Universitat de Lleida

Role of vitamin D signalling in vascular smooth muscle cells - morphological and molecular study

Petya Vladeva Valcheva

Universitat de Lleida
Departament de Medicina

Doctoral Thesis

Role of vitamin D signalling in vascular smooth muscle cells - morphological and molecular study

by

Petya Vladeva Valcheva

Supervised by:

Elvira Fernández Giráldez, MD, PhD

José Manuel Valdivielso Revilla, PhD

Lleida, February 2011

Elvira Fernández Giráldez, MD, PhD, Head of Nephrology Service, HUAV; Professor in the Department of Medicine, UdL and

José Manuel Valdivielso Revilla, PhD, Principal investigator of the Experimental Nephrology Laboratory, IRBLLeida

As supervisors of the doctoral thesis entitled **"ROLE OF VITAMIN D SIGNALLING IN VASCULAR SMOOTH MUSCLE CELLS - MORPHOLOGICAL AND MOLECULAR STUDY"**, presented by **Petya Vladeva Valcheva,**

Hereby state that this work fulfils the requirements to be defended in front of the Thesis committee and if it is the case, to obtain the degree "**Doctor of Philosophy**" from the University of Lleida.

Signed:

Dr Elvira Fernández Giráldez **Dr José Manuel Valdivielso Revilla**

Lleida, 2011

"El secreto de la felicidad no es hacer siempre lo que se quiere sino querer siempre lo que se hace" Lev Tolstoy

Dedicated to my family and my boyfriend

For their love and support

Antes de empezar a contar la historia de mi vida laboral en el grupo de "Nefrología experimental" me gustaría agradecer a toda la gente que participó en ella de una manera directa o indirecta:

A mis padres, Olya y Vladi, por confiar en mí y apoyarme en mi decisión de hacer la carrera de biología molecular y posteriormente venir en España/Catalunya para poder formarme como investigador, un sueño que marcó mi vida desde mi infancia (ser bióloga y venir en el país del "Verano Azul"). (На моите родители, Оля и Влади, за тяхното доверие в мен, за подкрепата им в решението ми да стана молекулярен биолог и в последствие да дойда в Испания/Каталуния за да се формирам като изследовател, една моя детска мечта (да бъда биолог и да дойда в страната на "Синьо лято").

A mis jefes, Elvira y José, por darme la oportunidad de formar parte de su grupo y por hacer posible la realización de esta tesis. A José agradezco personalmente la libertad que me dió en opinar sobre el proyecto de mi trabajo y aportar ideas, aunque no siempre "iban al grano" y todos los congresos a los que mando mi "abstract" y así pude ver en persona y escuchar muchos de los científicos cuyos artículos cito al final de este libro. A Elvira doy mil gracias por su apoyo y motivación a lo largo de mi trabajo.

A Dr Matias-Guiu como director científic de IRBLLEIDA, a la Fundació Dr Pifarré, a la Universitat de Lleida y a la AGAUR (Generalitat de Catalunya), por el apoyo económico sin el cual no podría realizar mi estancia en Lleida y Cardiff.

A Maya, por enseñarme donde está Lleida (la cual en los mapas del mundo en búlgaro era imposible encontrar por ser escrita con su nombre castellano) y convencerme que aquí hay una Universidad donde podré aprender mucho, porque cuenta con gente muy preparada y muy abierta a ayudar.

A las maravillosas "Chicas de NEFRO" Eva, Anna Cardús, Sara, Ana Martínez (lo siento pero para mi estas una de nosotras), Milica, Noelia y Montse. Vosotras os convertisteis en mi familia para lo malo y para lo bueno. De todo mi corazón os agradezco la ayuda que me habéis dado para poder aprender las técnicas en el laboratorio/animalario; poner las maquinas en el labo sin miedo; hablar castellano, entender catalán y practicar inglés; y el arte de disfrutar de la vida de estudiante de doctorado.

A Vicki y Adriana por la paciencia de escucharme siempre cuando lo necesitaba y aconsejarme sobre mis presentaciones.

A los chicos del Servicio de Nefrología de HUAV y UDETMA, especialmente a Lourdes, Olga, Felipe, Blai y Angels por aclararme mis dudas sobre algún fenómeno clínico o fármaco, y por a veces ser mis médicos.

A los profesores del grupo "Cicle Cel·lular" (especialmente a Marti, Carme y Eloi) por todo lo que me han enseñado sobre el mundo del ciclo celular y las maneras de estudiarlo.

A los doctores Pamplona y Boada, y todo el grupo "Fisiopatologia metabólica" por su colaboración en el nuestro proyecto y especialmente a Jordi por su dedicación a los experimentos con la respirometría y los niveles de ATP.

A Dra Anaïs Panosa por todas las horas que hemos pasado juntas delante del FACS y a Xavier Calomarde por las muestras de la microscopía electrónica.

A todos los profesores del departament de Ciències Mèdiques Bàsiques y especialmente a estos con los que compartíamos el laboratorio de investigación en la 1ra planta de ARNAU a los que acudía siempre cuando necesitaba consejo o algún anticuerpo/reactivo (Mario, Xavi, Dani, Marta, Judit, Carles, Andree) y a los doctores Carme Piñol y José Antonio Moreno por enseñarme como trabajar con los animales según las normas.

A Dr Luis Pérez-Ruiz por su ayuda en la realización del complicado método del daño en la arteria carótida en ratón.

A los chicos del animalario – Roser, Jessica, Marc, Emilia y Manolo por su gran ayuda en mantener la colonia de los ratones "VDRKO" y en todas las manipulaciones en las cuales estos animales fueron sometidos.

A las chicas de la Unitat Docent: Teresa, Montse y María por su apoyo y ánimo.

A la Unitat de Gestió d'Ajuts Interns y especialmente a Fermina, la que siempre estaba dispuesta de ayudarme en todas las dudas y problemas que yo tenía con las becas y los contratos predoctorales.

A todos los compañeros y becarios de ARNAU y de la Facultat (espero que no me olvide a nadíe): David, Crispi, Elizabet, Patricia, Nuria Bahí, Mary y Miguel, Carme, Raffi, Esteban, Mónica, Jinsheng, Anabel, Nuria Eritja, Cristina, Anna Macia, Myriam, Gemma, Esmeralda, Ana Madris, Dolos, Manu, María José, Marcelino, Rita, Marta, Xènia, Alba, Mariona, Dani, Hugo, Arindam, Mireia, María, Junmei, Deepshikha, Charumathi,… con los que hemos pasado unas horas muy agradables en el labo, durante los seminarios y las cenas nacionales y/o internacionales.

A mis profesoras de español de la EOI LLeida, Elena y Paloma por haber me insistido en aprender escribir cartas formales y prepararme en un nivel de castellano suficientemente bueno para poder escribir ahora estas líneas.

To Professor Jorge D. Erusalimsky, head of the Cellular Senescence and Vascular Biology Group, Cardiff School of Health Sciences, University of Wales Institute, Cardiff, UK to accept me in his group for a short stay and to all the people there who made my stay very pleasant. Y a Anna y Alberto por no sentir me sola en ningún momento.

A Stefi y Ariel por su amistad, apoyo y por ser los mejores compañeros de piso.

A toda la peña búlgara – Petar, Anton, Katya, Mima, Kaloyan y Tzveti por su amistad y por hacer que el nuestro país no este tan lejos.

A mis colegas del laboratorio "Parasitología experimental y aplicada" en Sofía donde aprendí hacer Westerns, especialmente a Ud Dr Rainova. (*На колегите ми от лаборатория "Експериментална и приложна паразитология" в София, където се научих да правя уестерни, и специално на Вас, Д-р Райнова.)*

A mi hermana Magdalena, su marido Georgi y especialmente a mis sobrinitos Viki y Miteto por su ánimo y todos los besos aéreos que me mandaban por Skype durante mis momentos más difíciles. (На сестра ми Магдалена и съпруга й Георги, и особено на моите племенничета Вики и Митето за това, че винаги са ме окуражавали и за всички въздушни целувки, които ми пращаха по Скайп в най-трудните ми моменти.)

A Josep María por su amor y apoyo, y a toda su familia por hacer me sentir como en mi casa cada vez cuando nos íbamos a comer en Termens. A Espie por su ayuda con todos los idiomas que tenía que utilizar a lo largo de mi trabajo y por ser una guía estupenda durante mi visita en Londres.

A mis abuelos que ya no están con nosotros pero con su confianza en mi y su ejemplo personal siempre me han motivado para continuar adelante y hacia arriba. (На баба ми и дядовците ми, които вече не са сред нас, но със своето доверие в мен и своя личен пример винаги са ме мотивирали да продължавам напред и нагоре.)

A todos vosotros muchas gracias!

(На всички вас благодаря много!)

INDEX

ABBREVIATIONS

1αOHase	*25-hydroxyvitamin D_3-1-α-hydroxylase*
1,25(OH)$_2$D$_3$	*Calcitriol (1,25-dihydroxyvitamin D_3)*
2HPT	*Secondary hyperparatiroidism*
24OHase	*25-hydroxyvitamin D3*-24-hydroxylase
25(OH)D$_3$	*25-hydroxyvitamin D_3*
ACE	*Angiotensin-converting enzyme*
AF-2	*Transcriptional* activation *function 2*
Agt	*Angiotensinogen*
AMPK	*Adenosine monophosphate activated kinase*
Ang II	*Aniotesin II*
ANT	*Adenine nucleotide transporter*
AT1/2-R	*Angiotensin II type 1/2 receptor*
ATP	*Adenosine triphosphate*
BMP4	*Bone morphogenetic protein 4*
bFGF	*Basic fibroblast growth factor*
BrdU	*Bromodeoxyuridine*
Ca	*Calcium*
CAK	*CDK-activating kinase*
Ca•PO$_4$	*Calcium phosphorus ion product*
CaR	*Calcium sensing receptor*
CDK	*Cyclin-dependent kinase*
CRE	*cAMP response element*
CREB	*cAMP response element-binding*
CRF	*Chronic renal failure*
CKD	*Chronic kidney disease*
CVD	*Cardiovascular disease*
DBD	*DNA binding domain*
DBP	*Vitamin D binding protein*
DC	*Dendritic cell*
DHE	*Dihydroethidium*
DMEM	*Dulbecco`s Modified Eagle`s medium*
DPI	*Diphenyleneiodonium sulfate*
DR	*Direct repeat*
DRIP	*VDR- interacting protein*
EC	*Endothelial cell*
ECM	*Extracellular matrix*
ERK1/2	*Extracellular-signal regulated kinase ½*
ETC	*Electron transport chain*
FBS	*Foetal bovine serum*

Abbreviations

FGF23	*Fibroblast growth factor 23*
FGFR1	*Fibroblast growth factor receptor*
FOXO1	*Forkhead box O1 transcriptional factor*
GAPDH	*Glyceraldehyde-3-phosphate dehydrogenase*
GFR	*Glomerular filtration rate*
HAT	*Histone acetyl transferase*
HDAC	*Histone deacetylase complex*
HT	*Hypertension*
HVDRR-II	*Hereditary vitamin D resistant rickets type II*
IGF	*Insulin-like growth factor*
IL-6	*Interleukin 6*
iNOS	*Inducible nitric oxide synthase*
IP3	*Inositol trisphosphate*
KO	*Knockout*
LBD	*Ligand binding domain*
LDL	*Low density lipoprotein*
MAPK	*Mitogen activated protein kinase*
LVH	*Left ventricular hypertrophy*
MTT	*3-(4,5-dimethylthiazol-2-yl)-2,5-diphenyltetrazolium bromide*
mVDR	*Putative cell membrane vitamin D receptor*
NAD(P)H	*Nicotinamide adenine dinucleotide (phosphate)*
N-CoR	*Nuclear receptor corepressor*
NFκB	*Nuclear factor κB*
NO	*Nitric oxide*
oxLDL	*Oxidised LDL*
P	*Phosphorus*
PBS	*Phosphate buffered saline*
PDDR	*Pseudo–vitamin D–deficiency rickets*
PDGF	*Platelet-derived growth factor*
PI	*Propidium iodide*
PI3K	*Phosphoinositide-3 kinase*
PKC	*Protein kinase C*
PLC	*Phospholipase C*
PTG	*Parathyroid gland*
PTH	*Parathyroid hormone*
PTHrP	*Parathyroid hormone related peptide*
Q	*Quiescent state*
Rank	*Receptor activator of NFκB*
RAS	*Renin-angiotensin system*
Rb (pRb)	*Retinoblastoma protein*

ROS	*Reactive oxygen species*
RP	*Rocking platform*
RT	*Room temperature*
RXR	*Retinoid X receptor*
SEM	*Standard* error *of the mean*
SIPS	*Stress-induced premature senescence*
SM22α	*Smooth muscle lineage restricted protein*
SMRT	*Silent mediator for retinoid and thyroid hormone receptors*
SOD	*Superoxide dismutase*
SRC	*Steroid receptor coactivator*
TGF-β	*Transforming growth factor β*
TRAP	*T3 receptor auxiliary protein*
VEGF	*Vascular endothelial growth factor*
VDR	*Vitamin D receptor*
VDRE	*Vitamin D responsive element*
VSMC	*Vascular smooth muscle cell*
WT	*Wild type*

ABSTRACTS

Vitamin D has long been known for its important role in regulating the levels of calcium and phosphorus, and in mineralization of bone. The biological effects of the hormonally active form of vitamin D ($1,25(OH)_2D_3$, or calcitriol) are mediated by the binding to the vitamin D receptor (VDR) which in turn acts over specific responsive elements (VDRE) in the promoter region of the vitamin D - target genes, modifying their expression. In the last decades, it has been shown that VDR is present not only in the classical vitamin D targets such as bone, kidney, and intestine, but also in many other tissues, like skeletal, smooth, and heart muscles, and in brain, skin, and liver. In addition to the control of the mineral homeostasis, vitamin D exerts pleiotropic actions in a variety of cell types, influencing important physiological processes such as cellular proliferation and differentiation, the immune response as well as different pathological conditions like cancer, cardiovascular, metabolic and autoimmune diseases. Moreover, together with its endocrine effects, vitamin D has important autocrine/paracrine roles. In vascular smooth muscle cells (VSMC), vitamin D regulates proliferation and calcification. Both processes, together with VSMC senescence occur during the atherosclerotic process. To be able to divide, VSMC need the energy of ATP produced by mitochondria. Alterations in the mitochondrial function are related to increased production of free radicals. In the artery wall, angiotensin II (Ang II) serves as a potent mediator of oxidative stress, provoking stress-induced premature senescence (SIPS). Ang II levels are controlled by renin, which gene expression is regulated by vitamin D. Thus, a defect of vitamin D signalling could lead to an increase in Ang II levels and its adverse effects in the artery wall.

When we cultured VSMC, obtained from VDR knockout (VDRKO) mice we found an increment in the production of Ang II in the culture medium of these cells in comparison with the wild type (WT), which was in accordance with the increased activation of the renin-angiotensin system at systemic level, found in the VDR mutant mice. Moreover, a decrease in the proliferation rates of VDRKO VSMC was found *in vitro* and *in vivo*. This decrease was in parallel to an increase in the cell volume. In quiescent state, VDRKO cells presented significantly increased expression of $p57^{Kip2}$ together with elevated levels of $p19^{Arf}$, $p21^{Cip1}$ and $p27^{Kip1}$, and lower levels of phosphorilated pRb and cyclins D and E, thus preventing their proliferation. Furthermore, VDRKO cells showed an increase in the expression of cathepsin D, an enzyme with renin-like activity, and of the Ang II receptor type 1. Also, superoxide anion production was higher in the mutant cells, and was inhibited with both, losartan and DPI. Moreover, the VDR ablated cells presented a significant decrease in the expression of the mitochondrial antioxidant enzyme manganese superoxide dismutase (SOD2) and the inducible nitric oxide synthase, which produces the vasodilatator molecule NO. By high-resolution respirometry we found that the mitochondria of VDRKO VSMC were less efficient which could explain the lower content of ATP in these cells. All of these findings were associated with the senescent phenotype, presented by around 20% of the VSMC lacking VDR in culture.

In conclusion, the absence of VDR signalling in VSMC leads to SIPS due to the increased local production of Ang II, with a subsequent increase in free radicals, produced by the activation of the NADPH oxidase, which suggests a possible role of the vitamin D system in vascular conditions which show hyperproliferation of VSMC.

La vitamina D ha sido durante mucho tiempo conocida por su importante papel en la regulación de los niveles de calcio y fósforo, y en la mineralización del hueso. Los efectos biológicos de la forma hormonalmente activa de la vitamina D ($1,25(OH)_2D_3$, o calcitriol) están mediados por la unión al receptor de la vitamina D (VDR), que a su vez actúa sobre los elementos de respuesta a la vitamina D (VDRE) en el promotor de los genes diana, modificando su expresión. En las últimas décadas, se ha demostrado que el VDR está presente no sólo en las dianas clásicas de la vitamina D, como los huesos, los riñones y el intestino, sino también en muchos otros tejidos, como los músculos esqueléticos, lisos, y cardíacos, y en el cerebro, la piel y el hígado. Además del control de la homeostasis mineral, la vitamina D ejerce acciones pleiotrópicos en diferentes tipos celulares, influyendo en procesos fisiológicos importantes tales como la proliferación y diferenciación celular, la respuesta inmune, así como diferentes condiciones patológicas como el cáncer, las enfermedades cardiovasculares, metabólicas y autoinmunes. Además, junto con sus efectos endocrinos, la vitamina D tiene papeles autocrinas/paracrinas importantes. En las células de músculo liso vascular (CMLV), la vitamina D regula la proliferación y la calcificación. Ambos procesos, junto con la senescencia de las CMLV surgen durante el proceso aterosclerótico. Para poder dividirse, las CMLV necesitan la energía del ATP producido por las mitocondrias. Las alteraciones en la función mitocondrial están relacionadas con una mayor producción de radicales libres. En la pared arterial, la angiotensina II (Ang II) actúa como un potente mediador de estrés oxidativo, provocando senescencia prematura inducida por estrés (SIPS). Los niveles de Ang II son controlados por la renina, cuya expresión génica se regula por la vitamina D. Por lo tanto, un defecto en la señalización de la vitamina D puede conducir a un aumento en los niveles de Ang II y sus efectos adversos en la pared arterial.

Cuando se cultivaron CMLV, obtenidas de ratones *knockout* para VDR (VDRKO) se encontró un aumento en la producción de Ang II en el medio de cultivo de estas células, comparando con el tipo salvaje (WT), lo que estaba de acuerdo con la mayor activación de la sistema renina-angiotensina a nivel sistémico, que fue encontrada en los ratones mutantes de VDR. Por otra parte, una disminución en la tasa de proliferación de las VDRKO CMLV fue encontrada *in vitro* e *in vivo*. Este descenso era en paralelo a un aumento en el volumen celular. En estado de reposo, las células VDRKO presentaron un aumento significativo en la expresión de $p57^{Kip2}$ junto con niveles elevados de $p19^{Arf}$, $p21^{Cip1}$ y $p27^{Kip1}$, y menores niveles de pRb fosforilada y ciclinas D y E, asi previniendo su proliferación. Además, las células VDRKO mostraron un aumento en la expresión de la catepsina D, una enzima con actividad parecida a la del renina, y del receptor de Ang II tipo 1. Además, la producción del anión superóxido fue mayor en las células mutantes, y fue inhibida tanto con losartán como con DPI. Por otra parte, las células VDRKO presentaron una disminución significativa en la expresión de la enzima antioxidante mitocondrial superóxido dismutasa de manganeso (SOD2) y la óxido nítrico sintetasa inducible, que produce la molécula vasodilatadora NO. Por respirometría de alta resolución fue determinado que las mitocondrias de las CMLV VDRKO fueron menos eficientes que podría explicar el menor contenido de ATP en estas células. Todos estos factores se relacionaron con el fenotipo senescente, presentado por alrededor de 20% de las CMLV que carecían VDR en cultivo.

En conclusión, la ausencia de señalización por VDR en CMLV lleva a SIPS debido al aumento en la producción local de Ang II, con el consiguiente aumento de los radicales libres, producidos por la activación de la NADPH oxidasa, lo que sugiere un posible papel del sistema de la vitamina D en enfermedades vasculares, que muestran una hiperproliferación de las CMLV.

La vitamina D ha estat durant molt de temps coneguda pel seu important paper en la regulació dels nivells de calci i fòsfor, i en la mineralització de l'os. Els efectes biològics de la forma hormonalment activa de vitamina D ($1,25(OH)_2D_3$, o calcitriol) estan mediats per la unió al receptor de vitamina D (VDR), que alhora actua sobre els elements de resposta específics (VDRE) en el promotor dels gens diana de vitamina D, modificant-ne l'expressió. En les últimes dècades, s'ha demostrat que el VDR no solament és present en les dianes clàssiques de la vitamina D com els ossos, els ronyons i l'intestí, sinó també en molts altres teixits, com els músculs esquelètics, llisos, i cardíacs, i també en el cervell, la pell i el fetge. A més del control de l'homeòstasi mineral, la vitamina D exerceix accions pleiotròpiques en diferents tipus cel·lulars, influint en processos fisiològics importants com la proliferació, la diferenciació cel·lular, la resposta immune, així com també en les diferents condicions patològiques: el càncer, les malalties cardiovasculars, metabòliques i autoimmunes. A més, juntament amb els seus efectes endocrins, la vitamina D té funcions importants autocrines/paracrines. En les cèl·lules de múscul llis vascular (CMLV), la vitamina D regula la proliferació i la calcificació, aquests dos processos, juntament amb la senescència de les CMLV es produeixen durant el procés ateroscleròtic. Per poder-se dividir, les CMLV necessiten l'energia de l'ATP produïda per les mitocòndries. Les alteracions de la funció mitocondrial estan relacionades amb una major producció de radicals lliures. A la paret arterial, l'angiotensina II (Ang II) actua com un potent mediador d'estrès oxidatiu, provocant senescència prematura induïda per l'estrès (SIPS). Els nivells d'Ang II són controlats per la renina, l'expressió de la qual es regulada per la vitamina D. Per tant, un defecte en la senyalització de la vitamina D pot conduir a un augment en els nivells d'Ang II i produir els seus efectes adversos en la paret de l'artèria.

Quan es van cultivar les CMLV, obtingudes de ratolins *knockout* per VDR (VDRKO) es va trobar un augment en la producció d'Ang II en el medi de cultiu d'aquestes cèl·lules en comparació amb el tipus salvatge (WT), que estava d'acord amb la major activació del sistema renina-angiotensina a nivell sistèmic, que es va trobar en els ratolins mutants de VDR. D'una banda, una disminució en les taxes de proliferació de les CMLV VDRKO es va trobar in vitro i in vivo. Aquest descens va ser en paral·lel a un augment en el volum cel·lular. En estat de repòs, les cèl·lules VDRKO presentaven un augment significatiu de l'expressió de $p57^{Kip2}$ juntament amb els nivells elevats de $p19^{Arf}$, $p21^{Cip1}$ i $p27^{Kip1}$, i nivells inferiors de PRB fosforilada, ciclines D i E, i axi es prevé la seva proliferació. A més, les cèl·lules VDRKO van mostrar un augment en l'expressió de la catepsina D, un enzim amb activitat com renina, i del receptor d'Ang II tipus 1. A més, la producció d'anió superòxid va ser major en les cèl·lules mutants, i va ser inhibida tant amb losartan com amb DPI. D'altra banda, les cèl·lules VDRKO presenten una disminució significativa en l'expressió de l'enzim mitocondrial antioxidant, la superòxid dismutasa de manganès (SOD2) i l'òxid nítric sintetasa induïble que produeix la molècula vasodilatadora NO,. Per respirometria d'alta resolució es va determinar que les mitocòndries de VDRKO CMLV van ser menys eficients que podria explicar el menor contingut d'ATP en aquestes cèl·lules. Tots aquests factors es van relacionar amb el fenotip senescent, que presentaven al voltant del 20% de les CMLV sense VDR en cultiu.

En conclusió, l'absència de senyalització per VDR en CMLV porta a SIPS causada per l'augment en la producció local d'Ang II, amb el consegüent augment dels radicals lliures, produïts per l'activació de la NADPH oxidasa, el què suggereix un possible paper del sistema de la vitamina D en malalties vasculars, que mostren una hiperproliferació de les CMLV.

Витамин Д е известен със своята важна роля в регулирането на нивата на калций и фосфор, както и в минерализацията на костите. Биологичните ефекти на хормонално активната форма на витамин Д ($1,25(OH)_2Д_3$, или калцитриол) се опосредстват от свързването с рецептора на витамин Д (РВД), който от своя страна въздейства върху специфични елементи, отговорящи на витамин Д в промотора на витамин Д таргетните гени, променяйки тяхната експресия. През последните десетилетия беше показано, че РВД има установено присъствие не само в класическите таргети на витамин Д, като костите, бъбреците и червата, но и в много други тъкани, като скелетната, гладката и сърдечната мускулатура, и в мозъка, кожата и черния дроб. В допълнение към контрола на минералната хомеостаза, витамин Д оказва плеотропни действия в различни клетъчни типове, влияейки върху важни физиологични процеси като клетъчната пролиферация и диференциация, на имунния отговор, както и различни патологични състояния, като рак, сърдечно-съдови, метаболитни и автоимунни заболявания. Освен това, заедно с ендокринните ефекти, витамин Д има важна авто/паракринна роля. Витамин Д регулира пролиферацията и калцификацията на гладкомускулните клетки (ГМК), двата процеса, които заедно с клетъчното стареене се проявяват по време на атеросклеротичния процес. За да може да се раздели, ГМК се нуждае от енергията на АТФ, произведен от митохондриите. Промените в митохондриалната функция са свързани с увеличаване на производството на свободни радикали. В артериалната стена, ангиотензин II (Анг II) служи като мощен медиатор на оксидативен стрес, предизвиквайки стрес-индуцирано преждевременно стареене (СИПС). Нивата на Анг II се контролират от ренина, чиято генната експресия се регулира от витамин Д. По този начин, дефект във сигнализацията, медиирана от витамин Д може да доведе до повишение на нивата на Анг II и неговите неблагоприятни ефекти във артериалната стена.

Когато култивирахме ГМК, получени от РВД нокаут (РВД-/-) мишки намерихме увеличено производството на Анг II в клетъчната среда на тези клетки в сравнение с дивия тип (ДТ), което е в съответствие с увеличената активация на ренин-ангиотензиновата система на системно равнище, намерена във РВД мутантни мишки. Установено бе и намаление в пролиферацията на РВД-/- ГМК, ин витро и ин виво. Това намаление бе успоредно с увеличаване на клетъчния обем. В латентно състояние, РВД-/- клетки представиха значително повишена експресия на $p57^{Kip2}$ заедно с повишени нива на $p19^{Arf}$, $p21^{Cip1}$ and $p27^{Kip1}$, и по-ниски нива на фосфорилация на ретинобластома протеин и циклините Д и Е, възпрепятствайки пролиферацията им. Освен това, РВД-/- клетки, показаха увеличение в експресията на катепсин Д, ензим чиято активност е подобна на тази на ренина, и на рецептора за Анг II тип 1. Беше манерено също така и по-високо производство на супероксидни аниони в мутантните клетки, което бе потиснато както с лосартан така и с дифенилен йодониум. Освен това, клетките без РВД представиха значителен спад в експресията на митохондриалния антиоксидантен ензим манганова супероксид дисмутаза (СОД2) и индуцируемата азот-оксид синтетаза, произвеждаща вазодилататорната молекула NO,. Чрез респирометрия с висока резолюция открихме, че митохондриите на РВД-/- ГМК са по-малко ефективни, което би могло да обясни по-ниското съдържание на АТФ в тези клетки. Всички тези находки са свързани със сенесентния фенотип, представен от около 20% от ГМК лишени от РВД в култура.

В заключение, липсата на сигнализация през РВД в ГМК води до СИПС, дължащо се на увеличеното местно производство на Анг II, с последващо увеличение на свободните радикали, произведени след активирането на НАДФН оксидазата, което предполага една евентуалната роля на системата на витамин Д в съдови заболявания, показващи хиперпролиферация на ГМК.

INTRODUCTION

1. CHRONIC KIDNEY DISEASE

Chronic kidney disease (CKD) is a progressive and irreversible loss of the renal functions, which grade is determined depending on the glomerular filtration rate (the volume of the fluid filtered through the glomerular capillaries into the Bowman's capsule per unit time, ml/min). The normal values of GFR in humans, adjusted for body surface area is similar in men and women, and is in the range of 100-130 ml/min/1.73m^2. The compound usually used for the determination of the GFR is the endogenously synthesized creatinine, a breake-down product of creatine phosphate in muscle, which does not bind to serum proteins, and is able to pass through the glomerular capillaries without being reabsorbed or secreted by the renal tubules. When the GFR is less than 60 ml/min/1.73 m^2 this means that the kidneys are loosing their capacity to eliminate the waste products, to concentrate the urine, to keep the electrolytes and present some other alterations as a result of retention of products of the cellular catabolism and the consequent acid-base imbalance. CKD begins with progressive decrease in the GFR as a result of the appearance of damaged nephrons, changes in the tubular homeostasis, failure in kidney hormone functions and when the GFR decreases below 15%, the uremic syndrome. Among the metabolical abnormalities associated with loss of renal endocrine function are the functional alterations in the production of hormones and mediators (per default $1,25(OH)_2D_3$ and erythropoietin and per excess - renin) or increased degradation (insulin and PTH).[1] In the *Study to Evaluate Early Kidney Disease (SEEK),* it has been found that vitamin D deficiency (serum levels <22 pg/ml) was a normal finding at all estimated GFR levels: 13% in those patients with eGFR >80 ml/min and more than 60% in CKD patients in stages 4 and 5 (eGFR <30 ml/min), together with elevated PTH (>65pm/dl).[2] As the renal tubular cells are the active sites of calcitriol synthesis, vitamin D deficiency could be a result of the decreased kidney mass. Furthermore, adequate local concentrations of calcitriol are needed for the maintenance of the kidney structure and function, thus the lower levels of this hormone could be considered among the factors that cause the initiation and support the progression of kidney damage, leading finally to CKD.

Usually, the diagnosis CKD is assigned after the routine examination of patients with high blood pressure, anaemia, pericarditis or diabetes, as well as people who smoke, elderly, Afro-Americans and narcotic users. The prevalence of CKD worldwide is estimated to 7.2% in people around 30 years old, with an increase from 23.4% to 35.8% in aged persons (64 years or older).[3] Otero et al. have shown that the prevalence of CKD at any stage in Spain is relatively high

(6.8%), thus being very similar to countries like Italy, Switzerland, Norway and Iceland.[4]

2. MAIN COMPLICATIONS RELATED TO CKD

The main complications that the patients with CKD develop are uremic syndrome, secondary hyperparathyroidism (2HPT) and cardiovascular disease (CVD) in parallel to number of abnormalities of the calcium-vitamin D metabolic pathway, such as hypocalcemia, hyperphosphatemia, and renal bone disease (osteodystrophy) (Figure 1).

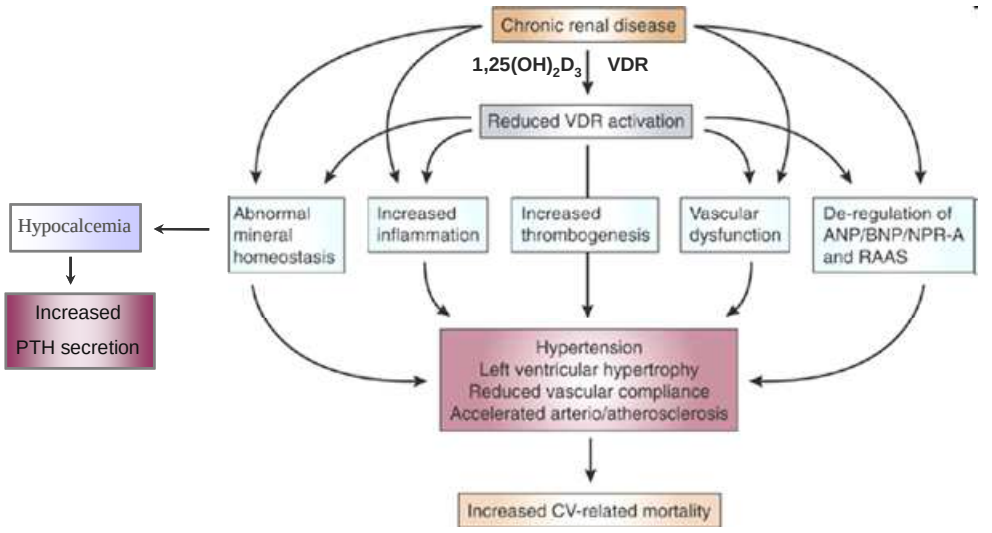

Figure 1. The main complications that the CKD patients suffer as a result of the reduced kidney functioning (*modified from Wu-Wong, 2007*).

2.1. Uremic syndrome

The term "uremia" literally means "urine in the blood" and usually accompanies the severe renal failure, when the GFR falls to less than 10 ml/min. Uremia is considered as a syndrome, associated with disruption in the fluid, electrolyte and hormone balances and is due to the incapacity of the damaged nephrons to secrete the urea and all the end-products of the protein metabolism. Several metabolic abnormalities could be related to this syndrome, such as malnutrition, anemia, acidemia, hyperkalemia, hypertension[5,6] as well as disorders characterized by hormone misbalance like disturbances in menstruation and fertility in women and impotence in men,[7] and 2HPT.

2.2. Hyperparathyroidism secondary to CKD

The secondary hyperparathyroidism is characterized by a functional disorder of the parathyroid glands (PTG). The main function of the PTG is to control the amount of calcium (Ca) and phosphorus (P) in the blood and within the bones. Ca is a divalent ion that is present in millimolar concentrations in the extracellular fluid, whereas in the parathyroid cell it is present in 10,000-fold lower concentrations. This ion plays a very important role in the intracellular signalling, in the coagulation and in the muscular function. The concentration of extracellular Ca is detected by the calcium sensing receptor (CaR), expressed in a broad range of cells, including parathyroid chief cells,[8] the C cells in the thyroid gland[9] and cells of the kidney tubule.[10] In low Ca conditions, the CaR is relaxed, PTH is released and the activation of a specific PTH receptor on bone and kidney occurs in order to release Ca and complete the feedback loop. In contrary, the hormone that is released by the parafollicular cells (C cells) of the thyroid gland, calcitonin, acts to decrease the Ca concentrations. Moreover, in the PTG cells a membrane co-transporter of P that is likely to function as a P sensor has been described.[11]

In the kidney, PTH favours the activation of 25-hydroxyvitamin D_3-1-α-hydroxylase (1αOHase), leading to un augment in the concentration of the active form of vitamin D ($1,25(OH)_2D_3$). By their side, the high levels of Ca and $1,25(OH)_2D_3$ exert a negative feedback control over the synthesis and secretion of PTH (Figure 2).

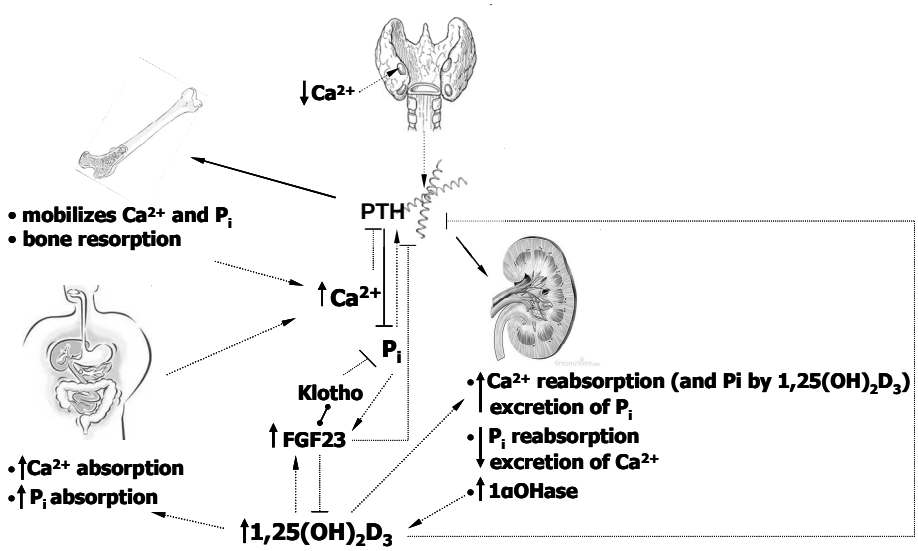

Figure 2. Schematic representation of the effects of PTH and the control of its secretion.

In order to regulate the PTH, Ca and P affect post-transcriptionally the binding of parathyroid proteins (trans factors) from the cytoplasm to a defined cis-sequence in the PTH mRNA 3'-untranslated region (UTR), thereby determining the stability of the transcript.[12] Apart of the direct influence of P over the PTH mRNA stability, the stimulatory effect of P over PTH could be indirect, mediated by the inhibition of $1,25(OH)_2D_3$ synthesis trough fibroblast growth factor 23 (FGF23) – dependant mechanism.[13] FGF23 is a circulating phosphaturic factor formed in the bone that acts as a hormone in the kidneys. It has been shown that the serum levels of FGF23 continuously increase as renal function declines in CKD, which has been proposed to play a role in the development of 2HPT. In the principal cells of the PTGs and in the kidneys, a permissive receptor cofactor for FGF23, called Klotho, is abundantly expressed. Urakawa et al. have shown that Klotho directly converts the canonical fibroblast growth factor receptor (FGFR1) into FGF23 receptor.[14]

After the detection of low levels of Ca and vitamin D and prolonged high levels of P, common findings in renal failure, an increase in PTH gene expression, synthesis, and secretion, as well as in the proliferation of the parathyroid cells occur. CKD patients suffer from this disorder for various reasons: the elimination of phosphate is impaired, there is no vitamin D due to the disappearance of the renal parenchyma, intestinal absorption of calcium is low and blood levels of calcium decrease.[15]

2.3. Cardiovascular disease in CKD

Cardiovascular disease currently is the major social health problem in the developed countries, and atherosclerosis is the most prominent contributor. Some of the traditional risk factors to develop a vascular disorder are gender, race, heredity, age, tobacco smoking, alcoholism, socioeconomic stress, dyslipidemia, obesity, diabetes mellitus and hypertension.[16] Out of the general population, higher prevalence of CVD was found in patients suffering CKD. Cardiovascular events are common finding in these patients and usually are the cause of death. The CKD patients are at high risk of CVD development because as a result of the kidney failure they suffer more severe oxidative stress and inflammation. It has been shown that CKD contributes to accelerated atherosclerotic disease in the coronary, cerebral, and peripheral circulations. This could be due to the fact that CKD patients have higher incidences of many major risk factors, such as diabetes or hypertension. The main features of the cardiovascular complications in CKD are the cardiomyopathy and the uremic arteriopathy.

2.3.1. Left ventricular hypertrophy

The left ventricular hypertrophy (LVH) appears in parallel with the progression of the CKD and is the result of the prolonged increase in the diastolic pressure, due to a chronic enhancement of flow/volume and the high cardiac output, associated with three factors – retention of salt and water, arteriovenose shunt and anaemia. Among the major factors, found to contribute to the LVH is the activation of the renin-angiotensin-aldosterone system (RAAS) and the main strategy to reduce the LVH is by the administration of angiotensin converting enzyme inhibitors. In patients with terminal kidney failure the LVH is very common (60% to 80%).[17]

2.3.2. Uremic arteriopathy

Uremic arteriopathy consists of two main events, atheromatosis and arteriosclerosis. These processes affect the walls of medium and large arteries. Atheromatosis is associated with fibrosis and calcifications of the innermost layer of the artery, which lead to the narrowing of the diameter because of the formation of atherosclerotic plaques (Figure 3). During this process the proliferation of vascular cells, coming from the media layer of the wall, makes the plaque bigger and more stable. If the cells lose irreversible their ability to divide, which is a common feature of cellular senescence, or the number of apoptotic cells within the plaque increases, the plaque becomes more susceptible to rupture. Thrombus formation on disrupted atherosclerotic plaques frequently causes acute coronary syndromes.

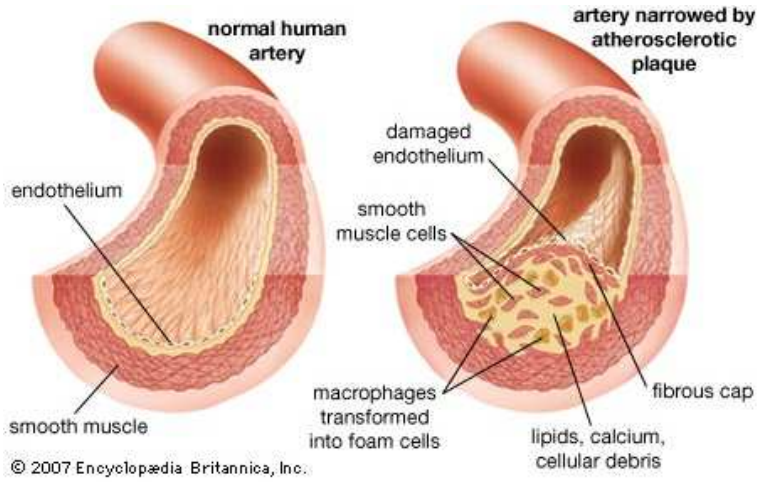

Figure 3. Representation of a normal human artery wall and of an artery affected by atherosclerosis.

In arteriosclerosis, calcification together with vascular hypertrophy, are found in both, the inner and medial layers, which make the artery wall thicker and harder, and therefore more rigid. This change in the wall affects the pulse wave velocity, used as a very valuable predictive factor in the population of the CKD patients.[18] This increase in the size of the artery wall is due mainly to the proliferation of the smooth muscle cells and the production of extracellular matrix (ECM). Thus, vascular smooth muscle cells (VSMCs) play a critical role in vascular remodeling associated with hypertension, atherosclerosis, and restenosis, participating in the vascular wall inflammation and lipoprotein retention, as well as to the formation of the fibrous cap that provides stability to the plaque. Thus, the proliferation of VSMC in pathological conditions could be considered beneficial, but several human and experimental studies provided evidence for the positive effect of the therapeutic inhibition of VSMC for in-stent restenosis, bypass graft failure and other vascular proliferative disorders.[19]

3. COMPONENTS OF THE ARTERY WALL

3.1. Structure

The normal structure of an artery consists of three well defined layers - tunica intima (I), tunica media (M), and tunica adventicia (A) (Figure 4).

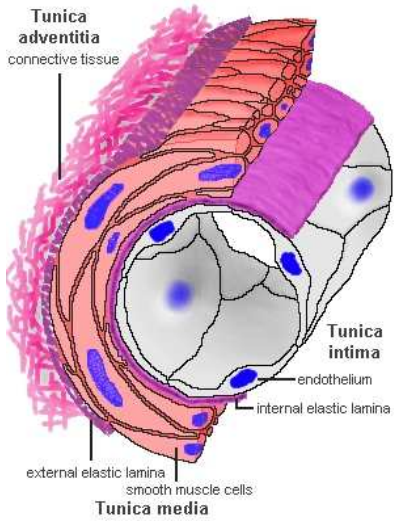

Figure 4. Structure of a normal artery (*by Professor John McGeachi, University of Western Australia*).

The intima is formed by a monolayer of endothelial cells (EC) and subendothelium or the basal laminae, formed by connective tissue containing ECM proteins like collagen, elastan, proteoglicans and other glicoproteins. This layer is the luminal surface of the artery and is in contact with the blood. The medial layer, formed by VSMCs provides the elasticity and the contractility of the artery wall. This layer is bordered by elastic laminaes, which consist of elastic fibres. The elastic laminaes possess fenestrations which permit the trafficking of substances and cells in both directions. The outmost part of the artery, the adventitia, is formed by connective tissue and beam of collagen, VSMC and fibroblasts. The connective tissue is the one that communicate with the surrounded structures.

3.2. Vascular smooth muscle cells

VSMCs are the contractile component of blood vessels, and express a set of smooth muscle (SM)-specific proteins such as SM α-actin and SM22α (SM lineage-restricted protein), which are characteristic of their contractile, differentiated phenotype.[20] In contrast to skeletal and cardiac myocytes, VSMCs are not terminally differentiated, and are able to undergo phenotypic changes both, *in vivo* and *in vitro* in response to environmental signals. This process involves changes in gene expression, which convert the cells from a non-proliferative contractile phenotype to a proliferating synthetic one.[21] It has been shown that VSMC can adopt also osteoblast-like phenotype which is essential for mineralization within the vascular wall.[22,23] The last modification is driven by the upregulation of factors, like core-binding factor 1α (Runx2), and bone morphogenetic protein-2, which control the expression of a number of osteoblastic markers, such as osteocalcin, alkaline phosphatase, and collagen-1. These markers were found to be elevated in the vasculature of patients with CKD.[23] Vascular calcification is a very important process because it leads to reduced elasticity of the arteries and is also found within the advanced atherosclerotic plaques. Thus, the activated VSMC could participate in the development and the progression of vascular pathologies.

3.2.1. VSMC proliferation

As commented above, a common finding in the CKD patients is the hardening of the artery wall, which in part is due to the increase in the size of the wall because of the dedifferentiation, migration, and proliferation of medial VSMCs in

response to arterial injury. VSMC proliferation plays also a central role in the repairing process. Under different environmental stimuli, like mechanical injury or release of growth factors such as basic fibroblast growth factor (bFGF), insulin-like growth factor (IGF) and platelet-derived growth factor (PDGF) by inflammatory cells increased VSMC proliferation is observed in the vasculature. VSMCs can suffer a switch to the so called "synthetic" phenotype, when they acquire characteristics of embryonic VSMCs that are able to proliferate, migrate and synthesise ECM, with morphology similar to the one of fibroblasts (fibroblast-like cells).[24]

3.2.1.1. Cell cycle

"Cell proliferation" is the increase in the content of molecules and organelles (cell growth) and the duplication of the genetic material with a following nucleus and then cell division to two daughter cells, genetically identical. This is a continuous and very finely controlled process, called cell cycle. Depending on the cell type, the regulation of the cell cycle could be different, for example, the terminally differentiated neuronal cells loose forever their ability to divide, meanwhile the smooth muscle cells conserve their capacity to divide, but normally are in quiescent state (Q). In general, in order to start the cytokinesis, the quiescent cell, which is found in the so-called Go phase, needs a signal to go back to the active presynthetic gap phase of the cell cycle, called G1. These signals could be provided from several molecules like mitogens, growth factors or cytokines. During this phase, the cell produces all the molecules and organelles, together with the energy in the form of macroergic bounds of ATP, which are necessary for the DNA-synthetic phase (S). In the S phase the DNA replication results in the production of two identical sets of chromosomes. The DNA replication is a very complex biochemical process that requires a lot of energy. In order to recover the lost ATP, the cell enters in the second gap period, G2 (premitotic phase), where new molecules of ATP are produced and the cell volume increases. Once the interphase period (G1/S/G2) is finished, the cell starts the mitosis (M). The main check points are the G1 to S and the G2 to M transitions (Figure 5).

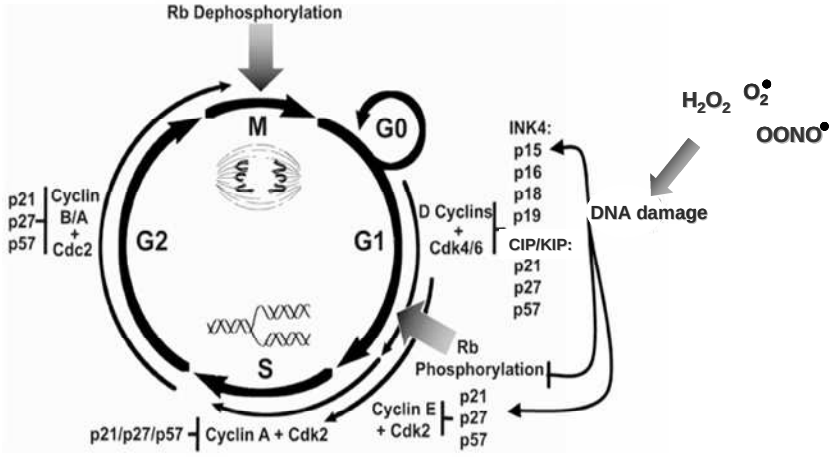

Figure 5. Cell cycle events and regulators (*modified from Donovan and Slingerland, 2000* [25]).

3.2.1.1.1. Positive regulators of the cell cycle

In the G1 phase of the cell cycle the cell decide whether to continue or exit the cell cycle. G1 phase is under the control of so-called cyclin-dependent kinases (CDKs). The constitutively expressed CDKs assemble with their regulatory co-partners the cyclins, which are sequentially synthesized and degraded throughout the cell cycle. For the complete activation of the complex CDK/cyclin, the kinase should be phosphorylated by the so called CDK-activating kinase (CAK). The first cyclin which expression is induced after the exposure of the cells to mitogenic stimuli is cyclin D. On one hand, the extracellular-signal regulated kinase ERK1/2 increases the transcription of the cyclin D gene and post-translationally regulates its assembly with the cyclin D-dependent kinases CDK4 or CDK6. The activated serine/threonine protein kinase AKT/PKB, on the other hand, prevents cyclin D degradation. The CDK4 and CDK6 after being bound to cyclin D initiate the phosphorylation of retinoblastoma protein (pRb), which is part of the pocket protein family. pRb, in its hypophosphorylated, active state, is bound to promoter-bound members of the E2F family of transcription factors, thus inhibiting their transcriptional activity and consequently the transcription of E2F-responsive genes. These genes encode for many of the components of the replication machinery, including cyclin E and DNA polymerase α. The hyperphosphorylated pRb, which releases E2F, is finally achieved by the activity of the cyclin E/CDK2 complex. These complexes phosphorylate, in addition to pRb, also several proteins such as the CDK inhibitor $p27^{KIP1}$, which leads to its degradation.[26]

3.2.1.1.2. Inhibitors of the cyclin-dependent kinases

The negative cell cycle control is exerted by the members of two main families of cyclin-dependent kinase inhibitors (CKIs) - INK and CIP/KIP families. INK proteins (p15 ^{INK4b}, p16 ^{INK4a}, p18 ^{INK4c}, p19 ^{INK4d}) specifically inhibit the catalytic subunits of CDK4/6 and the CIP/KIP proteins (p21 ^{CIP1}, p27 ^{KIP1} and p57 ^{KIP2}) affect the catalytic activity of cyclin D, E- and A-dependent kinases by binding to both, the catalytic and the cyclin subunit (Figure 5). The signals that provoke the synthesis of INK4 proteins are different, as $p15^{INK4b}$ is induced by TGF-β and mediates its ability to induce G1-phase arrest;[27] $p16^{INK4a}$ accumulates progressively during the cell aging,[28] meanwhile $p18^{INK4c}$ and $p19^{INK4d}$ are expressed during foetal development and may play a role in the terminal differentiation.[29] In VSMCs, the CDK inhibitors $p27^{KIP1}$ and $p21^{CIP1}$ have been implicated in terminating VSMC proliferation in intimal lesions[30] and the $p57^{KIP2}$ has been found to participate in the inhibition of the G1 to S transition. Moreover, microsatellite variants in the $p57^{KIP2}$ promoter were positively correlated with myocardial infarction in patients with atherosclerotic vessels.[31]

Furthermore, the CKIs expression is also controlled by environmental conditions that modulate cell growth, including exposure to reactive oxygen species (Figure 5), γ-irradiation, cell-cell contact, and cytokine stimulation.

3.2.2. VSMC hypertrophy

VSMC hypertrophy is an irreversible modulation of the VSMC phenotype, defined as an increase in the cell size in parallel to cell cycle progression block. This process is accompanied by elevated extracellular matrix deposition and could be the cause of systolic hypertension, altered coronary perfusion, and hypertrophy of the left ventricle. This modulation of the VSMC phenotype is also seen in the end stages of renal failure.[32] VSMC hypertrophy is found in large capacitance arteries such as the aorta of hypertensive animals or humans and is associated with the development of polyploidy, which occurs when the cells replicate their DNA but do not complete mitosis.[33] Braun-Dullaeus *et al*. provided evidence that $p27^{KIP1}$ acts as a molecular switch in determining whether VSMCs undergo hypertrophy or hyperplasia. Their experiments showed that after both, serum and angiotensin II (Ang II) treatments of VSMCs various cyclins and CDK were up-regulated, but meanwhile the serum downregulated the expression of the CKI $p27^{KIP1}$ and thus promoted cell proliferation, Ang II induced hypertrophy and protein synthesis was associated with no decline in the $p27^{KIP2}$ levels. Moreover, the acute ablation of this

CKI blocked the hypertrophy and promoted hyperplasia in VSMC upon incubation with angiotensin II.[34] Furthermore, the VSMC response to Ang II by hyperplasia vs. hypertrophy, is determined by the autocrine expression of transforming growth factor beta (TGFβ).[35] Ang II stimulates the production of biologically active TGFβ1 which, in turn, exerts an antiproliferative influence on the growth stimulatory effects of Ang II. Consequently, the net growth response to Ang II is hypertrophy without hyperplasia thus Ang II does not increase DNA synthesis in VSMCs, but increases protein synthesis and causes hypertrophy.[34] The hypertrophy of VSMC induced by Ang II is an important feature of hypertension, and the structural changes in the vessel wall contribute to an increase in the vascular resistance.[33]

3.2.3. VSMC senescence

One phenomenon that has been implicated both in ageing and in development of vascular pathologies is the cellular senescence. This stable form of cell cycle arrest has been shown to be related also to decrease in the proliferation of damaged cells and could be considered as a natural barrier to cancer progression. For the first time this phenomenon has been described by Hayflick and Moorhead (1961).[36] Replicative senescence is observed after a certain number of cell divisions in culture, when the cells stopped their growth process. In general, primary cells, freshly removed from an organism to be grown in culture, initially present tendency to divide rapidly and then the rate of division become slower until it reaches a division arrest.[37] When the cell enters the senescent state, it cannot be stimulated by physiological mitogens to enter again into the cell cycle.[38] Some typical morphological alterations could be also found – increased cell volume, flattened stella-like shape, nuclear changes, different gene expression, like the stable repression of the E2F target genes,[39] metabolism as well as the resistance to cell death by apoptosis. At mechanistic level, the replicative senescence has been linked to the erosion of telomeres. Telomeres in the vasculature shorten with age and this erosion is more pronounced in atherosclerotic-prone areas. Oxidative stress also can induce or accelerate the development of senescence. The pro-oxidant stimuli induce an acute form of senescence, which doesn't need extensive cell proliferation and is normally considered to be unrelated to telomere damage.[40] This form was called "stress-induced premature senescence" (SIPS) (Figure 6).

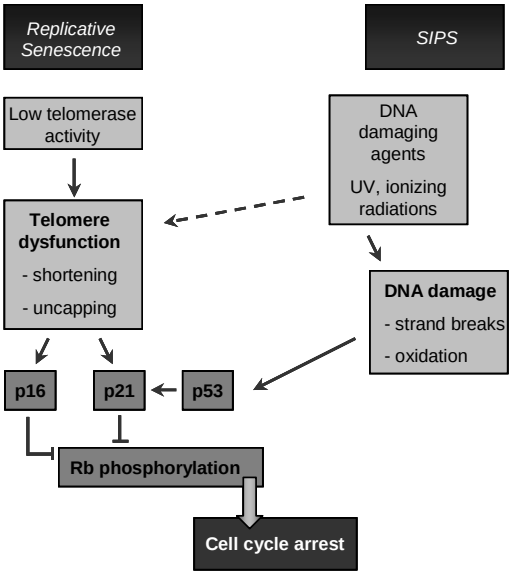

Figure 6. Pathways leading to replicative and stress-induced premature senescence (*modified from Gorenne et al., 2006* [41]).

Senescent VSMCs express genes, highly expressed in osteoblasts, such as alkaline phosphatase and collagen type I, pointing to a posible osteoblastic transition during the senescence, which could impair the main function of VSMCs, thus contributing to cardiovascular dysfunction.[42] Another characteristic of the senescent vascular cells is the increased interleukin-8 (IL-8) release and decreased endothelial nitric oxide synthase (eNOS) expression and activity, resulting in lower NO levels and mitochondrial membrane potential.[43,44]

In the vasculature cells exhibiting the typical senescence morphology are found within the advanced atherosclerotic plaque. These cells proliferate at very low levels, due to the decreased cyclin D/E expression, increased $p16^{INK4}$, $p21^{CIP1}$, and hypophosphorylated pRb and show increase in the marker senescence-associated ß-galactosidase (SA-ß-Gal) activity.[45] Furthermore, higher levels of ROS were found in all layers of the diseased arterial wall, and particularly in the plaque itself.[46] No matter which is the source of these free radicals, NAD(P)H oxidases, xanthine oxidase, myeloperoxidase or the mitochondrial oxidative metabolism, the pro-oxidant milieu in the atherosclerotic plaque may account for the appearance of more DNA lesions,[41] which modulate vascular cell life span leading to the onset of cellular senescence.

As commented above, the appearance of non-proliferating VSMCs in the plaque core is related to decreased stability with higher plaque susceptibility to rupture and subsequent thrombotic occlusion of the affected artery.[47] One of the

factors that induces premature senescence in human VSMCs trough a p53/p21^{CIP1}-dependent pathway in vitro as well as pro-inflammatory cytokines production in mouse model of atherosclerosis is angiotensin II.[48]

3.2.4. Oxidative phosphorylation system

In mammalian cells, the mitochondria are partially autonomous organelles with very high dynamics which possess their own genome (mtDNA) with transcriptional and translational machinery.[49] The human mtDNA lacks the protection of the histones and some of the nuclear repair mechanisms which make it vulnerable to damage by the produced also there free radicals.[50] It has been found that mutations in the mtDNA and mitochondrial dysfunctions are associated with increased arterial blood pressure and thus CVD and accumulate with age. In some *in vitro* studies with vascular cells (VSMCs and ECs) an increase in the mtDNA damage, decrease in the levels of mtDNA – encoded mRNA and protein synthesis, membrane potential, and total cellular ATP pools were observed when these cells were subjected to oxidative stress.[51] In 1971 it has been shown that the circular mitochondrial DNA of mammalian cells included a short segment of three strands called displacement loop (D-loop), which is located in the main non-coding control region of the molecule, where the replication of the mitochondrial DNA starts.[52] The region contains promoters for the transcription of genes from the two strands of mitochondrial DNA[53] for genes like ND subunits 1 to 6 and the ATP synthase subunit 6 and 8 genes. In this D-loop putative glucocorticoid (GRE), vitamin D (VDRE), thyroid hormone (TRE), and retinoic acid (RARE) responsive elements have been found to be present.[54]

3.2.4.1. Electron transport chain

In aerobically growing cells, the mitochondria play a very important role in the generation of the bigger part of the cellular energy through the oxidative phosphorylation system (OXPHOS). OXPHOS consists of four respiratory chain complexes (I–IV), two electron carriers (coenzyme Q10 and cytochrome c) and F1F0-ATP synthase, sometimes described as complex V, and the complex I is the largest and most complicated one. Thirteen of the around 80 essential OXPHOS subunits are encoded by maternally inherited mitochondrial DNA and the remainder by nuclear DNA. The first two complexes are where the electrons enter the chain. Complex I (NADH-ubiquinone reductase) accepts the substrate NADH from the citric acid cycle and donates electrons to the chain. Complex II (succinate-ubiquinone reductase) accepts electrons from FADH2 and pass them to Complex III

(ubiquinolcytochrome *c* reductase) via CoQ 10. From Complex III the electrons go to Complex IV (cytochrome *c* oxidase) trough cytochrome C. On acceptance of electron, complex IV then converts H^+ and O_2 to water (Figure 7). If electron flow through the cytochrome pathway is compromised, the alternative oxidase branched at the level of ubiquinone is activated. The transfer of electrons through the complexes generates energy, stored in the form of proton gradient across the inner membrane, the mitochondrial transmembrane potential ($\Delta\Psi m$) which couples the electron transport chain to the oxidative phosphorylation. The energy formed by the protons entry from the inter-membrane space into the matrix of the mitochondria finally is used for ATP synthesis from adenosine diphosphate (ADP) and inorganic phosphate by oxidative phosphorylation, accomplished through complex V.[55]

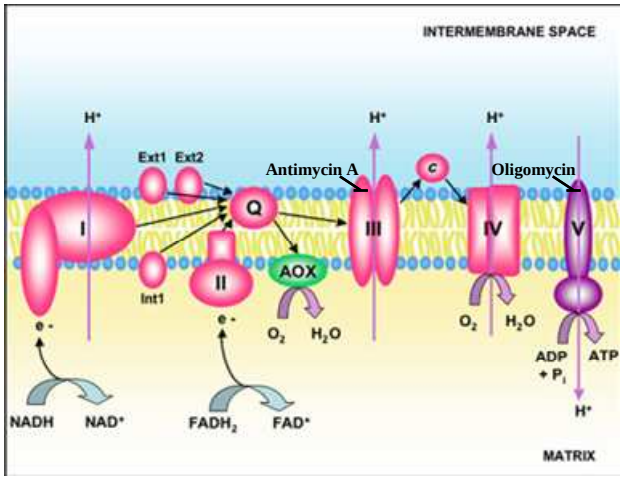

Figure 7. Schematic representation of the respiratory chain. I: Complex I, II: Complex II, III: Complex III, IV: Complex IV, Q: ubiquinone pool, AOX: alternative oxidase, *c*: cytochrome *c*, Ext1 and Ext2: external NAD(P)H dehydrogenase (*modified from Annie SAINSARD-CHANET*). Some respiratory inhibitors are represented: antimycin A as a complex III inhibitor and oligomycin as a complex V inhibitor.

ATP is then released into the cytosol via the adenine nucleotide transporter (ANT) and the voltage-dependent anion channel. Once cytosolic, ATP is converted to ADP during ATP-dependent processes in the cell and re-enters the mitochondrial matrix. Cellular stresses that inhibit ATP production or increase its consumption activate the adenosine monophosphate activated kinase (AMPK). AMPK is a redox sensor of the change in the AMP/ATP ratio and regulator, promoting ATP-producing and inhibiting ATP-consuming pathways in various tissues. AMPK is a heterotrimer composed of alpha-catalytic and beta and gamma-regulatory subunits. The binding of AMP to the gamma subunit of AMPK leads to conformational changes that activate AMPK by phosphorylation at Thr172. AMPK is predominantly involved in the regulation of lipid metabolism, stimulating fatty acids oxidation and inhibits their

synthesis. Moreover, AMPK is also involved in the increasing of the glucose uptake and utilization with potential impact over the energy expenditure. Due to its roles in fuel regulation, the AMPK pathway is regarded as a potential therapeutic target for diabetes type II, obesity and metabolic syndrome. As a note, drugs used in the treatment of insulin resistance and diabetes can activate AMPK.

3.2.4.2. Complex I deficiency

A number of specific mitochondrial disorders have been associated with mitochondrial malformations, which appear in early childhood (e.g. Leigh disease) to severe diseases of adulthood (e.g. Parkinson's disease, Alzheimer's disease,[56] type II Diabetes mellitus[57]). Complex I (CI) is the most common site for mitochondrial abnormalities, representing as much as one third of the respiratory chain deficiencies. CI is a giant multiheteromeric enzyme located in the inner membrane of mitochondria, consisting of a mitochondrial matrix protruding domain, and a membrane-embedded domain. CI contains seven mitochondrial DNA (mtDNA)-encoded NADH-dehydrogenase (ND) subunits (ND subunit 1, 2, 3, 4, 4L, 5 and 6) and at least 38 nuclear-encoded subunits.[58] The big importance of mutations in these genes on neurodevelopment and patient survival is related to critical alterations in cell metabolism, energy homeostasis and reactive oxygen species (ROS) production.[59] Moreover, the very low CI activity has been related to high ROS levels and a fragmented mitochondrial morphology. Recent investigations suggest that CI is a potent source of ROS[60] (superoxide as well as hydrogen peroxide) during both, forward electron transfer (very small amounts of superoxide)[61] and reverse electron transfer (from the reduced ubiquinol pool back to CI to reduce NAD^+ to NADH) with up to 5% of electrons being diverted to superoxide formation.[62] Furthermore, ROS levels were also tightly related to cellular NAD(P)H levels, which is indicative of substrate accumulation due to impaired CI function (Figure 8). Obviously, structural integrity of CI is essential to maintain its functionality. Therefore, changes in one of its "building bricks" may provoke catalytic problems or instability of the complete assembly. The nuclear-encoded NDUFA9 (39kDa) is an accessory subunit of CI and is believed not to be involved in catalysis, but in the stabilization of the multiprotein complex I after the binding of NADPH, and is used as a marker of fully assembled CI.[63,64]

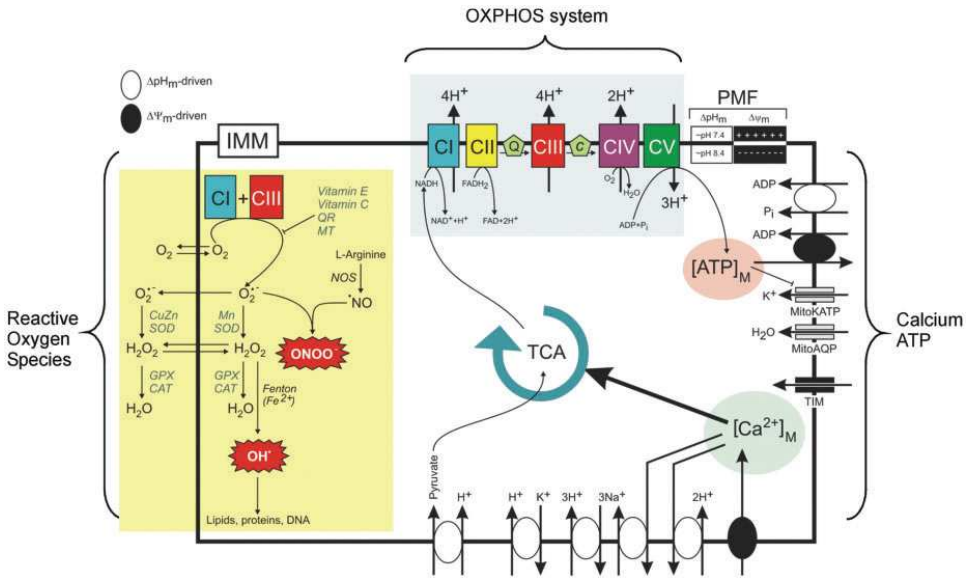

Figure 8. Affected cellular pathways in CI deficiency (*by Distelmaier et al,* 2009 [65]).

The ATP production is a Ca^{2+}-dependant prossess, as the entry of Ca ions from the cellular cytosol stores into the mitochondrial matrix is necessary to occur. It has been shown that in patients with CI-deficiency this process have been disrupted.[65] Furthermore, it has been shown that the ATP content in calcium deficient hearts was significantly decreased which associates the overall deficiency in energy production trough OXPHOS with chronic calcium deficiency secondary to vitamin D deficiency. In the study of Mukherjee et al.[66] the treatment of vitamin D deficient chicks with vitamin D_3, returned the respiration rate to normal levels.

4. RENIN-ANGIOTENSIN SYSTEM

Angiotensin II is the major effector molecule of the renin-angiotensin system (RAS). The main function of RAS is the regulation of the blood pressure, as well as the electrolyte and volume homeostasis, but it is also involved in some pathological conditions like fibrogenesis, hypertrophy, cell growth and senescence.[67] Moreover, Ang II can act as an endocrine hormone or, when synthesized locally in kidney, heart or brain, as an autocrine or paracrine effector. Renin, a protease synthesized in the renal juxtaglomerular cells from the precursor, pro-renin, cleaves liver-derived α-2-globulin angiotensinogen (Agt) in a rate-limiting step to produce

angiotensin I, which is then further converted in the lungs by the dipeptidyl carboxypeptidase angiotensin-converting enzyme (ACE) into Ang II. The main renin secretion stimuli are the blood flow reduction of the glomerular afferent arteriole, sympathetic stimuli and local factors such as vasodilating nitric oxide (NO)[68], prostaglandins[69] and adrenomedullin.[70] Other factors mediating renin expression are renal perfusion pressure, tubular sodium load and vasoconstrictors like vasopressin[71] and the product Ang II itself via a negative feedback loop.[72] Renin expression can be suppressed by endothelin-1 signalling via phospholipase C and the release of intracellular calcium.[73] Ang II is an octapeptide hormone that could be produced not only systemically via the circulating, also termed renal RAS, but also alternatively, by local proteinases, such as cathepsin D, chymase, carboxypeptidase and cathepsin G, which form the alternative pathways for Ang II production that occurs in some extrarenal tissues (Figure 9).[74,75] Cathepsin D, a lysosomal aspartic protease with high homology to renin, converts Agt to Ang I, meanwhile cathepsin G converts the Agt directly to Ang II[76], and chymase and cathepsin A convert Ang I to Ang II. However, although the chymase is also present in atherosclerotic lesions, Ang II co-localises with ACE rather than with chymase, suggesting that Ang II generation in the atherosclerotic vessel depends predominantly on ACE.[77] In addition, Ang I can be transformed to the heptapetide Ang II (1-7) by tissue endopeptidases. Ang II (1-7) is likely to be a naturally occurring antagonist of Ang II. Furthermore, the degradation of Ang II to Ang III and Ang IV is performed by aminopeptidases.[78]

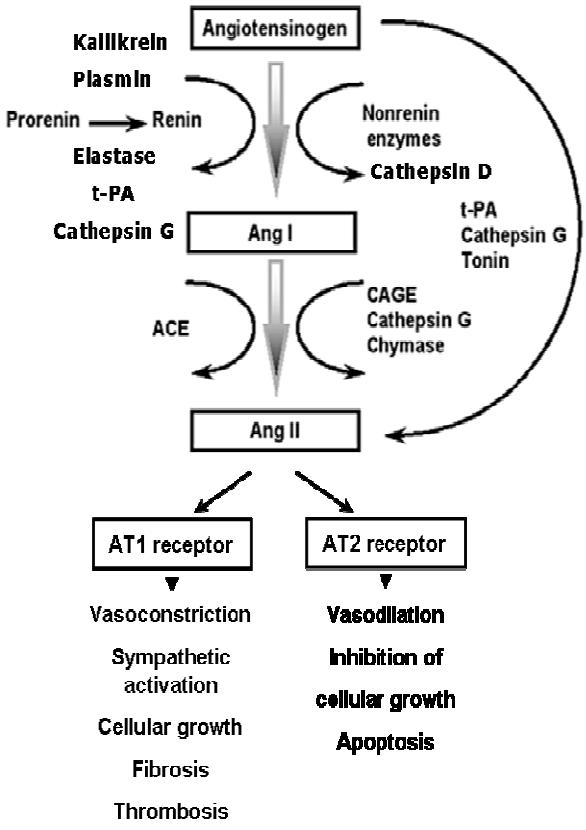

Figure 9. Canonical and alternative pathways for Ang II synthesis and its principle functions, mediated by the activation of the main Ang II receptors, AT1 and AT2 (*modified from Medscape*®).

4.1. Angiotensin II (Ang II) receptors

Ang II exerts its effects mainly through the activation of the G protein-coupled receptors AT1-R and AT2-R, which are localized in the vessels within the adventitia, on VSMCs (AT1-R), and on ECs (AT2-R). In rodents, two subtypes called, AT1a-R and AT1b-R, sharing 94% sequence homology, have been characterised, meanwhile there is only one AT1-R in humans.[79] Most of the vascular effects of Ang II are mediated by AT1-R, a glycoprotein composed of 359 amino acids that activates phospholipase C (PLC) *via* a heterotrimeric Gq protein.[78] In the vessel wall, AT1-Rs are localized mainly in VSMCs and the density of AT1-R increases in the media of diseased vessels compared to healthy animals.[80] The levels of this receptor in the tunica adventitia are low, whereas endothelial cells present even less amounts of AT1-R.[79] The AT2-R is also a seven-transmembrane protein, but its sequence homology with the AT1-R is low, around 32%. It is a 363 amino acid protein expressed at high levels in foetal tissues and decreases rapidly after birth.[81] In

healthy blood vessels, only 10% of the total angiotensin receptors are of the AT2-type.[77] AT2-R seem to be localised predominantly in adventitia and endothelial cells.[82] Until now, it has been considered that the functions of AT2-R antagonize the vasoconstrictor actions of the AT1-R by the inhibition of the proliferative and growth-promoting effects of AT1-R.[79]

In their study, Abdalla et al. have shown that in the co-expression of AT1-R and AT2-R the cellular effects of AT1-R are abrogated after the direct binding of AT2-R to AT1-R, leading to their heterodimerization which induces an AT1-R conformation that can not undergo the conformational change necessary for G-protein activation.[83] In fibroblasts, obtained from failing hearts, the elevated expression of AT2-R has been shown to inhibit the mitogenic stimuli of Ang II.[84] Similar findings are found in the study of Nakajima et al. with cultured smooth muscle cells, where AT2-R transfection reduced proliferation and inhibited mitogen-activated protein kinase activity.[85] Further, Warnecke et al. provide evidence that the impairment of the effect of Ang II in cultured porcine cardiac fibroblasts overexpressing AT2-R is mediated by the inhibition of the phosphotyrosine phosphatase 1B (PTP1B) which doesn't affect the Ang II-induced TGFβ1-mediated collagen type I expression. The inhibition of the PTP1B could result in an increase in the insulin response and sensitivity, thus linking the AT2-R to the insulin signalling.[86]

Thus it has been postulated that the activation of AT2-R has beneficial effects, but some recent data have shown that the AT2-R stimulation may be even harmful, mediating cell growth, fibrosis and hypertrophy, as well as being pro-atherogenic and pro-inflammatory.[87] Furthermore, the AT1a-R deficiency has been associated with increase longevity, due to decreased cardiac, vascular and renal injury as well as less oxidative stress. Thus, the AT1-R blockage by antagonists (Losartan) could improve the life expectancy.[88]

4.2. Role of Ang II in the development of cardiovascular disease

Atherosclerosis is now considered to be a chronic inflammatory disease, initiated by accumulation of lipid-laden macrophages and endothelial dysfunction.[89] In the vascular wall, the pro-inflammatory effects of Ang II have been shown, which includes the production of reactive oxygen species and inflammatory cytokines.[90]

Table 1. Direct vascular effects of angiotensin II (*modified from Dzau et al., 2001* [67])

Effect	Manifestation
Vasoconstriction	Stimulates Ang II type 1 receptor Releases endothelin and norepinephrin. Reduces NO bioactivity and produces peroxynitrit Activates NADH/NADPH oxidase and produces superoxide anion.
Inflammation	Induces expression of MCP-1, VCAM, TNF-a, IL-6 Activates monocytes/macrophages
Remodeling	Stimulates smooth muscle migration, hypertrophy, and replication Induces PDGF, bFGF, IGF-1, TGF-b expression Stimulates production of matrix glycoproteins and metalloproteinases
Thrombosis	Stimulates PAI-1 synthesis and alters tPA/PAI-1 ratio Activates platelets with increased aggregation and adhesion

Ang II actions in VSMCs extend far beyond vasoconstriction (Table 1). The stimulation of phospholipase D by Ang II in VSMCs has been involved in the activation of NADPH oxidase,[91] ERK,[92] AKT,[93] and cell growth[94]. Furthermore, Ushio-Fukai et al. have shown that the phosphoinositol-3 kinase (PI3K) and the serine/threonine protein kinase AKT pathway are essential for Ang II–induced VSMC hypertrophy.[95] Moreover, Ang II is critically involved in generation of ROS in the vessel wall. The most important source of ROS in the vessel is NAD(P)H oxidase, xanthine oxidase, lipoxygenases, cytochrom P450 monooxigenases and myeloperoxidase.[96,97] The Ang II-induced enhanced ROS production leads to endothelial dysfunction and oxidation of the low density lipoprotein (LDL), rich in the so called bad cholesterol. The oxidised LDL (oxiLDL) chemoattract monocytes and T-lymphocytes, thus being involved in the inflammation of the vessel. The subsequent ingestion of oxLDL by tissue macrophages result in the formation of foam cells, a major constituent of atherosclerotic plaques.[77]

4.3. Mitogen activated protein kinases

Ang II stimulation of the AT1-R in VSMCs leads to the activation of the mitogen activated protein kinases (MAPK). MAPK are ubiquitously expressed serine/threonine kinases involved in the control a variety of physiological processes, including cell growth, differentiation and apoptosis. For activation, these kinases need dual phosphorylation on threonine and tyrosine. Inactivation occurs by the action of specific MAPK phosphatases. In this way, the balance between

phosphorylation and dephosphorylation regulates MAPK activity, allowing the cell to rapidly adjust to environmental changes.[98] There are three well characterised subfamilies of MAPK:

- Extracellular-signal regulated kinases Erk 1 and Erk 2. Erk 1/2 is essentially involved in proliferation after stimulation with mitogenic agents.

- c-Jun N-terminal kinases (JNK) 1, 2 and 3. JNKs are stress-activated protein kinases that activate the transcription factor c-Jun, a component of the AP-1 transcription factor.
- Four p38 isoenzymes termed p38α, β, γ and δ. p38 is activated by a similar range of stimuli than JNK, and seems to overlap with JNK in some but not all functions.

In VSMC, Ang II leads to a rapid activation of all three MAPK subfamilies.[99]

5. ANTIOXIDANT DEFENCES OF VSMC

5.1. Nitric oxide (NO) synthase and NO in the vasculature

Nitric oxide is a molecule, synthesized from the amino acid L-arginine under the catalytic activity of the enzyme nitric oxide synthase (NOS). In the vascular wall the three isoforms are present, the endothelial (eNOS), inducible (iNOS) and the neuronal (nNOS). In VSMCs the main form is the iNOS. The NO has vasodilator effects, permitting the adaptation of the arteries to blood flow changes. Moreover, NO protects the vessels from endogenous injury, preventing leucocyte and platelet adhesion and inhibiting VSMC proliferation.[100,101] It has been shown that the endothelial dysfunction causes decrease in the NO production with subsequent structural and functional changes in the vasculature, due to the decrease in the vasodilator tone control, even in the absence of vasoconstriction, and is translated to the appearance of arterial hypertension, seen in CKD and chronic heart failure (CHF).[102] One of the early processes participating in the development of endothelial dysfunction in CVD is the oxidative stress. The free radicals such as superoxide anion react with NO forming peroxynitrites, thus reducing the NO bioavailability, leading to vasoconstriction (Figure 10).[103] Moreover, NO is produced also in mitochondria and is an important modulator of superoxide production.[104] At physiological concentrations, NO modulates mitochondrial oxygen consumption by inhibiting cytochrome *c* oxidase in a reversible process. It has been demonstrated

that ROS produced initially in mitochondria or in the cytoplasm by enzymes such as NAD(P)H oxidase act in a positive feedback, leading to more ROS production from mitochondria in a process termed "ROS-induced ROS release".

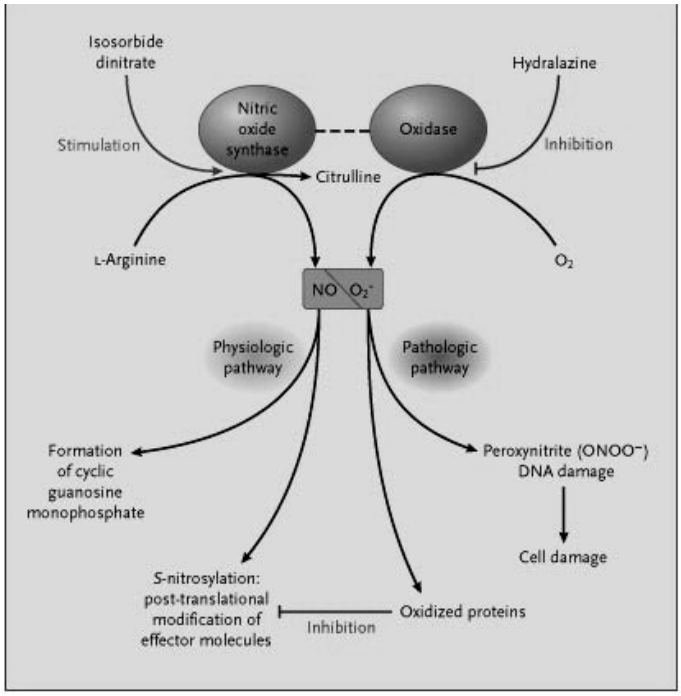

Figure 10. Role of the nitroso-redox balance in cardiovascular system (*Modified from Hare JM., 2004* [103])

Normally during some metabolic reactions and throughout the electron transport chain in the mitochondria minimal amounts of ROS are produced, but on pathological conditions like inflammation, CKD and CHF, the activation of NADPH oxidase increases the quantity of ROS.[105] The pro-inflammatory cytokines induces the expression of iNOS during the inflammatory response, and the increased NO concentrations could cause hypetension.

5.2. Superoxide dismutase

The mitochondrial respiratory chain reduces oxygen to water during the aerobic metabolism. However, the leakage of reactive species such as superoxide anion (O^-_2) from the respiratory chain is an important threat, inducing mitochondrial damage. The mitochondria are protected from oxidative stress from one hand by low oxygen levels and by other, trough complex defense systems against ROS. The TRX system (TRX, TRX reductase, and NADPH) is thiol antioxidant system of the cardiovascular system that regulates the reduction of intracellular

ROS.[106] It has been demonstrated that the upregulation of thioredoxin-interacting protein (Txnip) and subsequent impairment of thioredoxin antioxidative system through p38MAPK and FOXO1 may participate in the intracellular ROS increase.[107] VSMCs produce several superoxide scavenger enzymes, superoxide dismutase (SOD) which constitutes a family of antioxidant enzymes that catalyze the conversion of superoxide to hydrogen peroxide (H_2O_2), which is further converted to water by the mitochondrial glutathione peroxidase, using reduced glutathione (GSH) as the hydrogen donor, or to water and oxygen by catalase, which is present only in the mitochondria from the heart. The copper- and zinc-containing SOD (SOD1) is located principally in the cytoplasm, nucleus, and a small fraction located in the intermembrane space of mitochondria forming until 80% of the SOD in the blood vessel. The manganese-containing SOD (SOD2) that is located in the mitochondrial matrix to capture superoxide released during respiration is presented in fewer quantities in VSMC and abundantly in endothelial cells. The SOD3 has extracellular localization and is predominantly produced by VSMC.[108] The SOD1- and SOD-2 partial deficiency in VSMCs, together with the H_2O_2 provokes an activation of ERK1/2, p38MAPK,[109] meanwhile the mitochondrial-dependently H_2O_2 activates in a mitochondria-dependant way the JNK and the AKT[110] (Figure 11). Moreover, mitochondrial dysfunction that appears as a result from SOD2 deficiency is considered an early event in the initiation of atherosclerosis.

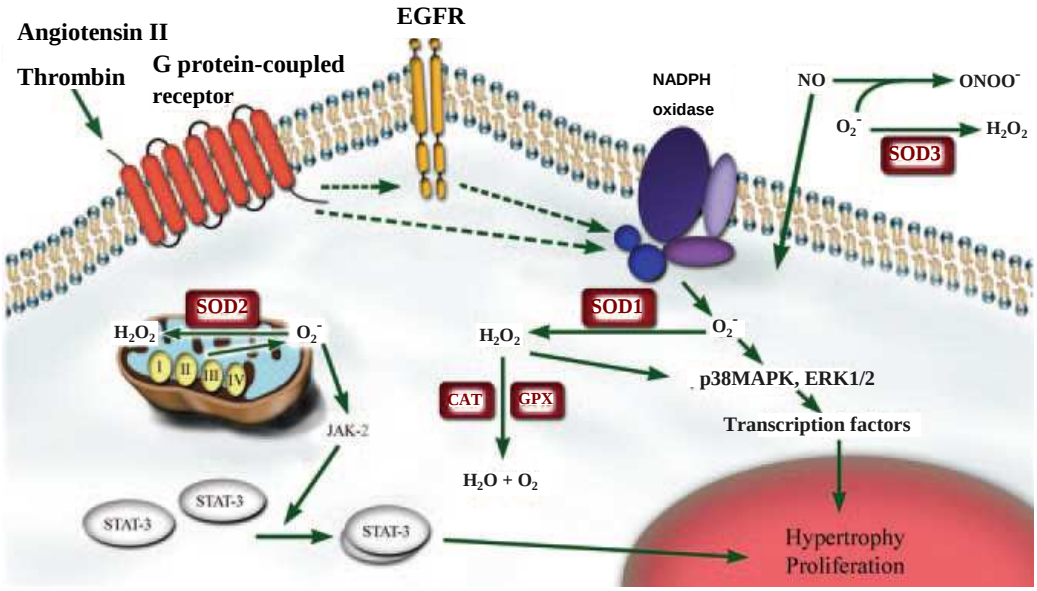

Figure 11. Schematic representation of the anti-oxidant enzymes in VSMC (*modified from Mendez et al., 2005* [108]). EGFR, epidermal growth factor receptor; SOD, superoxide dismutase; CAT, catalase; GPX, glutathione peroxidise.

6. VITAMIN D

In the recent decades a number of basic and clinical studies point to the important role that vitamin D plays in various physiological and pathological processes throughout the body and the beneficial role of its active form is believed to be due to the anti-proliferative (cancer), anti-inflammatory, anti-oxidant, anti-fibrotic and anti-thrombotic actions of vitamin D.

6.1. Vitamin D metabolism

Vitamin D has been discovered in the cod liver oil, used occasionally for the treatment of rickets in the late 18th century. McCollum and his collaborators in 1789 concluded that the anti-rachitic substance in this oil was different than vitamin A and that this new substance possesses specific properties to regulate the metabolism of bone. In the sequence of discovered vitamins, this was the fourth one, so they called it vitamin D, but later it has been shown that vitamin D is a fat soluble pre-hormone with seco-steroid nature. Vitamin D shows structural characteristics that make it conformationally flexible, because one of the rings of its cyclopentanoperhydrophenanthrene ring structure is cleaved (C_9–C_{10} bond of ring B). Therefore, it possesses the possibility of facile rotation about its C_6-C_7 single carbon bond which lead to the generation of potential ligand shapes (6-s-*cis* or 6-s-*trans* analogs).[111] Vitamin D in humans is delivered from the diet (vegetal ergocalciferol, or vitamin D_2 and animal cholecalciferol, or vitamin D_3). Vitamin D enters the plasma as a chylomicron/liproprotein complex after intestinal absorption.[112] However, the main source of vitamin D is the endogenously synthesized from the precursor molecule 7-dehydrocholesterol in the skin by the photolytic action of the solar UVB light. Once pre-vitamin D_3 is formed, it undergoes a spontaneous temperature-dependent isomerisation to vitamin D_3, which is then transported into the circulation, bound to the vitamin D binding protein (DBP). At this metabolic stage, vitamin D does not have biological activity. DBP drives vitamin D_3 subsequently to the liver and then to the kidney for bioactivation as well as carries away inactive metabolites for catabolism and excretion (Figure 12).

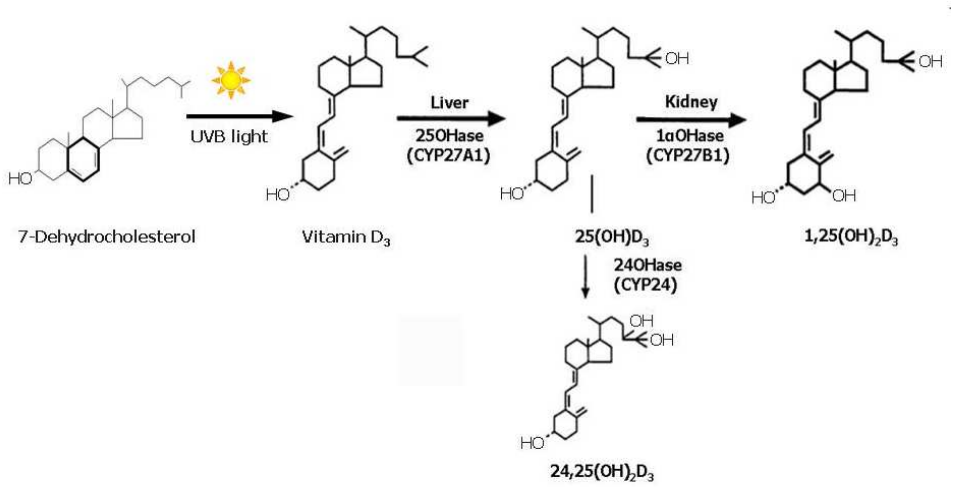

Figure 12. Basic metabolism of vitamin D from the precursor molecule 7-dehydrocholesterol to the biologically most active form, $1,25(OH)_2D_3$. The structure of the catabolic product $24,25(OH)_2D_3$ is also shown.

In the first activation step, vitamin D_3 is hydroxylated by the cytochrome P450 enzyme 25-hydroxylase (CYP27A1) to 25-hydroxyvitamin D_3 ($25(OH)D_3$) mainly in the liver, but also in the kidney, intestine, brain, lung, skin, prostate gland, blood vessels and macrophages.[113] This enzyme 25-hydroxylates both vitamin D_2 and D_3. This first hydroxylation is poorly regulated, that's why the level of $25(OH)D_3$ in serum increases in proportion to vitamin D_3 intake. $25(OH)D_3$ has a long half-life and being the most abundant form, its levels are used as a marker for the vitamin D status. Vitamin D deficiency is considered when $25(OH)D_3$ levels are below 15 ng/ml, being normal levels between 30 and 100 ng/ml. Serum levels of $25(OH)D_3$ are low in many people of all ages who live at northern latitudes and lower altitude, especially in the winter.[114]

In the second step, the biologically active hormone 1,25-dihydroxyvitamin D_3 ($1,25(OH)_2D_3$) is generated by the mitochondrial enzyme 1aOHase. 1aOHase is a monooxygenase attached to the inner mitochondrial membrane, with a molecular mass of approximately 52 kDa. In order to exert its actions, this enzyme requires molecular oxygen and NADPH-reducing equivalents from a group of iron-sulfur proteins called ferredoxins. The affinity of 1aOHase for $25(OH)D_3$ differs between species and tissues with Km values ranging from 1 to 16 μM.[115] The hydroxylation at carbon 1 in the vitamin D molecule occurs mainly in the kidney. Thus, expression of this enzyme is found in both the proximal (endocrine function) and distal convoluted tubules (autocrine/paracrine function), but also in numerous other tissues (lung, brain, liver, intestine, bone, stomach, spleen, colon, thymus, lymph

nodes, skin, placenta, monocytes, dendritic cells, vascular smooth muscle cells, endothelial cells, etc).[116, 117] However, in humans, these extrarenal sources of $1,25(OH)_2D_3$ only contribute significantly to circulating $1,25(OH)_2D_3$ levels during pregnancy, in chronic renal failure (CRF), and in pathological conditions such as tuberculosis, granulomatous disorders, and rheumatoid arthritis. Nevertheless, local production of $1,25(OH)_2D_3$ could be important as a autocrine or paracrine regulator of certain cell functions.

Circulating levels of $1,25(OH)_2D_3$ are tightly regulated. However, low levels can be found in several conditions like CRF and pseudo–vitamin D–deficiency rickets (PDDR). However, the pathophysiology of PDDR is different because in CRF, the compromised renal mass reduces 1aOHase activity, whereas in PDDR there is a hereditary defect in the gene that code for the 1aOHase. Some of the factors that influence the expression of the enzyme are parathyroid hormone (PTH), calcitonin, interferon gamma, calcium, phosphorus, and the active form of vitamin D by itself. $1,25(OH)_2D_3$ represses directly 1aOHase expression by a feedback loop as well as by suppressing the synthesis and secretion of PTH, which is the primary tropic hormone that stimulates the 1aOHase expression.[118,115]

Under conditions of adequate plasma Ca^{2+} levels, the 24-hydroxylation of both $25\text{-}(OH)D_3$ and $1,25\text{-}(OH)_2D_3$ occurs under the enzymatic activity of 24-hydroxylase (24OHase). The CYP24 is a mitochondrial enzyme (~53 kDa) that is found mainly in kidney, but also in intestine, skin, bone, placenta, and macrophages.[119] The expression of this catabolic enzyme is very tightly regulated at transcriptional level by the active form of vitamin D in almost all tissues where VDR expression could be found, thus making possible the negative feedback mechanism.[120] The concentration of $25(OH)_2D_3$ that gives half-maximal activity (Km) for the 24-hydroxylation range from 0.5 to 3 μM, but the preferred substrate for 24OHase is $1,25(OH)_2D_3$, even though its Km values are approximately 10-fold lower (0.1–0.25μM), making the enzyme very important in control of the ambient $1,25(OH)_2D_3$ levels. The $24,25(OH)_2D_3$ is the major circulating dihydroxy metabolite and is believed to have some biological activity in the intramembranous bone formation and the early stages of the fracture repair.[119] It is known that $1,25(OH)_2D_3$ can be rapidly metabolized either to $1,24,25(OH)_3D_3$ and then to calcitroic acid or to the $25(OH)D_3$-lactone. The first pathway consists of five sequential steps – C24 hydroxylation, C24 ketonization (C24-oxo) and C23 hydroxylation (C23-OH/C24-oxo), followed by an oxidative reaction in which 24,25,26,27-tetranor-1-alpha,$23(OH)_2D_3$ is formed and finally the calcitroic acid, a water-soluble metabolite, which is filtered in the kidney and excreted in the urine. The other

pathway involves C26 hydroxylation, C23 hydroxylation and lactonization to form (23S,25R)-1,25$(OH)_2D_3$-26,23-lactone.[121] Similar C23/C24 oxidation pathways exist for 24,25$(OH)_2D_3$.

6.2. Vitamin D receptor

There are two known proteins with structurally different ligand binding domains that could specifically bind the biologically most active form of vitamin D: vitamin D receptor (VDR) (Kd =1.2 nM) and DBP (Kd = 60 nM).[122]

VDR is a member of the superfamily of nuclear trans-acting hormone receptors that regulate gene expression in a ligand-dependent manner. VDR has nearly ubiquitous tissue distribution (kidney, bone, paratiroid gland, intestine, lymphocytes, macrophages, tumour cells, etc). Biochemical and in situ immunocytochemical localization studies have shown that VDR is predominantly a nuclear protein, even in the unoccupied state.[123] Unliganded VDR in the nucleus is likely bound to a corepressor related to the so called silencing mediator for retinoid and thyroid hormone receptors (SMRT). VDR–SMRT complex is linked to histone deacetylase that maintains chromatin in a repressed state, thus repressing the transcription of target genes.[124] Other studies reported that VDR mainly resided in the cytoplasm in the absence of VDR ligands and the binding of 1,25$(OH)_2D_3$ or some of its analogues, makes the VDR move from the cytoplasm into the nucleus.[125] Some authors believe that the initiation of the rapid cellular responses to vitamin D occurs through a putative plasma membrane-associated receptor (mVDR). Candidates for the mVDR have been suggested, including annexin II,[126] the MARRS binding protein[127] and the classical VDR or a slightly truncated form of VDR, associated with caveolae.[122] It has been proposed that the conformation of the ligand (6-s-*cis* versus 6-s-*trans*) mediates to certain extend the type of response, either rapid or genomic, as 6-s-*cis* configuration of the ligand favors activation of the nongenomic pathway, whereas the 6-s-*trans* mediates preferentially genomic responses.[111] However, numerous studies have confirmed that the presence of functional VDR is necessary for both the genomic and the nongenomic rapid responses to the active vitamin D_3 metabolite.[128]

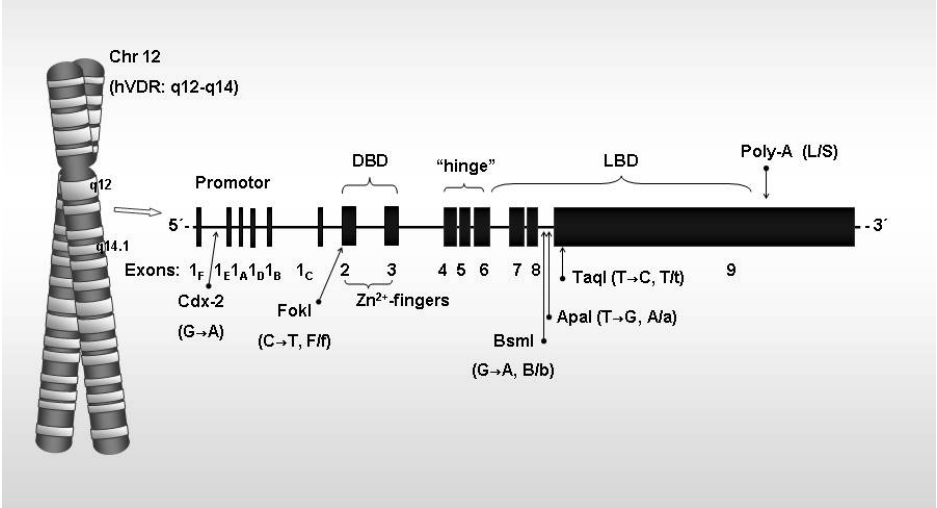

Figure 13. Schematic representation of the chromosomal localization and the domain organization of the human VDR gene: DNA Binding Domain (DBD), "hinge" and Ligand Binding Domain (LBD), together with the positions of the five frequently studied single nucleotide polymorphism (SNP) sites.

The human VDR is a product of a single chromosomal gene which locates on chromosome 12. The gene is comprised of at least 14 exons and span approximately 75 kb [129] (Figure 13). Six exons (1A to 1F) occupy the 5´-noncoding region, and eight additional exons (exons 2–9) encode the structural component of the VDR. In kidney, at least three VDR mRNA transcripts are produced, possibly by differential splicing of 5´- noncoding exons. Most of the variant transcripts produce the same classical VDR protein of 427 amino acids with a molecular mass of ~ 48kDa. VDR expression is regulated at both transcriptional and posttranslational levels. Single-nucleotide polymorphisms (SNP) in the VDR locus can be used to predict the susceptibility to suffer several disorders like osteoporosis, cardiovascular diseases and different types of cancer.[130] The most frequently studied polymorphisms in the VDR gene are the restriction fragment length polymorphisms (RFLP) for *BsmI*, *ApaI* and *TaqI*, found in intron 8/exon 9 at the 3´- end of the gene, together with the *FokI* polymorphism in exon 2 and the *Cdx2* polymorphism in the promoter region of the gene [131](Figure 13).

As a nuclear receptor, VDR has several functional domains. In the amino terminal there is the A/B domain 20 (AA long). The DNA-binding domain (DBD, C domain), locates between amino acids 21 and 92. As other nuclear receptors, all VDRs described to date possess a conserved DNA binding domain consisting of two zinc finger motifs (residues 24–90 in hVDR), an α-helix resides on the C-terminal side of each zinc finger, with helix A and helix B constituting the DNA-recognition

and phosphate backbone binding helices, respectively. One unique feature in the DNA binding domain of VDR is the presence of a cluster of five basic amino acids in the intervening sequence between the two zinc fingers (residues 49–55). Another interesting finding is that the DBD possesses a site (ser-51) for hVDR phosphorylation by protein kinase C. This posttranslational modification makes the receptor unable to bind DNA. The flexible linker region locates approximately between amino acids 93 and 123, followed by the E- or ligand binding domain (LBD) between amino acids 124 and 427. The C-terminal LBD is a globular multifunctional domain. It is responsible for hormone binding, strong receptor dimerization and interaction with co-repressors and co-activators, which are critical for the regulation of transcriptional activities. The LBD is formed by 12 α-helical structures. The twelve helix contain a transactivation function 2 (AF-2) domain which suffers conformational change upon ligand binding and the orientation of the helix 12 determine the state of the receptor – silent or activated.[132]

The ligand-bound VDR controls gene expression heterodimerizing with retinoid X receptor (RXR) and associating with specific genomic sequences in the promoter region of its target genes, known as vitamin D responsive elements (VDRE). However, some studies suggest that VDR represses some genes using a different than RXR co-partner [133]. Several VDRE have been described in a variety of genes (Table 2).

Table 2. List of some of the vitamin D responsive genes in normal and malignant cells. The genes with described vitamin D response element (VDRE) are shown like positively (+) or negatively (-) regulated genes, and the ones which transcription vitamin D regulates by antagonizing other transcription factors are presented as TFA genes.

Gene	Species	Type of VDRE		Reference
CYP24	Human	DR3	(++)	[134]
Atrial natriuretic factor	Rat	DR3	(+)	[135]
Osteopontin	Mouse	DR3	(+)	[136]
Carbonic anhydrase II	Chicken	DR3	(+)	[137]
NPT2	Human	DR3	(+)	[138]
Osteocalcin	Rat	DR3	(+)	[139]
$p21^{Cip1}$	Human	DR3	(+)	[140]
Cyclin C	Human	DR3	(+)	[141]
Integrin β_3	Chicken	DR3	(+)	[142]
5-Lipoxygenase	Human	DR3	(+)	[143]
VEGF	Rat	DR3	(+)	[144]
PPARβ/δ	Human	DR3	(+)	[145]
IGFBP-3	Human	DR3	(+)	[146]
IGFBP-5	Human	DR3	(+)	[147]
$TGF\beta_2$	Human	DR3	(+)	[148]
PTH	Human	DR3	(-)	[149]
PTHrP	Rat	DR3	(-)	[150]
Growth hormone	Human	DR3	(-)	[151]
RelB	Human	DR3	(-)	[152]

Type αI collagen	Rat	DR3	(-)	[153]
hTERT	Human	DR3	(-)	[154]
Calbindin D28k	Mouse	DR4	(+)	[155]
MYC	Human	DR4	(-)	[156]
Phospholipase C-γ1	Human	DR6	(+)	[157]
Fibronectin	Mouse	DR6	(+)	[158]
Calbindin D9k	Mouse	IP9	(+)	[159]
c-fos	Mouse	IP9	(+)	[160]
CYP3A4	Human	ER6	(+)	[161]
1α-hydroxylase	Human	VDIR	(-)	[162]
Renin	Mouse	TFA		[163]
IL-2	Human	TFA		[164]
IL-12	Human	TRA		[165]
GM-CSF	Human	TFA		[166]

The typical responsive element has two hexameric half-sites with consensus sequence of RGKTCA (R=A or G, K=G or T). An example of a response element, formed by direct repeat (DR) of two hexameric core binding motifs spaced by three nucleotides (DR3-type) is the one found in the proximal promoter of the human 24-hydroxilase (CYP24). Moreover, VDRE with direct repeats spaced by four nucleotides (DR4-type) and six nucleotides (DR6-type) have been described.[167] Another important type of VDRE, the IP9-type, has an inverted palindromic structure with nine intervening nucleotides.[168] Another type of noncanonical VDRE are the everted repeat of hexanucleotide motif with a spacer of 6 bp (ER6 motif), described in the promoter region of human Cyp3A4 gene,[161] coding for one of the most important enzymes involved in the metabolism of xenobiotics in the body.

It has been shown that VDR binds to the 3´- half-site of the VDRE, while its heteropartner RXR interacts with the 5´- half-site.[169] Haussler et al. proposed that in order to influence the gene expression of the targets genes VDR could reside on both, the 3´- and the 5´- half-elements of the VDRE. Moreover, in the positive VDRE VDR is situated on the 3´- half-element, meanwhile in the negative VDRE, VDR may have a reverse orientation, residing on the 5´- half-element.[118]

Vitamin D can influence the expression of its responsive genes in two main ways – directly interacting with positive or negative VDRE in the promoter region and indirectly, antagonizing the action of some transcription factors.

Ligand binding induces conformational change in the VDR which initiates a series of events that promotes the tight association of the receptor to its responsive element, enhances receptor dimerization and generates new surfaces on the receptor that allows the binding of co-activator molecules, which are essential factors in the gene activation cascade.[170] However, some authors report that ligand binding occurs in the cytoplasm, induces VDR-RXR heterodimerization and then translocation of the complex into the nucleus where a recruitment of various co-

regulatory molecules occurs with a final binding to VDRE.[171] Co-activators mediate induction of transcription, whereas the members of the family of co-repressors bind to the nonliganded nuclear receptors thus suppressing the expression of the target genes. The releasing of nucleosomal repression occurs trough the replacement of the repressor by the co-activator complex, thus leading to the initiation of gene transcription.[172]

The presence of co-repressors mediates the silencing of the receptor (non-agonistic conformation) in which histone deacetylases are recruited which deacetylate the lysine residues present in the N-terminally located histone tails, resulting in chromatin compaction and silencing of genes. The $1,25(OH)_2D_3$ binding to VDR provokes conformational changes in the helix 12 of the LBD making it to be closed, which characterize the activation state (agonistic conformation). In this state the receptor promotes the dissociation of co-repressor molecules like the nuclear receptor corepressor (N-CoR) and Alien and the subsequent interaction of coactivators like the members of the p160 family (steroid receptor co-activator, SRC). The subsequent recruitment of VDR-SRC or a VDR-histone acetyltransferase activity complex to a responsive promoter facilitates the destabilization of the nucleosomal core. These co-activator complexes probably act in a two-step process. Firstly, co-activator complex with histone acetyltransferase activity (CBP/p160) modifies chromatin and is then replaced by another co-activator complex (DRIP/TRAP) that lacks this enzyme activity but interacts with RNA polymerase II. The unwound DNA then becomes a target for the VDR-DRIP (VDR-interacting proteins) complex, which contains mediator factors that are required for interaction with basal transcription factors and polymerase II.[171,173] These protein complexes act as a direct link between the ligand activated receptor and RNA polymerase II holoenzyme complex and possibly recruit limiting components into the preinitiation complex.

In the 24OHase gene two VDRE are reported. In the absence of $1,25(OH)_2D_3$, the heterodimer VDR/RXR binds to one or both VDRE to recruit a co-repressor. Upon ligand binding to VDR, the co-repressor is replaced by a co-activator. When elevated levels of $1,25(OH)_2D_3$ are present, both VDREs are used synergistically in order to induce high levels of 24OHase which in turn leads to efficient inactivation of the hormone. There are some factors like the PKC, that could inhibit or enhance the $1,25(OH)_2D_3$ induction of 24OHase promoter activity.[115]

In the promoter of PTH and PTH-related peptide (PTHrP) genes, VDR binds to a negative VDRE (nVDRE). This kind of VDRE is shown to be structurally different due to the fact that it contains a homologous sequence to only one of the two

hexameric DNA sequences that form the VDRE for positive gene regulation by vitamin D [174]. In the case of the rat PTHrP two VDRE were reported by Falzon et al. to be responsible for the negative modulation of this gene.[175]

A negative VDRE was found also in the 1aOHase (CYP27B1) gene promoter. However, a direct binding of VDR/RXR to this VDRE was not detected. In their study, Murayama et al. have shown that vitamin D suppresses the transcription of 1aOHase via interaction with the bHLH-type transcription factor called VDR interacting repressor (VDIR). VDIR was found to be a direct sequence-specific activator of negative VDRE. The interaction between liganded VDR and VDIR induces p300 dissociation and association of histone deacetylase and corepressors to directly mediate transcriptional repression.[162]

One example for indirect regulation of gene expression is the negative action of vitamin D over the renin gene expression. Liganded VDR inhibits nuclear cAMP response element-binding (CREB) binding to the cAMP response elements (CRE) located in enhancer of the renin gene by directly interacting with CREB in ligand-binding domain, thus blocking the formation of CRE-CREB-CBP complex leading to reduction in renin gene expression.[163] Another example could be the suppression of the IL-2 expression after the inhibition of the formation of lymphoid cell-specific transcription factor NFAT-1/AP-1 transcriptional complex in the IL-2 gene promoter by the ligand-VDR-RXR binding.[164] In a similar way, after the binding of $1,25(OH)_2D_3$, VDR represses the activated transcription of the granulocyte-macrophage colony-stimulating factor gene.

It has been shown that the transcriptional activity of VDR can be modulated in a positive and negative way in response to phosphorylation. The dihydroxy metabolite of vitamin D has an essential role in this process activating different signalling pathways, including several kinases. For example, $1,25(OH)_2D_3$ provokes the translocation of the protein kinase C (PKC-β) to the nucleus and enhance its activity [176]. Furthermore, Hsieh at al. have shown that PKC-β plays a role in the control of VDR – mediated transcription, phosphorylating the hVDR in the region between the two zinc finger DNA-binding motifs (Ser-51).[177] VDR is also a target of casein kinase II (CK-II), but in this case the phosphorylation of VDR is $1,25(OH)_2D_3$ – independent.[178] The phosphorylation at Ser-208 by CK-II leads to an increase in the transcriptional activation capacity of hVDR.[179] The phosphorylation in the region between the DBD and the LBD (at serine-182) in the hVDR has been shown to be achieved by protein kinase A and that this post-translation modification leads to an attenuation of both RXR heterodimerization and transactivation of $1,25(OH)_2D_3$ target genes.[180]

It has been shown that there are many other factors in addition to VDR that are important for the regulation of the hormone responsiveness. Among them we can find the DBP and some "acceptor" proteins that promote internalization of steroid hormones, such as megalin (multiligand endocytosis receptor) and cubulin (endocytic glycoprotein receptor), both colocalized in the brush border of the renal proximal tubule epithelium.[181] Even if assembled for maximal transcriptional effectiveness, the transactivating complex must be able to interact with a specific promoter element in order to achieve its transcriptional potential. It has been shown the existence of a group of cis-acting proteins that compete with VDR-RXR for binding to VDRE, called VDRE-binding protein (VDRE-BP). These BP have high capacity and relatively high affinity (2–20 nM) for 25-hydroxylated vitamin D metabolites and the VDRE-BP2 is capable to squelch to a higher extend vitamin D-mediated transactivation. It has been shown that in the absence of liganded VDR, the VDRE-BP normally occupies VDRE and then the liganded VDR should compete with VDRE-BP for binding to the proximal promoter of target genes.

Moreover, there is a group of hsp-70-related intracellular transporters for vitamin D, called "co-integrator" chaperone proteins that direct the intracellular trafficking of vitamin D metabolites by one hand to the mitochondria for their bioactivation and by other hand, directly to VDR. Thus more ligand for VDR is available, that could activate the receptor for heterodimerization with RXR, and thus formed complex be able to compete more efficient with the so called VDRE-binding proteins.[182]

6.3. Physiological functions of vitamin D

The metabolically active form of vitamin D, $1,25(OH)_2D_3$ regulates several functions in the body. Classically, the main role of $1,25(OH)_2D_3$ is to regulate the calcium and phosphorus concentrations in serum via actions in bone, parathyroid gland, kidney and intestine. $1,25(OH)_2D_3$ is able to elevate serum calcium and phosphorus levels. In addition, $1,25(OH)_2D_3$ is able to generate several other biological responses (nonclassical actions of vitamin D) that are not related to the control of mineral homeostasis.

6.3.1. Control of mineral homeostasis

Ambient calcium is highly regulated in order to support its roles in bone mineralization and cellular processes that include neuromuscular activity, intracellular signal transduction, and blood coagulation. The principal function of $1,25(OH)_2D_3$, together with the parathyroid hormone (PTH) and FGF23 is to control

the calcium and phosphorus status in order to ensure the availability of these minerals for biological functions as well as skeletal mineralization. This is achieved by coordinated actions of the parathyroid gland, kidney, intestine and bone. The most critical role of $1,25(OH)_2D_3$ in mineral homeostasis is to enhance the efficiency of the small intestine to absorb dietary calcium and phosphorus, together with the bone calcium and phosphorus resorption, and renal calcium and phosphate reabsorption, thus increasing the blood Ca•PO4 ion product. Calcium absorption occurs by both vitamin D–dependent active process in the ileum and passive diffusion process that can be positively affected by vitamin D. The active calcium absorption pass trough three primary components - epithelial calcium channels, intracellular calbindins and ATP-activated basolateral membrane calcium pump. It has been already shown that $1,25(OH)_2D_3$ positively regulates the synthesis of all of these three components.[183] Thus, $1,25(OH)_2D_3$ increases the entry of calcium through the plasma membrane into the enterocytes and enhances the movement of calcium through the cytoplasm and across the basolateral membrane into the circulation. Furthermore, $1,25(OH)_2D_3$ is capable of reducing the excretion of calcium in urine by increasing the reabsorption of calcium in the kidneys. Moreover, $1,25(OH)_2D_3$ is able to increase the mobilization of calcium from bone into the circulation through the enhancement of osteoclastogenesis and osteoclastic activity.

In relation to the ability of vitamin D to control the levels of phosphorus, one possible mechanism is the induction of phosphate translocating proteins in kidney (renal sodium-phosphate cotransporter-2, NPT2) and probably in the small intestine. It has been shown that in hypophosphatemic conditions a stimulation of 1aOHase occurs in order to produce adequate levels of the active form of vitamin D. On the one hand, $1,25(OH)_2D_3$ suppresses the PTH levels and by other hand induces both, the PEX (phosphate-regulating gene with homologies to endopeptidases located on the X-chromosome) and the NPT2 genes. NPT2 has a direct effect over the phosphate reabsorbtion and the PEX enzyme is able to destroy the phosphatonin (a novel phosphaturic humoral factor).[118] Indeed, $1,25(OH)_2D_3$ has an essential role in bone development, mineralization and in the maintenance of the dynamic nature of the bone by controlling the availability of calcium and phosphorus and regulating the level of PTH, PTH related protein (PTHrP) and insulin-like growth factor (IGF). Increased levels of $1,25(OH)_2D_3$ and calcium in a coordinated manner suppress PTH synthesis and secretion, being thus a negative feedback mechanism for the development of hypercalcemia.

In addition, it is also involved in the synthesis of bone matrix proteins such as type I collagen, alkaline phosphatases, osteocalcin, osteopontin and matrix-Gla protein.[184]

6.3.2. Nonclasical functions of vitamin D

Recently, it has been shown that vitamin D exerts pleiotropic effects in a variety of target cells, controlling the VSMC proliferation and calcification,[185,186,187] regulating RAS[188] and, in general, participate in cardiovascular health.[189] Vitamin D regulates negatively the growth of breast, prostate and colon cancer cells. This effect may be related to the ability of the hormone to arrest the neoplastic cells in the G_1 phase of the cell cycle by influencing the regulator proteins, such as $p21^{Cip1}$ and $p27^{Kip1}$,[190] to control the proto-oncogenes c-*myc* and c-*fos*[159] or to provoke apoptosis, downregulating *Bcl*-2 gene.[191]

It is known that vitamin D functions as a general suppressor of the immune system, including the activated B- and T- lymphocytes, especially the T-helper cells. Most immune cells possess express VDR as well as the enzymes responsible for its methabolism – 1aOHase and CYP24. Dendritic cells (DC) are also targets for the immunosuppressive activity of $1,25(OH)_2D_3$ which role is to inhibit their differentiation and maturation.[192] In some in vitro experiments with DC, the $1,25(OH)_2D_3$ treatment leads to downregulated expression of the costimulatory molecules CD40, CD80, CD86 as well as to decreased production of the proinflamatory IL-12 and enhanced production of the IL-10 that has potent anti-inflammatory properties. By other hand, the short treatment with vitamin D is able to induce DC with tolerogenic properties and thus increasing the number of the CD4+CD25+ suppressor T cells that are able to mediate transplantation tolerance. In addition, $1,25(OH)_2D_3$ inhibits the secretion of IL-2 by impairing the formation of the transcription factor complex NF-AT and of the IFN-γ through VDRE mediated pathway.[193]

There are some studies showing that $1,25(OH)_2D_3$ also affects several major endocrine processes, such as TRH/TSH action and pancreatic insulin secretion with subsequent regulation of glucose homeostasis. Vitamin D improves both, insulin secretion and insulin sensitivity which is associated with lower incidence of type II diabetes mellitus. This effect of vitamin D is mediated by the presence of its receptor and the enzyme that catalyze the formation of its active form (1aOHase) in the pancreatic β-cells. Vitamin D also influences the expression of the human insulin gene as well as to the one of its receptor (InsR) and enhances insulin-mediated glucose transport in vitro.[194]

$1,25(OH)_2D_3$ is likely to be an autocrine or paracrine factor for epidermal differentiation since it is produced by the keratinocytes. Cultured keratinocytes contain the enzymes required for the synthesis of $1,25(OH)_2D_3$ from 7-dehydrocholesterol. In keratinocytes, the active form of vitamin D, together with calcium trough a PLC-γ1-dependent pathway, regulate the differentiation by turning on and off the corresponding genes and activating those enzymes involved in the differentiation. It has been shown that during the differentiation of the keratinocytes VDR binds sequentially to two major coactivator complexes, DRIP (mainly the subunit DRIP205/TRAP220) and SRC with a hypotetical transition from DRIP in proliferating cells to SRC in more differentiated cells.[195] Moreover, $1,25(OH)_2D_3$ increases the expression of calcium receptor, thus making the cell more responsive to calcium.[112] In keratinocytes, vitamin D is able to either promote or inhibit proliferation. The antiproliferative effects are accompanied by an increase in TGF-β[196] and a reduction in the number of high-affinity receptors for epidermal growth factor and c-myc[197] mRNA levels.

The anti-oxidative effects of vitamin D have been suggested by epidemiological and many in vitro and in vivo laboratory studies. It is likely that 7-dehydrocholesterol and both, vitamin D_2 and vitamin D_3, as well as the metabolically active form, $1,25(OH)_2D_3$, are able to stabilize the membrane of normal cells against iron-dependent lipid peroxidation via an interaction between their hydrophobic rings and saturated and unsaturated residues of the phospholipid fatty acid side chains, which decreases the fluidity of the membrane.[198] In a recent study Bao et al. showed that the active form of vitamin D can protect nonmalignant prostate cells from oxidative stress-induced cell death by elimination of ROS-induced cellular injuries through transcriptional activation of glucose-6-phosphate dehydrogenase activity, a key antioxidant enzyme, dose- and time-dependently induced by calcitriol.[199] By other hand, the anti-oxidant activity of vitamin D could be due to the fact that the supplementation with this hormone increases the activities of two antioxidant enzyme – superoxide dismutase (SOD) and catalase to an extend, comparable to the one of vitamin E.[200] In studies on cancers, a pro-oxidant activity for vitamin D was revealed, but in this case one should consider the fact that this finding was made in a group of unhealthy people.[201] It has been shown an accumulation of oxidative stress-induced modification in proteins, lipids and DNA in tissues during the aging process. There are some studies which have shown that vitamin D deficiency is associated with a normal aging process, whereas excessive levels of vitamin D are associated with an accelerated aging process.[202] Moreover, it has been described that higher vitamin D concentrations are

associated with longer leukocyte telomere length, which underline the potentially beneficial effects of this hormone on aging and age-related diseases.[203] Clinical and experimental data showed that vitamin D regulates also some physiological brain functions like neuroprotection, regulation of behaviour, antiepileptic effects and motor functions. It has been shown that vitamin D is able to induce the expression of some neurotrophic hormones like glial cell-derived neurotrophic factor, leukemia inhibitory factor, neurotrophin-3 mRNA and nerve growth factor.[118]

The fact that the active vitamin D metabolite exerts a variety of actions throughout the body, affecting different organs and systems, led to its usage in the treatment of several disorders like secondary hyperparathyroidism, osteoporosis, psoriasis, autoimmune diseases and different type of cancer (breast, prostate, colon). The targets of vitamin D therapy in CKD involve renal inflammation, RAS and glomerular (mesangial cells and podocytes) and tubulointerstitial (tubular epithelial cells and interstitial fibroblasts) fibrosis. Active vitamin D has been shown to inhibit multiple pathogenic pathways in renal fibrosis. Active vitamin D (1) has anti-inflammatory effects; (2) inhibits mesangial and podocyte proliferation; (3) down-regulates the RAS by inhibiting renin production; (4) prevents glomerular hypertrophy as measured by glomerular volume in 5/6 subtotal nephrectomized rats; (5) decreases proteinuria in different animal models of CKD; (6) decreases fibrogenic cytokine production in the kidney by regulating Smad3 and TGF-β pathways; (7) has the potential to block the EMT and myofibroblast activation.[204]

However, the therapy with vitamin D has some limitations because of the hypercalcemic and phosphataemic activity of this compound with main unwanted side effect, the soft tissue calcification. In the last decades special attention has been paid to the development of structurally modified analogs that influence to a less extend the mineral metabolism, but the beneficial properties of vitamin D are retained.[205] Calcitriol (1α,25$(OH)_2D_3$) and VDRAs such as paricalcitol (19-nor-1α,25$(OH)_2D_2$) and doxercalciferol (1α$(OH)D_2$) and calcimimetics are currently used to manage secondary hyperparathyroidism (SHPT) associated with CKD.[206]

6.4. Effects of vitamin D in the vascular wall

VDR is nearly ubiquitously expressed and in the last decades great attention has been paid to the presence of VDR, together with all the components of the vitamin D system, in the vascular wall.

6.4.1. Distribution of VDR and vitamin D metabolic enzymes in the vasculature

There is growing interest in the potential role of vitamin D metabolites in the vasculature. Both ECs and VSMCs express high-affinity receptors for $1,25(OH)_2D_3$. Recent publications indicated that 1αOHase is expressed in endothelial cells, in which it appears to modulate cell growth and increase monocyte adhesion. Given the high ciculating levels of $25(OH)D_3$, the precursor of $1,25(OH)_2D_3$, it is possible that a locally expressed 1αOHse system might enable VSMCs to regulate the concentrations of $1,25(OH)_2D_3$ in an autocrine and/or paracrine manner so it can be governed by local factors and provide intracellular ligands for the vitamin D receptor. The mitochondria of the vascular cells possess also a functional 24OHse that regulates the first step of its catabolism. Thus, local production of $1,25(OH)_2D_3$ is considered to be important as an auto/paracrine regulator of certain vascular cell functions.

6.4.2. Specific functions of vitamin D in the vascular wall

In previous studies from our laboratory it has been found that $1,25(OH)_2D_3$ increases the proliferation and calcification of VSMC through a vitamin D response element in the promoter of vascular endothelial growth factor (VEGF)[185,144] and via RANK-BMP4 - dependent pathway,[187] respectively. $1,25(OH)_2D_3$ induces the proliferation of VSMC in vitro in dose-dependent manner in parallel with an increased expression of vascular endothelial growth factor (VEGF). Furthermore, inhibition of VEGF activity neutralizes proliferation induced by $1,25(OH)_2D_3$.

6.4.3. Beneficial effects of vitamin D and its synthetic analogs for the cardiovascular health

Vitamin D status has been proved to be an independent predictor of cardiovascular morbidity and mortality and vitamin D sufficiency is believed to promote cardiovascular health. Blood vitamin D levels depend mainly on solar exposure, but geographic and social factors can also influence.[114] Moreover, various pathological conditions like CKD, Crohn disease, rheumatoid arthritis, systemic lupus erythematosus and type 2 diabetes mellitus are associated with prevalence of low vitamin D levels with consequent cardiovascular complications. Thus, supplementation with vitamin D is now an important point in the treatment guidelines for these disorders.

One of the effects of vitamin D that mediates its beneficial role in the vasculature is the negative regulation of renin production, the rate-limiting

component of RAS. Li et al. have shown that vitamin D suppresses renin gene expression by targeting the cyclic AMP signalling pathway that is known to be the major stimulator of the renin production in the juxtaglomerular cells.[188, 207] However, kidney is not the only source of Ang II. It has been shown that the vasculature possesses the components needed for the local production of Ang II, and that their expression is increased in the atherosclerotic vessel. By inhibiting the rate-limiting step in RAS, vitamin D analogs might have some advantages over the ACE inhibitors and Ang II receptor blockers, as Ang II can be generated through ACE-independent pathways, and one Ang II receptor antagonist cannot completely block the effects of Ang II, as Ang II has multiple receptors.

As a putative positive vitamin D response element has been described within the mitogen activated kinase phosphatase MKP5 promoter, one of the beneficial aspects of the vitamin D treatment could be because MKP5 dephosphorylates/inactivates the stress-activated protein kinase p38MAPK. Activation of p38MAPK has like a downstream effector the production of IL-6, which is a proinflammatory agent in VSMC. Thus, $1,25(OH)_2D_3$ treatment could inhibit the IL-6 production in normal cells via p38MAPK inhibition.[208]

Moreover, it has been described that higher vitamin D concentrations, which are easily modifiable through nutritional supplementation, are associated with longer leukocyte telomere length, which underscores the potentially beneficial effects of this hormone on aging and age-related diseases.[203] The anti-oxidative effects of vitamin D have been suggested by epidemiological and many in vitro and in vivo laboratory studies. The active form of vitamin D can protect nonmalignant prostate cells from oxidative stress-induced cell death by elimination of ROS-induced cellular injuries through transcriptional activation of Glucose-6-phosphate dehydrogenase (G6PD) activity, a key antioxidant enzyme, which is a primary target of $1,25(OH)_2D_3$.[199]

7. KNOCKOUT MODELS FOR STUDYING THE ROLE OF VITAMIN D/VDR SIGNALLING

7.1. VDR knockout mice

Gene knockout studies in mice and VDR mutations in humans have provided considerable insights into the physiological functions of vitamin D. Four groups have created VDR knockout animals (Table 3).[209,210,211,212]

Table 3. Strains of VDRKO mice

Year	Strain of VDR null mice	Authors	Modified exon	Encoded region
1997	**Tokyo**	**Yoshizawa *et al*.**	**2**	**First zinc finger**
1997	**Boston**	**Li, Y. C. *et al*.**	**3**	**Second zinc finger**
2001	**Leuven**	**Van Cromphaut *et al*.**	**2**	**First zinc finger**
2002	**Munich**	**Erben *et al*.**	**2**	**First zinc finger**

VDR null mice were phenotypically normal at birth, but developed growth retardation, hypocalcemia, hypophosphatemia, hyperparathyroidism, high serum concentrations of alkaline phosphatase, rickets/osteomalacia, alopecia, bone growth retardation with loss of bone density, few whiskers, flat face and short nose after weaning, similar to the symptoms that occur in people with VDR mutations in vitamin D-dependent rickets type II (vitamin D resistance, hypocalcaemia, hypophosphataemia, secondary hyperparatiroidism, osteomalacia). These findings were accompanied by serum levels of $1,25(OH)_2D_3$ found to be around 10 times higher than in the WT, meanwhile the 24, $25(OH)_2D_3$ were almost undetectable at 4 weeks.[209] VDR knockout mice were also found to have impaired insulin secretory capacity (77) and showed gonad insufficiencies. In females a uterine hypoplasia and impaired folliculogenesis were observed and in males the lack of the receptor was associated with decreased sperm count and motility.[213]

Interestingly, feeding the VDR null mice with a diet rich in calcium, phosphate, and lactose all the symptoms were normalized, except the hair abnormalities. These observations suggest that increased intestinal calcium absorption is critical for 1, $25(OH)_2D_3$ action on bone and calcium homeostasis. The calcium homeostasis defect could be explained by the reduced expression of duodenal epithelial calcium channels CAT1 and CAT2 in VDR null mice.

Moreover, increased platelet aggregation, down-regulated expression of antithrombin and anticoagulant glycoprotein thrombomodulin along with upregulation of critical coagulation factor tissue factor expression in both hypo- and normocalcemic VDRKO mice can all contribute to the enhanced thrombogenicity, found in VDRKO mice. [214] In a study with LPS-induced disseminated intravascular coagulation rat model, a beneficial effect of the active form of vitamin D3 against thrombosis has been demonstrated.[215]

The study of Li et al., investigating the effect of VDR gene ablation in mice on the renin-angiotensin system revealed significant up-regulation of renin expression

in VDRKO mouse kidney. Blood diastolic and systolic blood pressure in VDRKO mice were significantly elevated, as was the heart weight / body weight ratio, a potential indication for the onset of hypertension-induced cardiac hypertrophy. Treatment of WT mice with active vitamin D and in vitro experiments on mouse glomerular AS4.1 cells, transfected with human VDR and a reporter gene fused to the murine renin 5' promoter region, showed VDR-mediated suppression of renin expression.[188] The disruption of this suppressing mechanism in VDRKO mice explains the up-regulation of renin expression in VDRKO mouse kidney.

7.2. 1αOHase knockout mice

Mutations in the gene coding for 1α-OHase lead to severe disorders including pseudovitamin D-deficiency rickets (PDDR)[216]. PDDR is an autosomal recessive disease characterized by growth retardation, failure to thrive, hypocalcemia, osteomalacia, and rickets. Recently, the genetic association of 1α-OHase with PDDR has been confirmed by deletion of the 1-OHase gene in mice.[217,218] 1α-OHase knockout mice were rescued by $1,25(OH)_2D_3$ depletions or high dietary Ca^{2+} intake.

7.3. 24OHase knockout mice

In order to examine the physiological role of the enzyme 24OHase and address the putative role of $24,25(OH)_2D_3$, St-Arnaud et al. have generated 24OHase knockout mice (24OHaseKO).[219] Initial reports suggest that 24OHaseKO mice showed poor viability and tendency to hypercalcemia, hypercalciuria and nephrocalcinosis during the neonatal period. The mice that managed to reach adulthood presented elevated plasma $1,25(OH)_2D_3$ levels after exogenous $1,25(OH)_2D_3$ administration. Unexpectedly, 24OHse mutated animals showed lower baseline levels of circulating $1,25(OH)_2D_3$ than wild-type controls and it has been proven that the surviving 24OHaseKO mice owe their survival in part to down-regulation of 1aOHase gene expression.[220] It has been postulated that these animals may use an alternative pathway of $24,25(OH)_2D_3$ catabolism to regulate circulating levels of the hormone.

OBJECTIVES

HYPOTHESIS

Vitamin D trough its nuclear receptor VDR increases the proliferation and migration of vascular smooth muscle cells, thus being involved in the development of atherosclerosis. Lacking the signalling via VDR would affect the proliferation rates in VSMC.

OBJECTIVES

1. Determine the effect of absence of VDR over the proliferation of vascular smooth muscle cells.

2. Study the metabolic activity of the VDR ablated VSMC.

3. Find the factors that could mediate the differential behaviour of the mutant cells at molecular level.

4. Determine how the sustained activation of Angiotensin II affects the proliferation of VDRKO vascular smooth muscle cells.

MATERIALS AND METHODS

The work, presented here, was carried out in the **Experimental nephrology laboratory**, part of the Nephrology department of University Hospital Arnau de Vilanova, Lleida under the direction of Dr José Manuel Valdivielso and Dr Elvira Fernández.

1. CHEMICALS AND STOCK SOLUTIONS, USED IN THE EXPERIMENTAL WORK

The following chemical substances were utilized as a ready to use solution or a solution that was *ex tempore* made from an already prepared stock solution:

- **1α,25-Dihydroxyvitamin D_3** (SIGMA, cat. Nº 076K4067) - 1mM stock solutions of 1α,25$(OH)_2D_3$ were prepared in 100% ethanol and stored in 10 µl aliquots at –20°C;
- **2-butyl-4-chloro-1-[*p*-(*o*-1*H*-tetrazol-5-ylphenyl) benzyl] imidazole-5-methanol monopotassium salt** (Losartan) (SIGMA, cat.Nº 61188) - 50 mM stock in water;
- **3-(4,5-dimethylthiazol-2-yl)-2,5-diphenyltetrazolium bromide** (MTT): 5 mg/ml stock and kept at –20°C;
- **Basic fibroblast growth factor** (bFGF) (PeproTech, cat. Nº 100-18B) - the recombinant substance was reconstituted in 5mM TRIS-HCL solution, pH 7.6 to 0.1 mg/ml;
- **Charcoal/dextran treated FBS** (charcoal stripped serum, CSS) (HyClone, cat. Nº SH30068.02) – this serum is obtained after activated carbon absorption of non-polar lipophilic substances such as certain growth factors, hormones and cytokines from the whole FBS. CSS was used in the determination of the growth curves of WT and VDRKO cells;
- **Dihydroethidium** (DHE) – was prepared as 15.85 mM stock solution in DMSO and was used in the measurements of the superoxide production in WT and VDRKO cells;
- **Diphenyleneiodonium sulfate** (DPI, SIGMA, cat. Nº D2926) - DPI (gift from Dr Jordi Boada) was dissolved in DMSO to 5mM stock concentration;
- **DNA molecular weight marker** (Roche, cat. Nº 11721933001) following the instructions of the manufacturer, using Oringe G (SIGMA) as a stain;
- **Dulbecco's modified Eagle's medium** (DMEM, GIBCO, cat. № 41965) – the medium was kept at 4°C and used always pre-heated at 37°C;
- **Fibronectin** (SIGMA, cat. Nº F1141) was reconstituted with sterile destilated water to 100 µg/ml and kept in 500 µl aliquots at -20°C;

- **Foetal bovine serum** (FBS, GIBCO, cat. Nº 10500) was aliquoted and stored at –20°C. For experiments, 10% concentration was used;
- **Hoechst 33258** (Bisbenzimide H, SIGMA, cat. Nº B2883) - stock solutions of 200 µM were prepared in water and kept in dark at –20°C;
- **Orange G** (SIGMA, cat. 03756) loading buffer – the salt was dissolved in water solution of 10mM EDTA, 10mM TRIS and 30% glycerol;
- **Paraformaldehyde (4%)** - 80g of paraformaldehyde were dissolved in 800 ml H_2O under high temperature and stirring in a hood. When the temperature is 60°C, few drops of 5M NaOH were put, until the solution became transparent. Then the solution was cooled the volume of adjusted to 1L, and pH to 7.4. Then the paraformaldehyde solution was mixed with 1L 0.2M phosphate buffer and the pH adjusted again to 7.4;
- **Penicillin & streptomycin solution** (SIGMA, cat. № P4458) – aliquots of 10 ml (one for a bottle of DMEM, 500 ml) were and frozen at - 20°C;
- **Phosphate buffer (0.2M)** – 13.79g NaH_2PO_4 in 500 ml H_2O, 53.39g $Na_2HPO_4x2\ H_2O$ in 1500 ml H_2O. First, the dibasic sodium phosphate solution was prepared to pH 7.0 and then the other phosphate solution was added slowly, until pH 7.4;
- **Phosphate buffered saline** (PBS) – 17.52g NaCl, 400mg KCl, 100ml 0.2M phosphate buffer, H_2O to 2L;
- **Propidium iodide** (PI, SIGMA, cat. Nº P4170) – the solution of PI (25 mg of PI were dissolved in 10 ml 20x SSC and 490 ml H_2O) at 50 µg/ml, was covered with aluminium paper in order to project it from the sunlight, and was kept at 4°C;
- **Sodium saline citrate** (SSC, 20x) – 3M NaCl, 0.3M sodium citrate, H_2O to 1L, pH 7.0;
- **Tiron –** antioxidant, stock solution of 1M, kept at -20°C (gift from Dr Xavier Dolcet);
- **Trypsin** (0.05% Trypsin-EDTA 1x, Gibco, cat. Nº 25300) was used for the detachment of the cells.

2. EXPERIMENTAL ANIMALS

The animal experiments were done in accordance with the following legal directives:

- Llei 5/1995, 21st of June, of the Generalitat de Catalunya for protection of the animals used for experimental work and other scientific purposes.

- Decret 214/1997, 30th of July, that develops the upper law.
- Real Decreto 1201/2005, 10th of October, for protection of the animals used for experimental work and other scientific purposes.

We bred VDR knockout (VDRKO) mice, initially generated by targeted ablation of exon 2,[209] using wild type (WT) littermates as a control in all the experiments. A breeding colony of heterozygous for VDR (VDRHZ) mice was established from 10 mice (males and females), a generous gift by Dr. Kato. C57Bl/6 mice strain was used like genetic background for these KO mice. On day 21 postpartum pups were weaned and assigned to different cages based on their genotype and gender.

2.1 Diets

Mice were fed the standard rodent chow (0.6% calcium and 0.8% phosphorus, and 0.6 IU/g vitamin D_3 with 2.9Kcal/g (Harlan Teklad) and housed in the animal facility of the University of Lleida at temperature of 21°C with 12 hours dark/light cycle with food and water freely available. In order to normalize mineral homeostasis and thus exclude hypocalcaemia as a factor in our experiments, VDRKO mice only were fed on a "rescue diet" upon weaning, containing 20% lactose, 2.0% calcium, 1.25% phosphorus, 2.2 IU/g vitamin D_3 diet with 3.5 Kcal/g (Harlan Teklad, TD.96348). We used 3 months-old mice for all experiments.

2.2. Genotyping

Mice were identified by polymerase chain reaction (PCR) with tail genomic DNA as template, obtained by a standard digestion with proteinase K (High Pure PCR Template Preparation Kit, Roche, cat. Nº 11796828001). Four primers were used to amplify a 140 bp VDR band and a 455-bp Neo band from the inserted targeting vector:

WT *forward*: **5´-ATG GAG GCA ATG GCA GCC AGC ACC TC-3´**
reverse: **5´- GAA ACC CTT GCA GCC TTC ACA GGT CA-3´**
VDRKO *forward*: **5´- GCC TGC TTG CGC AAT ATC ATG GTG GA-3´**
reverse: **5´- AGC CAG GTG AGT TTA CCT ACC ACT TCC-3´**

The PCR mixture consists of 1x PCR buffer minus Mg, 1.5 mM $MgCl_2$, 0.2 mM dNTP mixture, 0.2 µM of each primer and 1 U/µl Taq DNA polymerase (cat. Nº 18038-034), all from Invitrogen, and the reaction conditions were: 35 cycles at

94°C for 15s, 66°C for 30s, 72°C for 1 min, with a final extension at 72°C during 10 min. [221]. Then, the reaction product together with DNA molecular weight marker in Orange G loading buffer, were visualized after running a 1.5% low melting agarose (Conda laboratories, cat. № 8050) gel. SYBR green was used as a DNA staining.

The VDRKO mice and their WT littermates were subjected to several in vitro and in vivo experiments.

3. IN VITRO STUDIES

3.1. Cell cultures

In order to achieve the purpose of our work, we employed primary aortic mouse VSMCs, as these cells are widely used and accepted in cardiovascular research.

3.1.1. Primary culture of mouse VSMC

3.1.1.1. Explant method

Primary aortic VSMCs of 3-month-old WT and VDRKO mice were obtained by explants outgrowth culture, as previously described with slight modifications [222]. In brief, WT and VDRKO mice were anesthetized with isoflurane, administered in conjunction with pure oxygen; the thoracic and the abdominal aorta was extracted and stored in ice-cold sterile phosphate-buffered saline (PBS) on ice. The following steps were carried out under a laminar flow hood in sterile conditions. After three washes in PBS and excision of the lateral vessels, aorta was cut into small fragments (<1 mm^3) and placed in 6-well culture plate, previously coated with 100 µg/ml fibronectin. The explants were maintained in DMEM, supplemented with 20% (vol/vol) heat-inactivated FBS, 2 mM glutamine, penicillin (100 U/ml) and streptomycin (100 µg/ml), in a humid atmosphere at 37°C with 5% CO_2. Two weeks later, the cells migrated from the tissue had occupied the culture plate. Then, the explants were removed with a sterile pancetta and the cells were detached by trypsinization with subsequent planting in a new plate with bigger size (60 mm).

The cells obtained by this method were identified as VSMC by the following criteria: the characteristic for VSMC morphology at confluence ("hill-and-valley" pattern) and by positive indirect fluorescent immunocytochemistry for smooth muscle α-actin.

3.1.1.2. Fluorescent immunochemistry for smooth muscle α-actin

In order to confirm the vascular smooth muscle origin of the primary cultures, WT and VDRKO cells at passage 2 were grown in 6-well plates. When the cells reached 80% of confluence they were washed with DMEM without FBS and 1 ml of ITC medium, containing insulin and transferin (100x, GIBCO, cat. № 41400), supplemented with 0.25mM ascorbic acid and 0.01nM $FeCL_3$. Cells were left to grow in this medium for three days. Then, the cells were rinsed with cold PBS three times five minutes each, fixed with ice-cold 100% methanol for 15 minutes at 4°C and washed with cold PBS. The fixed cells were then incubated in blocking solution (4% FBS in PBS) for one hour at room temperature (RT) on a rocking platform. After washing with cold PBS, a monoclonal anti-smooth muscle α-actin, alkaline phosphatase conjugated antibody (SIGMA, clone 1A4, cat. № A5691) was added in a 1:50 dilution in blocking solution for one hour at RT. Some wells were incubated only with blocking solution (negative control). The wells were washed three times with PBS and a fluorescent rabbit anti-mouse (Table 7) was added in a 1: 200 dilution in blocking solution for one hour at RT. Finally, after the last washing in PBS, 50 μl of SlowFade component A (Molecular Probes, cat. № S7461) were put, together with 0.5 μg/ml Hoechst 33258 dye, covered with cover slip and viewed under a microscope equipped with epifluorescence (OLYMPUS IX70) and photographed.

3.1.1.3. Maintainance of primary VSMC cultures

Cells were passaged twice a week. All the mediums and solutions were pre-wormed at 37°C. Growth medium was removed and cells were washed once with PBS and then 1 ml (for 35 mm) or 2 ml (for 100 mm) of Trypsin/EDTA solution were added. The cells were brought back to the incubator for approximately 5 minutes to allow the detachment of the cells. After one washing in DMEM, containing 10% FBS, cells were subcultured in 1:3 ratio in 100 mm plates.

3.1.1.4. Freezing, storage and thawing of VSMC

For freezing, VSMCs were trypsinized, spun down and resuspended in ice-cold freezing medium containing 0.1 ml DMSO plus 0.9 ml FBS per vial. The cell suspension was placed in cryotubes and first frowzen at -80°C during three days before the long time storage at -196°C in liquid nitrogen. For thawing, cells were warmed to 37°C and immediately dissolved in pre-warmed culture medium. After centrifugation, cells were resuspended in culture medium and placed in 100 mm plate for overnight incubation.

3.2. Cell culture treatments

For all experiments VSMCs between passage 2 and 8 were cultured in 4, 6, 24 or 96-well plates and used at 70-80% confluence. In order to synchronize the cell population in Go phase of the cell cycle, before each experiment cells were serum starved during 24h in DMEM supplemented with 0.2% FBS, after which cells were switched to DMEM supplemented with 0.2%FBS again or to 10%FBS DMEM. The culturing in 0.2% FBS was used to maintain the VSMC in quiescent state, the one that they have in natural conditions, being part of the artery wall. When a reference to this state is made, the term "basic conditions" is usually used. As FBS is a classical mitogen, 10%FBS was utilized in the induction of cellular proliferation.

To check if there was a difference in the responsiveness of WT and VDRKO VSMCs to molecules that influence different cell events, the following substances were used:

- 10% **CCS**, that has very low concentrations of any liposoluble substances, among them growth factors, was used in the experiments in which the growing curves of WT and VDRKO cells were obtained.
- 100 nM (10^{-7}M) **$1,25(OH)_2D_3$** was added first to both, WT and VDRKO cells, but as the mutant cells were unresponsive to the treatment, the effects of vitamin D over mouse WT cells only are listed in the Results chapter;
- 0.4mM **H_2O_2** was added to the cells during one hour in order to provoke oxidative stress;
- 2 µg/ml **Oligomycin** was used in order to induce phosphorylation of adenosine monophosphate – activated protein kinase (AMPK) in WT and VDRKO cells;
- 10 µM **Losartan** was used as an inhibitor of the activation of Ang II receptor type 1 (AT1) in WT and VDRKO cells;
- 10 µM **DPI**, inhibitor of the enzyme NADPH oxidase, was used in both cell population in the monitoring of the superoxide production by FACS analysis;
- 10 µM **Tiron** was added to the cells, because of its antioxidant properties.

3.3. In vitro experiments with mouse VSMC

The differences in the cell cycle regulation and some metabolical characteristics of WT and VDRKO VSMCs were determined in vitro.

3.3.1. Determination of the proliferation rates of WT and VDRKO VSMC

In order to test the effect of the activation of VDR on VSMC growth WT and VDRKO VSMCs were proceeded in the following assays:

3.3.1.1. BrdU incorporation

The incorporation of 5-bromo-2´-deoxyuridine (BrdU) into the new synthesized DNA was detected using a commercial colorimetric enzyme-linked immunosorbent assay (5-bromo-2´-deoxy-uridine Labeling and Detection Kit III, Roche Diagnostics, cat. Nº 1444611). In brief, WT and VDRKO VSMCs were cultured in 96-well microtiter plates ($3x10^3$ cells/well). After reaching 60-80% of confluence, VSMCs were serum starved for 24 hours and then the medium was changed to fresh 0.2% FBS (basic condition) or 10% FBS DMEM (stimulated condition) for an additional period of 24h. After that time, the cells were incubated with 10 μM BrdU overnight at 37°C and fixed. After washing with 10% FBS DMEM three times, the cells were partially digested by incubation with nuclease working solution during 30 minutes in an incubator without CO_2 at 37 °C. Then, the cells were washed and a working solution of peroxidase-conjugated anti-BrdU antibody was added for 30 minutes at 37 °C. Finally, the cells were washed three times, and the peroxidise substrate was added. Optical density (OD) was measured at 405 nm against a reference wavelength of 490 nm using a microplate reader (BIO RAD, model 680). Measurements were done on six wells for each condition. The cell number was determined in three wells for each cell culture (WT and VDRKO) before fixation, in order to normalize the amount of incorporated BrdU.

3.3.1.2. Determination of the growth curves

The growth curves of WT and VDRKO VSMCs were obtained using 6-well plates ($1x10^5$ cells/well) in DMEM supplemented with 10% FBS or 10% Charcoal CSS. Cells were left to reach 50% of confluence, the medium was changed and then, considering this moment as a start point, the cells were harvested by trypsinization and the cell number was count manually in triplicate at 3, 6, 12, 18, 24, 32 and 48 hours, using a Neubauer hemocytometer.

In experiment with the AT1-R antagonist Losartan, $3x10^4$ WT and VDRKO cells/well were cultured in 6-well plates in triplicate, the cell number was counted after the addition of 10 μM Losartan to complete DMEM, and the growing curves were done. In this experiment the medium ± losartan was changed every 24 hours.

3.3.2. Cell volume measurement

To measure the cell volume WT and VDRKO cells were cultured in 100 mm plates ($5x10^5$ cells/ plate) in 10% DMEM. The cells were left to attach overnight, then FBS deprivation was done during 24 hours and past this time, the culture medium was changed to 10%FBS DMEM. Starting from this moment (point 0), 18, 32 and 48 hours later the cells were trypsinized. The cell pellet was resuspended in 0.5 ml of PBS, previously passed through a 0.2 μm filter. Then, a 1:100 solution in 0.9% saline, also filtered, was made. The cell volume was recorded using a Coulter Z2 particle count and size analyzer (Beckman), equipped with a 100-μm-aperture for determination of cell volume. The Coulter method of sizing is based on the sensation of the small aperture from the cells that passed through it, displacing a volume of liquid, and measuring it as a voltage pulse, which is converted and shown as volume histograms.

3.3.3. Flow cytometry study of the cell cycle distribution

We analyzed the distribution of WT and VDRKO VSMC in the different phases of the cell cycle using fluorescence-activated cell sorter (FACS). Cells were cultured in 100 mm plates ($2x10^5$cells/well) and left to reach 50% of confluence, time point that we considered as a zero moment. Then, the culture medium was changed and the cells were trypsinized and fixed with 70% ethanol overnight at 4°C. Ethanol was removed and the cells were incubated with 1 mg/ml RNase solution for 30 min at 37°C. Then, the cell nuclei were stained during 30 min with 50 μg/ml propidium iodide. Cell fluorescence distributions in the cell cycle phases were obtained using Coulter Epics XL flow cytometer (Beckman). PI is a dye that intercalates into DNA. The intensity with which a cell's nucleus emits fluorescence light is directly proportional to the amount of PI and therefore to the cell's DNA content. Flow cytometry permits the evaluation of every cell that pass a laser beam in a single file.

3.3.4. Gene expression analysis

3.3.4.1. RNA extraction

In order to assess the expression of genes of interest, we scrapped and lysed the cells, usually grown in 6-well plates, directly in 1 ml of TRIzol®Reagent (Invitrogen, cat. № 15596-018). To homogenize the cells we passed the lysate several times through the pipette tip. After five minutes incubation at room temperature (RT) which permit the complete dissociation of nucleoprotein complexes, 0.2 ml of chloroform was added and the samples were centrifuged at

12,000×g during 15 minutes at 4°C (Eppendorf centrifuge, 5415R). The total RNA was then separated in the colourless upper aqueous phase which was transferred to a new tube. Precipitation of the RNA from the aqueous phase was done by mixing with 0.5 ml isopropanol per 1 ml of TRIZOL® Reagent used for the initial homogenization. The samples were incubated at RT for 10 minutes, forming an invisible RNA precipitate, and centrifuged at 12,000×g for 10 minutes at 4°C. To the RNA pellet 1 ml of 75% ethanol was added, mixed at Vortex to dissolve the pellet in the ethanol and centrifuged at 9,400×g for 5 minutes at 4°C. Then, the supernatant was removed and the pellet was air-dried for 15 minutes. Afterwards, the RNA pellet was dissolved in diethyl pyrocarbonate (DEPC) - treated water (RNase-free water) and stored at -80°C. The total RNA concentration was quantified by its absorption maximum at 260 nm, using a spectrophotometer (NanoDrop 2000, Thermo Scientific). The ratio of the absorbance at 260 to 280 was used to assess the RNA purity and a sample with A_{260}/A_{280} of 1.8÷2.0 was considered to be pure RNA.

3.3.4.2. DNA microarray

For this analysis, WT and VDRKO cell were cultured at 100mm plates (four plates per each). The cells were left to attach 24 hours in 10%FBS DMEM, and afterwards, the medium was switched to 0.2% FBS. The cultures were grown in quiescent conditions during 24/48 hours. At the end of the experiment, the cells were collected in Tryzol. In order to obtain a pure RNA which was necessary for the DNA microarray, the RNeasy mini kit (QIAGEN) was used, following the protocol, provided by the manufacturer. The DNA microarray (Mouse WMG 4X44K (Agilent microarray design ID 014868, P/N G4122F) and the consequent retrieval and significance analysis of the microarray data were carried out in the Unidad de Genómica, Centro Nacional de Investigaciones Oncológicas (CNIO), Madrid.

3.3.4.2.1. Microarray design

Labeling-hybridization-scanning methodology

Samples: total RNA fraction. RNA Integrity Numbers were in the range 8.1 to 9.5 when assayed by Lab-chip technology on an Agilent 2100 Bioanalyzer.

Label protocol: Amount of nucleic acid labeled: 1µg. Amplification: by RNA polymerases. Commercial "Two-Color Microarray-Based Gene Expression Analysis (Quick Amp Labeling)" kit by following manufacturer instructions. Briefly, MMLV-RT retrotranscription of sample from a T7 promoter primer is followed by a T7 RNA pol catalysed in vitro transcription reaction in the presence of either Cy3-CTP or Cy5-

CTP fluorophores. Labeled samples are purified with silica-based RNeasy spin columns (Qiagen).

Hyb protocol: Chamber type: SureHyb hybridization chamber (Agilent). Quantity of each labeled extract used: 825 ng; Volume: 100 uL; Temperature: 65ºC; Duration: 17 hours.

Scan protocol: Scanned on an G2565C DNA microarray scanner (Agilent). Images were quantified using Agilent Feature Extraction Software (ver. 10.1.1).

Analysis: Hybridized microarray images were analyzed and backgound subtracted with Agilent FeatureExtraction (FE) Software. Raw data was subsequently normalized with GeneSpring software. The term ''raw'' signal values refer to the linear data after thresholding and summarization.

Significance analysis: In order to derive some statistical confidence and depending on the experimental grouping, either t-test, LIMMA or ANOVA are performed. Two important factors used to estimate whether a gene is differentially expressed are the magnitude of the difference between groups and the variability of the gene. Sample size, data noise and signal distribution are additional factors that affect the output of statistical tests. Since the P-value is only statistically valid when a single score is computed, a 'multiple testing correction' is used to adjust the statistical confidence measures to the number of tests performed. P-value adjustment changes the raw p values (individual genes) into a false discovery rate for the whole experiment.

Table 4. To find changes in the expression profile of VDRKO and WT celld, RNA from 4 VDRKO cell cultures were hybridised in 5 microarray experiments against a reference RNA from WT. RIN, RNA integrity number

Dye	CNIO ID	Sample ID	RIN	Microarray ID
Cy3	116WT_(1+2+3+4)	pool WT	8,9	251486830228_3
Cy5	116-5	VSMC VDRKO 1	8,1	
Cy3	116WT_(1+2+3+4)	pool WT	8,9	251486830228_4
Cy5	116-6	VSMC VDRKO 2	9,4	
Cy3	116WT_(1+2+3+4)	pool WT	8,9	251486830230_1
Cy5	116-7	VSMC VDRKO 3	9,5	
Cy3	116WT_(1+2+3+4)	pool WT	8,9	251486830230_2
Cy5	116-8	VSMC VDRKO 4	9,1	
Cy3	116KO_(5+6+7+8)	pool KO	9	251486830230_3
Cy5	116WT_(1+2+3+4)	pool WT	8,9	
Experiment grouping				
Samples				**Comparison**
poolWT vs poolVDRKO_251486830230_1_3.txt				dye swap
VDRKO1 vs poolWT_ 251486830228_1_3.txt				VDRKO vs WT
VDRKO2 vs poolWT_ 251486830228_1_4.txt				VDRKO vs WT
VDRKO3 vs poolWT_251486830230_1_1.txt				VDRKO vs WT
VDRKO4 vs poolWT_251486830230_1_2.txt				VDRKO vs WT

3.3.4.3. cDNA synthesis

The reverse transcription was performed, using "1st-strand DNA synthesis kit for RT-PCR (AMV)" (Roche Diagnostics, cat.№ 11483188001). 1 μg of RNA was used for the copy DNA (cDNA) conversion. After the reaction mix was prepared according to the manufacture's instructions, one hour at 42°C was run before inactivating the reverse transcriptase at 99°C for 5 min in a thermal cycler (TC-412, Techne, Cambridge, Ltd). The obtained in this way cDNA was used as a template in a real time polymerase chain reaction (RT-PCR).

3.3.4.4. Real time polymerase chain reaction

Taqman real-time PCR method was used in order to determine the relative mRNA levels of the target genes. The reaction mix consists of Taqman universal PCR Mastermix (Applied Biosystems, 4324018), specific primers, already prepared as stock solutions, and water. The primers for all the genes of interest and the glyceraldehyde-3-phosphate dehydrogenase (GAPDH), used as a house-keeping gene, were purchased from Applied Biosystems (Table 5). This gene was used as a control, because it has been found that its expression is not affected by vitamin D and many studies related to vitamin D, present the expression levels of their genes of interest as ratio to GAPDH. Moreover, in our DNA microarray there was no statistically significant difference between VDRKO and WT cell expression of Gapdh. We used optical 96-well reaction plates with barcode (MicroAmp®, Applied Biosystems, 4306737). Forty cycles at 95°C for 15s and 60°C for 1 min were performed with an ABI Prism 7000 Sequence Detection System (Applied Biosystems). The relative RNA amount was calculated by the "delta delta Ct method". Threshold cycle (Ct) is the fractional cycle number at which the fluorescence crosses the threshold. For every gene, one of the control samples was selected to have value equal to 1 and the values of the other samples were related to it.

Table 5. List of primers, used for the RT-PCR analysis

Assay ID	Gene symbol	Gene name	RefSeq	Species	Amplicon length
Mm00437297_m1	**Vdr**	Vitamin D receptor	NM_009504.3	*Mus musculus*	95
Mm99999915_g1	**Gapdh**	Glyceraldehyde-3-phosphate	NM_008084.2	*Mus musculus*	107

		dehydrogenase			
Mm01303209_m1	**Cdkn1a**	Cyclin-dependent kinase inhibitor 1A (p21)	NM_007669.4	*Mus musculus*	62
Mm00438170_m1	**Cdkn1c**	Cyclin-dependent kinase inhibitor 1C (p57)	NM_001161624 NM_009876	*Mus musculus*	115
Mm01546133_m1	**Acta2**	Actin, alpha 2, smooth muscle, aorta	NM_007392.2	*Mus musculus*	88
Mm00483888_m1	**Col1a2**	Collagen, type I, α2	NM_007743.2	*Mus musculus*	67
Mm00441724_m1	**Tgfb1**	Transforming growth factor, beta 1	NM_011577.1	*Mus musculus*	99
Mm02342887_mH	**Ren1**	Renin 1 structural	NM_031192.2	*Mus musculus*	143
Mm00515587_m1	**Ctsd**	Cathepsin D	NM_009983.2	*Mus musculus*	88
Mm01165918_g1	**Cyp27b1**	Cytochrome P450, family 27, subfamily b	NM_010009.2	*Mus musculus*	73
Mm01166161_m1	**Agtr1a**	Angiotensin II receptor, type 1a	NM_177322.3	*Mus musculus*	63
Mm01341373_m1	**Agtr2**	Angiotensin II receptor, type 2	NM_007429.4	*Mus musculus*	86

3.3.5. Protein/DNA ratio

WT and VDRKO VSMCs were serum starved by incubation in DMEM containing 0.2% FBS for 24 hours before being grown in DMEM with FBS. 24 hours later, the cells were harvested by trypsinization and each sample was then split in two separate tubes and spun by centrifugation. Lysis buffer was added to the pellet of one of these two tubes. The pellet in the other tube was subjected to genomic DNA extraction, using the kit, mentioned in the genotyping section. Protein was measured using the method of Lowry et al. with albumin as a standard, as explain in the next section. DNA concentration was measured spectrophotometrically. After measuring the protein and DNA concentrations, the protein/DNA ratio was calculated, as a sign of average cell size and presence of hypertrophy.

3.3.6. Protein analysis

3.3.6.1. Solutions

Before the initiation of the protein analysis, the following stock or ready to use solutions were prepared:

- Lysis buffer: 2% SDS, 125 mM TRIS, pH 6.8 (Store at RT). Just before use for every 1 ml buffer 5 µl of the DMSO protein inhibitors cocktail solution (PIC, SIGMA, cat. Nº P8340) and 10 µl of 1mM Phenylmethylsulfonyl fluoride (PMSF, SIGMA, cat. Nº P7626), dissolved in 100% ethanol.
- 5x SDS sample buffer: 50mM TRIS-HCl (pH 6.8), 2% SDS, 10% glycerol, 144mM β-mercaptoethanol, 0.1% bromophenol blue.
- TRIS–HCl – 0.12g TRIS were dissolved in 20 ml 0.9% NaCl, and the pH was adjusted to 8.8 or 6.8 with 5% HCl;

Table 6. Components of the polyacrylamide gels

	Resolving gels				**Stacking gels**	
	15%	**12%**	**10%**	**8%**	**5%**	**4%**
30%AA:0.8% bis AA, ml	4	3.2	2.6	2.2	0.845	0.163
1.5MTRIS-HCl pH 8.8, ml	2	2	2	2	-	-
0.5MTRIS-HCl pH 6.8, ml	-	-	-	-	1.25	0.313
10% SDS, ml	0.081	0.081	0.08	0.081	0.1	0.0125
10% APS, ml	0.081	0.081	0.08	0.081	0.1	0.0125
TEMED, ml	0.00325	0.00325	0.008	0.00485	0.01	0.0025
H_2O, ml	1.86	2.65	3.28	3.75	2.86	0.76
Linear range of separation (kDa)	**50 – 10**	**200 - 20**	**200 - 25**	**200 - 50**		

- Electrophoresis buffer**:** 1.92M glycin, 250mM TRIS, 10% SDS, pH 8.3;
- Blotting buffer (10x): 1.92M glycine, 250mM TRIS. *Ex tempore* to 1x buffer methanol at 10% (8% and 10% resolving gels) or at 20% (12% and 15% running gels) was added.
- 20x TBS/T – 146.1g NaCl, 48.44g TRIS, and H_2O until 1L, pH 7.4; Ex tempore to 1L of 1x TBS, 1 ml of Tween 20 was added;
- Stripping solution: 0.2M glycin, pH 2.5
- Coomassie staining solution: 0.1% Acid violet (SIGMA, cat. Nº 210579-50Q), 10% Acetic acid, 25% isopropanol and 10% acetic acid;
- Coomassie distaining solution: mixture of 10% Acetic acid, 10% isopropanol, used in the estimation of the protein load in western blot;

3.3.6.2. Protein extraction

Cell extracts were collected in lysis buffer, supplemented *ex tempore* with PIC and PMSF. The cell lysate was subjected to three freeze-thaw cycles. Then, an

ultrasonication was carried out three times, 10" each (Digital sonifier model 450, Branson). Insoluble materials were cleared through centrifugation at 4°C for 10 minutes at 10,000×g, the supernatant was removed by aspiration and stored at -80 °C. Protein concentrations were determined by an improved Lawry's method (DC protein assay, BioRad, cat. Nº 500-0116).

3.3.6.3. Western blotting

For western blot (WB) analysis 20 µg of total protein per well were used. After boiling 5 min in the sample buffer, the proteins were separated in SDS-polyacrylamide gel electrophoresis (SDS-PAGE) under reducing conditions according to Laemmli. Pre-stained protein ladder (Invitrogen, cat. Nº 10748-010) was run in parallel. After running, the separated proteins were blotted to 0.45 µm pore size polyvinylidine fluoride membranes (Immobilon®-P transfer membrane, Millipore, cat. Nº IPVH00010) during one hour at 70 V. Blocking of non-specific binding was achieved by placing the membrane during one hour in solution of 3% nonfat dry milk in TRIS-buffered saline with 0.1% Tween 20 (TBST), except for retinoblastoma protein (pRb), where bovine serum albumin (BSA) was used. Then, blots were incubated with primary antibodies (Table 7) overnight at 4°C on RP. After washing with TBST, appropriate horseradish peroxidise-conjugated secondary was added for an extra hour. Binding was detected with ECL™ Advance Western Blotting Detection Kit (Amersham Biosciences, cat. Nº RPN2135) or EZ-ECL chemiluminescence detection kit for HRP (Biological industries, cat. Nº 20-500-120), according to the recommendations of the manufacturer, using VersaDoc Imaging system Model 4000 (BioRad). Signals were quantified with the Quantity One software (BioRad).

Table 7. Primary and secondary antibodies used for western blotting analysis

Protein	Source	Dilution of use	Storage	Band, kDa	Company
VDR	rabbit	1: 1000	4°C	51	Santa Cruz Biotechnology
Rb protein	mouse	1: 250	- 20°C	110-115	Generous gift from Dr Marti Aldea and Dr Carme Gallego
Cyclin D	rabbit	1: 200	- 20°C	36, 34	
Cyclin E	rabbit	1: 500	- 20°C	52	
$p21^{Cip1}$	rabbit	1: 500	- 20°C	21	
$p27^{Kip1}$	mouse	1: 500	- 20°C	27	
$p57^{Kip2}$	rabbit	1: 500	- 20°C	57	
$p19^{ARF}$	rabbit	1: 1000	- 20°C	19	Upstate
Cathepsin D	rabbit	1: 5000	- 20°C	46,28	Abcam
AT_1	rabbit	1: 1000	4°C	43	Santa Cruz Biotechnology
AT_2	rabbit	1: 1000	4°C	43	Santa Cruz Biotechnology
NOS Type II	rabbit	1: 1000	- 20°C	130	BD Transduction Laboratories
AMPKα	rabbit	1: 1000	- 20°C	62	Generous gift from

Phosphor-AMPKα	rabbit	1: 1000	- 20°C	62	Dr Jordi Boada
p38	rabbit	1: 2000	4°C	38	eBioscience
P-p38	rabbit	1: 2000	4°C	38	eBioscience
SOD1	rabbit	1: 2500	- 20°C	2x 16.6	Chemicon
SOD2	mouse	1: 2500	- 80°C	25	StressGen
Complex I	mouse	1: 2000	4°C	39	Generous gift from Dr R. Pamplona
Complex II	mouse	1: 2000	4°C	70	
Complex III	mouse	1: 2000	4°C	48.5	
Complex IV	mouse	1: 8000	4°C	35	
Porine	mouse	1: 5000	4°C	32	
ERK1/2	mouse	1: 1000	- 20°C	44-42	Cell signalling
P- ERK1/2	rabbit	1: 1000	- 20°C	44-42	Cell signalling
α-tubulin	mouse	1: 30000	- 20°C	50	SIGMA
Rabbit IgG + HRP	goat	1: 10000	- 20°C	-	Cell signalling
Mouse IgG + HRP	goat	1: 10000	- 20°C	-	Jackson Immuno Research Laboratories
Goat IgG + HRP	bovine	1: 10000	4°C	-	Santa Cruz Biotechnology
Sheep IgG + HRP	donkey	1: 10000	- 20°C	-	Abcam
Alexa Fluor 488: Mouse IgG Rabbit IgG + fluorescein	rabbit goat		- 20°C	-	Molecular probes

3.3.6.4. Stripping of an already probed membrane

When incubation with another primary antibody was needed, a previous stripping of the blot was made using a low pH stripping solution. Then, one hour of blocking was done, and after three washings, the membrane was incubated with another Ab. For example, in order to assess the loading, we probed the membranes with anti-tubulin antibody.

3.3.6.5. Coomassie blue staining

In order to control equal loading and transfer of proteins, the membranes were stained with Coomassie blue staining solution after the last revealing. In brief, gels were incubated in the staining solution for one hour and subsequently washed 3 times for one hour each in distaining solution.

3.3.7. Morphological studies of WT and VDRKO cells

3.3.7.1. Hoechst staining

WT and VDRKO cells were planted in 4-well plates and left to attach overnight. Then, the cells were cultured during 48 hours in 10%FBS DMEM. After 24 hours of serum deprivation the medium was removed, the cells were washed once in PBS and fixed with 4% paraformaldehyde in PBS for 30 min. Subsequently, the cells were stained with 0.5 μg/ml bisbenzimidazole (Hoechst 33258 dye) during 30 min and were mounted with glass coverslips using 70% glycerol. Hoechst 33258 is a cell

permeable adenine-thymine specific fluorescent dye, used to stain DNA. It gives a bright blue staining of the condensed chromatin. The nuclear fluorescence was detected by Olympus IX70 microscope, equipped with epifluorescence optics and a camera Olympus OM-4 Ti. From each sample, at least 500 nuclei were counted, and the data is present as mean values ± SE of the percentage of picnotic nuclei.

3.3.7.2. Transmission electron microscopy

The ultrastructure of the studied VSMC was determined by transmission electron microscopy (TEM). The samples were washed with PBS, fixed for 6 h with 2.5 % glutaraldehyde in 0.1 mol/l phosphate buffer (pH 7.4) at 4ºC, post-fixed with 1 % osmium tetroxide in solution of potassium ferricianide for 2h, and dehydrated with increasing concentrations of ethanol - water mixtures. After embedment in resin (Embed-812 Epon), ultrathin sections (70-80 nm) were stained with uranyl acetate and Reynold´s lead citrate and were observed under TEM (ZEISS, EM910, 80Kv). (Electron microscopy facility, SCT-ME, University of Lleida).

3.3.8 Metabolic studies of VSMC

The metabolic activity of WT and VDRKO VSMC were determined by the assessment of the mitochondrial function, measured by the conversion of MTT to formazan, high resolution respirometry, and the concentration of ATP, produced by the cells. The expression of the complexes of the mitochondrial electron chain was checked by WB analysis.

3.3.8.1. MTT viability assay

The viability and the metabolic activity of WT and VDRKO VSMC were determined by the mitochondrial reduction of the yellow-coloured MTT to the purple formazan. The cells were grown in 96-well plates (10^4 cells per well) and left to attach overnight. Then a 24 hours starving (0.2% FBS) was made in order to synchronize the cells. After this period, a working solution of MTT (1 mg/ml) in DMEM without FBS was added to each well for one hour in CO_2 incubator at 37°C. The produced formazan was dissolved in 50µl DMSO, protected from light, and the spectrophotometric absorbance was taken at 540 nm wavelength, using microplate reader (BIO RAD, model 680). The levels in the control wells were designated as 100% viability.

3.3.8.2. High-resolution respirometry

The oxygen flux of WT and VDRKO VSMC (2×10^5 cells/ml) was measured at 37°C in DMEM culture medium with 10% FBS by high-resolution respirometry, using Oroboros® Oxygraph-2k. The chamber volumes were set at 2 mL and the stirring speed at 400 rpm. DatLab software (Oroboros Instruments, Innsbruck, Austria) was used for data acquisition (2 s time intervals) and analysis, which includes calculation of the time derivative of oxygen concentration and correction for instrumental background oxygen flux.[223] The experimental regime started with routine respiration, which is defined as respiration in cell culture medium without additional substrates or effectors. After observing steady-state respiratory flux in the time interval between 15 and 20 minutes after closing the chamber, the ATP synthase (complex 5) was inhibited with oligomycin (1 µg/ml), followed by uncoupling of oxidative phosphorylation by stepwise titration of carbonyl cyanide p-trifluoromethoxyphenylhydrazone (FCCP) up to optimum concentrations in the range 4-5 µM. After the addition of FCCP, protons entered the mitochondrial matrix via complex 5, provoking maximal respiratory stimulation. Finally, respiration was inhibited by addition of antimycin A at 2.5 µM (inhibiting complex III of the mitochondrial electron transport chain). This titration method was completed within 60 min. In order to avoid oxygen limitations, all the experiments were performed above 50% oxygen saturation. Oxygen consumption was normalized by cell number and citrate synthase activity.

The respiratory control ratios: RCR, UCR and RCRp were calculated from the titrations with oligomycin and the uncoupling agent FCCP, where routine respiration (**R**), inhibitited by oligomycin (**4o**) and the respiration after the FCCP-induced uncoupling; total mitochondrial capacity (**3u**) were used:

- Respiratory control ratio, **RCR=3u/4o**
- Uncoupling control ratio, **UCR=3u/R**
- Phorphorylation respiratory control ratio, **RCRp=(R-4o)/3u**.

There were strong arguments to replace the conventional UCR and RCR by the inverse ratios:

1/UCR = Routine respiration / Uncoupled respiration

1/RCR = Oligomycine inhibited / Uncoupled respiration

3.3.8.2.1. Citrate synthase activity measurement

The cell pellets, obtained by the WT and VDRKO samples, used for the measurement of the oxygen flux, were homogenized on ice in 0.1 M Tris buffer containing 0.1% Triton X-100, pH 8.35. Citrate synthase activity, a marker of the mitochondrial mass, in a specific tissue is frequently constant when expressed per mitochondrial protein. Some metabolic mitochondrial parameters, therefore, may be expressed per citrate synthase for specific applications.[224-226] The activity of citrate synthase in the cell homogenate supernatants was measured spectrophotometrically at 412 nM and 30°C in a medium containing 0.1 mM 5,5-dithiobis-(2-nitrobenzoic) acid, 0.5 mM oxaloacetate, 50 mM EDTA, 0.31 mM acetyl coenzyme A, 5 mM triethanolamine hydrochloride and 0.1 M Tris–HCl, pH 8.1, as described previously.[227]

3.3.8.3 Measurement of ATP content

In order to determine ATP content, WT and VDRKO cells were seeded on 100 mm culture plates. After reaching a confluence of 50-75%, the cells were washed with cold PBS and 0.5 ml of ice-cold extraction buffer (0.1 M Tris-acetate, 2 mM EDTA, pH 7.8) were added to the plates. The cells were detached with scrapper and heated at 90-95ºC during 90 sec. The cell extracts were centrifuged and the supernatants were immediately frozen at -80ºC until the assay. ATP was measured with the Adenosine 5'-triphosphate (ATP) Bioluminescent Assay Kit (SIGMA, cat. Nº FLAA), according to the manufacturer instructions, in a Tecan microplate reader. Briefly, samples were neutralized to pH 7.4 with 10 µl 4 M TRIS and 10 µl were added to a new tube with 90 µl ATP-free water. The luciferase reagent was added 1 s before the 5-s measurement in the luminometer, as described by the supplier. For each sample the amount of the produced light was immediately measured with a luminometer and was compared with the light of the ATP standard standards in order to calculate the ATP concentration. The protein content of the test samples was measured and used for normalization of the ATP concentration, expressed in nmol per mg protein.

3.3.9. Cytochemical staining for SA-β-Gal activity

In order to measure SA-β-gal activity, WT and VDRKO VSMC from passage two, four and six, were cultured in 6 well plates ($1x10^5$ cells/well) in 10% DMEM. When the cells reached 50% of confluence they were washed once in PBS (pH 7.2), fixed during 4 min (RT) in 0.5% glutaraldehyde and then rinsed again in PBS (pH 7.2, supplemented with 1mM $MgCl_2$). Finally, the cells were incubated overnight at

37°C (without CO_2) with a freshly prepared SA-β-Gal staining solution: 1mg/ml 5-bromo-4-chloro-3-indolyl β-D-galactoside (FLUCA, cat.№ 16665) (stock = 20mg per ml in DMSO)/ 5 mM potassium ferrocyanide/ 5 mM potassium ferricyanide/ 2 mM $MgCl_2$ in PBS, pH 6.0. For control, cells were stained at pH 4.0. After the removal of the staining solution, the cells were washed twice in PBS. For counting, the cells were covered with 70% glycerol, containing Hoechst 33258 dye.

3.3.10. Angiotensin II measurement

VSMC of WT and VDRKO mice were grown in 6-well plates with 10%DMEM for 24 hours. The cells were then washed twice with PBS and serum starved for un additional period of 24 hours. Then, three wells per condition were incubated in 1 ml of either serum free DMEM or DMEM with 10%FBS for 24 hours. The conditioned culture medium was then collected and centrifuged at 1000x*g* for 10 minutes, and the supernatant (medium) was collected. The cells were washed twice with ice-cold PBS, scraped in 75 µl lyses buffer, and disrupted by sonication. The cell homogenates were centrifuged at 10 000x*g* for 10 minutes, and the supernatants were collected. The conditioned medium and cell extracts stored at -80°C until analysis for Ang II by EIA. The Ang II concentration in the condition medium of WT and VDRKO VSMC was determined using a commercial EIA kit (SPI-bio, cat. Nº A05880) according to the manufacturer's instructions. In brief, in a 96-well plate, pre-coated with mouse anti-Ang II IgG, an immunological reaction with Ang II from the culture medium occurred and after washing, the trapped molecule was covalently linked to the plate by 0.5% glutaraldehyde treatment. After washing and denaturing treatment with borane-trimethylamine in 2N HCl/methanol (1:1) leading to epitope release, Ang II reacted with the acetylcholinesterase-labelled mAb (AChE) used as tracer. The plate was then washed and the sustrate/chromogen Ellman's reagent was added to the wells. The AChE tracer acts on the Ellman's reagent to form a yellow compound. The intensity of the colour was measured spectrophotometrically at 405 nm. Results are calculated by interpolation from the standard curve. The total protein concentration was measured by the Lawry's method, as explained before in order to normalize the amount of Ang II per mg protein.

3.3.11. Intracellular superoxide anion detection

3.3.11.1. Ethidium fluorescence

Quiescent WT and VDRKO cells were trypsinized, washed in PBS and counted manually in a Neubauer chamber. Equal amount of cells from both cell population were put in cuvettes for fluorescence measurements with 1 ml of PBS and the basal fluorescence was measured by fluorimeter (RF-5000, Shimadzu) at λ_{ex}= 520 nm and λ_{em}= 590 nm. Then, 10μM DHE, dissolved in DMSO, were added to the cell suspension and the fluorescence was measured every 5 minutes until 30 minutes. DHE is freely permeable to alive cells and can be directly oxidized by superoxide anion ($O^{\bullet}_2$) to ethidium bromide (EtBr), that intercalates with DNA and emits red fluorescence, which corresponds to the levels of $O^{\bullet}_2$, produced by the cells.

3.3.11.2. FACS analysis

For more precise measurements, the $O^{\bullet}_2$ levels in our VSMC model were analysed also by fluorescent activated cell sorter analysis, using the same method of detection (DHE). In one set of experiments, the DHE was added to the cells after one hour of treatment of normally growing WT and VDRKO cells with 0.4mM H_2O_2 in complete DMEM. Being an oxidant, it has been shown that H_2O_2 is able to induce superoxide production. The cells were incubated with DHE at 37°C 20 minutes. After trypsinization and several washings in PBS, the cells, resuspended in 800 μl of PBS were subjected to FACS analysis. The flow cytometry was carried out in BD FACSCanto™ II flow cytometer (FL2 channel) and FACSDiva Version 6.1.1 software was used to acquire and analyze the data. Simultaneous staining of two types control samples was done. First, staining with propidium iodide (2μg/ml) of WT and VDRKO cells was made in order to assess the cell viability and to set the gate of the cell populations. Second, samples without DHE staining were proceeded to determine the autofluorescence of VSMC to which the fluorescence of the test samples was normalized.

In order to find the source of the superoxide in another set of experiments WT and VDRKO cells were maintained for 48h in DMEM, containing 10% FBS. After quick detachment from the plate, cells were resuspended in PBS, for the control cells, or in 0.5 ml PBS containing one of the following compounds, 10 μM losartan or 10 μM DPI. Then, the cells were transferred into 5-ml polystyrene round bottom tubes (Becton Dickinson), protected from light and kept at 37°C for 30 min. During the last 20 min of incubation, dihydroethidium (DHE, 10 μM) was added. After the end of the incubation, the cells were washed twice in PBS in order to remove the unspecific staining and kept cold until subjected to analysis. The histogram

represents the fluorescence of 10 000 cells. The results are expressed as median ± SEM. All the FACS analysis were done with the help of a experienced fellow Anaïs Panosa Borràs, PhD in the Flow Cytometry and Confocal Microscopy Facility, IRBLLEIDA.

3.3.12. Determination of the migration of VSMC

We determined the ability of VSMC to migrate by the study of "wound healing" in vitro. Two lines on the bottom of 6-well plates were made in order to facilitate the subsequent measurements as shown in the figure 14.

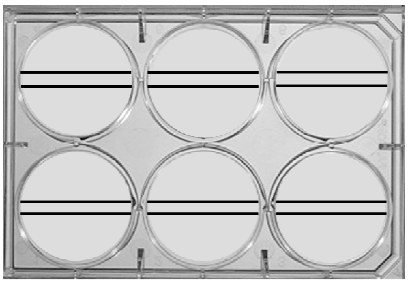

Figure 14. Plate, prepared for "wound healing" assay in vitro.

WT and VDRKO cells were seeded in thus prepared 6-well plates ($3x10^5$ cells/well) in 10%FBS DMEM. When the cells reached 100% confluence, the medium was switched to 0%FBS DMEM for 24 hours. After washing in PBS, with a tip for 0.2 ml micropipette, a scratch ("wound") in the cell monolayer was made. The, 0% FBS DMEM was added to the wells. One picture at that time (point 1) was used to compare with the one made 24 hours later (point 2). During these hours, the cells were left to migrate towards the "wound". At the end of the experiment, the two areas ($\mathbf{A_1}$ and $\mathbf{A_2}$) for each sample were quantified, using a computer image analysis programme (Leica IM50 Image Manager). The results were achieved at mm^2 and displayed as the percentage of the "healed" area ($\mathbf{A_H}$), calculated as:

$$\mathbf{A_H\% = (A_1 - A_2)/ A_1 * 100}$$

4. IN VIVO STUDIES

4.1. Carotid artery injury

The surgery was done with the help of a surgery fellow (Dr Luis Perez-Ruiz, PhD), assisted by experienced animal technicians (Roser Pane Doménech and Jessica Pairada Montero), using a dissecting microscope (Zeiss, Germany) at a magnification of x1.6. The recently described mouse carotid injury method [228] was

used, with minor modifications. In brief, on day 0, WT and VDRKO mice were anesthetized with isoflurane, administered in conjunction with pure oxygen and the left external carotid artery (CA) was exposed via midline neck incision. The primary bifurcation of the CA was located and two ligatures were placed around the external branch. Afterwards, the distal ligature was tied and the proximal was used to loop the common and internal carotid arteries for temporary vascular control during the procedure. A transverse arteriotomy was made in the CA and a 0,014 inch flexible angioplasty guide wire (Abbott Laboratories) was passed along the vessel three times with a rotating motion, with care taken to use the identical injury procedure for each animal. The wire increased the lumen size by overstretching and denuding the endothelium from the vessel. The wire was removed, the proximal CA silk secured, and the incision closed with a 5-0 nylon suture (Ethicon). Animals were returned to appropriate cages and allowed to awaken under a warming lamp. A 200 µl of 0,003 mg/ml Buprex® (0.3 mg/ml buprenorphine, dilute 1/100 with sterile water for injections, 0.024 µg/g) were injected intraperitonially.

4.1.1. Tissue harvest and histology

21 days after carotid injury, animals were re-anesthetized, the injured CA located and looped. Mice were killed by placement of a 22-gauge butterfly angiocatheter in the left ventricle and in situ fixation with 3% glutaldehyde in 0.2 M phosphate buffer, pH 7.3. The artery was harvested and left in the fixative solution for an additional period of 48h at 4°C. Each artery was imbedded in paraffin, assigned a number and various sections were cut. Parallel sections were subjected to standard hematoxylin & eosin staining.

4.1.2. Hematoxylin & eosin staining

Hematoxylin is a basic stain and has affinity to the acid structures of the cell, thus staining the nucleus in blue-violet. The eosin has the opposite affinity and stains the cell cytoplasm in red. Prior to staining, paraffin slides must be baked at temperature of around 70°C to inhibit detachment of sections during the staining procedure. Then, the samples should be rehydrated by passing trough a sequence of xilol, 100% ethanol, 96% ethanol, 70% ethanol. After washing in water (2x 5 min), the slides were left in Harri´s hematoxylin (Panreac) for 15 minutes. The following washing in tap water from helps thew oxidation of hematoxylin over the nucleus, giving it blue colour. One washing in the mixture of 1.2% HCl in 80% ethanol was made and again the slides were washed in running tap water during 10 minutes. Then 5 minutes incubation in eosin was made. The eosin has affinity to

basic structures and stains the cell cytoplasm in red. Finally, the samples were dehydrated in ethanol – xilol series (70% ethanol, 96% ethanol, 100% ethanol, xilol, xilol – eucalyptus oil). The cover slips were mounted in DPX (BDH Laboratory Supplies).

4.1.3. Morphometry

The injured vessels were analyzed for the development of maximum narrowing. Vessel dimensions were measured at original magnification 200x, using an image analysis program (Leica IM50 Image Manager). For each artery section, two types of measurements were made: area inside the innermost elastic lamina and area inside the adventitial (outermost) elastic lamina. The area of the media was calculated by subtracting the measured area inside the innermost internal elastic lamina from the area within the outermost elastic lamina.[229]

4.2. Matrigel plug assay

The Matrigel plug assay was used to check the ability of endothelial cells in WT and VDRKO mice to form microcapillaries as a feature of the angiogenesis process. High concentration basement membrane matrix (BD Biosciences, cat. № 354248) was used for in vivo formation of a plug. Ex tempore, aliquots of Matrigel were supplemented with 500ng bFGF and kept on ice few minutes until use. The mixture (0.5 ml) was injected in the back of anesthetised WT and VDRKO mice (isoflurane, administered in conjunction with pure oxygen). After one week, a 0.25 $mg.ml^{-1}$ solution of FITC-dextran (SIGMA, cat. № 056K5312) was injected i.v. trough the tail vein of re-anesthetised animals. Twenty minutes later, a blood sample (around 0.2 ml) was taken by cardiac punction made with a "heparin syringe" (insulin syringe, trough which a small amount of heparin was passed, enough to avoid the coagulation of the blood). 5 µl of the total blood were kept in a separate tube to be used for measurement of the haemoglobin (Hb) concentration. The rest of the blood was centrifuged 10 min at 10.000 rpm in order to obtain plasma in which to measure the FITC fluorescence. Then, post-mortem, the skin of the back of each animal was taken off and the plug (as clean as possible, without hair) was placed in a pre-weight tube in order to measure its weight. The plugs were kept overnight at 4°C. On the next day, the plugs were homogenized 10 min on ice (Ultra-turrax T8, IKA-WERKE, Gmb&Co). After a centrifugation of 6 min at 10.000xg, the supernatant was poured in a new tube.

4.2.1. Fluorescence measurements

The blood sample was diluted 100x in H_2O and the supernatant, obtained after the plug homoginization, was used directly. The fluorescence was measured against a standard curve of FITC-dextran (0.4 – 25 $\mu g.ml^{-1}$) in a black 96 well plate (BD, cat. Nº 353948) at 486/528 nm in a fluorescence reader (FLx800, Bio-Tek instruments, INC).

4.2.2. Hemoglobin determination

The determination of the hemoglobin (Hb) concentration was carried out in a 96 well plate with a standards (0, 25, 50, 100, 150, 200 µg/ml), prepared with haemoglobin from bovine blood (SIGMA, cat. Nº H2625-256). Simultaneously, 25 µl of plug supernatant and standard samples were put in duplicate. Then, 25 µl of tetramethylbenzidine solution, TMB (SIGMA, cat. Nº T8665) were added and the plate was incubated 20 minutes over a rocking platform at RT. The reaction was stopped with 75 µl 2N H_2SO_4. After an additional period of 5 minutes, the absorbance at 450 nm was taken.

5. STATISTICAL ANALYSIS

All results, if not specially indicated, are expressed as mean ± S.E.M. Differences between means of two groups were assessed by Student's t-test. A probability of less than 0.05 was considered statistically significant in all tests. To indicate a significant difference (p value from 0.01 to 0.05) we used *, and for very significant (p value: 0.001 to 0.01) and extremely significant (<0.001) ** or ***, respectively.

RESULTS

1. Phenotype of VDRKO mice

During the first month of age, all the pups of a couple of VDRHZ mice presented the same size. After weaning, VDRKO mice fed on regular rodent diet exhibited severe growth retardation, alopecia, impaired bone formation, infertility, and usually die within 3 months of age. When VDRKO mice fed on a rescue diet, containing higher contents of calcium, phosphorus and lactose, were able to reach the same size and weight of their WT littermates, as well as to reproduce. Another very obvious finding was the almost complete lack of intra-abdominal fat in the mutant mice. As shown by others, the alopecia was not able to be recovered by the calcium rich diet (Figure 15).

Figure 15. The photograph represents the typical appearance of WT and VDRKO mice at the same age. The smaller size and the severe alopecia are the phenotypical features that differentiate the mutant mice from the wild type. The VDRHZ mice are phenotipically identical to the WT. The genotypes of the mice, from left to right, are WT, VDRHZ, and VDRKO [210].

In order to detect the different genotypes, and especially to separate the knockout animals and give them the rescue diet as soon as possible after weaning, we performed a PCR with genomic DNA as a template. In figure 16, a representative agarose gel is shown.

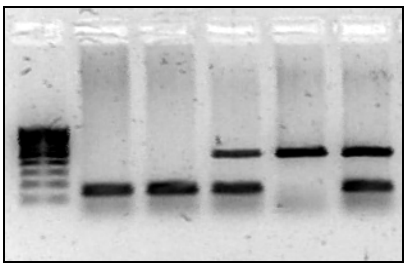

Figure 16. SYBR green - stained 1.5% agarose gel which represents the genotyping of 5 mice. Between the littermates, the three genotypes were present – WT (140 bp), VDRKO (455 bp) and VDRHZ (140bp and 455 bp)

2. Characterisation of aortic VSMCs obtained from WT and VDRKO mice

VSMC were obtained from WT and VDRKO mice aortas by the explant method, as described in the Materials and Methods section. The cells were spindle shaped and displayed the classic "hill-and-valley" pattern of growth at confluence, as shown in figure 17A and B. Figure 17C and 3D shows that the isolated cells stained with FITC-labelled anti-α-smooth muscle actin, exhibited a bright green fluorescence, identifying them as VSMC.

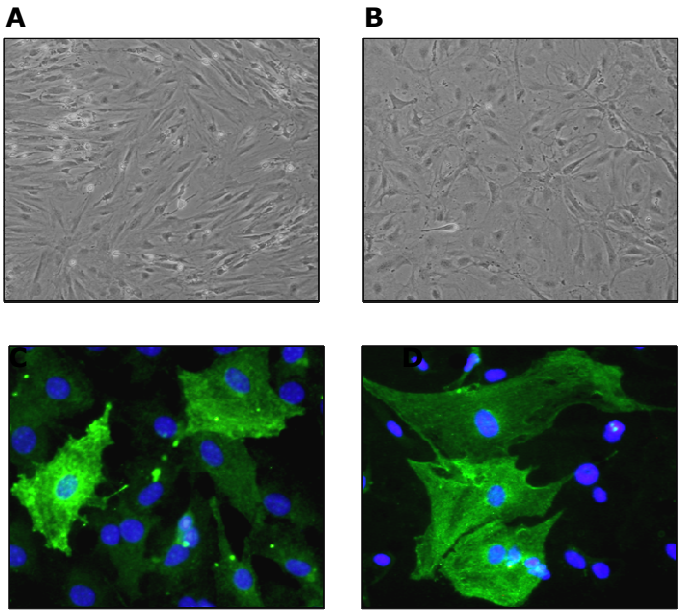

Figure 17. Appearance of WT (**A**) and VDRKO (**B**) cells in culture, stimulated to grow with 10%FBS. Immunocitochemistry for α-smooth muscle actin of WT (**C**) and VDRKO (**D**) cells. Hoechst 33258 dye was used to stain the cell nuclei.

Very obvious features of the knockout cell population were their lower rate of proliferation and the enlarged size of the cells. Moreover, the VDRKO cells were more resistant to the effect of growth factors (FBS) withdrawal.

3. Expression of the main components of the VDR system

By RT-PCR and WB analysis the absence of VDR in the mutant cells was confirmed. In order to check if the signalling through VDR is abrogated in these cells, the expression of the two main enzymes, regulating the vitamin D metabolism, which levels are under the transcriptional control of the active form of

vitamin D, $1,25(OH)_2D_3$, were determined. As shown in figure 18, the three principal proteins were expressed in our VSMC cultures – VDR (only in WT), 1αOHase and 24OHase. The levels of 1αOHase were higher in VDRKO cells, which is due to the lack of the metabolic negative feedback that $1,25(OH)_2D_3$ exerts trough its receptor. The catabolic enzyme 24OHase was expressed at very low level in the mutant cells. This finding was not expected because this protein has positive VDRE in its promoter. Thus, the lack of activation of VDR explains the low levels of 24OHase.

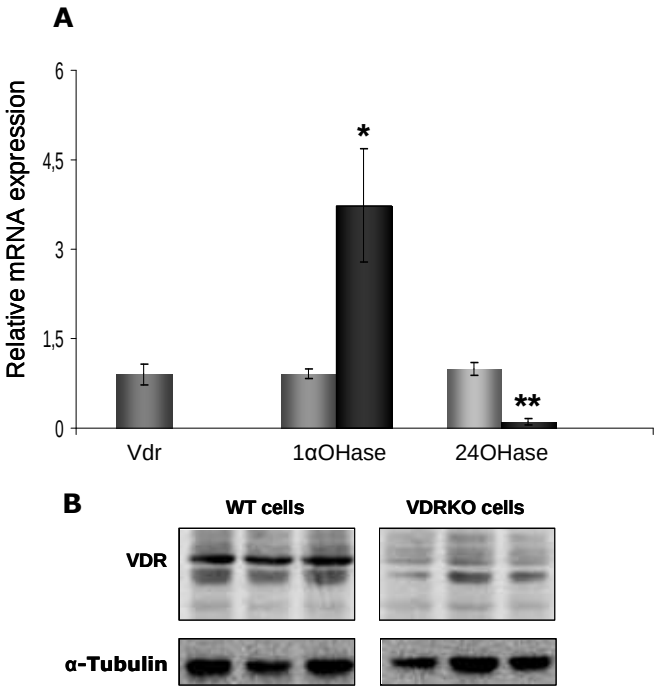

Figure 18. Expression of the main components of the VDR system in WT (grey bars) and VDRKO (black bars) vascular smooth muscle cells (A), assessed by RT-PCR, * $p< 0.05$. Representative Western blots of the VDR protein levels in the control and in the mutant cells (B). Tubulin was used as a loading control.

4. VSMC proliferation

VSMC replication and migration result from the combined action of several cytokines, growth factors, and extracellular matrix components. The proliferation of both VSMC cultures (WT and VDRKO) was assessed in several assays in which a significant reduction in the proliferation rates of the mutant cells was confirmed.

4.1. BrdU-ELISA

Starting with the same number of cells, we checked the levels of growth of both cell populations – WT and VDRKO. Since VSMC proliferate asynchronously under standard culture conditions, pre-synchronization by serum deprivation was done during 24 hours. The absence of mitotic signals (serum deprivation) leads to a rapid exit from the cell cycle into a non-dividing state, termed G_0, characterized by low metabolic activity. Then, VSMC were grown either in medium containing 0.2%FBS, referred as "basic condition" or stimulated to grow with the standard 10%FBS DMEM for an additional period of 24 hours. The proliferation rate, determined by the overnight incorporation of BrdU in the newly synthesized DNA, was found to be significantly lower in the VSMC from VDRKO mice in comparison to WT (Figure 19). Serum reduction led to rapid decrease in the number of dividing cells in both cell cultures. When the growth factors containing bovine serum was added, both populations increased significantly their cell number being significantly lower ($p < 0.05$) in the mutant cells.

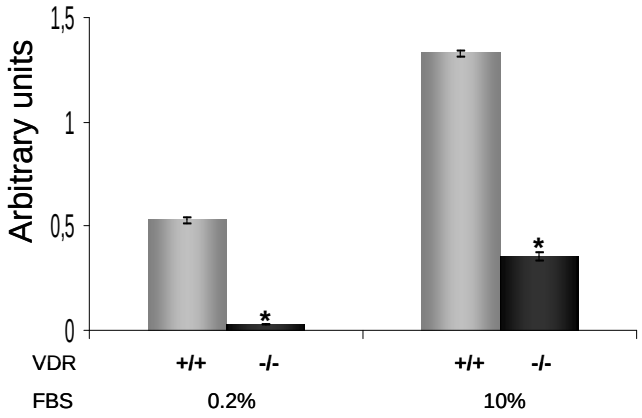

Figure 19. BrdU-incorporation of WT (grey bars) and VDRKO (black bars) cells was determined with a commercial ELISA kit. Starting with the same number of cells, in 24 hours after the addition of the growing conditions (0.2% or 10%FBS) the mutant cells incorporated significantly less BrdU, * $p < 0.05$.

4.2. Growth curves

The term cell growth in these experiments was used in the context of cell division (reproduction). We evaluated the proliferation characteristics of WT and VDRKO cells stimulated to grow with 10%FBS by manually counting them in Neubauer chamber at different time point in triplicate wells until 48 hours. The mean values of the cell number were plotted on a graph as a function of time

(hours). Wild type VSMC had a significant increase in the cell number after 48 hours in culture compared with that from VDRKO VSMC (4.2 ± 0.14 $x10^5$ vs 2.2 ± 0.11 $x10^5$; $p < 0.05$). We found that the growth of WT cells followed a typical exponential curve ($y = 87.445e^{0.0322x}$, $R^2 = 0.936$), meanwhile the one of the VDRKO cells was nearly linear ($y = 108.92e^{0.0154}$, $R^2 = 0.949$) (Figure 20A). The exponential, also sometimes called geometric growth is faster than the linear or also called arithmetic growth. The growth curves revealed that the primary culture of VDRKO VSMC showed a slower growth pattern than the WT cells with significant differences in the mean cell numbers observed over 18 hours after the addition of 10% serum to the culture medium. When a charcoal stripped serum (CSS) was used as a mitogen, a decrease in the growth rate of WT was seen ($y = 64.763e^{0.022x}$, $R^2 = 0.883$), meanwhile the mutant cells kept the same pattern ($y = 58.214e^{0.016x}$, $R^2 = 0.762$) (Figure 20B).

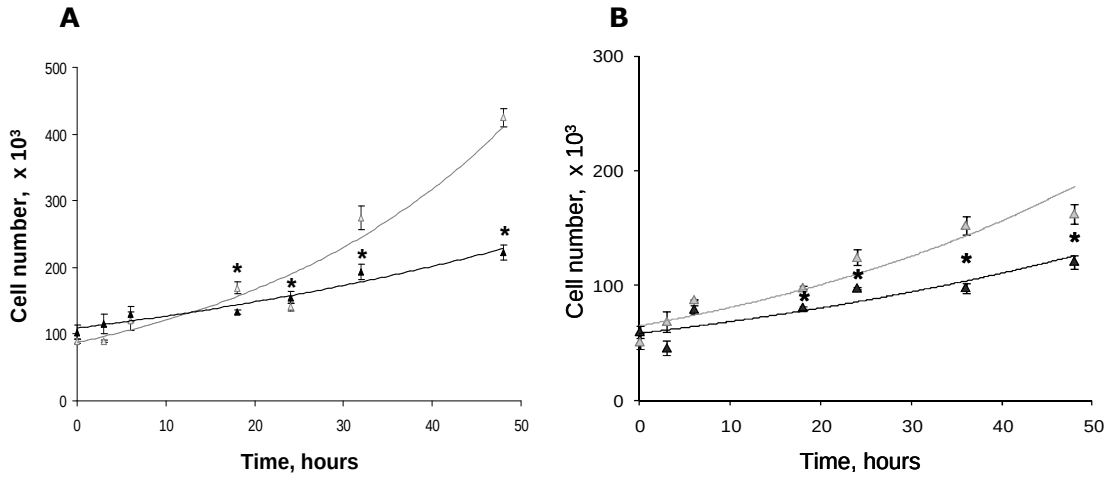

Figure 20. Growth curves of WT and VDRKO VSMC upon serum stimulation. Quiescent VSMC were stimulated with 10%FBS (A) or 10%CCS (B) for 3, 6, 18, 24 and 48 hours. Cells were harvested and manually counted, as described in Materials and Methods section. Each graph shows one representative experiment out of three. Values given are means, and error bars indicate SEM (n=3). WT cells are presented in grey and the VDRKO in black coloured triangles, the curve colour is grey for WT and black for VDRKO cells, * $p< 0.05$.

4.3. Protein/DNA ratio

Under bright light microscopy, the mutant cells appeared to be larger than their controls. For this reason we decided to check their relative size. In the same sample (WT and VDRKO, n =3) both, total protein and DNA concentrations were measured. Then, the ratio between the protein and the DNA content was calculated

and presented according to the control (WT=100%) (Figure 21). A slight increase in this ratio (118,4%) was seen in the VDRKO cells, without reaching statistical significance. This finding led us to thing that the lack of signalling trough VDR probably leads to an increase in the size of the mutant cells.

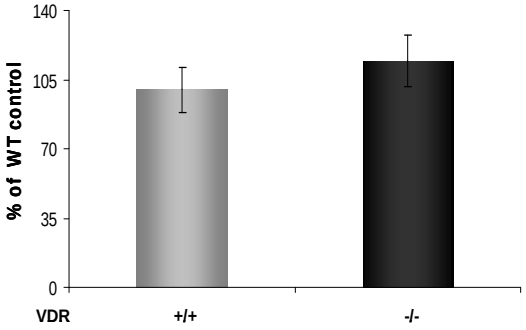

Figure 21. The total protein [µg/µl] to DNA [µg/µl] ratio was measured as an indicator of changes in the cell size in both cell populations (WT, +/+) and VDRKO (-/-).

The hypertrophy of vascular smooth muscle cells (VSMC) is critical event in vascular remodelling associated with hypertension, atherosclerosis, and restenosis. Further, we decided to measure directly the cell volume in order to clarify the tendency found by the protein/DNA ratios.

4.4. Cell volume

One typical feature of the cell response to mitogenic stimuli is the increase in the size of the cell, during the interface of the mitosis. To determine whether there were significant differences in cell size, the mean cell volume of both cell populations was measured. As it is shown in figure 22, from 0 to 48 hours in culture, both WT and VDRKO cells increased their volume, but at any moment the mutant cells were significantly larger.

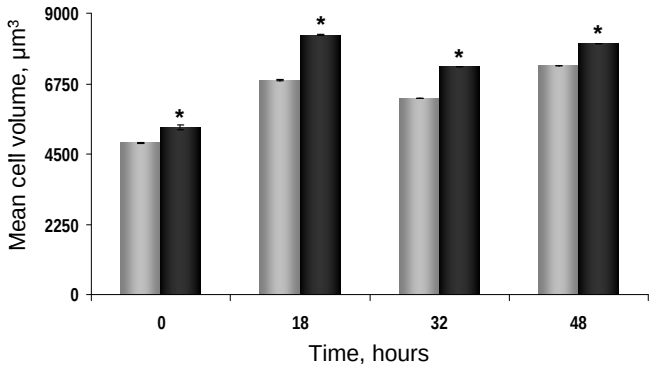

Figure 22. The mean cell volume was measured by Coulter Z2 cell counter at 4 time points. At any moment a significant difference in the cell volume of WT (grey bars) and VDRKO (black bars) cells was seen, * $p < 0.05$.

The lower cell number in the VDRKO population, together with the increase in the mean cell volume led us to thing that the mutant cells probably are stopped in the G_1/S transition check point of the cell cycle.

4.5. Fluorescence activated cell sorting for cell cycle distribution

In order to clarify if really there was a G_1-arrest of the VDRKO cells, a flow cytometry assay for the distribution of the cells in the cell cycle phases was performed. The first finding of the FACS analysis was the evident difference in the forward light scatter (FSC) and side light scatter (SSC) cell frequency profile, which was in accordance with the bigger VDRKO cell size and point to an increased granularity of our mutant cells (Figure 23).

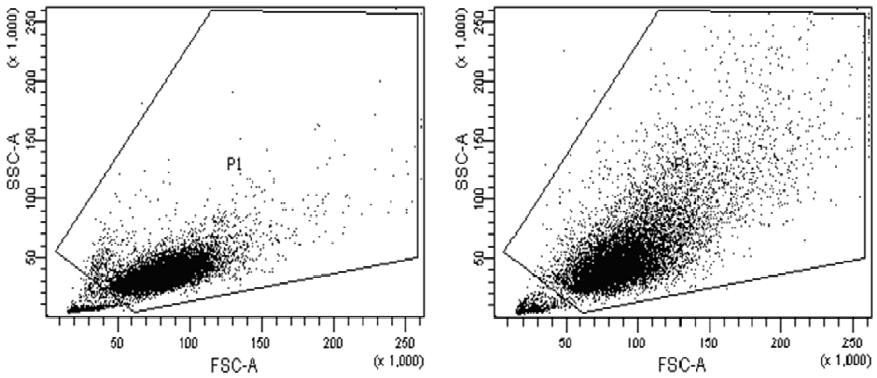

Figure 23. Representative FSC (cell volume) versus SSC (granularity) cell frequency dot-plots of WT (right) and VDRKO (left) VSMC, grown in the presence of 10%FBS. Each plot represents a minimum of 10 000 cellular events.

With respect to the distribution of the cells in the cell cycle phases, FACS analysis revealed that VDRKO cells after 48h in 10%FBS culture medium presented 72.9 ± 6 % in G_1 phase, 3.9 ± 0.4 % in S phase and 16.8 ± 3.9% in G_2/M phase in comparison to WT cells with 64.4 ± 3.9%, 15 ± 0.6%, 15.9 ± 3.5% in G_1, S and G_2/M phase, respectively (Figure 24). Thus, the difference between the WT and the VDRKO cells was mainly in the G_1 and S phases, meanwhile a constant percentage (approximately 14% of the cells) showed the 4n DNA content characteristic of the G_2/M phase. The very low percentage of knockout cells in the synthetic phase of the cell cycle points to a possible arrest of the mutant cells in the G_1/S transition, even in the presence of 10% FBS.

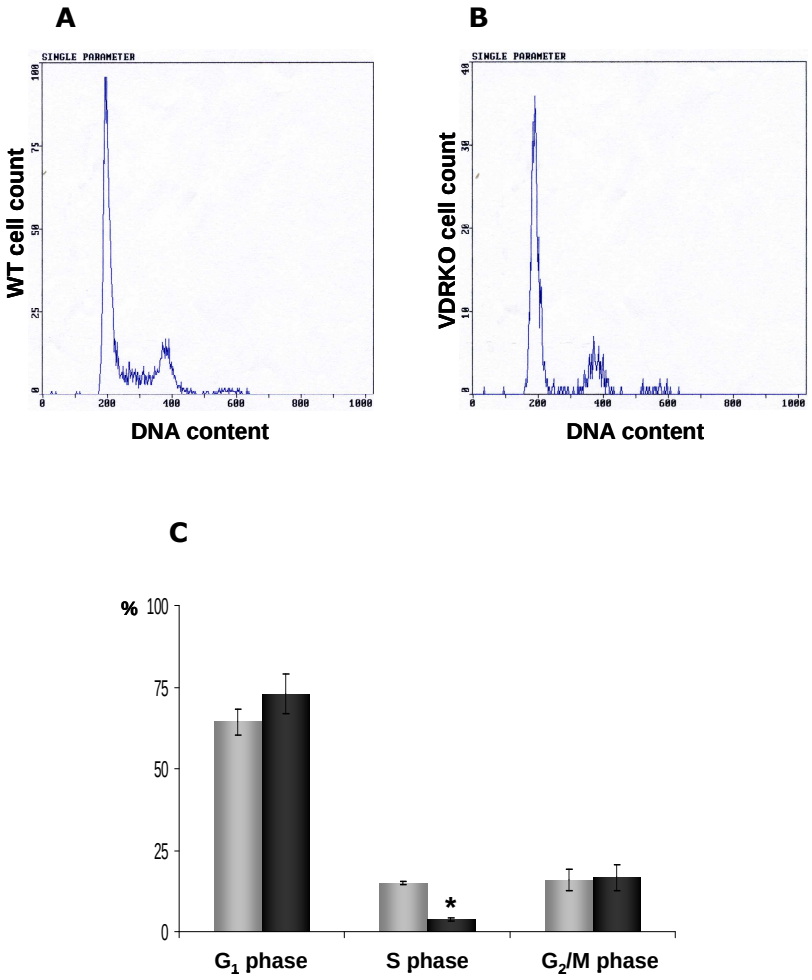

Figure 24. FACS analysis: frequency histograms of the distribution of WT (A) and VDRKO (B) cells in the phases of the cell cycle. The percentage in each cell-cycle phase was assayed for cells whose DNA content was between diploid (2n) for G_0/G_1 phase and tetraploid (4n) for G_2/M phase, as detected by propidium iodide fluorescence of RNase-treated cells. Representative graphic of WT (grey bars) and VDRKO (black bars) cell ranges of cell cycle distributions (C), * $p < 0.05$.

5. Nuclear morphology

In order to evaluate whether the lower cell number in the VDRKO populations was due to an increase in the cell death events, the nuclear morphology of both cell cultures was assessed by Hoechst 33258 staining. Following the guidelines of the Nomenclature Committee on Cell Death (NCCD) from 2009 [230] one of the criteria to considered a cell dead is when the cell, including its nucleus presents complete fragmentation into discrete ("apoptotic") bodies. The observation of the cell nuclei under fluorescent microscope revealed a similar percentage of cells with nuclear condensation of the chromatin between the WT and the cells lacking VDR, grown in parallel in 10%FBS DMEM during 48 hours and then serum deprived for 24 hours (Figure 25).

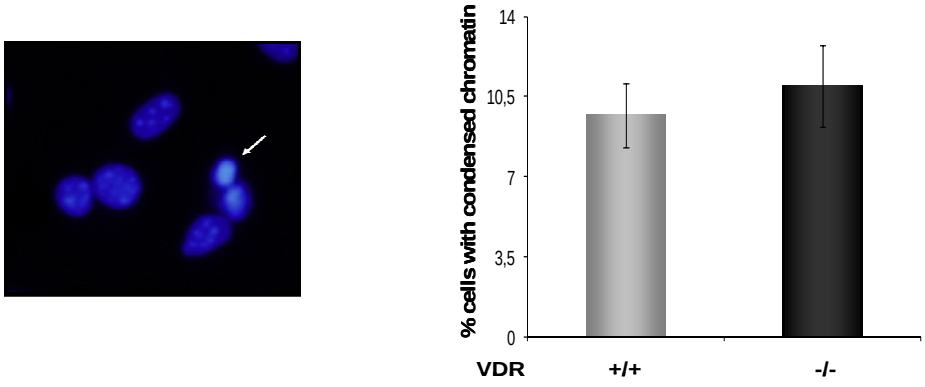

Figure 25. Fluorescence micrograph of cells stained with Hoechst 33258 dye to reveal nuclei. The white arrow shows chromatin condensation. The percentage of cells with condensed pyknotic nuclei for WT (grey bars, +/+) and VDRKO (black bars, -/-) VSMCs are presented in the graph. From each sample at least 500 nuclei were scored. Data are mean ± SEM for two independent experiments.

6. Expression of factors, involved in the regulation of the VSMC proliferation

6.1. Expression of cell cycle regulators

It is widely accepted that mitogens promote cell cycle progression of quiescent cells via accumulation of D-type cyclins in the early G1 phase. An important negative regulator of G1-cell cycle progression is pRb, the product of the retinoblastoma tumor-suppressor gene. Unphosphorylated pRb binds members of the E2F family of transcription factors, and thus inhibits the transcription of E2F-responsive genes necessary for cell cycle progression. In order to be inactivated by

phosphorylation, pRb needs the full activity of the cyclin D and cyclin E, together with their corresponding cyclin-dependent kineses (CDK4/6 and CDK2, respectively). The hyperphosphorylation of pRb by cyclin-dependent kinases leads to dissociation of pRb from E2F, allowing transcription of E2F regulated genes. The activity of the complexes is regulated by the so called cyclin-dependent kinase inhibitors (CKI). By Real Time PCR we checked the relative mRNA expression of two CKI – $p21^{Cip1}$ and $p57^{Kip2}$. They were both found to be significantly higher in VDRKO cells (Figure 26 A and B). After the addition of growth factors containing FBS, difference in the levels of $p57^{Kip2}$ only was still present between WT and VDRKO cell.

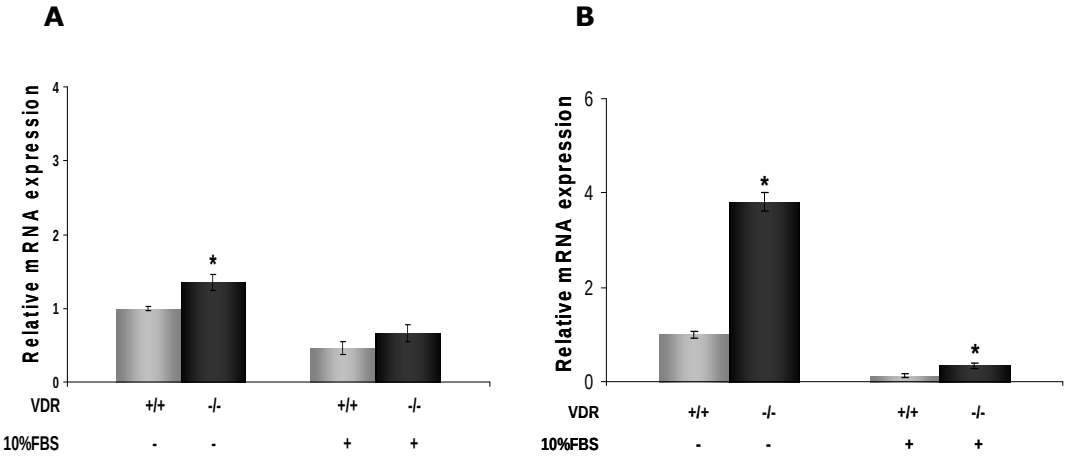

Figure 26. The relative mRNA expression of two of the CKI, $p21^{Cip1}$ (A) and $p57^{Kip2}$ (B) was assessed by Real time PCR. The levels of the WT cells are presented as grey bars, and of the VDRKO in black bars, *p< 0.05 (n=3).

These findings were confirmed at protein level (Figure 27). Several studies have shown that even though the members of the Cip/Kip family are potent inhibitors of cyclin E- and A-dependent kinases, rate-limiting and essential for DNA replication, they act as positive regulators of cyclin D-dependent kinases that starts the phosphorylation of pRb. In the mutant cells the levels of cyclin D were similar, meanwhile of the cyclin E were found to be decreased (Figure 27). Cyclin D with its co-partner CDK4/6, that is constitutively expressed, phosphorylates pRb, but in order to be hyperphosphorylated, pRb needs the activity of cyclin E. Thus, it was normal to expect that the levels of hyperphosphorylation of pRb were lower than in the control cells. By western blot we checked also the expression of $p27^{Kip1}$ and $p19^{Arf}$ (Ink4a-Arf family). There was a strong increase in their expression in the VDRKO cells, which was reduced when the cells were stimulated to grow (Figure

27). Therefore, it seemed possible that the lack of signalling trough VDR may influence the cell cycle arrest through upregulation of the cell cycle inhibitors $p21^{Cip1}$ and $p57^{Kip2}$.

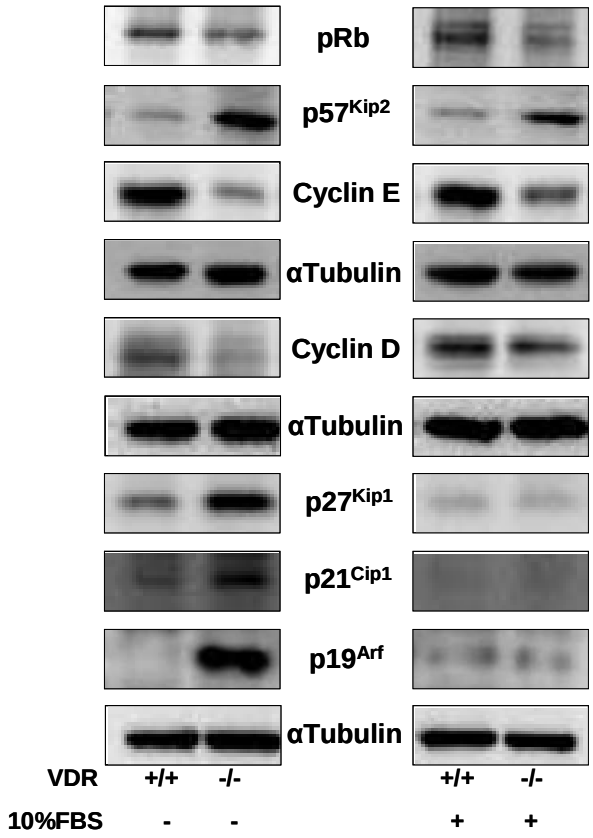

Figure 27. Expression pattern of cell cycle regulatory molecules in WT (+/+) and VDRKO (-/-) cells. The control of loading was done against α-tubulin. Panel depicts one representative western blot for every protein.

As $p57^{Kip2}$ was found to be differentially expressed at any moment during the VDRKO culturing we decided to search such genes that could intermediate the effect over $p57^{Kip2}$ expression, found in the VSMC lacking VDR.

6.2. Expression of transforming growth factor beta and two of its responsive genes in VSMC

6.2.1. TGF-β1 relative mRNA expression

Cell enlargement or hypertrophy plays a prominent role in the postnatal growth of many tissues, as well as in physiological and pathological hypertrophy of a variety of tissues. One possible candidate for a substance that might elicit hypertrophic response in smooth muscle cells is transforming growth factor-β

(TGF-β).[231] In a study after unilateral nephrectomy, $p57^{Kip2}$ was found to mediate the TGFβ -induced hypertrophy.[232]

As we already had found a significant increase in the $p57^{Kip2}$ expression, we decided to check the relative mRNA level of TGFβ1 in our model. By Real Time PCR we found a significantly higher expression of TGFβ1 in VDRKO cells under deprivation conditions. When the cells were switched to normal growth medium containing FBS, the TGFβ1 levels decrease significantly in both cell populations and the difference found in basic conditions was lost (Figure 28).

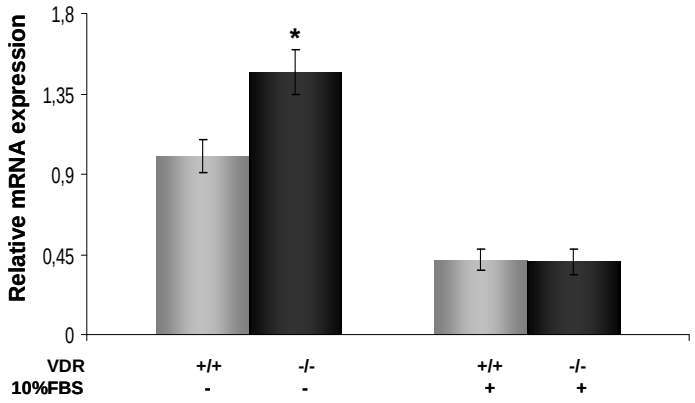

Figure 28. Relative mRNA TGFβ1 expression in WT (grey bars) and in VDRKO (black bars) VSMC, cultured under deprivation conditions (without FBS) and stimulated to grow (10%FBS).

6.2.2. TGFβ1 effectors genes: collagen type I and α-SMC

An important physiological characteristic of TGF-ß is the de novo synthesis of ECM proteins. Moreover, TGF-ß has been shown to inhibit the expression of matrix metalloproteinases, a family of proteins that degrade ECM proteins [233]. TGF-β, together with serum response factor (SRF), are the two major regulators of the α-smooth muscle actin (α-SMA) gene expression through CArG boxes for SRF and TGF-β-control elements (TCE).[234] TGF-β which expression was increased in the airways of individuals with severe asthma, increased cell size and total protein synthesis, expression of α-smooth muscle actin and smooth muscle myosin heavy chain and thus hypertrophy in primary bronchial smooth muscle cells.[235]

As these two proteins – collagen and α-SMA are very important molecules in the biology of VSMC we decided to check their levels in our model. We found differences in the expression of TGFβ1 only in basal conditions that's why the

expression of its responsive genes was checked also when the cells (WT and VDRKO) were cultured without FBS. For both genes, the expression levels in VDRKO cell were significantly higher (Figure 29).

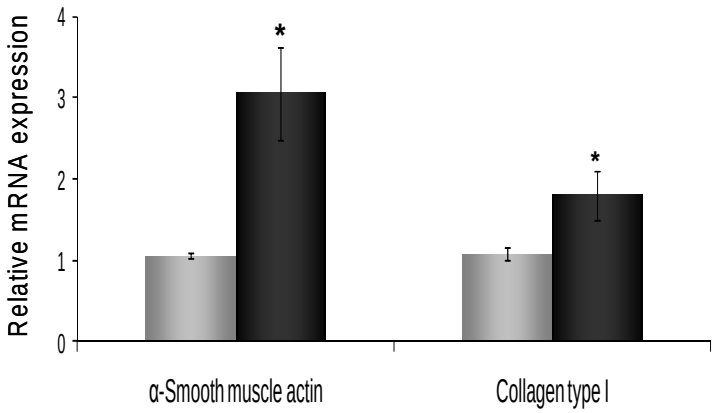

Figure 29. Relative mRNA expression of two TGFβ1 genes in WT (grey bars) and in VDRKO (black bars) VSMC, cultured under deprivation conditions (without FBS) and stimulated to grow (10%FBS).

It has been shown that the arteries from hypertensive patients and animals have a greater SMC content than normotensive individuals. The arterial thickening is thought to be an important adaptive response to the elevated wall stress provoked by the increased blood pressure [236]. As the renin-angiotensin-aldosteron (RAAS) has a leading role in the maintenance of the blood pressure, great number of studies explored the role of angiotensin II (Ang II) in the mediation of VSMC hypertrophy in large vessels during chronic hypertension. For this reason we decided to check the production of Ang II in the culture medium of both VSMC cultures.

7. Angiotensin II production

7.1. Cathepsin D expression

In VDRKO mice a higher renin expression was found and its increased activity was the reason for the elevated plasma angiotensin II levels [188]. VSMCs from these mice we were not able to find transcripts encoding for renin by RT-PCR. In contrast, VSMCs from both genotypes contained cathepsin D mRNA (an enzyme with renin-like activity), the abundance of which was significantly ($P<0.05$) higher in quiescent cells from VDRKO mice than in those from WT controls. When 10%FBS was added, the expression of cathepsin D in the mutant cells was reduced to the levels found in

the control cells. In WT cells the withdrawal of growth factors didn't play a role, because the mRNA levels of cathepsin D were similar in 0.2% and 10% (Figure 30).

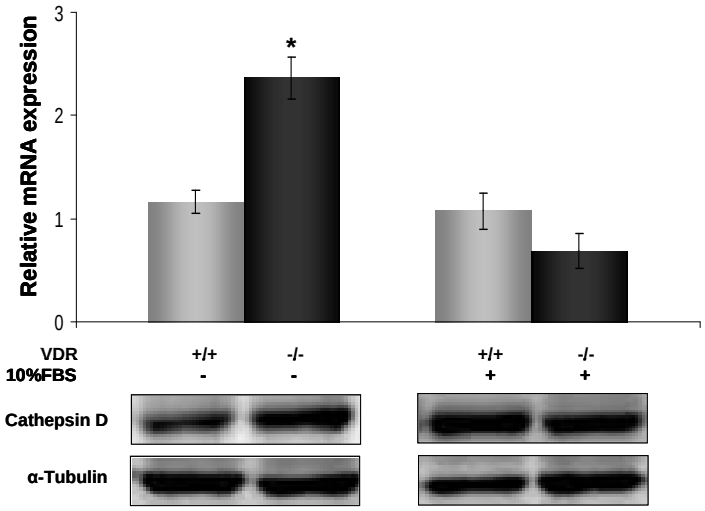

Figure 30. RT-PCR (up) and Western blot (down) analysis detected cathepsin D expression in WT (grey bars, +/+) and VDRKO (black bars, -/-) VSMC at mRNA and protein levels, respectively. The abundance of cathepsin D was significantly greater in quiescent (grown in medium without serum) VDRKO cells.

It has been demonstrated that this lysosomal aspartic proteinase cathepsin D has renin-like activity, being able to catalyze the hydrolysis of angiotensin I from angiotensinogen. Studies with spontaneously hypertensive rats have shown increased expression of cathepsin D, together with higher endogenous production of angiotensin II.[237] Moreover, cathepsin D induction was related to the cell response to oxidative stress, cytokines, and aging.

7.2. EIA for Ang II

The finding that the VDRKO cells are larger than the WT controls and they express higher levels of TGFß1, collagen, and α-SMA was the reason to measure the production of Ang II in the culture medium of the studied cells. In quiescent cells, the differences in the concentrations of Ang II in WT and VDRKO cells were extremely higher with a p value less than 0.001 compared to the levels in growth medium, containing 10%FBS. Moreover, the mutant cells showed a significant increase in the Ang II content in quiescent state, as well as when they were stimulated to grow by FBS in comparison to the WT (Figure 31).

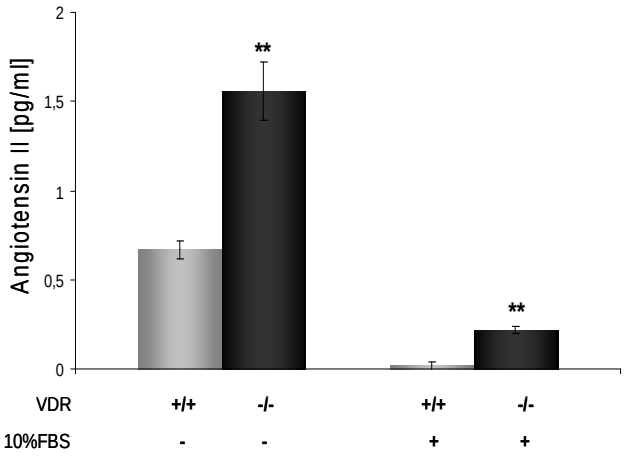

Figure 31. The Ang II concentrations (pg/ml) in the culture medium of WT and VDRKO cells were checked by a commercial EIA kit. WT (grey bars), VDRKO (black bars), ** statistical significance was considered at $p < 0.01$.

When the concentration of Ang II was normalized to the protein content, as a determinant of the cell mass, very similar results were obtained. As the graphic was the same it is not presented here.

7.3. Angiotensin II receptors expression

In order to exert its biological actions, Ang II interacts with a family of angiotensin receptors, and especially with the two main – angiotensin II receptor type I (AT1-R) and type 2 (AT2-R). In our model, we found higher mRNA levels of both, AT1a-R and AT2-R receptors in the mutant cells in quiescent conditions. After the incubation of the cells with 0.2%FBS the expression of both receptors was also higher in the VDRKO cells at protein level (Figure 32 panel A). When the cells were stimulated to grow, the elevated expression of AT1a-R in VDRKO cells was no more detectable, even became lower than in the control cells, meanwhile the expression of the other Ang II receptor (AT2-R) was maintained higher in the mutant cells (Figure 32 panel B).

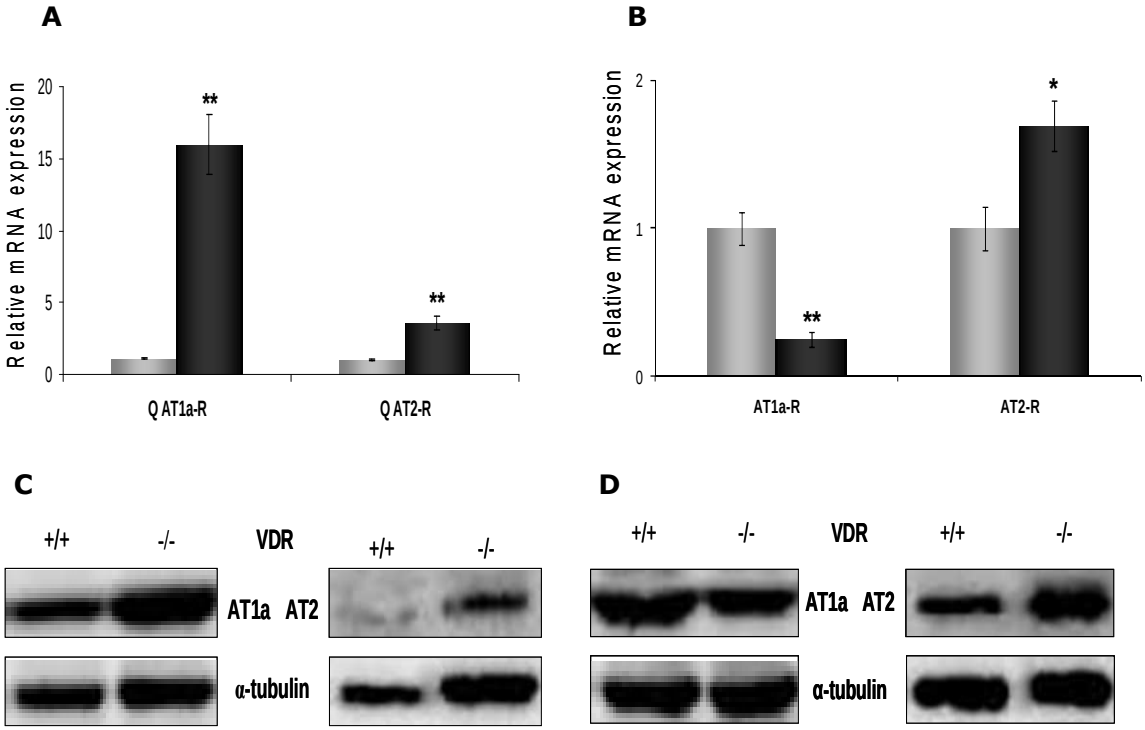

Figure 32. Messenger RNA (mRNA) and protein levels of both Ang II receptors, AT1a and AT2, in quiescent (A, C) and growing (B, D) WT (grey bars, +/+) and VDRKO (black bars, -/-) VSMC, * p< 0.05. In the mRNA measurements GAPDH was used like a housekeeping gene, and the α-tubulin expression was used as a loading control in the WB analysis.

8. IL-6 expression

Apart of the pro-fibrotic actions of Ang II, another very important feature are its pr-inflammatory effects in the cardiovascular system. Among the cytokines that mediate the inflammatory response in VSMC interleukin 6 (IL-6) play a central role. Funakoshi et al. have shown that exogenous Ang II treatment dose-dependently increases the expression of IL-6 sustained to 24 hours after stimulation.[238] The induction of IL-6 is also found to be mediated by TGBβ.[239]

In VDRKO cells the expression of pro-inflammatory IL-6 was measured by RT-PCR (Figure 33) and a significant increase in its expression was found in comparison to the WT cells.

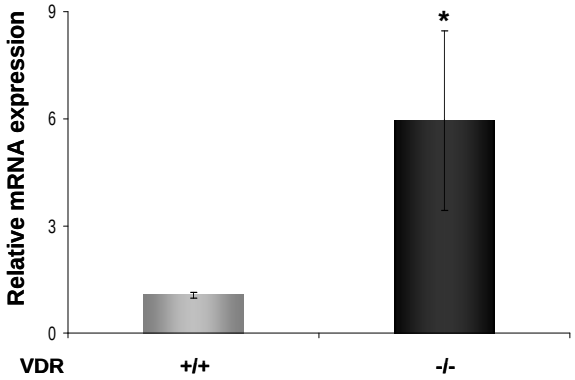

Figure 33. Expression of IL-6 checked by Real Time PCR in WT (grey bars) and VDRKO (black bars), * p< 0.05.

9. Expression of the inducible nitric oxide synthase (iNOS)

The inorganic molecule NO has been well documented as an inhibitor of total protein synthesis and of the expression of extracellular matrix proteins (collagen)[240] as well as a pro-inflammatory mediator. Studies with the TGF-beta family of cytokines and the enzyme nitric oxide synthase (NOS) have suggested that the interaction of these molecules represent a central homeostatic mechanism with implications for a variety of human diseases. Studies with several cell types in vitro indicate that TGF-beta1 negatively controls the inducible nitric oxide synthase (iNOS) by reducing its expression and activity at multiple levels. It has been shown that 1,25-dihydroxyvitamin D3 is also a potent stimulus for NO production in macrophage-like HL-60 line.[241] But in the literature the role of vitamin D over the iNOS expression is still controversial as others in vitro and in vivo studies report inhibitory actions of $1,25(OH)_2D_3$ on iNOS levels.[242]

As we already have found decrease in the proliferation rates in our mutant cells, together with increased TGFβ1 expression, we decided to check the expression levels of iNOS by Western blot. After the densitometry analysis, we found that when the cells were stimulated to grow with 10%FBS, there was a minimal expression of iNOS in both cell cultures. Then, the serum starvation significantly increased the iNos expression, but this increase was significantly lower in the mutant cells (Figure 34).

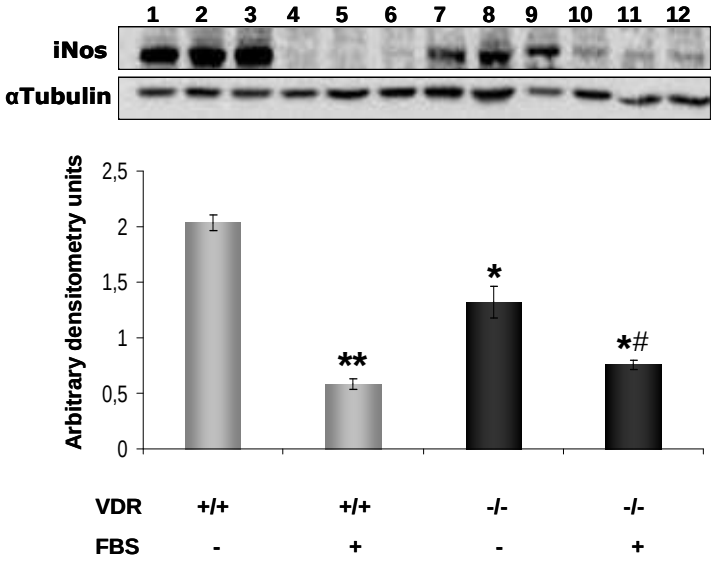

Figure 34. Expression of iNos in WT (lines 1,2,3; grey bars) and VDRKO (lines 7,8,9; black bars) quiescent cells, and cell, stimulated to grow (WT: lines 4,5,6) and (VDRKO: lines 10,11,12), *<0.05, **< 0.001 vs growth arrested WT, and # vs growth arrested VDRKO.

10. Treatments of wild type VSMC

In previous work of our laboratory it has been found that $1,25(OH)_2D_3$ (5-100 nM) induces a dose-dependent increase in rat VSMC proliferation in both quiescent cells and cells stimulated to grow. This increase in the proliferation was achieved by shortening the G_1 phase [185]. In these experiments a dose of 10^{-7}M was found sufficient in order to induce $1,25(OH)_2D_3$ gene regulation.[243]

In the present work, after a 24 hours growth factor starvation, we treated only WT cell with 100nM $1,25(OH)_2D_3$ during 24 hours in basal conditions (without FBS). For two genes that are known to be vitamin D responsive, VDR and 24OHase, we found a significant increase after the stimulation with $1,25(OH)_2D_3$. The genes which we observed to be upregulated in VDRKO cells ($p21^{Cip1}$, $p57^{Kip2}$, collagen type I, α-smooth muscle actin) the active form of vitamin D was able to reduce their expression significantly to almost 50% (Figure 35). A decrease in the expression of cathepsin D was also found, without reaching statistical significance.

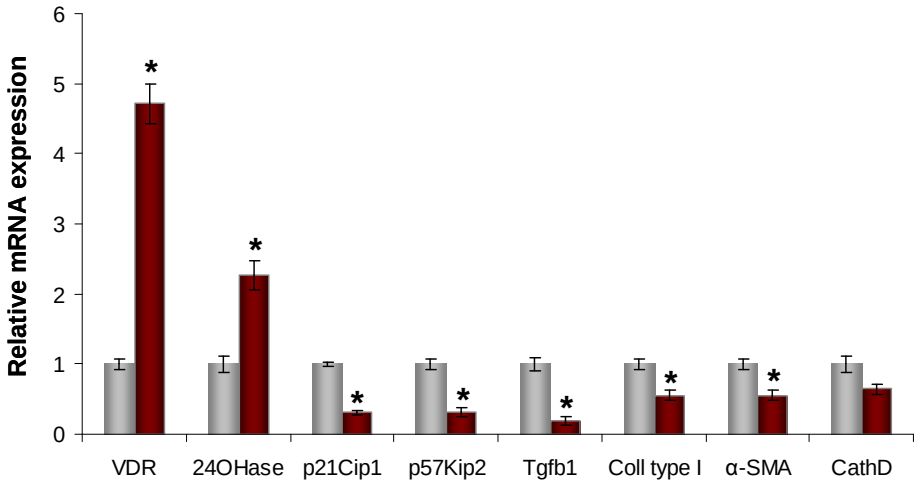

Figure 35. Reprisentative RT-PCR analysis of some vitamin D responsive genes. The control cells are presented as grey bars and the cells with 100nM 1,25$(OH)_2D_3$ treatment in red bars. The expression of all genes of interest in the control cells was considered as 1 and the one of the treated cells – as fold change in relation to the expression of the control, * $p<0.05$. The data is presented as mean ± SEM.

11. Metabolic studies

11.1. Senescence associated β-Galactosidase activity

The pre-aged phenotype of the VDRKO mice and the enlarged stella-like shape of the aortic VSMC, obtained from these mice, together with the decreased proliferation rates in culture and their different gene profile, made us check if these cells suffered cellular aging. To confirm the presence of senescence in our VDRKO cultures, we investigated the expression of the senescence biomarker senescence-associated β-galactosidase (SA-β-Gal). Dimri et al. described at pH 6.0 β-galactosidase activity was found specifically in senescent human fibroblast cultures, but not in quiescent or terminally differentiated cells.[244] We performed a cytochemical staining for SA-β-Gal activity at pH 6.0 in WT and VDRKO and the SA-β-galactosidase positive cells was determined by the blue cells under bright field illumination, and then the total number of cells in the same field under phase contrast. Representative fields were photographed. We found that some of the mutant cells presented blue perinuclear staining even in passage 4, meanwhile WT cells stayed negative until passage 10. In figure 36 we present some typical cell of both types.

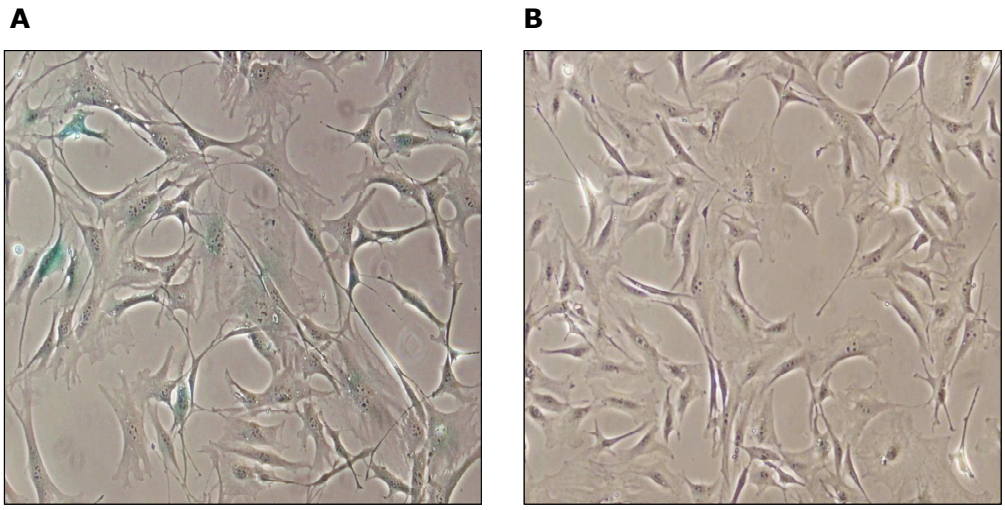

Figure 36. Cytochemical staining of SA-β-gal activity in VDRKO (A) and WT (B) after 20 hours in the X-gal solution at pH 6.0.

11.2. MTT assay

Starting with the same cell number on day 0, 72 hours later, 3-(4,5-dimethylthiazol-2-yl)-2,5-diphenyltetrazolium bromide was added for one hour and during this time the alive adherent cells present in the well formed water-insoluble crystals of formazan which were dissolved in DMSO and colorimetrically detected at 540 nm. Absorbance readings were proportional to the number of living and metabolically active cells. In parallel wells, the cell number of both WT and VDRKO cells was determined. The decrease in the absorbance at 540nm seen in the VDRKO cells was associated with a lower number of adherent viable cells. But even when the absorbance was normalized to the cell number, there still was a significant decrease, probably due to the impaired mitochondrial function (Figure 37).

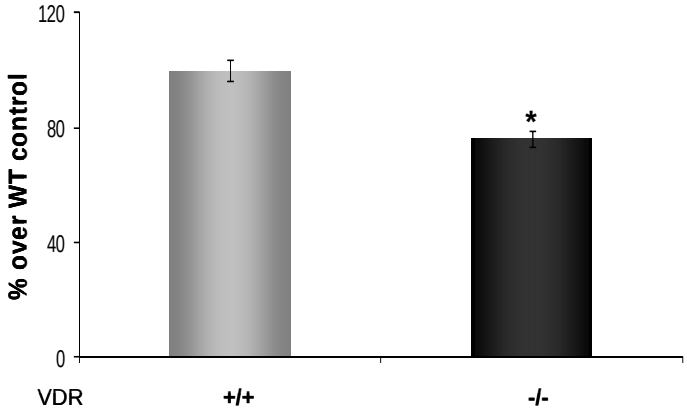

Figure 37. Starting with the same cell number on day 0, after synchronization of the cells in the Go of the cell cycle and 24 hours in quiescent conditions afterwards, VDRKO (black bars) cells presented lower conversion of the MTT to formazan in comparison to the WT (grey bars)* $p < 0.05$.

12. Analytical cytology by transmission electron microscopy (TEM)

The morphology of growing subconfluent WT and VDRKO was analyzed by transmission electron microscopy. The nucleus of the VDRKO cells was irregular with wrinkled membrane, predominantly found in the central area. Its chromatin appeared clear, with levels of heterochromatin lower than in WT. In some of the mutant cells, the heterochromatin was agglomerated and stuck against the inside of the nuclear membrane. Also, the number of vacuoles of various sizes and lysosomes were notably increased in the cytoplasm of these cells in comparison to the control. Moreover, the cytoplasm was occluded with electron dense substances and contained more vesicles. Besides, double-membrane bound autophagosomal vacuoles were also observed. We observed that the VDRKO cells contained swollen mitochondria with damaged cristae (Figure 38). The mitochondria of the mutant cells were either dispersed in this central area or aggregated close to the nucleus and appearing very contracted and oxidized. Some of these altered mitochondria were found inside the autophagic vacuoles. The morphology of our mutant cells were to a great extend similar to the one observed in senescent keratinocytes which displayed altered mitochondria and nuclei.[245]

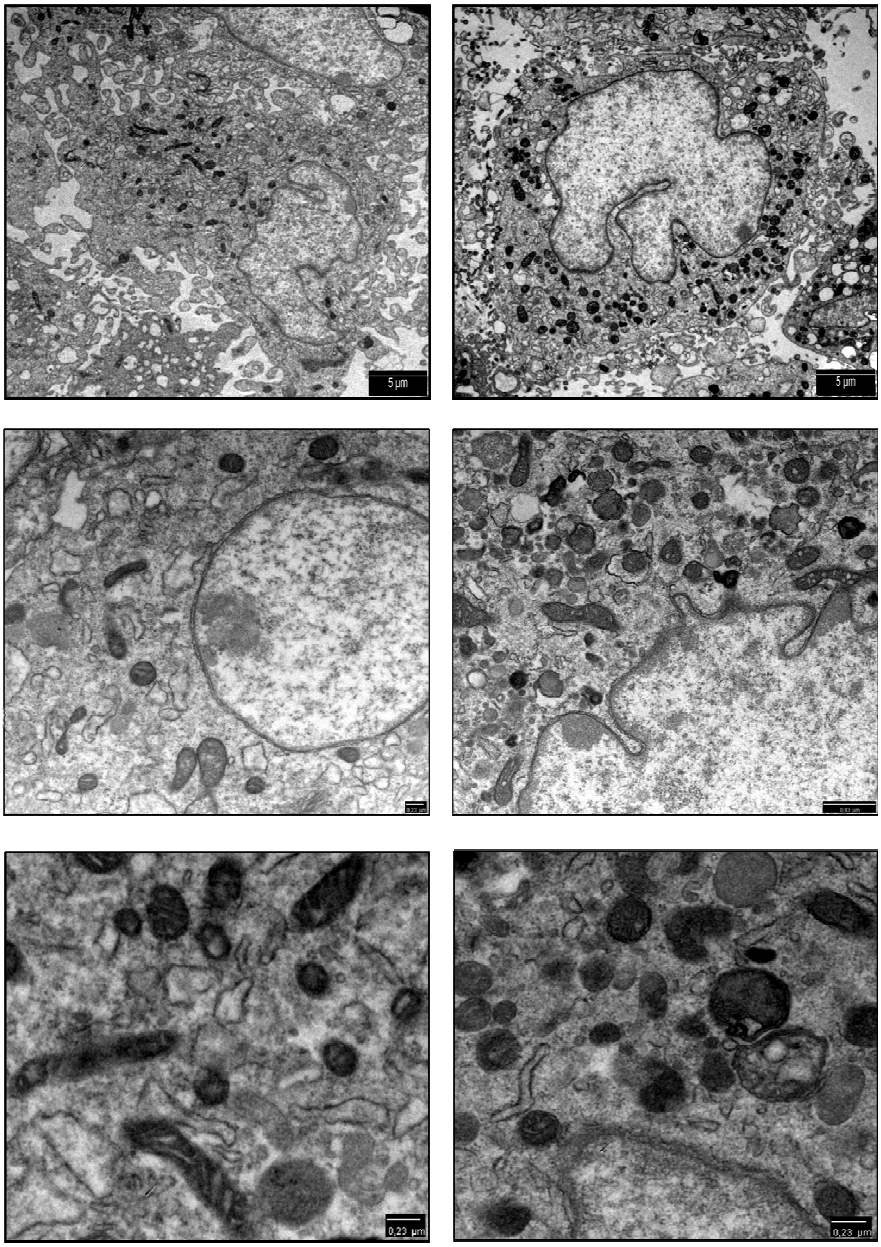

Figure 38. Transmission electron microscopy analysis. Representative photographs of VSMC from WT (panel A, C, E) and VDRKO (panel B, D, F) mice showed stronger staining and swelling mitochondria in the mutant cells. Bars are 5µm (A, B), 0.23 µm (C, E, F) and 0.93 µm (D).

The mitochondrial damage, seen in the TEM analysis, made us check if there were any differences in the mitochondria at functional level, as a possible free radical source.

13. Western blot analysis for the complexes forming the mitochondrial respiratory chain

Representative subunits of mitochondrial respiratory complexes I to IV were analyzed by Western blotting and representative blots are presented in figure 25A. In our experimental model, the only complex that showed different expression in the mutant cells was complex I. Complex I, or NADH ubiquinone oxidoreductase, provides the input from the NAD-linked dehydrogenases of the citric acid cycle to the respiratory chain. The complex couples the oxidation of NADH and the reduction of ubiquinone, to the generation of $4H^+$/NADH across the coupling membrane, thus forming a proton gradient which is used for ATP synthesis. The channel-forming protein porin is localized in the outer membrane of mitochondria where it forms the primary pathway of metabolites across the membrane. After the densitometry analysis and normalization to the expression of porin as a control for variations in mitochondrial protein loading, this decrease was found to be significant (Figure 39B).

A **B**

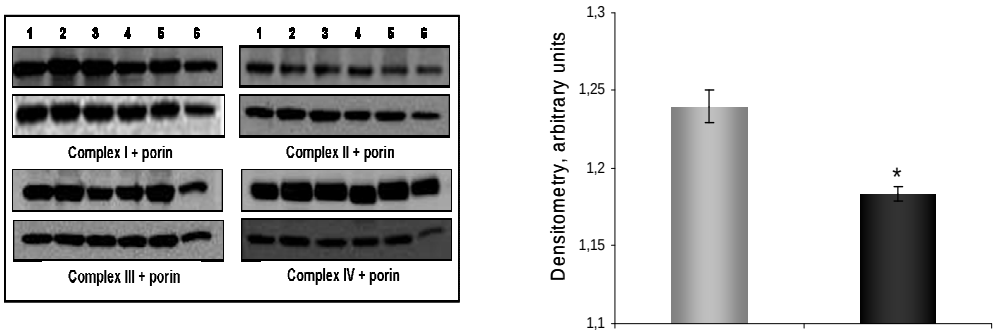

Figure 39. Representative western blots of the mitochondrial Complexes I to IV, together with the porin expression in WT (lines 1, 2, 3) and VDRKO (lines 4, 5, 6) cells (A). The expression of Complex I was determined by densitometry and normalized by porin signals (Complex I/Porin). Results are presented in grey (WT) and black (VDRKO) bar graphs as means ± SE. *, p <0.05.

It has been shown excessive reactive oxygen species production in families with cardiomyopathy, cataracts, and complex I deficiency of the mitochondrial respiratory chain.[246] For this reason, we decided to measure the respiration of the VDRKO cells and compare it to the one of the WT.

14. ATP content

In order to estimate the bioenergetic state of the VSMC, we determined its ATP content. The ATP content in VDRKO cells was lower than in WT cells, indicating a metabolic dysfunction, either a higher ATP consumption or an impaired ATP production (Figure 40).

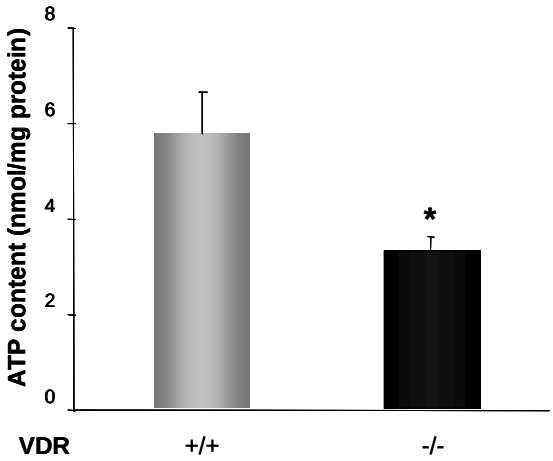

Figure 40. ATP content (nmol/mg protein) of WT (grey bars) and VDRKO (black bars). Bars represent the means ± SD for 4 parallel experiments, * p <0.05 with respect to WT cells.

In order to confirm the lower content of ATP in the mutant cells we performed an immunoblotting, in which the levels of the phosphorylation of adenosine monophosphate (AMP)-activated protein kinase or AMPK were measured. This enzyme is a sensor of cellular energy status, activated by a variety of cellular stresses that deplete ATP, which increasing the AMP/ATP ratio. After synchronization of the cells by overnight serum starvation, we treated both, WT and VDRKO cells with 0.4mM H_2O_2, 2µg/ml oligomycin, and 10%FBS for a period of one hour. We used oligomycin which is a mitochondrial ATP synthase inhibitor (complex V) and as an additional control H_2O_2, because it has been shown that this compound also induces AMPK activation [247, 248]. Then, the cell lysates were probed with anti-AMPK, basal and phosphorylated, antibodies. As it can be seen in the representative WB (Figure 41) after the normalization of the phosphorylated levels of AMPK to its basal expression VDRKO presented higher activation of the enzyme, with was in accordance with the lower ATP content. Moreover, in the same samples, the phosphorylation of ERK1/2 was checked. It has been shown that some metabolic inhibitors rescued cell death in vitro, activating ERK pro-survival

signalling, which is known to be induced by growth factors addition. The treatment with oligomycin slightly induced the phosphorylation of ERK in WT cells, meanwhile in the mutant cells had the opposite effect, decreasing its phosphotylation.

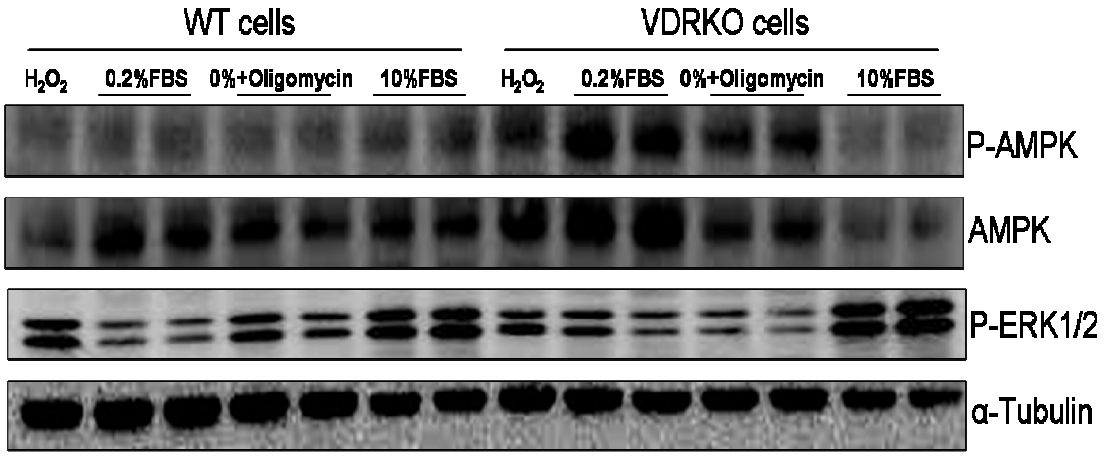

Figure 41. Representative western blot with anti P-AMPK and P-ERK antibodies of WT (grey bars) and VDRKO (black bars) cells grown in 0,2%FBS DMEM, and treated with 0.4mM H2O2, 2 µg/ml Oligomycin or 10%FBS during 1 hour. Data is means ± SD.

15. Respiratory flux measurements

To assess the second hypothesis about the impaired ATP production and because mitochondria are the main source of cellular ATP, we measured the mitochondrial function by high resolution respirometry. The experimental work with the Oroboros® Oxygraph-2k and the analysis of the data, using the specific software, were kindly done by Dr Jordi Boada. As it is shown in figure 42, the experiments started with the registration of the routine respiration of the cells, followed by the inhibition of complex V of the mitochondria electron chain by oligomicin to the final inhibition of the complex III with antimycin A.

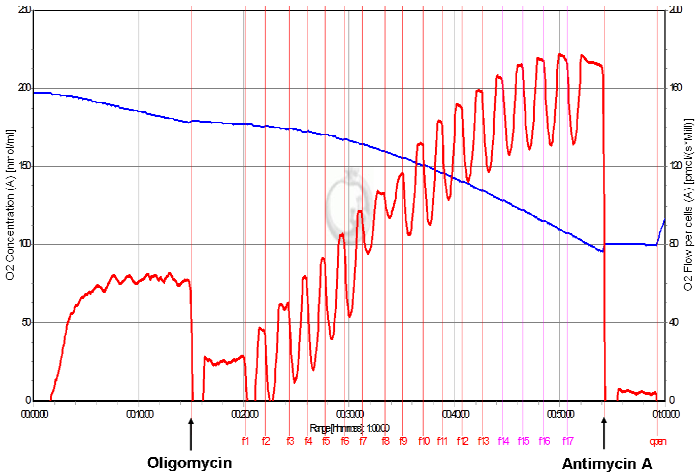

Figure 42. Representative traces of oxygen concentration and respiration in the closed respirometer chamber at 37°C. Arrows show two steps of the titration, the initial with oligomycin, leading to the inhibition of ATP synthase, thus achieving an ADP-independent state, followed by maximal stimulation by FCCP and the final one with antimycin A.

The results of the high-resolution respirometry normalized to the cell number showed that the respiration per cell is lower in VDRKO, both coupled and uncoupled (Figure 43).

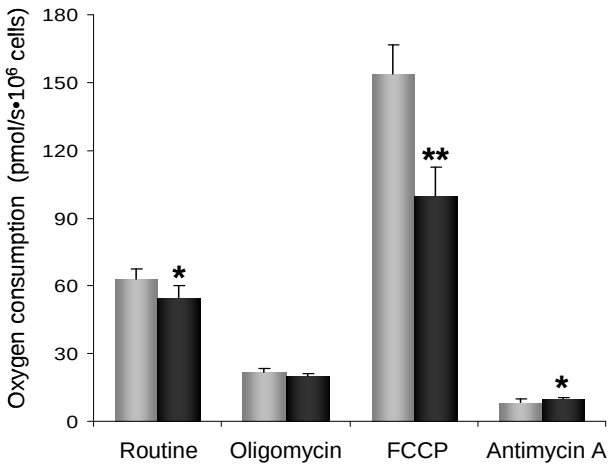

Figure 43. Representative respiration of WT (grey bars) and VDRKO (black bars) cells in various states of mitochondrial respiratory control. Bars represent the means ± SD for 6 parallel experiments. Values were normalized by cell number, * p <0.05 and **, P <0.01 with respect to WT cells.

As we already knew that the mutant cells had bigger size, we normalized the respiration by the activity of the enzyme citrate synthase, which reflects the

mitochondrial mass of the cell. As a result, the former difference in oxygen flux was lost (Figure 44). The only type that was still significantly higher was the residual respiration after the inhibition with actinomycin A.

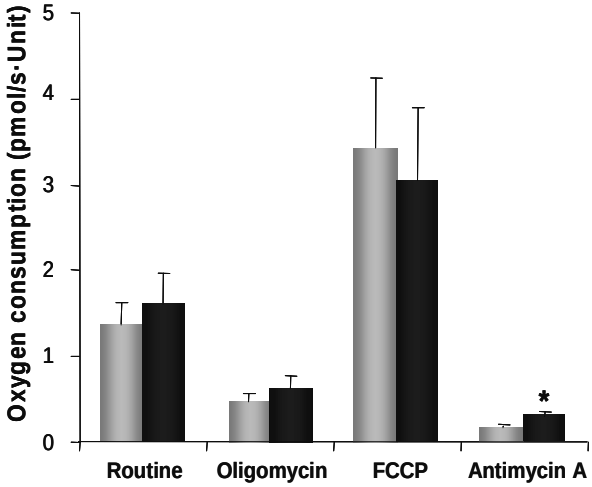

Figure 44. Respiration of WT and VDRKO cells in various states of mitochondrial respiratory control. Respiration of WT (grey bars) and VDRKO (black bars) cells. Bars represent the means ± SD for 6 parallel experiments. Values were normalized by citrate synthase activity that was determined in parallel, * p <0.05 and **, P <0.01, with respect to WT cells.

However, when the same data were used to calculate the mitochondrial respiratory control ratios, an estimation of the mitochondria efficiency, the differences between WT and VDRKO cells were significant again (Figure 45).

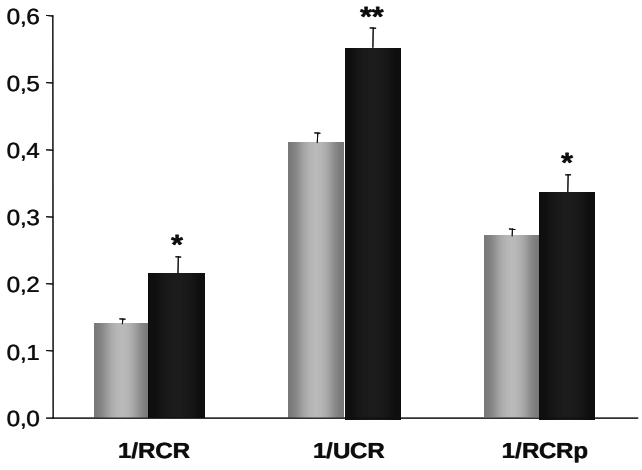

Figure 45. Respiration of WT and VDRKO cells in various states of mitochondrial respiratory control. Calculated inverse control ratios of WT (light bars) and VDRKO (dark bars) cells. RCR, respiratory control ratio; UCR, uncoupling control ratio; RCRp, phosphorylating control ratio. *, P < 0.05 and **, P <0.01, with respect to WT cells.

These findings, together with the lower ATP content in VDRKO cells, indicated that the mitochondria of VDRKO cells are less efficient. Moreover, the significantly higher residual respiration in the mutant cells in the presence of antimycin A is probably due to extra-mitochondrial consumption of oxygen which could be associated with increased production of reactive oxygen species (ROS).

16. Superoxide levels measurements

Reactive oxygen species (ROS) are derivatives of O_2 metabolism, including superoxide anions, hydrogen peroxide, hydroxyl radicals and nitric oxide. In vascular cells, ROS are important intracellular signalling molecules that regulate vascular function, modulating cell growth/apoptosis, migration and extracellular matrix protein turnover, thus contributing to vascular remodelling. Cardiovascular diseases, such as hypertension, are associated with increased ROS formation [249]. In the literature is shown by one hand that the VDRKO mice develop hypertension and due to the increased expression of renin and subsequently systemical Ang II, we decided to check the levels of superoxide anion in the VSMC obtained from these mice. We resuspended cell pellets of quiescent WT and VDRKO cells with equal cell number in PBS and the fluorescence at λ = 520ex/590em nm was measured, which then was used as basal or auto fluorescence of the cells. Then, after the addition of 10μM dehydroethidium (DHE) we measured the fluorescence of the samples at different time point until 30 minutes. The mean fluorescence of both cell populations at the indicated below time point were plotted to a graph, presented in figure 46. The resulted curves of the increase of ethidium, result of the oxidation of DHE by the intracellular superoxide anion, showed that the mutant cells had higher tendency to produce superoxide.

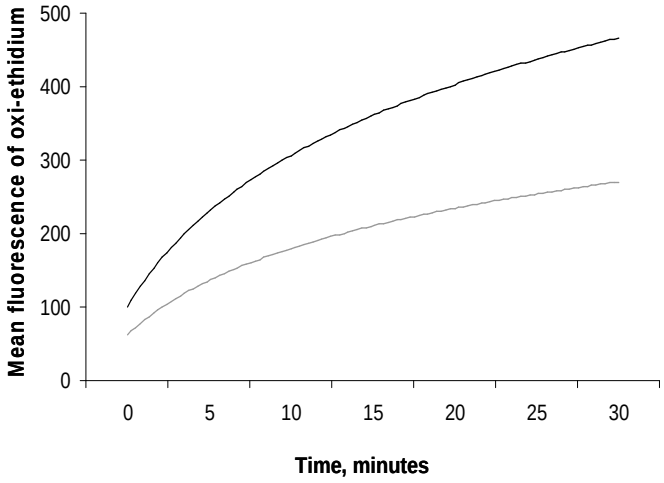

Figure 46. Change in the oxi-ethidium fluorescence, produced by the oxidation of dehidroethidium by the intracellular superoxide anion during the 30 minutes of incubation in WT (grey curve) and VDRKO (black curve) cells.

Oxidative stress in the vasculature reduces the levels of the vasodilator nitric oxide, causes tissue injury, promotes protein oxidation and DNA damage, and induces proinflammatory responses.

17.Stress-induced protein kinases

In order to check if our mutant cells were subjected to oxidative stress, due to the increased levels of superoxide anion, the activation of stress-induced kinases was determined by WB. The p38 kinase belongs to the MAP kinase superfamily which transduces signals from the cell membrane to the nucleus in response to various stimuli. Furthermore, generation of ROS in response to various external stimuli is known to activate MAP kinases, e.g. angiotensin II stimulates p38MAP kinase by a redox sensitive mechanism in vascular smooth muscle cells, which mediates VSMC hypertrophy. For Ang II-induced hypertrophy in these cells, the mitogen activated protein kinase (MAPK) ERK½ has also shown to be implicated [250]. Therefore, we performed western blot analysis using antibodies against both phosphorylated kinases. As depicted in Figure 33, in quiescent conditions, VDRKO cells showed increase phosphorylation of the above-mentioned kinases and this difference was lost when the cells were stimulated with FBS.

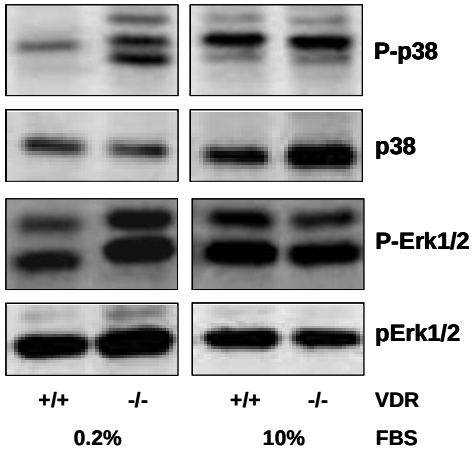

Figure 47. Quiescent VSMC were treated with fresh 0.2%FBS or 10%FBS for 24 hours and lysates were prepared as described in Materials and Methods. Representative western blots out of three for phosphorylated P-p38 and P-Erk1/2 kinases. Top panels show the phosphorylated form and the lower panels show the total (pan) levels of these kinases in WT (+/+) and VDRKO (-/-) cells.

18. Western blot analysis of superoxide dismutases, SOD1 and SOD2

The members of the superoxide dismutase (SOD) family are involved in ROS detoxification, catalyzing the dismutation of superoxide radical (O_2^-) into hydrogen peroxide (H_2O_2) and oxygen (O_2). In order to check the antioxidant levels in our VSMC cultures, we performed immunoblotting against the two main forms of SOD – the cytosolic Cu-Zn SOD1 and the intramitochondrial Mn SOD2. In figure 48 a representative out of three WB is shown. In quiescent conditions, the expression of both enzymes presented a significant increase in the WT cells; meanwhile in VDRKO cells the levels of expression of SOD1 were without change and of SOD2 showed a strong decrease when the cells were serum starved. In general the comparison between WT and VDRKO revealed that the expression levels of both enzymes were lower in VDRKO cells in quiescent conditions, and when the growth factors were added, this difference was lost. This finding could be explained with the possibility that during the basal growth of the cells there some factors that inhibits or prevent the expression of the antioxidant enzymes.

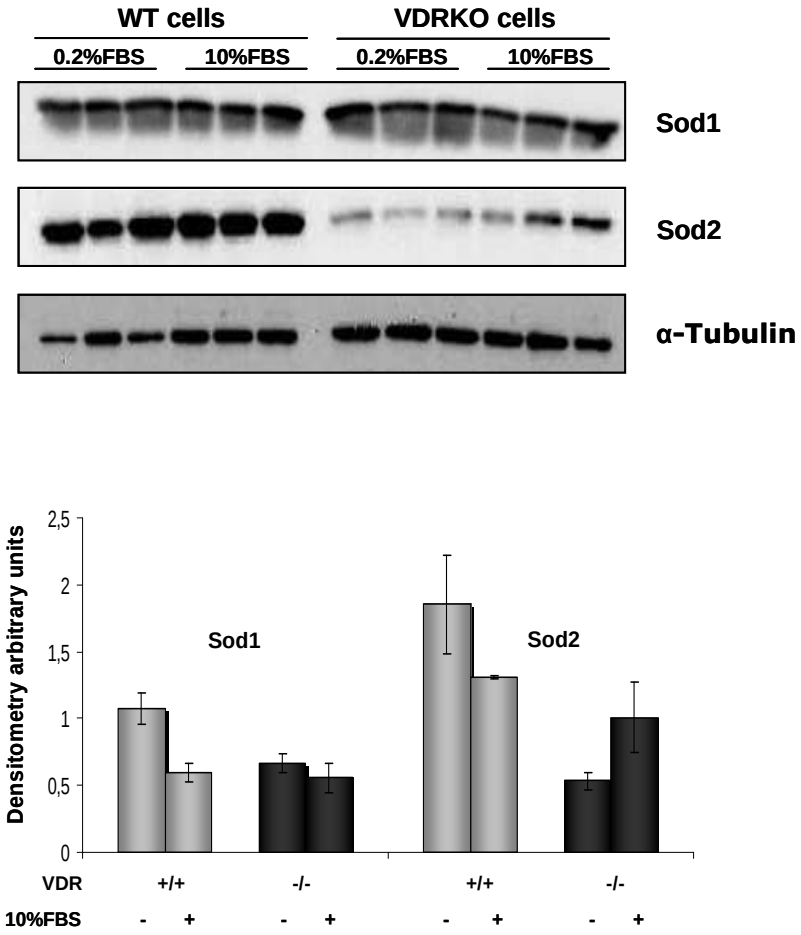

Figure 48. Representative western blots of the citoplasmic Sod1 and the mitochondrial Sod2. The graphic represents the densitometry analysis in which the expression of the enzymes in WT (grey bars, +/+) and VDRKO (black bars, -/-) was related to the tubulin levels.

19. Treatments with H_2O_2

Since the superoxide anion is rapidly dismutated to hydrogen peroxide (H_2O_2), we decided to treat our cells with this pro-oxidative compound in order to check if there were differences in the way how our cells react to the induced stress.

19.1. Expression of iNOS

In quiescent conditions we found increase in the expression of iNos. In order to check if this expression is somehow related to the levels of pro-oxidant substances, we added 0.4mM H_2O_2 to the basal medium during one hour. As it is shown in figure 35, the expression of iNos was decreased in the presence of H_2O_2 in both cell cultures, WT and VDRKO, although that in the VDRKO cells this decrease was not

significant. As we already have shown in figure 34, in the mutant cells the expression of iNos was significantly lower. The fact that the in oxidant conditions the expression of iNos was inhibited is in accordance with the statement that the ROS are able to reduce the expression of the enzyme and thus the production of NO which is believed to have protective role, counteracting the ROS.

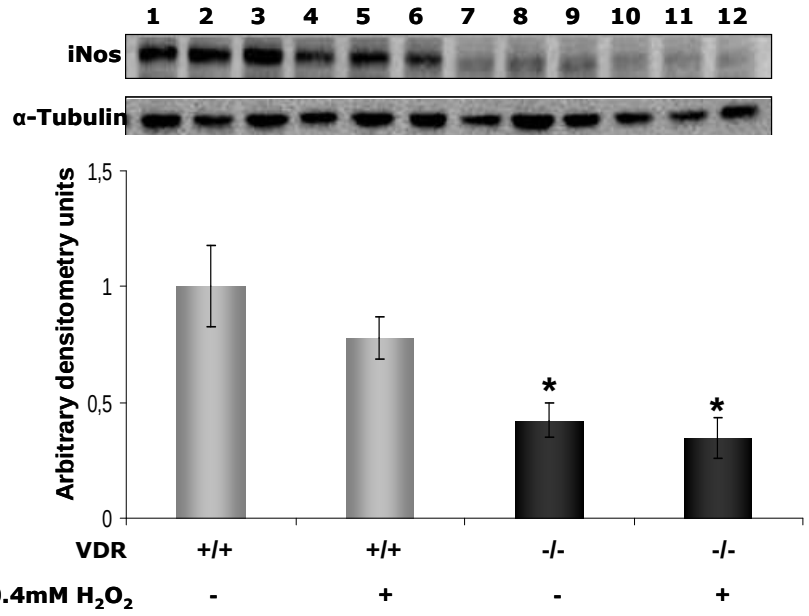

Figure 49. Expression of iNos in quiescent WT (lines 1, 2, 3; grey bars) and VDR (7, 8, 9; black bars) cell without treatment and after the addition of 0.4mM H_2O_2 of WT (lines 4, 5, 6; grey bars) and VDRKO (lines 10, 11, 12; black bars) cells.

19.2. AKT phosphorylation

The same samples from 18.1 were probed with anti-phospho and anti-pan AKT antibodies. The western blot revealed that the mutant cells had significantly higher levels of AKT phosphorylation in quiescent conditions, and that the pro-oxidant treatment increases it significantly in both cell cultures (Figure 50).

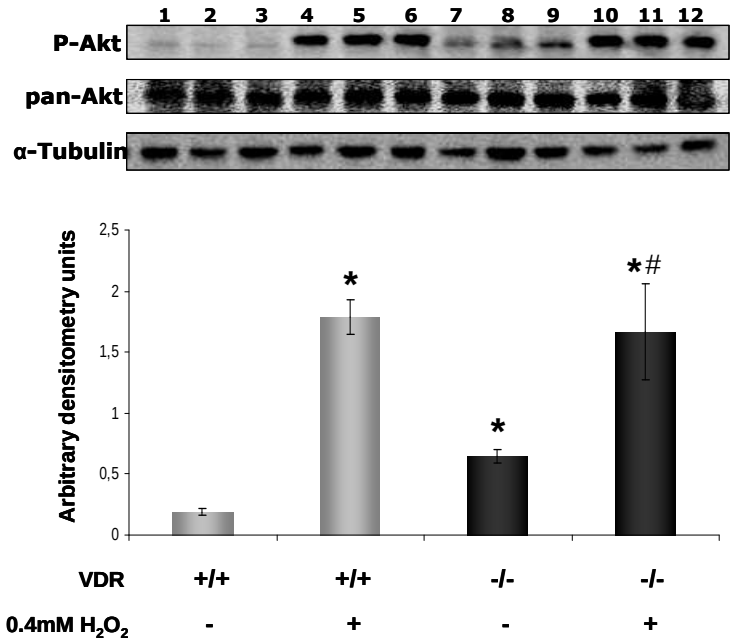

Figure 50. Expression of P-Akt and pan-Akt in quiescent WT (lines 1, 2, 3; grey bars) and VDRKO (7, 8, 9; black bars) cell without treatment and after the addition of 0.4mM H_2O_2 of WT (lines 4, 5, 6; grey bars) and VDRKO (lines 10, 11, 12; black bars) cells. The phosphotylation was calculated over the pan levels of Akt and the tubulin is shown like a loading control.

19.3. Superoxide production

In another set of experiments, H_2O_2-treated cells were processed by FACS analysis in order to measure the levels of superoxide anion. The auto fluorescence of both WT and VDRKO cells was low and similar. We used dehidroethidium (DHE), a probe useful in detecting oxidative activities in live cells, which fluoresces upon exposure to oxidants. Cellular redox status, monitored by flow cytometry clearly indicated the presence of "basal" differences between VSMC from WT and VDRKO mice in terms of redox balance. In fact, in the mutant cells O_2^- production was significantly higher than in the control VSMCs (Figure 51A). Moreover, in the presence of H_2O_2 the superoxide production was not changed in WT cells (Figure 51B), meanwhile this one hour of treatment with 0.4mM H_2O_2 was enough for the further increase in the superoxide levels in the mutant cells (Figure 51C).

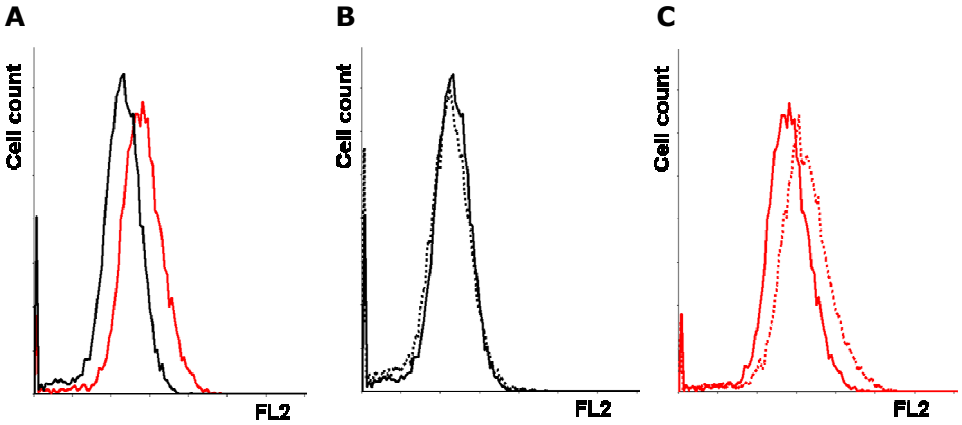

Figure 51. Representative cytofluorimetric histograms of superoxide anion production in (A) untreated WT (black curve) and VDRKO (red curve) cells and after 0.4 mM H_2O_2 treatment in (B) WT (black dotted line), and (C) VDRKO (red dotted line).

These results confirmed that VDRKO cells are exposed and are more susceptible to oxidative stress. VDRKO displayed a sort of "physiological oxidative imbalance" when compared with basal WT. The mutant cells produced more superoxide anions and had a major decrement of antioxidant defences in terms of the antioxidant enzymes superoxide dismutase with respect to WT.

20. Inhibition of the increased superoxide anion levels in VDRKO cells

It has been previously demonstrated that in cultured VSMC, the hypertrophic agent Ang II caused a delayed, sustained superoxide production by activating a membrane-associated NADH/NADPH oxidase. This enzyme appears to be the major source of O_2^- in this cell type and is believed to play a role in Ang II-induced hypertrophy.[96] In order to find the source of the increased basal levels of superoxide anion in the VDR mutant cells, we used an Ang II receptor 1 (AT1-R) blocker, losartan and the inhibitor of the flavoprotein component of the neutrophil NADPH oxidase, diphenylene iodonium (DPI). WT cells showed a low concentration of ethidium fluorescence, whereas, there was a significant increase in ROS in VDRKO cells. The inhibition of either AT1-R or NADPH oxidase provoked a decrease in the levels of superoxide anion in the VDRKO cells, reaching the levels in the WT control (Figure 52).

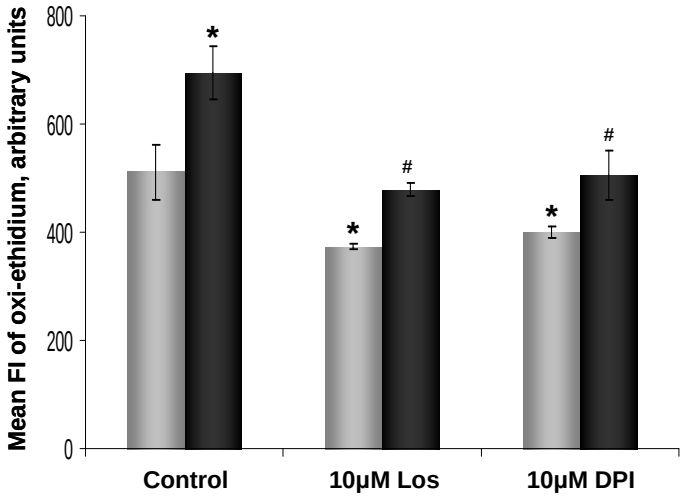

Figure 52. The higher mean fluorescent intensity of oxi-ethidium in VDRKO cells was inhibitited by 10 μM of both losartan and DPI. WT (grey bars), VDRKO (black bars). Statistical significance, p <0.05 * versus the correspondent WT control, # vs VDRKO control.

21. Oxidative stress and cell cycle

21.1. Expression levels of $p21^{Cip1}$ and $p57^{Kip2}$ after challenge with antioxidant

In order to check if the increased oxidative stress in the mutant cells could be the reason of the decreased proliferation rates in these cells, we treat both cell populations with the membrane-permeant non-enzymatic O^{-}_{2} scavenger. After reaching 50% confluence, WT and VDRKO VSMC were serum starved during 24h, and then cultured in 0.2%FBS DMEM with or without Tiron at 10μM concentration. Then, we checked the expression levels of two CDI, $p21^{Cip1}$ and $p57^{Kip2}$, by RT-PCR. We saw that in the WT cells neither $p21^{Cip1}$ nor $p57^{Kip2}$ expression was affected by the antioxidant treatment. Meanwhile in the mutant cells, decreasing the oxidative levels we were able to downregulate significantly the expression of $p57^{Kip2}$, meanwhile in the $p21^{Cip1}$ there was not a difference (Figure 53).

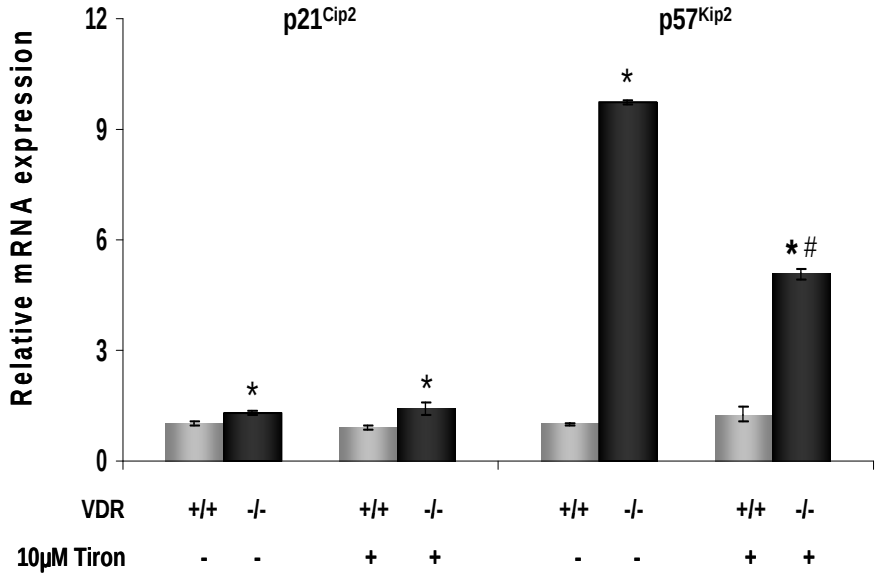

Figure 53. Quiescent WT (gray bars) and VDRKO (black bars) were treated with 10μM Tiron during 24 hours and the relative mRNA levels of two cell cycle inhibitors, $p21^{Cip1}$ and $p57^{Kip2}$ was measured by RT-PCR. p<O.05, * vs WT control, # vs VDRKO control.

21.2. $p57^{Kip2}$ after blocking the activation of AT_1

In our FACS analysis we found that blocking the activation of Ang II receptor type 1 (AT1-R) by Losartan treatment, we were able to decrease the production of superoxide anion and by the treatment with the antioxidant Tiron, the expression of the cell cycle inhibitor $p57^{Kip2}$ was decreased.

21.2.1. Expression levels of $p57^{Kip2}$ after Losartan treatment

In order to determine if the activation of AT1-R is involved in the regulation of the cell cycle, we treated quiescent VDRKO cells in parallel with Tiron or Losartan, both at 10μM concentration. The blocking of the AT1 receptor reduced significantly the levels of $p57^{Kip2}$ to a similar extend as Tiron (Figure 54).

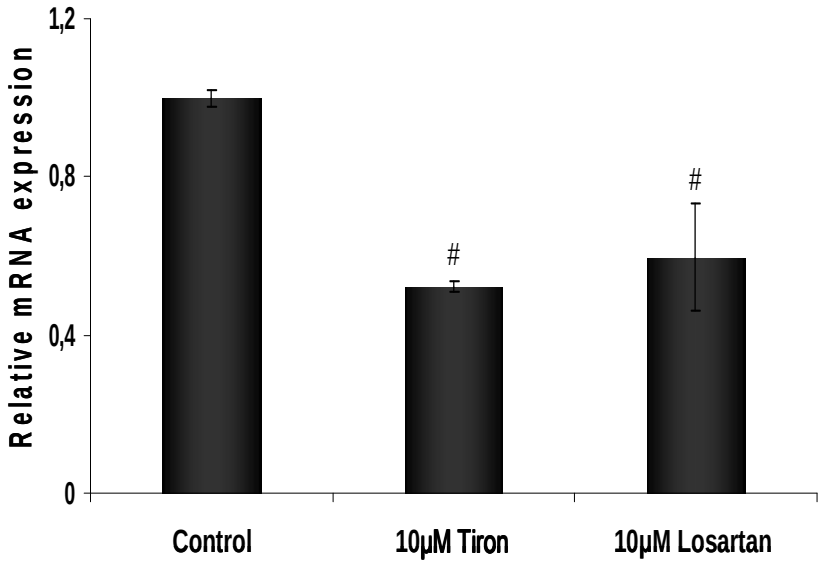

Figure 54. The relative mRNA expression of p57Kip2 was assessed in VDRKO cells in parallel treatment with the superoxide scavenger Tiron and AT1 inhibitor Losartan. # $p<0.05$ vs VDRKO cells without treatment.

21.2.2. Effect of Losartan treatment over the proliferation of VSMC

Then, we decided to determine how the activation of AT1-R affects the proliferation rates in VDRKO cells incubating both WT and VDRKO cells with losartan up to 96 hours. Every day fresh losartan containing medium was added to the cells. At 72 hours after the beginning of the experiment we were able to see a significant decrease in the proliferation of the treated WT cells. In contrary, when the receptor for Ang II (AT1-R) was blocked, the VDRKO presented significantly higher cell numbers in comparison with the untreated mutant cells (Figure 55).

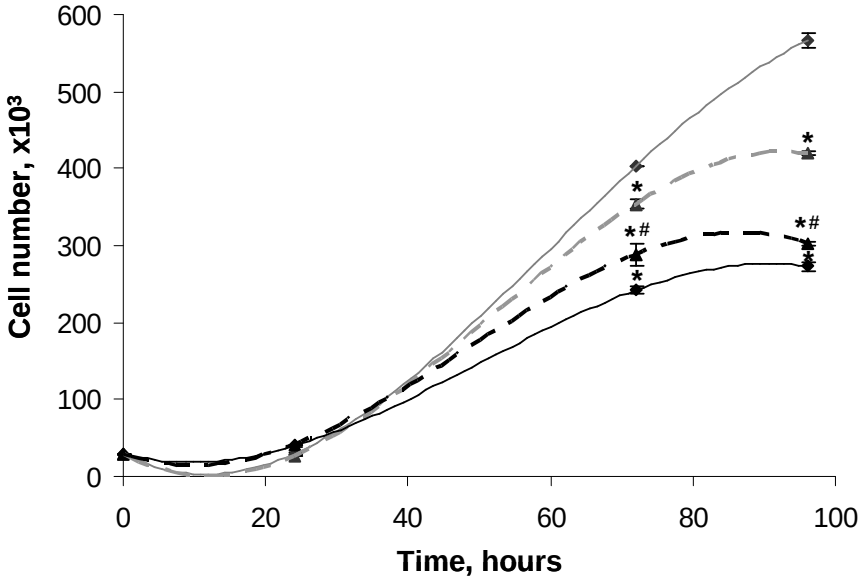

Figure 55. Effect of losartan over the proliferation of VSMC in FBS-stimulated cells. The growth rates of WT (grey curve) and VDRKO (black curve) without treatment or after the addition of Losartan at 10μM (dotted grey curve for WT and dotted black curve for VDRKO) were determined after manually counting of the cell number. The curves were fit with a polynomial equation (order = 3). Statistical significance was considered at $p < 0.05$, * vs the WT control and # vs VDRKO control. The graphic is one representative experiment.

The deceased proliferation rates of VDRKO VSMC are likely due to the activation of the AT1-R with a subsequent elevation in the production of free radicals.

22. Migration of VSMC in vitro

As the migration of VSMC is a critical component of VSMC response to injury, we decided to determine if this process is also impaired in the mutant cells. In quiescent conditions we performed an in vitro "wound" in the cell monolayer. 24 hours later, the WT cells had reoccupied 34.4 ± 4.4% of the "wound", meanwhile the VDRKO cells only 7.6 ± 1,9% (Figure 56).

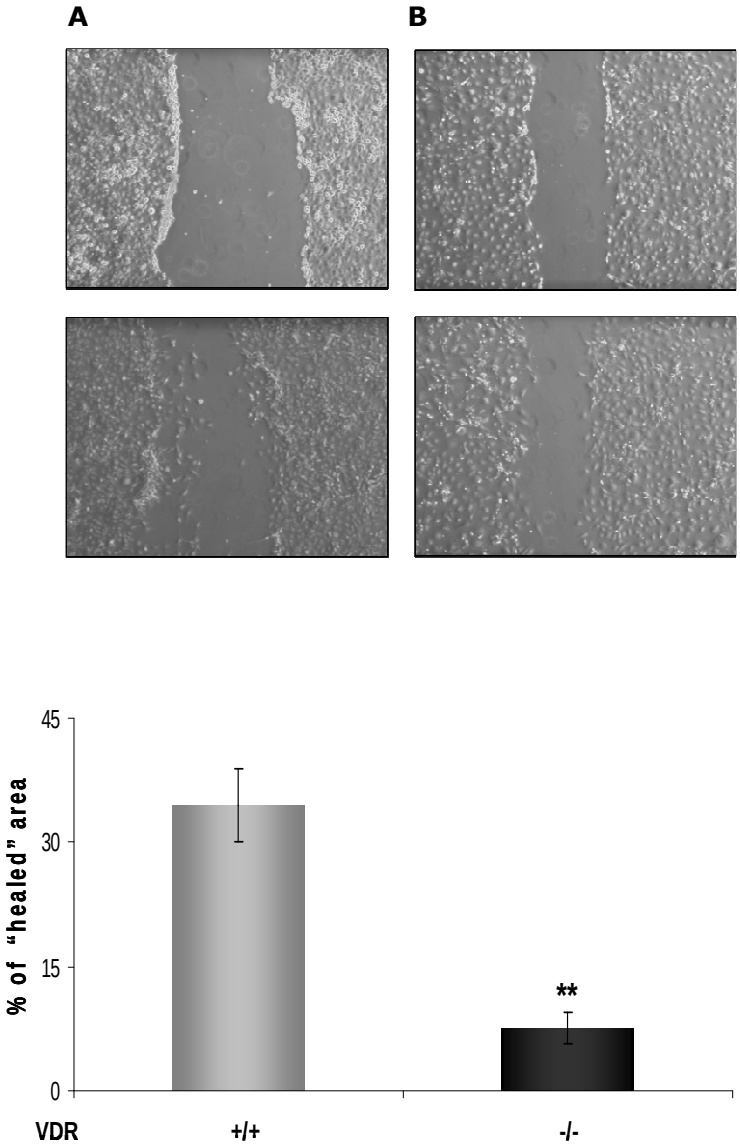

Figure 56. In vitro wound-healing motility assay in WT (grey, +/+) and VDRKO (black, -/-) cells was done as described in Materials and Methods. In contrast to control cells, the VDRKO cells showed a decreased migration into the denuded area and in vitro closure of the "wound".

23. In vivo studies

A part from our in vitro studies, we assessed the in vivo behaviour of the vascular cells in our knockout mouse model, using the WT mice as a control. We performed two approaches – in vivo angiogenesis in which the endothelial cells took a part, and carotid artery injury, which permitted us to speculate about the proliferative capacity mainly of the medial vascular smooth muscle cells.

23.1. Matrigel plug assay

In order to confirm our finding about the reduced capacity of the mutant cells to migrate in vitro, we decided to perform an in vivo study of angiogenesis. Angiogenesis involves a combination of endothelial cell and pericyte migration, proliferation, and appropriate spatial orientation to form new tubular formations for the passage of blood under the stimulus of different factors. The process is important physiologically during embryological development and in wound repair, and is also relevant in the pathological conditions like atherosclerosis, tumor vascularization, and diabetic retinopathy.

In this assay, WT (n=6) and VDRKO (n=6) were used. The microcapillaries formation was assessed in a Matrigel plug, containing 500ng basic fibroblast growth factor (bFGF) by measure both, the haemoglobin (Hb) content and the fluorescence of the plug. The Hb content as an indicator of the blood passing trough the newly formed capillaries in the plug was measured and presented in relation to the whole blood Hb concentration, normalized to the weight of the plug. After the in vivo perfusion of the animals with FITC-labeled dextrans, which were distributed throughout the whole body, including the Matrigel plug, the resulted fluorescence of the plug was measured and, as in the case of the Hb, was presented in relation to the total fluorescence of the plasma. The picture in figure 57 represents the appearance of the newly formed blood tubules inside the plug, viewed under fluorescence microscopy. The quantity of blood passing through the plug measured by the FITC florescence was half of that found by the measurement of the Hb content, because the first parameter was determined in plasma, which volume is known to be around 50% of the whole blood volume. By both measurements the blood content of the plug in the VDRKO mice was lower. Measuring the fluorescence of the plug gave significantly lower levels in the VDRKO mice, and by the quantification of the Hb concentration the tendency was the same, even that was not found to be statistically significant.

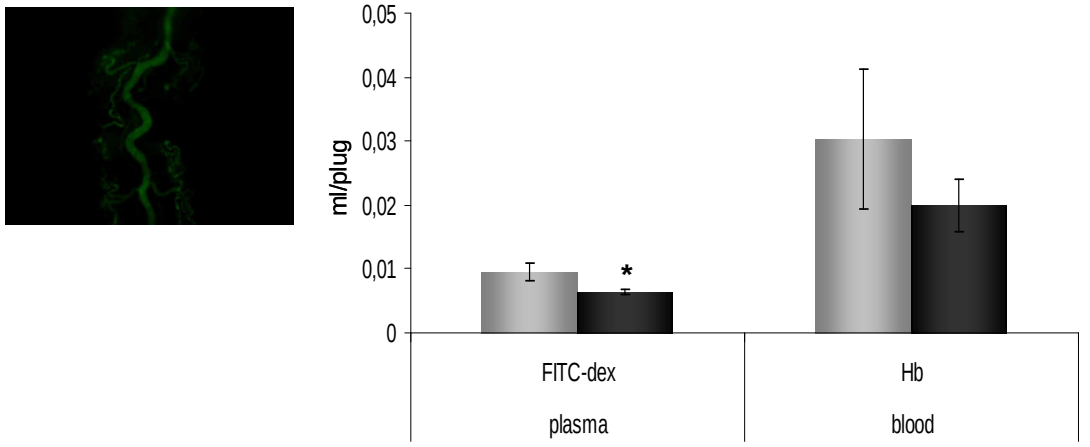

Figure 57. Representative picture of the newly formed capillaries of plug in WT mouse. The graphic presents the quantification of the in vivo angiogenesis in WT (grey bars) and VDRKO (black bars) mice, measured by the plasma or blood quantity (ml) of the Matrigel plugs.

23.2. Carotid artery injury

Intimal thickening, induced after endothelial denudation of an artery is though to be due to migration and proliferation of smooth muscle cells (SMC). After vascular injury, VSMC rapidly leave their quiescent state and enter back to the cell cycle [89]. In vivo experiments have shown that after arterial injury the expression of the endogenous $p27^{Kip1}$ protein in the VSMC is diminished, thus triggering VSMC proliferation [251].

In our model of artery injury, the carotid artery of age-matched WT (n=6) and VDRKO (n=6), was damaged by the insertion of a wire and denudation of the endothelium. 21 days after the procedure, the carotid arteries were perfuse with 3% glutaraldehyde solution and embedded in paraffin. The observation of the hetatoxilin-eosin sections of the arteries revealed that the artery injury provoked a disorganization and increase in the medial layer, which reflects the ability of the VSMC to migrate and proliferate. The quantification of this increase showed that the VSMC of the VDR mutant mice proliferated in a significantly lower rate than the WT controls (Figure 58).

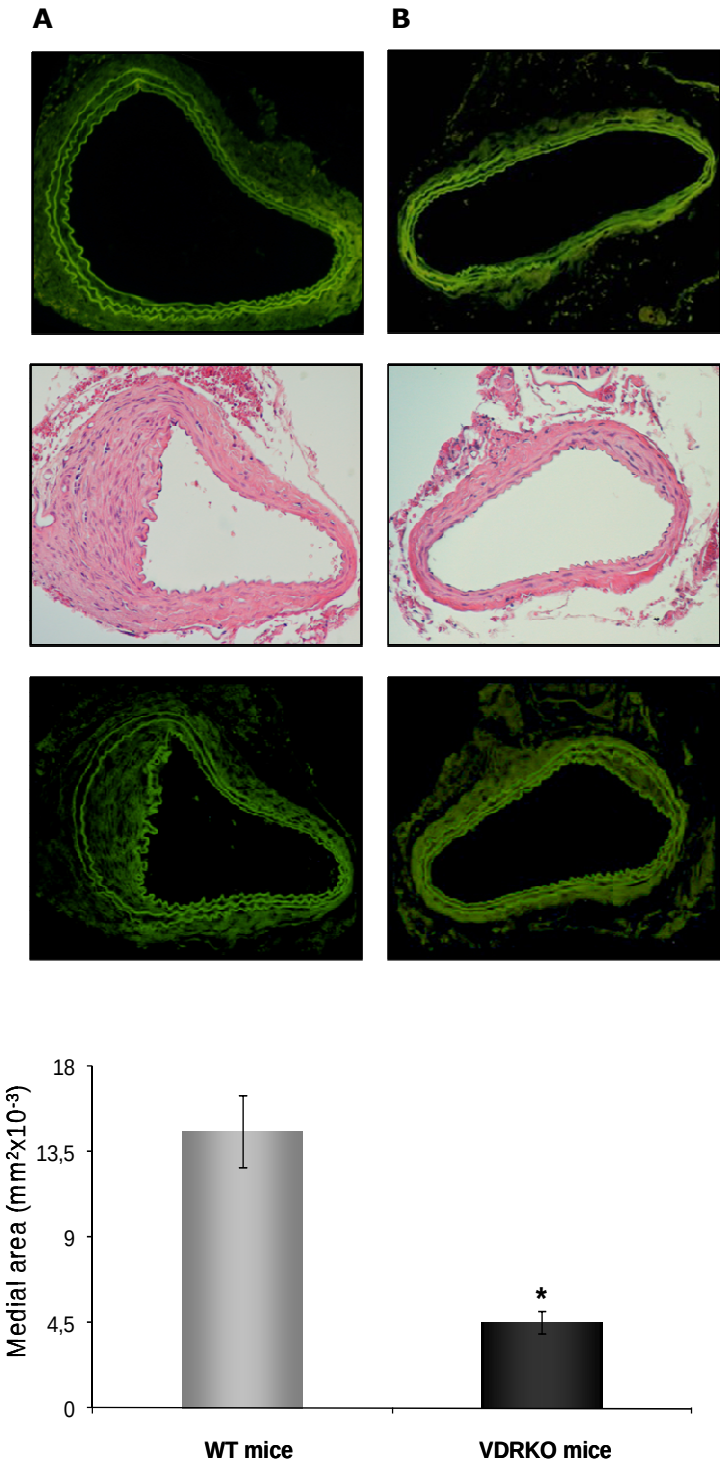

Figure 58. The proliferation capacity of WT (panel A) and VDRKO (panel B) VSMC in vivo was assessed in a carotid artery injury model. The morphology of the carotid artery in the uninjured vessels is presented by the autofluorescence of the arteries in the upper picture of each panel. The hematoxylin&eosin staining shows the increased medial layer 21 days after the injury, which is better visible by the autofluorescence of the elastic laminae, presented in the last picture of both panels. The graphic represents the medial area of the injured vessels in WT (grey bars) and VDRKO (black bars) mice. * p <0.05 vs the WT control.

24. Main cell functions affected by VDR ablation, detected by DNA-microarray

In our in vitro and in vivo studies we found that the lack of signalling trough the vitamin D receptor in VSMC affects processes that are physiologically very important. In order to complete our findings about the VDRKO VSMC and open new fields for our future work, a DNA microarray was performed, in which the differential expression of around 41000 genes was assessed in quiescent VDRKO cells, compared to the WT control. Probe sets were filtered by Present-Marginal (PM) flags and analyzed by a T-test against zero. After the statistical analysis, 14000 genes have been found to be significantly up- or down- regulated in the mutant cells. Using the IPA software the gene annotations were found, as well as the main functions/pathways for the most significantly up- and down-regulated genes. Among these candidate genes, a big part has functions in the regulation of the immune system (antimicrobial and inflammatory response); cellular growth and proliferation; cell-to-cell signalling and interaction; lipid metabolism, ion transport, or were reported to be induced in cancer, cardiovascular diseases, hypertension or by hypoxia. The main cell functions, affected by the lack of vitamin D receptor in VSMC, together with some of the candidate genes are listed below.

- **VDR/RXR activation**

Down-regulated: cathelicidin antimicrobial peptide (CAMP); S100 calcium binding protein G; semaphorin 3B (SEMA3B); Wilms tumor 1 (WT1).
Up-regulated: chemokine (C-C motif) ligand 5; insulin-like growth factor binding protein 5 (IGFBP-5); protein kinase C zeta; homeobox A1 (HOXA10); PTHrP.

- **Ion transport and calcium homeostasis**

Down-regulated: calbindin D9K; ATPase, Ca++-sequesterin

- **Steorid/cholesterol metabolism**

Down-regulated: 3-hydroxy 3-methylglutaryl-Coenzyme A synthase 1; 3-hydroxy-3-methylglutaryl-Coenzyme A reductase
Up-regulated: apolipoprotein E

- **Lipid metabolism and energy supply**

Down-regulated: fatty acid synthase; lipin 1, lipoprotein lipase; Na+/K+-ATPase.
Up-regulated: monoglyceride lipase.

- **Regulation of cell cycle and proliferation**

Down-regulated: Vascular endothelial growth factor B, Dual specificity phosphatase 10.

Up-regulated: p27, p19, CDC28 protein kinase 1b, S-phase kinase-associated protein 2 (p45), vascular endothelial growth factor A, cyclin C; dualspecific phosphatase 6.

- **VEGF signalling**

Down-regulated: actinin, alpha 3

Up-regulated: actin, alpha 1, skeletal muscle; actin, alpha, cardiac muscle 1; actin, gamma 2, smooth muscle, enteric.

- **Apoptosis**

Down-regulated: Bcl2

Up-regulated: Nur77

- **Atherosclerosis**

Down-regulated: collagen, type V; alpha 3, interleukin 1 beta; matrixmetallopeptidase 3.

Up-regulated: arachidonate 5-lipoxygenase; chemokine (C-C motif) ligand 11; platelet derived growth factor D; WNT1 inducible signalling pathway protein 2.

- **Hypertension and cardiac hypertrophy**

Down-regulated: calcipressin-1

Up-regulated: connective tissue growth factor, atrial natriuretic peptide type B,

- **Immune response**

Down-regulated: actinin, alpha 3; matrix metallopeptidase 3; matrix metallopeptidase 8; matrix metallopeptidase 10; matrix metallopeptidase 12; claudin 10; claudin 19; calgranulin A

Up-regulated: actin, alpha 1, skeletal muscle; actin, alpha, cardiac muscle 1; actin, gamma 2, smooth muscle, enteric; claudin 1; claudin 3; cadherin-associated protein; ICAM-1; VCAM-1;

- **Chemopreventive and genoprotective effects**

Down-regulated: GADD45A, Glutathione peroxidise 1, Thioredoxin reductase 1

- **Mitochondrial disfunction**

Down-regulated: **Components of complex I** (Nduf s1, Nduf v1)
Up-regulated: **Synuclein α** (provokes increase in ROS by one hand and mitochondrial structural abnormalities, thus leads to MD)

- **Nuclear factor-erythroid 2-related factor 2 -mediated oxidative stress response**

Down-regulated: glutathione S-transferase; Sod2; Nfr2; catalase; thioredoxin reductase 1
Up-regulated: flavin containing monooxygenase 1 (FMO1); Sod3; thioredoxin

To summarize, gene expression profiling of VDRKO cells found in the DNA microarray, compared to the WT cells, showed impairments in the regulation of different physiological functions and biochemical pathways. The high number of differentially expressed genes coding for proteins that participate in lipid metabolism and blood pressure control is in accordance with the possible association between vitamin D action and metabolic disorders, which could explain the increase in the gene expression of markers for inflammatory diseases and cardiac hypertrophy.

DISCUSSION

The active vitamin D metabolite ($1,25(OH)_2D_3$, calcitriol) plays a central role in phosphorus and calcium homeostasis and is essential for the development and the maintenance of bone tissue. In order to control these processes, $1,25(OH)_2D_3$ coordinates different actions in its classical targets, the kidney, intestine, bone and parathyroid glands. Together with the control of the rapid (seconds to minutes) changes in the ion channels activity, vitamin D exerts genomic effects, mediated by the interaction of $1,25(OH)_2D_3$ in a ligand dependent manner with its nuclear receptor VDR, which functions as a transcription factor.[118,252] It has been proved that for all actions of vitamin D (genomic and nongenomic) the presence of a functional VDR is required.[128] The expression of VDR has been shown in several nonclassical targets like the skin, muscle, pancreas, reproductive organs, both white and brown adipose tissue, where vitamin D and its metabolites are stored,[253] vascular wall and in the haematopoietic, immune and nervous systems.[254] In these tissues, $1,25(OH)_2D_3$ exerts different biological actions, including the control of cell proliferation and differentiation, modulates hormonal secretion of some endocrine glands, regulates reproductive function and protects from neuronal degeneration. The effect of $1,25(OH)_2D_3$ on proliferation is well studied in different cell types such as colon, prostate, breast cancer, osteoblasts and parathyroid gland cells. In all these cells, $1,25(OH)_2D_3$ acts as a potent inhibitor of proliferation and inductor of differentiation. However, in previous studies from our laboratory, it has been demonstrated that vitamin D has a positive effect in the VSMC proliferation[185] and calcification in a VEGF- and RANK-BMP4-dependent pathways, respectively. As the role of $1,25(OH)_2D_3$ in the proliferation of VSMC is still controversial, we decided to use mice, in which the VDR is mutated and thus the signalling trough it is disrupted. Nowadays, four different strains of VDRKO mice are in use.[209,210,211,212] In our group we maintain a colony of so called "Tokyo strain" VDRKO mice. Ablation of the functional vitamin D receptor in mice created an excellent model of hereditary type hypocalcemic vitamin D resistant rickets (HVDDR) also known as vitamin D-dependent rickets type II, which is caused by mutations in the human VDR gene, and provided options to study the molecular biology of vitamin D signalling.

After mating of HZ mice, offspring of all three genotypes, WT, HZ and VDRKO, were obtained. Usually the number of knockout mice was not as expected by the Mendelian ratio, probably because of higher prenatal mortality of the mice with this genotype. Under regular rodent dietary conditions, VDRKO mice displayed a lean phenotype, similar to HVDDR, characterized by alopecia, hypocalcemia, hypophosphatemia, hyperparathyroidism, impaired growth and bone formation, absence of abdominal adipose tissue, hyperphagia, enhanced thrombogenicity and

infertility, and usually die within the first three months.[209,210,214] Following the standard therapy of HVDDR, these mice were fed on diet enriched in calcium, lactose and phosphorus.[255] This diet has been previously shown to prevent hypocalcemia and elevation in PTH levels in vitamin D-deficient rats.[256]

The use of primary cell cultures obtained from these mice provides a good tool to study different processes, related to the vasculature in which vitamin D is involved. In the literature there are plenty of studies, in which different cell types, obtained from VDRKO mice are used.[257,258,259,260] To our knowledge, a study with VSMC from VDRKO mice is still missing. For this reason we obtained primary VSMC from age-matched VDRKO and WT mice, as a control.

The absence of VDR expression in the mutant cells was confirmed at mRNA and protein levels. It has been shown that a truncated form of vitamin D receptor was found in the Tokyo strain,[261] which could explain the bands seen in the Western blot. In order to check if the signalling through VDR is really abrogated in VDRKO cells, the expression of the two genes, which levels are under the transcriptional control of the active form of vitamin D were determined. Both cell populations, WT and VDRKO, express 1αOHase and 24OHase. The higher levels of 1αOHase, found in the VDRKO vascular cells, point to the increased production of the active form of vitamin D at local level. It has been shown that VDRKO mice have dramatically elevated systemic levels of $1,25(OH)_2D_3$ (WT: 380 ± 60 pmol/l and VDRKO: 7705 ± 360 pmol/l).[262]

The almost null expression of 24OHase in the VDRKO cells was expected, because the stimulating effect of $1,25\text{-}(OH)_2D_3$ on 24OHase gene activation is mediated by the activation of VDR, trough the functional vitamin D-responsive elements in its promoter.[134,263] In a study with VDRKO mouse keratinocytes it has been shown that VDR ablation leads to a loss of basal 24OHase gene expression even in the presence of $1,25(OH)_2D_3$.[264] In our study, when we treat WT VSMC with 100nM $1,25(OH)_2D_3$ a significant increase in the expression of 24OHase was found. The expression of VDR and both enzymes that participate in vitamin D metabolism shows that the vitamin D system is present in mouse VSMC and VDRKO VSMC could be an usufull tool for understanding the role of VDR in the vasculature.

Very obvious features of the knockout cell population were their lower rate of proliferation and the enlarged, stella–like shape of the cells. These findings made us look at the molecules that are involved in the regulation of the cell cycle, as well as in the control of the metabolism.

In general, we used two main groups, cells growing in basic conditions (serum starved) and cells growing after the administration of growth factors (10%FBS).

The withdrawal of mitotic signals induces the cell to exit from the cell cycle into a non-dividing state, termed G_0, characterized by low metabolic activity. In contrary, in the presence of growth factors, the cell goes back and progresses trough the cycle and its metabolic activity is increased. The proliferation of both VSMC cultures (WT and VDRKO) was assessed in a number of assays in which a decrease in the proliferation rates of the mutant cells was confirmed. The incorporation of the synthetic thymidine analog BrdU in the newly synthesized DNA, marker of the number of dividing cells, was found to be significantly lower in the VSMC from VDRKO mice in comparison to WT in both growth-arrested and stimulated cells. These experiments showed that the VDRKO VSMC proliferate less, and that this effect is independent of the amount of serum in the incubation medium. This finding was confirmed by manually counting the cell number of both populations in the presence of 10% bovine serum. In cell culture, serum provides a wide variety of proteins, low molecular weight nutrients, carrier proteins for water – insoluble components, and other compounds necessary for in vitro growth of cells, such as hormones and attachment factors. As shown in the growth curves, VDRKO cells followed almost a linear profile and as soon as 18 hours, the differences in cell number between them and the WT cells reached statistical significance. When we used serum processed with activated charcoal for global removal of hormones we found that the WT cells were not able to grow at the same rate like when the complete serum was used, indicating that the steroid hormones with vitamin D among them, are necessary for their normal growth. However, the proliferation of the mutant cells seemed to be not affected by the reduced amount of sterols. The fact that the growth of the VDRKO cells was similar in both complete and stripped FBS made us use complete FBS for all further in vitro studies.

The study of the cell cycle distribution of the cells by FACS analysis showed that the VDRKO cells presented very low percentage in the S phase meanwhile the percentage of cells in G1 was higher than in the control cells. The FSC and SSC cell frequency profile of the mutant cells pointed to an increase in their size and granularity. By the measurements of the cell volume we found that at all studied time points the mutant cells were larger. Thus, the VDRKO cell probably was preparing itself for an entrance in the cycle, increasing its size as the biosynthetic activities of the cell usually increase in G1,[265] but then it was not able to overcome the G1/S check point. These results support those previously published by our group in which the treatment with the active form of vitamin D in rat VSMC has been shown to induce a dose-dependent increase in VSMC proliferation in both, quiescent and cells stimulated to grow and that this increase was achieved by a

shortening of the G1 phase.[185] The increase in the proliferation was in parallel with the upregulation of VDR at 1,25$(OH)_2D_3$ concentration of 100 nM. Thus, with the measurements of the proliferation rates in cells that lack functional VDR, we provide additional evidence for the importance of this nuclear receptor for the proliferation of VSMC.

In order to check if the lower cell number was due to higher cell death events, we performed staining of the cell nuclei with Hoechst 33258 in FBS-deprived cells. The fluorescent staining showed a slight increase in the number of cells with pyknotic nuclei among the mutant cell population, without reaching statistical significance. Furthermore, the PI staining of intact WT and VDRKO cells analyzed by FACS didn´t show differences between both cell populations. By WB we cheched for the presence of the cleaved product of the acticated pro-apoptotic caspase 3, but neither in the WT not in the VDRKO cells we were able to detect it (data not shown).

Having established that VSMCs from VDRKO mice present a defect in the proliferation, we analyzed the proteins involved in the cell cycle entry into S phase. The entry into S phase is finely regulated by series of positive (cyclin-CDK complexes) and negative (CKI) regulators. All signals relevant for G1 progression into S-phase finally culminate in the pRb hyperphosphorylation. Its hipophosphorylated form joins the transcription factor E2F preventing its movement to the nucleus. Once hyperphosphorylated, pRb liberates E2F, thus initiating the transcription of factors needed in the S phase. By immunoblotting, we found that the VDRKO cell expression of cyclin D was lower in the resting phase but when the cells enter the cell cycle after stimulation with 10%FBS this difference was lost. Cyclin D, together with its co-partner Cdk 4/6 plays a role in mid-G1-phase and is responsible for the initiation of the phosphorylation of pRb. In order to complete the inactivation of pRb, cyclin E-cdk2 activity is needed. In the mutant cells the expression of cyclin E was decreased which was in accordance with the lower phosphorylation of pRb, seen during the proliferation of these cells. The inhibition of the cyclin E expression was probably due to the increased levels of the CKI. By real time PCR and WB we found a significantly higher expression of $p21^{Cip1}$ and $p57^{Kip2}$ in quiescent conditions. The treatment of WT cells with 100nM 1,25-$(OH)_2D_3$ during 24 hours was able to reduce significantly the mRNA expression of both, $p21^{Cip1}$ and $p57^{Kip2}$. The $p27^{Kip1}$ and $p19^{Arf}$ were found to be also upregulated in the mutant cells by western blot. After the addition of FBS only the difference in the levels of $p57^{Kip2}$ was still present between WT and VDRKO cell. Therefore, we can speculate that during the quiescent state, the one in which the VSMC are present in the normal

arteries, the VDRKO cells are in G1 phase growth arrest, due to increased cell cycle repressor protein levels, and probably they have more difficulties to pass the cell cycle check point and phosphorylate pRb.

Even after the stimulation with growth factors, the CKI $p57^{Kip2}$ protein presents extremely higher levels in the mutant cells than in the control. Nakano et al. [266] studied the effects of $p57^{Kip2}$ overexpression on the cell cycle of VSMC proliferation. They found that the supplemental overexpression of $p57^{Kip2}$ inhibited the activations of G1 cyclin/CDKs and subsequent hyperphosphorylation of pRb as well as G1/S transition of cell cycle. In addition, mice lacking $p57^{Kip2}$ die soon after birth, demonstrating multi-organ dysplasia and growth retardation with hyperproliferation and marked apoptosis.[267]

A similar pattern of cell cycle regulators expression has been demonstrated during the development of the compensatory tubular cell hypertrophy, following unilateral nephrectomy[268, 269] and that $p57^{kip2}$ is the one that mediates the TGFβ-induced compensatory hypertrophy after subtotal nephrectomy in the remaining kidney.[232] Moreover, it has been demonstrated that TGFβ might elicit hypertrophic response in smooth muscle cells.[231] The medial hypertrophy in the aorta of spontaneously hypertensive rats was found to be due almost exclusively to hypertrophy of pre-existing VSMCs, without changes in VSMC number, and was implicated in the pathogenesis of the disease [270]. It has been shown by several in vivo studies that the lack of VDR leads to ventricular hypertrophy and hypertension [271] and we found that the VDRKO VSMCs were larger and proliferate less than the WT. Further, we decided to check the expression of TGFβ in the VDRKO cells. This cytokine is a natural growth inhibitor of a variety of cell types, including epithelial, endothelial, and hematopoietic cells, but its effect on VSMC proliferation and apoptosis are controversial. TGF-β-mediated growth arrest occurs by blocking all cycle transits at mid- and late-G_1 phase of the cell cycle and the mechanism of this arrest is cell-type specific. In epithelial cells, TGFβ can trigger cell cycle arrest by up-regulating CKI $p15^{INK4B}$ [272] and $p21^{Cip1}$.[273] Studies related to hematopoietic cell cycle arrest and stem cell quiescence have proven that neither $p21^{Cip1}$ nor $p27^{Kip1}$ appears to be required for the inhibition by TGFβ treatment.[274] Scandura et al. have identified $p57^{KIP2}$ as an immediate–early target of TGFβ in normal human CD34β hematopoietic stem cells, required for TGFβ-mediated cell cycle arrest of these cells as the basal expression of $p57^{KIP2}$ restrains their proliferation. Using HeLa cells and truncation mutant plasmids, these authors had identified a region in the $p57^{KIP2}$ gene promoter just upstream of the TATA box (extending from - 165 to - 77) to be critical for TGFβ-mediated activation. It is known that this region is highly

conserved in the mouse, rat, and human promoters. Thus, TGFβ induces transcription of $p57^{KIP2}$. They also used siRNA technique to knock-down expression of $p57^{KIP2}$ in M091 cells (acute myelogenous leukemia-derived cell line) and observed marked reduction in the cytostatic response to TGFβ, indicating that $p57^{KIP2}$ is a critical downstream mediator of TGFβ in these cells.[275]

As expected, in basal conditions VDRKO cells showed higher mRNA levels for TGFβ1, meanwhile treating WT cells with 100 nM $1,25(OH)_2D_3$, the mRNA expression of TGFβ1 was significantly down-regulated. It has been shown that TGF-ß family could play an integral role in the development of fibrosis, characterized by uncontrolled fibroblast growth and a disproportional accumulation of extracellular matrix proteins (collagen and fibronectin) as a result from the cardiac hypertrophy.[276] This finding was not limited only to the myocardium. The lung fibrosis developed secondary to myocardial infarction was also associated with up-regulation of TGF-$ß_1$ and TGF-$ß_3$ mRNA.[277] An important physiological characteristic of TGF-ß is the de novo synthesis of ECM proteins. Moreover, TGF-ß has been shown to inhibit the expression of matrix metalloproteinases (MMP), a family of proteins that degrade ECM proteins.[233] Collagen and elastin are the main ECM proteins involved in the maintenance of the aortic wall mechanical properties and resistance. By RT-PCR we found significant increase in the mRNA for collagen type I in quiescent VDRKO cells. It has been found that the components of the ECM play an important role in the regulation of VSMC proliferation. For example, the polymerized collagen type I can arrest VSMCs in the G1 phase, inhibiting the phosphorylation of cyclin-dependent kinase 2 (cdk2).[278] Thus, the higher expression of collagen type I found in the VDRKO cells could be one of the factors that regulate their capacity to proliferate.

The gene profile and the increased cell size of the VDRKO VSMCs, together with the in vivo found cardiac hypertrophy, point to the possible hypertrophic phenotype of these cells. According to one theory, VSMC hypertrophy would involve an increase in the "contractile" protein content.[279] A study with primary human bronchial smooth muscle cells has shown that TGF-β increases the cell size and total protein synthesis, especially the expression of α-smooth muscle actin (α-SMA) through TGF-β-control elements (TCE) in its promoter[234] and smooth muscle myosin heavy chain, thus the hypertrophy in these cells.[235] By RT-PCR analysis together with the increased TGF-β1, the aorta smooth muscle actin α2 was found to be significantly up-regulated in VDR ablated VSMC in basal conditions. Moreover, the treatment of WT cells with the active form of vitamin D for 24 hours was able to reduce the mRNA level of TGFβ1 and both, α-SMA and collagen type I.

One of the factors that has been shown to induce the expression of TGF-ß1, collagen, and α-SMA in VSMC is angiotensin II.[280] Using VDRKO mice, Li et al. have explored the mechanism underlying the relationship between vitamin D and the renin-angiotensin system and its role in the cardiac hypertrophy and hypertension, found in these mice.[207] They showed that plasma Ang II levels were significantly elevated in both VDRKO and 1αOHaseKO mice, while no differences were found in the angiotensinogen expression in the liver in comparison to the WT mice, indicating that plasma Ang II elevation was likely to be due to increased renin activity. Further, in their studies Li et al. demonstrated that vitamin D deficient mice also had increased renin production, whereas $1,25(OH)_2D_3$ treatment of normal mice resulted in renin suppression.[188] Moreover, Nagpal et al. performed a study with captopril-treated VDR ablated mice, and they found a reduction of the elevated blood pressure, thus confirming that the hypertension in VDR null animals was due to activation of the renin-angiotensin system (RAS).[171]

The renal RAS play an fundamental role in the control of the hypertension, but it is has been shown that in the vasculature an alternative pathway for Ang II production exists,[281] including enzymes like cathepsin D, cathepsin G and chymase. When the sequence of porcine cathepsin D, renin, and pepsin were aligned, 32.7% of the residues were found to be identical and the three-dimensional structures of all three molecules to be similar.[282] Moreover, except of the structural homology, cathepsin D exerts renin-like activity, being able to catalyze the hydrolysis of angiotensin I from angiotensinogen. Studies with VSMCs obtained from spontaneously hypertensive rats have shown that although the renin expression was absent, these cells presented elevated production of Ang II, due to the increased expression of angiotensinogen, cathepsin D and angiotensin-converting enzyme.[237]

In our VSMC model, we didn't find renin expression either, but we do find transcripts encoding for cathepsin D. Quiescent VDRKO cells showed higher levels of this lysosomal aspartic protease than the WT cells in the same condition. Moreover, $1,25(OH)_2D_3$ treated WT cells presented lower, even not statistically significant, cathepsin D expression in comparison to the untreated WT cells.

It has been shown that the cathepsin D expression is controlled by both hormonal and mitogenic factors like transforming growth factor α, epidermal growth factor and insulin-like growth factor-I. One more factor found to influence the expression of cathepsin D in MCF-7 breast cancer cells is the cAMP analog 8-bromo-cAMP.[283] Moreover, it has been shown that the 8-bromo-cAMP increase also the expression of renin mRNA. In the renin promoter a cAMP responsive element

(CRE) was found and it has been shown that cAMP plays an important role at several control points for renin release, mRNA synthesis and mRNA stability. The intracellular production of cAMP enhances renin secretion, and cAMP is a critical second messenger that determines renin secretory rate.[284] Yuan et al. have demonstrated that vitamin D is a negative endocrine regulator of the renin expression by being able to block the formation of CRE-CREB-CBP complex and thus the activity of the cyclic AMP responsive element in the renin gene promoter.[163] Thus, we could speculate that it is highly likely that there is a CRE in the cathepsin D gene, susceptible to the same negative regulation by active vitamin D as the one reported in the renin gene.

As expected, when we collected the culture medium of both quiescent and cells stimulated to grow we found significantly elevated concentrations of Ang II in the VDRKO, in comparison to the WT culture medium, where they were slightly detectable. Ang II exerts its actions trough G protein-coupled receptors. The main Ang II receptors, AT type 1 (AT1-R in humans and AT1a-R in rodents) together with type 2 (AT2-R) have been shown to play a crucial role in most Ang II - mediated responses. Following birth, the level of AT2-R declines rapidly, but in certain pathological conditions such as vascular injury, the AT2 receptor is reexpressed.[85]

In basal conditions, when the effect of all the components of the FBS is excluded and we could monitor the real effect of the VDR ablation, VDRKO VSMC produce higher levels of Ang II with subsequent increase in the expression of both receptors, AT1a-R and AT2-R It has been shown that the acutely increased levels of Ang II, achieved by its exogenously addition, lead to an increased level of AT1-R activation; however, chronic exposure to Ang II downregulates its own receptors. In the case of endogenous production it is difficult to determine the exact moment in which Ang II is produced, but the fact that we have found its hypertrophic, pro-fibrotic and pro-oxidant effect over the mutant cells confirm the notion that in the absence of VDR, the local RAS is active. The changes in the mRNA expression of AT1a-R in VDRKO cells in complete medium further support the functioning of RAS in these cells.

Ang II has been found to exert pleiotropic effects being hypertrophic, pro-fibrotic, pro-inflammatory and pro-oxidant agent for VSMCs. The hypertrophic actions of Ang II, mediated by the increase of TGFβ and subsequently in collagen type I and α-SMA, were also seen in VDRKO cells in deprivation state with a decline when the growth factors were added. The pro-inflammatory effects of Ang II have been demonstrated in several studies in different cell types. For example, in a study with pancreatic cell line AR42J it has been shown that Ang II induces the expression

of IL-6, together with the activation of extracellular-regulated kinase (ERK)1/2 and superoxide generation, and that this increase was reversed by the AT1 receptor antagonist losartan.[285] Funakoshi et al. have shown that exogenous Ang II treatment of rat VSMCs dose-dependently increases the IL-6 levels sustained to 24 hours after stimulation,[238] which mediates the pro-inflammatory effects of Ang II as IL-6 has been found to play a central role in the inflammatory response of VSMCs. Moreover, the induction of IL-6 is also found to be mediated by TGFβ [239] which mRNA levels were found to be higher in quiescent VDRKO cells. Furthermore, it has been shown that IL-6 itself is able to increases angiotensinogen expression via STAT3 pathway in renal proximal tubular cells [286].

A significant increase in the IL-6 mRNA was found in the VDRKO cells in comparison to the WT cells which is in accordance with the anti-inflammatory effects that vitamin D exerts trough the VDR activation. These effects could mediate the beneficial role of vitamin D over the cardiovascular system, as atherosclerosis is considered to be a chronic inflammatory disease state as in its development an interaction between immune (macrophase/T-lymphocytes) and non-immune cells (endothelial and VSMC) occur. Moreover, the inflammatory pathways promote thrombosis, a late complication of atherosclerosis responsible for myocardial infarctions and most strokes [287]. It has been described that the inflammatory cytokines, released during vascular injury, increased the expression of the inducible NOS (iNOS) in the VSMCs and that the NO released from either source decreases vascular tone, inhibits VSMC proliferation, induces apoptosis, attenuates platelet aggregation, and reduces cell adhesion to vascular walls.[288]

By western blot analysis we found that the expression of iNOS was very low in the growing cells with an increase when the cells were serum starved. The induction of iNOS in the VDRKO cells was significantly lower in comparison to the one found in quiescent WT cells. This finding could be explained by the fact that 1,25-dihydroxyvitamin D_3 is also a potent stimulus for NO production, demonstrated in macrophage-like HL-60 line. In the study with HL-60 cells, iNOS mRNA was not detected in unstimulated cells, but was weakly expressed at 24 h and strongly expressed at 96 hours after vitamin D treatment.[241] But in the literature the role of vitamin D over the iNOS expression is still controversial as others studies in vitro and in vivo report inhibitory actions of $1,25(OH)_2D_3$ on iNOS levels.[242]

In order to check if the iNOS expression in VSMC is affected by the presence of oxidant agents, we performed experiments with one hour pulse of 0.4mM H_2O_2. It has been shown that this treatment also induces the phosphorylation of AKT,

which we used as a marker of the efficiency of the H_2O_2 treatment. By western blot we found that the VDRKO cells presented higher levels of phosphorylated AKT at basal conditions than the WT and the pro-oxidant treatment further increased it, meanwhile the expression of iNOS in the mutant cells after this treatment was even lower than in the untreated VDRKO cells. Thus, if the pro-oxidant conditions lead to even lower expression of iNOS in both cell populations we could give the role for the decreased iNOS expression also to a possible altered redox state in the mutant cells.

Redox imbalance is usually seen during the normal cell and whole body aging process. At cellular level, two types of aging, called senescence have been described - replicative senescence that appears as a result of exhausting of the cell potential to divide and maintain the telomere structures, and the oxidative stress induced premature senescence (SIPS). Many biomarkers of replicative senescence appear in SIPS: typical cell morphology, irreversible growth arrest, sharp decrease of the DNA synthesis, and an increase in cells positive for the senescent-associated β-galactosidase activity (SA β-gal). The phenotype of the VDRKO mice resembles premature aging that has been found in mice with hypervitaminosis D_3. The wrinkled thinner skin and the hair and hearing loss in the VDR-ablated mice made us check if the cells, obtained from these mice, would exhibit the typical for cellular aging appearance and markers (SA-β-gal activity). As expected, many of the mutant cells presented the typical flatten, stella-like shape with plenty of vacuoles, and around 22% (22 ± 2.3%) of them, the blue perinuclear staining after the overnight incubation with the chromogenic substrate for SA-β-gal at early passage, meanwhile the WT from the correspondent passage were negative. Dimri et al. described a pH 6.0 β-galactosidase activity, which was found specifically in senescent human fibroblast cultures, but not in quiescent or terminally differentiated cells.[244] In comparison to quiescence which is a reversible process involving the capacity of the cells to re-enter to the cell cycle, senescence is characterized by a lack of response to mitogenic stimuli such as growth factors.[289] The results of Kurz et al. demonstrated that the pH 6.0 β-galactosidase activity detected in senescent cells as well as their flow cytometric SSC characteristics are consequence of the increased lysosomal mass in these cells.[290] In our FACS analysis we also found an increase in the SSC profile of VDRKO cells. Apart of the increased cell size and granularity, many studies have reported the importance of $p19^{INK4d}$, $p21^{CIP1}$, $p27^{KIP1}$ and $p57^{KIP2}$ genes in cellular senescence. These molecules are considered as biological markers of cell senescence for their higher expression and accumulation in aged cells.[291,292,293] We found all of these genes to be up-regulated

in the VDRKO cells. Some environmental stress can also lead to the overexpression of these genes, which may induce premature senescent cells.[294,295] A long term overexpression of $p21^{Cip1}$ with the subsequent hypophosphorylation of pRb was observed in SIPS induced by H_2O_2.[296] Moreover it is well known that in the atherosclerotic lesions there are vascular cells that exhibit the morphological features of cellular senescence.[297] These cells also show impaired function, such as the decreased expression of endothelial NOS and the increased expression of proinflammatory molecules, two findings that we already discussed to be found in VDRKO mice. Furthermore, vasodilation has been found to be impaired with age due to the decreased endothelial production of vasodilators such as nitric oxide (NO) as well as to reduced responsiveness of VSMC to vasodilators.[298] The increased expression of proinflammatory and prothrombogenic molecules was also observed in vascular cells of aged arteries. Moreover, it has been shown that the arterial components of the Ang II signalling cascade increase with aging and contribute to the pathogenesis of atherosclerosis.[299] In this context, the impaired expression of iNOS, the higher expression of IL-6 and the elevated concentration of Ang II could be related to the senescent phenotype, found in some VDRKO cells. The higher levels of $p21^{Cip1}$, measured by RT-PCR and detected by immunoblotting, could mediated the effects of endogenously produced Ang II leading to the appearance of premature senescence in VDRKO cells.[48]

Senescent cells are metabolically active, but they lack the capacity to replicate, therefore are unable to perform DNA synthesis and continue to grow. This finding was confirmed for our mutant cells by the MTT assay. As the chemical reaction that leads to the formation of formazan is performed by mitochondrial enzymes, the lower absorbance measured in the VDRKO cells could be due to impaired mitochondrial function. The observation of the ultrastructure of the mutant cells in the TEM pictures gave us more evidence for the senescent phenotype of these cells. The wrinkled membrane of the irregular nucleus, the abundance of vacuoles and lysosomes and the mitochondria with damaged cristae pointed to the possibility that VDRKO cells are exposed to higher oxidative stress. Oxidative stress alters proteins and organelles and the proper cytoplasmic protein turnover influencing autophagic process.[300] This could explain the finding of autophagic vacuoles in the cytoplasm of VDRKO cells. Nowadays some authors consider autophagy to be a survival pathway that the cells bring into play in unfavorable microenvironmental conditions [301].

The presence of pro-oxidant conditions in the VDRKO cell environment was suspected by the decrease expression of NADH-ubiquinone oxireductase (complex I

of the mitochondrial respiratory chain) sununit ND1α subcomplex 9 (39kDa) found by WB. This subunit is important for the assembly of the complex I, a requisite for normal functioning. It has been shown that complex I and III are the possible places where a premature electron leakage occurs, thus being one of main sites of production of harmful superoxide. Complex I translocates four H^+ across the inner membrane per molecule of oxidized NADH, thus providing sources for the formation of the electrochemical potential, used to produce ATP. Thus, if complex I is not performing well, because of its lower expression, we could expect lower ATP production.

After the estimation of the bioenergetic state of the studied VSMCs we found that the mutant cells possessed lower levels of ATP than the WT, which indicated a metabolic dysfunction, either a higher ATP consumption or an impaired ATP production. The lower content of ATP was confirmed also indirectly by the increased phosphorylation of the cellular sensor of the energy status adenosine monophosphate (AMP)-activated protein kinase (AMPK). AMPK is activated in conditions that lead to depletion of cellular ATP (reflected as increased AMP), including glucose deprivation, exercise, hypoxia and ischaemia. After the oxidative stress produced in our cells by the addition of 0.4mM H_2O_2 or the inhibition of F1F0ATPase (comlex V of the mitochondrial oxidative phosphorylation system) with 2μg/ml oligomycin, which enables the synthesis of ATP, we found that the mutant cells presented higher AMPK phosphorylation which is in accordance with the lower ATP level. It has been shown that some metabolic inhibitors, like oligomycin, rescued cell death in vitro, activating ERK pro-survival signalling, which is known to be induced by growth factors addition. The treatment with oligomycin slightly induced the phosphorylation of ERK1/2 in WT cell. From the fact that the inhibition of ATP synthesis leads to an activation of ERK1/2 and the finding that the mutant cells present higher levels of P-ERK1/2 in quiescent state than the controls, we could speculate that the reason for this activation in the VDRKO cells probably is a signal for survival. Moreover, it has been demonstrated that Ang II induces AMPK activation in an AT1-R-dependent manner, and this activation leads to the inhibition of Ang II–induced ERK1/2 phosphorylation, which has as a consequence the inhibition of the Ang II– stimulated VSMC proliferation.[247]

The higher activation of AMPK in the VDRKO cells could be considered as a consequence of the lower ATP content, which the VDRKO cells used during the G1 phase arrest. Thus, the larger VDRKO cells need more ATP to maintain their vital functions. Once activated, AMPK phosphorylates downstream substrates, with an overall effect of switching off ATP consuming pathways (*e.g.* fatty acid and

cholesterol synthesis) as well as cell proliferation [302] and to switch on catabolic pathways that generate ATP (*e.g.* fatty acid oxidation and glycolysis). The overall decrease in the fatty acid synthesis is obvious from the VDRKO mice lean phenotype and very few amount of adipose tissue.

In a study with human fibroblasts as a model of in vitro senescence Zwerschke at al. showed that senescent fibroblasts entered into a metabolic imbalance leading to strong reduction in the levels of ATP, which was required for nucleotide biosynthesis and proliferation. They attributed the ATP depletion in senescent cells to deregulations of the glycolytic enzymes, which leads to a drastic increase in cellular AMP, which induces premature senescence [303].

In order to assess the hypothesis that the lower ATP content is because of an impaired ATP production, as a result of mitochondrial disfunction, the respiratory flux in WT and VDRKO cells was assessed by high resolution respirometry. The experiments started with the registration of the routine respiration of the cells. Respiratory capacity per cell, measured during the routine stady state phase and after uncoupling with FCCP was decreased in the VDRKO cells, meanwhile the inhibition of the ATPase with oligomycin decrease the respiration to a similar extend in VDRKO and WT cells. When the respiration was totally blocked by the inhibition of complex III, the residual respiration was even higher in the mutant cells. Huntter at al. showed that the senescent cells present higher expression of CS protein when equal cell numbers were used, which reflects the increased cell volume, total protein content and cellular respiration that occur with replicative age. Their results indicated that the increased mitochondrial respiration of the senescent cells was due to the increased mitochondrial content [225].

When we normalized the oxygen flux to the activity of CS, neither the coupled nor the uncoupled respiration was found to be different in the VDRKO cells. The only situation when the VDRKO cells consumed significantly more oxygen was during the residual respiration after the inhibition with actinomycin A, a finding found also after the normalization of the respiration per cell. Further, the respiratory control ratios were determined from the titrations with oligomycin and the uncoupling agent FCCP. Significantly increased mitochondrial inverse respiratory (1/RCR), uncoupling (1/UCR) and phosphorylating (1/RCRp) control ratios in VDRKO cells in comparison to the WT were found. These ratios are related to the control of the electron flux trough the respiratory chain to the ATP synthase. The higher inverse ratios of the VDRKO control ratios pointed to a lower efficiency of these cells. Huntter et al. had attributed the lower RCR and UCP ratios of the senescent cells to a partial uncoupling. They found that the senescent cells were

able to enhance the electron transport as a compensatory mechanism for the increased electron leakage.[225] In our case however, no electron leakage is detected, because the routine respiration is similar in WT and VDRKO cells.

The lower efficiency of the mitochondrial electron transport chain (ETC) resulting in lower ATP content in the VDRKO cells, could be due to the decreased expression/deficiency of complex I. It has been shown that the mitochondrial oxidation of NADH is diminished when a significant decline in the activity of complex I is present.[304] In this case flavin adenine dinucleotide (FADH2), produced after the oxidation of succinate to fumarate by complex II in the Krebs cycle, could give an alternative supply of reducing equivalents and maintain the oxidative phosphorylation as the electrons from $FADH_2$ enter the ETC distal to complex I (trough complex II). This phenomenon is observed during the reperfusion of an ischemic myocardium, where a switch to fatty acid oxidation, as a fuel, has been described. The usage of FADH2 as electron carrier is thermodynamically less efficient because it requires more electrons and more oxygen, but produces a fast flux of ATP. It has been calculated that the oxidation of NADH to NAD^+ pumps 3 protons which charges the electrochemical gradient with enough potential to generate between 2,5 and 3 ATP molecules, meanwhile the oxidation of FADH2 to FAD^+ pumps 2 protons which is calculated to be enough for the generation of 1.5 equivalents of ATP.

Moreover, the significantly higher residual respiration of the mutant cells in the presence of antimycin A is probably due to extra-mitochondrial consumption of oxygen which could be associated with increased production of reactive oxygen species (ROS). ROS are derivatives of O_2 metabolism, including superoxide anions, hydrogen peroxide, hydroxyl radicals and nitric oxide. In vascular cells, ROS are important intracellular signalling molecules that regulate vascular function, modulating cell growth/apoptosis, migration and extracellular matrix protein turnover, thus contributing to vascular remodelling. Cardiovascular diseases, such as hypertension, are associated with increased ROS formation.[249] Oxidative stress in the vasculature reduces the levels of the vasodilator nitric oxide, causes tissue injury, promotes protein oxidation and DNA damage, and induces proinflammatory responses.

By FACS analysis of the superoxide anion levels in the studied cells we found a significant increase in the content of this free radical in the VDRKO cells. The fact that the quiescent VDRKO cells were exposed to pro-oxidant conditions was suspected also by the increase phosphorylation of two stress-induced MAPK, p38

and ERK1/2 in comparison with the WT, but this difference was no more detectable after the addition of growth factors containing FBS. It has been shown that p38 MAPK together with forkhead box O1 transcriptional factor (FOXO1) are involved in the expression of thioredoxin interacting protein (Txnip) that inhibits the thioredoxin (Trx). The TRX system (TRX, TRX reductase, and NADPH) is thiol antioxidant system in the cardiovascular system that regulates the reduction of intracellular ROS [106]. It has been demonstrated that the upregulation of Txnip and subsequent impairment of thioredoxin antioxidative system through p38MAPK and FOXO1 may participate in the intracellular ROS increase [107]. The mitochondria are protected from oxidative stress by both low oxygen levels and complex defence systems against reactive oxygen species (ROS). Another family of enzymes that are involved in ROS detoxification by catalysing the dismutation of superoxide radical (O_2^-) into hydrogen peroxide (H_2O_2) and oxygen (O_2) is the superoxide dismutase (SOD) family. It has been shown that in prostatic primary cultures $1,25(OH)_2D_3$ induced the expression of thioredoxin reductase 1 and superoxide dismutase 2. By WB analysis of the protein expression of SOD1/SOD2 in quiescent cells we found that the cytosolic Cu-Zn SOD1 protein and the intramitochondrial Mn SOD2 were down-regulated in quiescent VDRKO cells, meanwhile in FBS-stimulated cells their was no difference. This finding could be explained with the possibility that during the basal growth of the cells the lack of signalling trough VDR impedes the activation of the SOD genes.

After the induction of oxidative stress by one hour treatment with 0.4mM H_2O_2, the FACS frequency diagrams showed that the WT cells didn't react to this treatment; meanwhile the exposure of the VDRKO cells to the pro-oxidant compound provoked a further increase in the superoxide anion levels. This reaction of the mutant cells could be due the lower expression and subsequently activity of the upper-mentioned anti-oxidant enzymes. Thus, the reduced anti-oxidant defence of the VDRKO cells could be one of the reasons for the increased levels of superoxide anion in these cells. These results confirmed that VSMC that lack the vitamin D signalling because of the VDR disruption are exposed and are more susceptible to oxidative stress, displaying a sort of "physiological oxidative imbalance" when compared with WT, a fact that was expected because of the well known antioxidant activities of vitamin D.

In the vascular wall there are some potential sources of superoxide production such as NAD(P)H oxidase, xanthine oxidase, lipooxigenase, etc. and NADPH oxidase is considered as the main one [305] and is believed to play a role in Ang II-induced hypertrophy [96]. Further, it has been demonstrate that this increase

in cell volume is mediated via the AT1 subtype receptor. In the study of Herbert at al. it has been found that the Ang II – induced ROS provoke senescence by two mechanisms: acute stress-induced premature senescence SIPS, the one that is telomere independent and replicative senescence, that depends on the telomere shortening [306]. Kunieda et al. reported that in VSMC Ang II induces both, premature senescence and inflammation via a $p21^{Cip1}$ pathway by 3 days of treatment without telomere shortening. They found that $p21^{Cip1}$ activates both, pro-inflammatory transcription factors and small G proteins that positively regulate NADPH oxidase activity, thus increasing the production of ROS [48]. Recent study has show that Ang II via its receptor AT1 produces senescence in rat VSMC by increasing the NADPH oxidase activity and superoxide production [307].

By blocking either the AT1-mediated signalling with losartan or the NADPH oxidase with DPI, we confirmed that the origin of the elevated superoxide anion levels was the Ang II, produced and functioning in the VDRKO cells by an auto/paracrine mechanism. Moreover, the oxidant milieu of the VDRKO cells could be the reason for the induction of the CDI $p57^{Kip2}$ as its levels were significantly reduced, even not to the levels in the WT cells, by the superoxide scavenger Tiron. The expression of this regulator of the cell cycle in the VDRKO was decreased to a similar extant and after the blocking of the Ang II-AT1-R action. The WT expression of neither $p21^{Cip1}$ nor $p57^{Kip2}$ was affected by the antioxidant treatment; meanwhile the inhibition of the AT1 receptor in 72 hours was able to decrease significant the proliferation of the treated WT cells, measured by the changes in the cell number. In contrary, when the AT1 receptor for Ang II was blocked, the VDRKO presented significantly higher cell numbers in comparison with the untreated mutant cells.

The in vitro migration of the VDRKO cells, assessed by "wound healing" assay was also found to be impaired, finding that was confirmed by our in vivo studies. First, in the angiogenesis model, the capacity of endothelial and pericyte cells to migrate, proliferate, and produce appropriate spatial orientation to form tubular formations in the Matrigel plug was found to be reduced in the VDR ablated mice. Reidy et al. have shown that the initiation of the neointima formation is a result of VSMC migratory rather than proliferation. The migration and proliferation of smooth muscle cells (SMC) were induced by endothelial denudation of the carotid artery. In our carotid artery injury model the increase in the thickness of medial layer of the artery wall of the VDRKO mice was significantly lower than in the control mice. In vivo, VSMCs are in quiescent state under normal conditions, and their entry into the cell cycle occurs in various situations. As a result of damage to the vessel, VSMCs are stimulated to proliferate in response to mitogens that cause

entry into S phase of cell cycle. Three critical processes has been shown to be important for the proliferation of VSMCs after injury – dedifferentiation and growth of medial VSMCs; migration, transdifferentiation and proliferation of adventitial fibroblasts and recruitment of progenitor cells. This proliferation is in order to produce the repair of the vessel, after which the cells enter again in a quiescent state. The uncontrolled proliferation of VSMCs has been linked to diseases such as hypertension and atherosclerosis. Moreover, it has been found that the proliferating and producing extracellular matrix components VSMCs play an essential role in the maintenance of the stability of an atherosclerotic plaque, preventing its rupture.

Thus, as a general conclusion of this work, the deceased proliferation rates of VSMC lacking functional vitamin D receptor are likely due to the increased endogenous production of Ang II that after the activation of the AT1-R upregulates NADPH oxidase with a subsequent elevation in the production of free radicals that are widely implicated in vascular inflammation and fibrosis and participate in the uncoupling of the cell growth from the proliferation, leading to growth arrest and senescence of VDRKO cells with increased expression of $p57^{Kip2}$ and hypertrophy.

CONCLUSIONS

Based on our results we can conclude that:

1. Vascular smooth muscle cells, obtained from mice lacking functional VDR present impaired proliferation capacity *in vitro* and *in vivo*.

2. The decreased proliferation of VDRKO VSMC is due to increased expression of cyclin dependent kinase inhibitors $p19^{Arf}$, $p21^{Cip1}$, $p27^{Kip1}$ and especially of $p57^{Kip2}$.

3. The VDRKO VSMC showed increased levels of angiotensin II production, related to the elevated levels of cathepsin D.

4. VDRKO vascular cells show hypertrophic changes due to the elevated Ang II levels.

5. The sustained signalling trough AT1 receptor in VDRKO cell leads to the activation of NADPH oxidase with subsequent elevation in the intracellular levels of superoxide anions.

6. The ablation of VDR in VSMC reduces their mitochondrial anti-oxidant capacity, decreasing the expression of manganese superoxide dismutase.

7. The mutant cells showed decreased expression of the assembling 39kDa subunit of the mitochondrial complex I and reduced efficiency.

8. All these findings in VDRKO vascular cells are associated with the presence of stress-induced premature senescence.

Thus, our results point to the important role of vitamin D trough its nuclear receptor in the prevention of VSMC hypertrophy and senescence, two processes that occur during the development of the atherosclerotic lesions.

1. Las células de musculo liso vascular, obtenidas de ratones que carecen VDR funcional presentan una capacidad de proliferación disminuida in vitro e in vivo.

2. La disminución en la proliferación de las CMLV VDRKO se debe al incremento en la expresión de los inhibidores la quinasas dependientes de ciclina, $p19^{Arf}$, $p21^{Cip1}$, $p27^{Kip1}$ y especialmente de $p57^{Kip2}$.

3. Las CMLV VDRKO mostraron un aumento de los niveles de producción de angiotensina II, relacionado con niveles elevados de catepsina D.

4. Las células vasculares VDRKO muestran cambios hipertroficos, debido a los niveles más altos de Ang II.

5. La señalización sostenida a través del receptor AT1 en la celulas VDRKO conduce a la activación de la NADPH oxidasa con posterior elevación en los niveles intracelulares del anión superóxido.

6. La carencia de VDR en CMLV reduce su capacidad antioxidante mitocondrial, disminuyendo la expresión de la superóxido dismutasa de manganeso.

7. Las células mutantes mostraron una disminución en la expresión de la subunidad de montaje del complejo I de 39kDa y una efficiencia reducida.

8. Todos estos encuentros en las células vasculares VDRKO se asocian con la presencia de senescencia prematura inducida por estrés.

Por lo tanto, nuestros resultados apuntan a la importancia de la vitamina D a través de su receptor nuclear en la prevención de la hipertrofia de CMLV y la senescencia, dos procesos que ocurren durante el desarrollo de las lesiones ateroscleróticas.

1. Cèl·lules de múscul llis vascular, obtingudes a partir de ratolins que no tenen VDR funcional presenten una capacitat de proliferació disminuïda in vitro i in vivo.

2. La disminució de la proliferació de les CMLV VDRKO es deu a l'increment en l'expressió dels inhibidors de quinasa depenents de ciclina $p19^{Arf}$, $p21^{Cip1}$, $p27^{Kip1}$ y especialment de $p57^{Kip2}$.

3. Les CMLV VDRKO van mostrar un augment dels nivells de producció d'angiotensina II, relacionat amb els nivells de catepsina D.

4. Les CMLV VDRKO van mostrar uns cambis hipertrofics que es deu a l'increment en els nivels de Ang II.

5. La senyalització sostinguda a través del receptor AT1 en cèl·lules VDRKO condueix a l'activació de la NADPH oxidasa amb una elevació posterior dels nivells intracel.lulars de l'anió superòxid.

6. L´ausència de VDR en CMLV redueix la seva capacitat antioxidant mitocondrial, disminuint l'expressió de la dismutasa de superòxid de manganès.

7. Les cèl·lules mutants van mostrar una disminució de l'expressió de la subunitat de muntatge del complex I de 39kDa i una eficiencia disminuinta.

8. Totes aquestes troballes en cèl·lules vasculars VDRKO s´associen amb la presència de senescència prematura induïda per estrès.

Per tant, els nostres resultats apunten a la importància de la vitamina D a través del seu receptor nuclear en la prevenció de la hipertròfia de CMLV i la senescència, dos processos que ocorren durant el desenvolupament de les lesions ateroscleròtiques.

1. Съдови гладкомускулните клетки, получени от мишки лишени от функционален РВД представят нарушен пролиферационен капацитет ин витро и ин виво.

2. Намалената пролиферация на РВД-/- ГМК се дължи на повишената експресия на инхибитори на циклин зависимите кинази, $p19^{Arf}$, $p21^{Cip1}$, $p27^{Kip1}$ и особенно на $p57^{Kip2}$.

3. РВД-/- ГМК показват повишени нива на производство на ангиотензин II, което е свързано с повишените нива на катепсин Д.

4. РВД-/- ГМК изявяват хипертрофични промени, свързани с увеличените нива на Анг II.

5. Постоянната сигнализация през АТ1 рецепторите в РВД-/- клетка води до активирането на НАДФН оксидазата с последващо увеличение на вътреклетъчното ниво на супероксидни аниони.

6. Премахването на РВД в ГМК намалява техния митохондриален антиоксидантен капацитет, понижавайки експресията на манганова супероксид дисмутаза.

7. Мутираните клетки показват намалена експресия на субединицата от митохондриалния комплекс I с големина 39kDa участваща в сглобяването на комплекса и понижена ефективност.

8. Всички тези находки в РВД-/- съдови клетки са свързани с наличието на стрес индуцирано преждевременно стареене.

Така, получените резултати насочват към важната роля на витамин Д посредствум ядрения си рецептор за предотвратяването на хипертрофия и стареене на гладкомускулните клетки, два процеса, които се случват по време на развитието на атеросклеротични лезии.

Annex

1. Scientific publications:

Petya Valcheva, Jordi Boada, Anna Cardus, Sara Panizo, Eva Parisi, Milica Bozic, Jose M Lopez-Novoa, Adriana Dusso, Elvira Fernandez, Jose M Valdivielso **Lack of Signalling through VDR Leads to Decreased Proliferation and Stress-induced Premature Senescence in VSMC** (*Manuscript in preparation*)

Eva Parisi, Milica Bozic, Merce Ibarz, Sara Panizo, **Petya Valcheva**, Blai Coll, Elvira Fernandez, Jose Valdivielso **Sustained activation of renal N-methyl-D-aspartate receptors decreases vitamin D synthesis: a possible role for glutamate on the onset of secondary HPT.** Am J Physiol Endocrinol Metab. (2010) Am J Physiol Endocrinol Metab. **2010**; 299(5):E825-831.

Sara Panizo, Anna Cardus, Mario Encinas, Eva Parisi, **Petya Valcheva**, Susana López-Ongil, Blai Coll, Elvira Fernandez, and Jose M. Valdivielso **RANKL Increases Vascular Smooth Muscle Cell Calcification Through a RANK-BMP4–dependent pathway**. Circ. Res. **2009**; 104(9):1041-1048.

Eva Parisi, Josep Maria Reñé, Anna Cardús, **Petya Valcheva**, Carme Piñol-Felis, José Manuel Valdivielso, Elvira Fernández. **Vitamin D receptor levels in colorectal cancer. Possible role of BsmI polymorphism**. J Steroid Biochem Mol Biol. **2008**; 111(1-2):87-90.

2. Participation in conferences and congresses:

Petya Valcheva, Jordi Boada, Milica Bozic, Adriana Dusso, Elvira Fernandez and Jose M Valdivielso. **La falta de senyalització per receptor de Vitamina D indueix Senescència prematura en cèl.lules de músculo llis vascular.** V Reunió de Joves Investigadors en Risc Vascular, 21-22 de gener de **2011**, Cardona (presentació dins la Taula "Marcadors sistèmic i lesió vascular")

Petya Valcheva, Sara Panizo, Eva Parisi, Milica Bozic, Juan F. Navarro, Blai Coll, Elvira Fernandez and Jose M. Valdivielso. **Lack of vitamin D receptor induces elevated production of angiotensin II that leads to oxidative stress induced premature senescence in vascular smooth muscle cells.** World Congress of Nephrology, May 22-26 2009, Milan, Italy; Poster, published as one of the Top 20 abstracts in NDT Plus **2009** 2 (suppl 2).

Petya Valcheva, Sara Panizo, Eva Parisi, Milica Bozic, Blai Coll, Elvira Fernandez, Jose Valdivielso. **Lack of vitamin D receptor leads to elevated production of angiotensin II which induces premature senescence in vascular smooth muscle cells.** V International Symposium "Advances in Bone and Mineral Disorders in CKD", P67, Oviedo, Spain, March 19-20**, 2009** (Poster, awarded with membership of ERA-EDTA for year 2009)

P.Valcheva, S.Panizo, E.Parisi, M.Bozic, B.Coll, E.Fernandez, J.M.Valdivielso. **La falta del receptor de la vitamina D lleva a elevada producción de angiotensina II que induce senescencia prematura en células del músculo liso vascular.** XXXVIII Congreso Nacional de la S.E.N, Donostia-San Sebastián, del 4 al 7 de octubre de octubre de **2008** (*Comunicación Oral*)

S.Panizo, A.Cardús, M.Encinas, E.Parisi, **P.Valcheva**, E.Fernández, J.M. Valdivielso. **RANKL incrementa la calcificación de células de músculo liso vascular a traves del aumento de BMP4 mediado por RANK.** XXXVIII Congreso Nacional de la S.E.N, Donostia-San Sebastián, del 4 al 7 de octubre de octubre de **2008** (*Comunicación Oral*)

E.Parisi, **P.Valcheva**, Y.Almadén, M.Ibarz, Sara Panizo, M.Rodríguez, E.Fernández, J.M. Valdivielso. **El receptor de N-Metil-D-Aspartato se expresa en la glándula paratiroides y regula la secreción de PTH.** XXXVIII Congreso

Nacional de la S.E.N, Donostia-San Sebastián, del 4 al 7 de octubre de octubre de **2008** (*Comunicación Oral*)

Petya Valcheva, Sara Panizo, Anna Cardus, Eva Parisi, Carme Gallego, Marti Aldea, Elvira Fernandez, Jose Valdivielso. **Lack of vitamin D receptor induces senescence in vascular smooth muscle cells.** XLV ERA-EDTA Congress, May 10-13 Stockholm, Sweden, **2008** (*Poster*)

Petya Valcheva, Sara Panizo, Anna Cardus, Eva Parisi, Carme Gallego, Marti Aldea, Elvira Fernandez, Jose M. Valdivielso. **Role of vitamin D receptor in vascular smooth muscle cell proliferation.** ASN, Renal Week, San Francisco, **2007** (*Poster*)

Sara Panizo, Anna Cardús, **Petya Valcheva**, Eva Parisi, Elvira Fernández, José M. Valdivielso. **Role of RANKL on the Vascular Smooth Muscle Cells calcification in vitro** ASN, Renal Week, San Francisco, **2007** (*Poster*)

P.Vladeva, S.Panizo, A.Cardús, E.Parisi, M.Aldea, C.Gallego, E Fernández Giráldez, J.M.Valdivielso. **Papel del receptor de vitamina D en la proliferación y migración de las células de músculo liso vascular.** XXXVII Congreso Nacional de la S.E.N, Cádiz, del 29 de septiembre al 2 de octubre de **2007** (*Póster*)

S.Panizo, A.Cardús, E Parisi, **P.Vladeva**, E.Fernández Giráldez, J.M. Valdivielso. **Efectos diferenciales del calcitriol y paricalcitol en la calcificación de células de músculo liso vascular in vitro. Papel de RANKL.** XXXVII Congreso Nacional de la S.E.N, Cádiz, del 29 de septiembre al 2 de octubre de **2007** (*Póster*)

O. Gracia, S. Panizo, M. Panadés, M. Ibars, M. Borrás, F. Sarró, **P. Valcheva**, J. Roig, E. Fernández, J. Valdivielso. **Efecto de la vitamina D sobre la nefropatía diabética.** XXIII Reunió anual de la societat catalana de nefrologia, Lleida, 31 de maig i 1 de juny de **2007** (*Presentación oral*)

Sara Panizo, Anna Cardús, Eva Parisi, **Petya Valcheva**; Elvira Fernández; Jose M. Valdivielso. **Differential Effects of the Calcitriol and Paricalcitol in the Calcification of Vascular Smooth Muscle Cells In Vitro.** J Am Soc Nephrol 17, p.687A, **2006** (*Poster*)

Eva Parisi, Merce Ibarz, Paula Gassiot, **Petya Valcheva**, Sara Panizo, Anna Cardús, Elvira Fernández, Jose M. Valdivielso. **Role of N-Methyl-D-Aspartate Receptor Activation in Renal Function.** J Am Soc Nephrol 17, p.474A, **2006** (*Poster*)

S Panizo, A Cardús, E Parisi, **P Valcheva**, E Fernández, J.M. Valdivielso. **Efectos diferenciales del calcitriol y paricalcitol en la calcificación de células de músculo liso vascular in vitro.** V Congreso Iberoamericano de Nefrología y XXXVI Congreso Nacional de la S.E.N, Madrid, del 18 al 21 de octubre de **2006** (*Póster*)

THE CARDIFF SCHOOL OF HEALTH SCIENCES
YSGOL GWYDDORAU IECHYD CAERDYDD

UWIC

Friday, 27 November 2009

TO WHOM IT MAY CONCERN

RE: Working Visit to Cardiff School of Health Sciences - Petya Valcheva

We are pleased confirm that Petya Valcheva from the University of Lleida, has completed her 3 month work placement with the Cardiff School of Health Sciences on 30th November 2009.

During this period she has been working under the supervision of Professor Jorge Erusalimsky, with the assistance of Dr Anna Cardus on the project: "The effect of calcitriol treatment over the onset of premature senescence in vascular endothelial cells"

We have enjoyed working with Petya and wish her every success for the future.

Yours sincerely

Jorge D.Erusalimsky, PhD
Professor of Biomedical Sciences
Cardiff School of Health Sciences
UNIVERSITY OF WALES INSTITUTE, CARDIFF
Western Avenue
Cardiff, Wales CF5 2YB, UK

Tel: +44 (0)29 2041 6853
Fax: +44 (0)29 2041 6982

http://www.uwic.ac.uk/cellsenescence

PO Box 377 Western Avenue Cardiff CF5 2YB UK
Tel: +44 (0)29 2041 6070 Fax: +44 (0)29 2041 6982
web: www.uwic.ac.uk
Cardiff's **metropolitan** university

Blwch SP 377 Rhodfa'r Gorllewin Caerdydd CF5 2YB DU
Ffôn: +44 (0)29 2041 6070 Ffacs: +44 (0)29 2041 6982
gwe: www.uwic.ac.uk
prifysgol **metropolitan** Caerdydd

REFERENCE LIST

References

1. Yao Q, Axelsson J, Heimburger O, Stenvinkel P, Lindholm B. Systemic inflammation in dialysis patients with end-stage renal disease: causes and consequences. *Minerva Urol Nefrol* 2004 September;56(3):237-48.

2. Levin A, Bakris GL, Molitch M et al. Prevalence of abnormal serum vitamin D, PTH, calcium, and phosphorus in patients with chronic kidney disease: results of the study to evaluate early kidney disease. *Kidney Int* 2007 January;71(1):31-8.

3. Zhang QL, Rothenbacher D. Prevalence of chronic kidney disease in population-based studies: systematic review. *BMC Public Health* 2008;8:117.

4. Otero A, de FA, Gayoso P, Garcia F. Prevalence of chronic renal disease in Spain: results of the EPIRCE study. *Nefrologia* 2010;30(1):78-86.

5. Ahmed J, Weisberg LS. Hyperkalemia in dialysis patients. *Semin Dial* 2001 September;14(5):348-56.

6. Levin A. Anemia and left ventricular hypertrophy in chronic kidney disease populations: a review of the current state of knowledge. *Kidney Int Suppl* 2002 May;(80):35-8.

7. Palmer BF. Sexual dysfunction in uremia. *J Am Soc Nephrol* 1999 June;10(6):1381-8.

8. Brown EM, Gamba G, Riccardi D et al. Cloning and characterization of an extracellular Ca(2+)-sensing receptor from bovine parathyroid. *Nature* 1993 December 9;366(6455):575-80.

9. Freichel M, Zink-Lorenz A, Holloschi A, Hafner M, Flockerzi V, Raue F. Expression of a calcium-sensing receptor in a human medullary thyroid carcinoma cell line and its contribution to calcitonin secretion. *Endocrinology* 1996 September;137(9):3842-8.

10. Aida K, Koishi S, Tawata M, Onaya T. Molecular cloning of a putativeCa(2+)-sensing receptor cDNA from human kidney. *Biochem Biophys Res Commun* 1995 September 14;214(2):524-9.

11. Miyamoto K, Tatsumi S, Morita K, Takeda E. Does the parathyroid 'see' phosphate? *Nephrol Dial Transplant* 1998 November;13(11):2727-9.

12. Silver J, Levi R. Regulation of PTH synthesis and secretion relevant to the management of secondary hyperparathyroidism in chronic kidney disease. *Kidney Int Suppl* 2005 June;(95):S8-12.

13. Krajisnik T, Bjorklund P, Marsell R et al. Fibroblast growth factor-23 regulates parathyroid hormone and 1alpha-hydroxylase expression in cultured bovine parathyroid cells. *J Endocrinol* 2007 October;195(1):125-31.

14. Urakawa I, Yamazaki Y, Shimada T et al. Klotho converts canonical FGF receptor into a specific receptor for FGF23. *Nature* 2006 December 7;444(7120):770-4.

15. Cozzolino M, Gallieni M, Corsi C, Bastagli A, Brancaccio D. Management of calcium refilling post-parathyroidectomy in end-stage renal disease. *J Nephrol* 2004 January;17(1):3-8.

16. D'Agostino RB, Sr., Vasan RS, Pencina MJ et al. General cardiovascular risk profile for use in primary care: the Framingham Heart Study. *Circulation* 2008 February 12;117(6):743-53.

17. Amann K, Rychlik I, Miltenberger-Milteny G, Ritz E. Left ventricular hypertrophy in renal failure. *Kidney Int Suppl* 1998 December;68:S78-S85.

18. Sarnak MJ, Levey AS, Schoolwerth AC et al. Kidney disease as a risk factor for development of cardiovascular disease: a statement from the American Heart Association Councils on Kidney in Cardiovascular Disease, High Blood Pressure Research, Clinical Cardiology, and Epidemiology and Prevention. *Circulation* 2003 October 28;108(17):2154-69.

19. Dzau VJ, Braun-Dullaeus RC, Sedding DG. Vascular proliferation and atherosclerosis: new perspectives and therapeutic strategies. *Nat Med* 2002 November;8(11):1249-56.

20. Weissberg PL, Cary NR, Shanahan CM. Gene expression and vascular smooth muscle cell phenotype. *Blood Press Suppl* 1995;2:68-73.

21. Owens GK. Molecular control of vascular smooth muscle cell differentiation. *Acta Physiol Scand* 1998 December;164(4):623-35.

22. Stompor T. An overview of the pathophysiology of vascular calcification in chronic kidney disease. *Perit Dial Int* 2007 June;27 Suppl 2:S215-S222.

23. Cozzolino M, Brancaccio D, Gallieni M, Slatopolsky E. Pathogenesis of vascular calcification in chronic kidney disease. *Kidney Int* 2005 August;68(2):429-36.

24. Bedalov A, Breault DT, Sokolov BP et al. Regulation of the alpha 1(I) collagen promoter in vascular smooth muscle cells. Comparison with other alpha 1(I) collagen-producing cells in transgenic animals and cultured cells. *J Biol Chem* 1994 February 18;269(7):4903-9.

25. Donovan J, Slingerland J. Transforming growth factor-beta and breast cancer: Cell cycle arrest by transforming growth factor-beta and its disruption in cancer. *Breast Cancer Res* 2000;2(2):116-24.

26. Sherr CJ. Cancer cell cycles. *Science* 1996 December 6;274(5293):1672-7.

27. Reynisdottir I, Massague J. The subcellular locations of p15(Ink4b) and p27(Kip1) coordinate their inhibitory interactions with cdk4 and cdk2. *Genes Dev* 1997 February 15;11(4):492-503.

28. Serrano M, Lin AW, McCurrach ME, Beach D, Lowe SW. Oncogenic ras provokes premature cell senescence associated with accumulation of p53 and p16INK4a. *Cell* 1997 March 7;88(5):593-602.

29. Phelps DE, Hsiao KM, Li Y et al. Coupled transcriptional and translational control of cyclin-dependent kinase inhibitor p18INK4c expression during myogenesis. *Mol Cell Biol* 1998 April;18(4):2334-43.

30. Chen D, Krasinski K, Sylvester A, Chen J, Nisen PD, Andres V. Downregulation of cyclin-dependent kinase 2 activity and cyclin A promoter activity in vascular smooth muscle cells by p27(KIP1), an inhibitor of neointima formation in the rat carotid artery. *J Clin Invest* 1997 May 15;99(10):2334-41.

31. Rodriguez I, Coto E, Reguero JR et al. Role of the CDKN1A/p21, CDKN1C/p57, and CDKN2A/p16 genes in the risk of atherosclerosis and myocardial infarction. *Cell Cycle* 2007 March 1;6(5):620-5.

32. Walsh K, Shiojima I, Gualberto A. DNA replication and smooth muscle cell hypertrophy. *J Clin Invest* 1999 September;104(6):673-4.

33. Owens GK, Schwartz SM. Alterations in vascular smooth muscle mass in the spontaneously hypertensive rat. Role of cellular hypertrophy, hyperploidy, and hyperplasia. *Circ Res* 1982 September;51(3):280-9.

34. Braun-Dullaeus RC, Mann MJ, Ziegler A, von der Leyen HE, Dzau VJ. A novel role for the cyclin-dependent kinase inhibitor p27(Kip1) in angiotensin II-stimulated vascular smooth muscle cell hypertrophy. *J Clin Invest* 1999 September;104(6):815-23.

35. Gibbons GH, Pratt RE, Dzau VJ. Vascular smooth muscle cell hypertrophy vs. hyperplasia. Autocrine transforming growth factor-beta 1 expression determines growth response to angiotensin II. *J Clin Invest* 1992 August;90(2):456-61.

36. HAYFLICK L, MOORHEAD PS. The serial cultivation of human diploid cell strains. *Exp Cell Res* 1961 December;25:585-621.

37. Ben-Porath I, Weinberg RA. When cells get stressed: an integrative view of cellular senescence. *J Clin Invest* 2004 January;113(1):8-13.

38. Campisi J. Cancer, aging and cellular senescence. *In Vivo* 2000 January;14(1):183-8.

39. Narita M, Nunez S, Heard E et al. Rb-mediated heterochromatin formation and silencing of E2F target genes during cellular senescence. *Cell* 2003 June 13;113(6):703-16.

40. Erusalimsky JD, Kurz DJ. Cellular senescence in vivo: its relevance in ageing and cardiovascular disease. *Exp Gerontol* 2005 August;40(8-9):634-42.

41. Gorenne I, Kavurma M, Scott S, Bennett M. Vascular smooth muscle cell senescence in atherosclerosis. *Cardiovasc Res* 2006 October 1;72(1):9-17.

42. Nakano-Kurimoto R, Ikeda K, Uraoka M et al. Replicative senescence of vascular smooth muscle cells enhances the calcification through initiating the osteoblastic transition. *Am J Physiol Heart Circ Physiol* 2009 November;297(5):H1673-H1684.

43. Sun C, Liu X, Qi L et al. Modulation of vascular endothelial cell senescence by integrin beta4. *J Cell Physiol* 2010 November;225(3):673-81.

44. Leopold JA, Zhang YY, Scribner AW, Stanton RC, Loscalzo J. Glucose-6-phosphate dehydrogenase overexpression decreases endothelial cell oxidant stress and increases bioavailable nitric oxide. *Arterioscler Thromb Vasc Biol* 2003 March 1;23(3):411-7.

45. Matthews C, Gorenne I, Scott S et al. Vascular smooth muscle cells undergo telomere-based senescence in human atherosclerosis: effects of telomerase and oxidative stress. *Circ Res* 2006 July 21;99(2):156-64.

46. Warnholtz A, Nickenig G, Schulz E et al. Increased NADH-oxidase-mediated superoxide production in the early stages of atherosclerosis: evidence for involvement of the renin-angiotensin system. *Circulation* 1999 April 20;99(15):2027-33.

47. Braganza DM, Bennett MR. New insights into atherosclerotic plaque rupture. *Postgrad Med J* 2001 February;77(904):94-8.

48. Kunieda T, Minamino T, Nishi J et al. Angiotensin II induces premature senescence of vascular smooth muscle cells and accelerates the development of atherosclerosis via a p21-dependent pathway. *Circulation* 2006 August 29;114(9):953-60.

49. Duchen MR. Mitochondria in health and disease: perspectives on a new mitochondrial biology. *Mol Aspects Med* 2004 August;25(4):365-451.

50. Yakes FM, Van HB. Mitochondrial DNA damage is more extensive and persists longer than nuclear DNA damage in human cells following oxidative stress. *Proc Natl Acad Sci U S A* 1997 January 21;94(2):514-9.

51. Ballinger SW, Patterson C, Yan CN et al. Hydrogen peroxide- and peroxynitrite-induced mitochondrial DNA damage and dysfunction in vascular endothelial and smooth muscle cells. *Circ Res* 2000 May 12;86(9):960-6.

52. Kasamatsu H, Robberson DL, Vinograd J. A novel closed-circular mitochondrial DNA with properties of a replicating intermediate. *Proc Natl Acad Sci U S A* 1971 September;68(9):2252-7.

53. Fish J, Raule N, Attardi G. Discovery of a major D-loop replication origin reveals two modes of human mtDNA synthesis. *Science* 2004 December 17;306(5704):2098-101.

54. Berdanier CD, Everts HB. Mitochondrial DNA in aging and degenerative disease. *Mutat Res* 2001 April 18;475(1-2):169-83.

55. Saraste M. Oxidative phosphorylation at the fin de siecle. *Science* 1999 March 5;283(5407):1488-93.

56. Lin MT, Beal MF. Mitochondrial dysfunction and oxidative stress in neurodegenerative diseases. *Nature* 2006 October 19;443(7113):787-95.

57. Civitarese AE, Ravussin E. Mitochondrial energetics and insulin resistance. *Endocrinology* 2008 March;149(3):950-4.

58. Janssen RJ, Nijtmans LG, van den Heuvel LP, Smeitink JA. Mitochondrial complex I: structure, function and pathology. *J Inherit Metab Dis* 2006 August;29(4):499-515.

59. Smeitink JA, van den Heuvel LW, Koopman WJ, Nijtmans LG, Ugalde C, Willems PH. Cell biological consequences of mitochondrial NADH: ubiquinone oxidoreductase deficiency. *Curr Neurovasc Res* 2004 January;1(1):29-40.

60. Murphy MP. How mitochondria produce reactive oxygen species. *Biochem J* 2009 January 1;417(1):1-13.

61. Hansford RG, Hogue BA, Mildaziene V. Dependence of H2O2 formation by rat heart mitochondria on substrate availability and donor age. *J Bioenerg Biomembr* 1997 February;29(1):89-95.

62. Muller FL, Liu Y, bdul-Ghani MA et al. High rates of superoxide production in skeletal-muscle mitochondria respiring on both complex I- and complex II-linked substrates. *Biochem J* 2008 January 15;409(2):491-9.

63. Verkaart S, Koopman WJ, van Emst-de Vries SE et al. Superoxide production is inversely related to complex I activity in inherited complex I deficiency. *Biochim Biophys Acta* 2007 March;1772(3):373-81.

64. Koopman WJ, Verkaart S, van Emst-de Vries SE et al. Mitigation of NADH: ubiquinone oxidoreductase deficiency by chronic Trolox treatment. *Biochim Biophys Acta* 2008 July;1777(7-8):853-9.

65. Distelmaier F, Koopman WJ, van den Heuvel LP et al. Mitochondrial complex I deficiency: from organelle dysfunction to clinical disease. *Brain* 2009 April;132(Pt 4):833-42.

66. Mukherjee A, Zerwekh JE, Nicar MJ, McCoy K, Buja LM. Effect of chronic vitamin D deficiency on chick heart mitochondrial oxidative phosphorylation. *J Mol Cell Cardiol* 1981 February;13(2):171-83.

67. Dzau VJ. Theodore Cooper Lecture: Tissue angiotensin and pathobiology of vascular disease: a unifying hypothesis. *Hypertension* 2001 April;37(4):1047-52.

68. Schricker K, Hegyi I, Hamann M, Kaissling B, Kurtz A. Tonic stimulation of renin gene expression by nitric oxide is counteracted by tonic inhibition through angiotensin II. *Proc Natl Acad Sci U S A* 1995 August 15;92(17):8006-10.

69. Schricker K, Hamann M, Kurtz A. Prostaglandins are involved in the stimulation of renin gene expression in 2 kidney-1 clip rats. *Pflugers Arch* 1995 June;430(2):188-94.

70. Jensen BL, Kramer BK, Kurtz A. Adrenomedullin stimulates renin release and renin mRNA in mouse juxtaglomerular granular cells. *Hypertension* 1997 May;29(5):1148-55.

71. Aoyagi T, Izumi Y, Hiroyama M et al. Vasopressin regulates the renin-angiotensin-aldosterone system via V1a receptors in macula densa cells. *Am J Physiol Renal Physiol* 2008 July;295(1):F100-F107.

72. Moosavi SM, Johns EJ. Effect of renal perfusion pressure on renal function, renin release and renin and angiotensinogen gene expression in rats. *J Physiol* 1999 October 1;520 Pt 1:261-9.

73. Ryan MJ, Black TA, Millard SL, Gross KW, Hajduczok G. Endothelin-1 increases calcium and attenuates renin gene expression in As4.1 cells. *Am J Physiol Heart Circ Physiol* 2002 December;283(6):H2458-H2465.

74. Resende MM, Mill JG. Alternate angiotensin II-forming pathways and their importance in physiological or physiopathological conditions. *Arq Bras Cardiol* 2002 April;78(4):425-38.

75. Paul M, Poyan MA, Kreutz R. Physiology of local renin-angiotensin systems. *Physiol Rev* 2006 July;86(3):747-803.

76. Desfontaines L, Hornebeck W, Wei SM, Robert L, Lafuma C. Susceptibility of baboon aorta elastin to proteolysis. *Biol Chem Hoppe Seyler* 1990 May;371(5):441-6.

77. Schmidt-Ott KM, Kagiyama S, Phillips MI. The multiple actions of angiotensin II in atherosclerosis. *Regul Pept* 2000 September 25;93(1-3):65-77.

78. Touyz RM, Schiffrin EL. Signal transduction mechanisms mediating the physiological and pathophysiological actions of angiotensin II in vascular smooth muscle cells. *Pharmacol Rev* 2000 December;52(4):639-72.

79. Allen AM, Zhuo J, Mendelsohn FA. Localization and function of angiotensin AT1 receptors. *Am J Hypertens* 2000 January;13(1 Pt 2):31S-8S.

80. Yang BC, Phillips MI, Mohuczy D et al. Increased angiotensin II type 1 receptor expression in hypercholesterolemic atherosclerosis in rabbits. *Arterioscler Thromb Vasc Biol* 1998 September;18(9):1433-9.

81. Yamada H, Akishita M, Ito M et al. AT2 receptor and vascular smooth muscle cell differentiation in vascular development. *Hypertension* 1999 June;33(6):1414-9.

82. Wang ZQ, Moore AF, Ozono R, Siragy HM, Carey RM. Immunolocalization of subtype 2 angiotensin II (AT2) receptor protein in rat heart. *Hypertension* 1998 July;32(1):78-83.

83. bdAlla S, Lother H, bdel-tawab AM, Quitterer U. The angiotensin II AT2 receptor is an AT1 receptor antagonist. *J Biol Chem* 2001 October 26;276(43):39721-6.

84. Tsutsumi Y, Matsubara H, Ohkubo N et al. Angiotensin II type 2 receptor is upregulated in human heart with interstitial fibrosis, and cardiac fibroblasts

are the major cell type for its expression. *Circ Res* 1998 November 16;83(10):1035-46.

85. Nakajima M, Hutchinson HG, Fujinaga M et al. The angiotensin II type 2 (AT2) receptor antagonizes the growth effects of the AT1 receptor: gain-of-function study using gene transfer. *Proc Natl Acad Sci U S A* 1995 November 7;92(23):10663-7.

86. Warnecke C, Kaup D, Marienfeld U et al. Adenovirus-mediated overexpression and stimulation of the human angiotensin II type 2 receptor in porcine cardiac fibroblasts does not modulate proliferation, collagen I mRNA expression and ERK1/ERK2 activity, but inhibits protein tyrosine phosphatases. *J Mol Med* 2001 September;79(9):510-21.

87. Andresen BT, Romero GG, Jackson EK. AT2 receptors attenuate AT1 receptor-induced phospholipase D activation in vascular smooth muscle cells. *J Pharmacol Exp Ther* 2004 April;309(1):425-31.

88. Nishiyama A, Matsusaka T, Miyata T. Angiotensin II type 1A receptor deficiency and longevity. *Nephrol Dial Transplant* 2009 November;24(11):3280-1.

89. Ross R. The pathogenesis of atherosclerosis: a perspective for the 1990s. *Nature* 1993 April 29;362(6423):801-9.

90. Touyz RM. Reactive oxygen species and angiotensin II signaling in vascular cells -- implications in cardiovascular disease. *Braz J Med Biol Res* 2004 August;37(8):1263-73.

91. Touyz RM, Schiffrin EL. Increased generation of superoxide by angiotensin II in smooth muscle cells from resistance arteries of hypertensive patients: role of phospholipase D-dependent NAD(P)H oxidase-sensitive pathways. *J Hypertens* 2001 July;19(7):1245-54.

92. Shome K, Rizzo MA, Vasudevan C, Andresen B, Romero G. The activation of phospholipase D by endothelin-1, angiotensin II, and platelet-derived growth factor in vascular smooth muscle A10 cells is mediated by small G proteins of the ADP-ribosylation factor family. *Endocrinology* 2000 June;141(6):2200-8.

93. Li F, Malik KU. Angiotensin II-induced Akt activation through the epidermal growth factor receptor in vascular smooth muscle cells is mediated by phospholipid metabolites derived by activation of phospholipase D. *J Pharmacol Exp Ther* 2005 March;312(3):1043-54.

94. Freeman EJ. The Ang II-induced growth of vascular smooth muscle cells involves a phospholipase D-mediated signaling mechanism. *Arch Biochem Biophys* 2000 February 15;374(2):363-70.

95. Ushio-Fukai M, Alexander RW, Akers M et al. Reactive oxygen species mediate the activation of Akt/protein kinase B by angiotensin II in vascular smooth muscle cells. *J Biol Chem* 1999 August 6;274(32):22699-704.

96. Griendling KK, Minieri CA, Ollerenshaw JD, Alexander RW. Angiotensin II stimulates NADH and NADPH oxidase activity in cultured vascular smooth muscle cells. *Circ Res* 1994 June;74(6):1141-8.

97. Hayashi K, Takahashi M, Nishida W et al. Phenotypic modulation of vascular smooth muscle cells induced by unsaturated lysophosphatidic acids. *Circ Res* 2001 August 3;89(3):251-8.

98. Johnson GL, Lapadat R. Mitogen-activated protein kinase pathways mediated by ERK, JNK, and p38 protein kinases. *Science* 2002 December 6;298(5600):1911-2.

99. Takahashi E, Berk BC. MAP kinases and vascular smooth muscle function. *Acta Physiol Scand* 1998 December;164(4):611-21.

100. Pugsley MK, Tabrizchi R. The vascular system. An overview of structure and function. *J Pharmacol Toxicol Methods* 2000 September;44(2):333-40.

101. Davis KL, Martin E, Turko IV, Murad F. Novel effects of nitric oxide. *Annu Rev Pharmacol Toxicol* 2001;41:203-36.

102. Harrison DG. Cellular and molecular mechanisms of endothelial cell dysfunction. *J Clin Invest* 1997 November 1;100(9):2153-7.

103. Hare JM. Nitroso-redox balance in the cardiovascular system. *N Engl J Med* 2004 November 11;351(20):2112-4.

104. Giulivi C, Poderoso JJ, Boveris A. Production of nitric oxide by mitochondria. *J Biol Chem* 1998 May 1;273(18):11038-43.

105. Napoli C, Ignarro LJ. Nitric oxide and atherosclerosis. *Nitric Oxide* 2001 April;5(2):88-97.

106. World CJ, Yamawaki H, Berk BC. Thioredoxin in the cardiovascular system. *J Mol Med* 2006 December;84(12):997-1003.

107. Li X, Rong Y, Zhang M et al. Up-regulation of thioredoxin interacting protein (Txnip) by p38 MAPK and FOXO1 contributes to the impaired thioredoxin activity and increased ROS in glucose-treated endothelial cells. *Biochem Biophys Res Commun* 2009 April 17;381(4):660-5.

108. Mendez JI, Nicholson WJ, Taylor WR. SOD isoforms and signaling in blood vessels: evidence for the importance of ROS compartmentalization. *Arterioscler Thromb Vasc Biol* 2005 May;25(5):887-8.

109. Madamanchi NR, Moon SK, Hakim ZS et al. Differential activation of mitogenic signaling pathways in aortic smooth muscle cells deficient in superoxide dismutase isoforms. *Arterioscler Thromb Vasc Biol* 2005 May;25(5):950-6.

110. Chen K, Thomas SR, Albano A, Murphy MP, Keaney JF, Jr. Mitochondrial function is required for hydrogen peroxide-induced growth factor receptor transactivation and downstream signaling. *J Biol Chem* 2004 August 13;279(33):35079-86.

111. Norman AW, Song X, Zanello L, Bula C, Okamura WH. Rapid and genomic biological responses are mediated by different shapes of the agonist steroid hormone, 1alpha,25(OH)2vitamin D3. *Steroids* 1999 January;64(1-2):120-8.

112. Bikle DD. Vitamin D regulated keratinocyte differentiation. *J Cell Biochem* 2004 June 1;92(3):436-44.

113. Ichikawa Y, Hiwatashi A, Nishii Y. Tissue and subcellular distributions of cholecalciferol 25-hydroxylase: cytochrome P-450D25-linked monooxygenase system. *Comp Biochem Physiol B* 1983;75(3):479-88.

114. Valdivielso JM, Coll B, Fernandez E. Vitamin D and the vasculature: can we teach an old drug new tricks? *Expert Opin Ther Targets* 2009 January;13(1):29-38.

115. Omdahl JL, Morris HA, May BK. Hydroxylase enzymes of the vitamin D pathway: expression, function, and regulation. *Annu Rev Nutr* 2002;22:139-66.

116. Hewison M, Zehnder D, Bland R, Stewart PM. 1alpha-Hydroxylase and the action of vitamin D. *J Mol Endocrinol* 2000 October;25(2):141-8.

117. Zehnder D, Bland R, Williams MC et al. Extrarenal expression of 25-hydroxyvitamin d(3)-1 alpha-hydroxylase. *J Clin Endocrinol Metab* 2001 February;86(2):888-94.

118. Haussler MR, Whitfield GK, Haussler CA et al. The nuclear vitamin D receptor: biological and molecular regulatory properties revealed. *J Bone Miner Res* 1998 March;13(3):325-49.

119. St-Arnaud R, Glorieux FH. 24,25-Dihydroxyvitamin D--active metabolite or inactive catabolite? *Endocrinology* 1998 August;139(8):3371-4.

120. Townsend K, Evans KN, Campbell MJ, Colston KW, Adams JS, Hewison M. Biological actions of extra-renal 25-hydroxyvitamin D-1alpha-hydroxylase and implications for chemoprevention and treatment. *J Steroid Biochem Mol Biol* 2005 October;97(1-2):103-9.

121. Ishizuka S, Reichel H, Norman AW. Synthesis and biological activity of 1 alpha,23,25,26-tetrahydroxyvitamin D3. *Arch Biochem Biophys* 1987 April;254(1):188-95.

122. Huhtakangas JA, Olivera CJ, Bishop JE, Zanello LP, Norman AW. The vitamin D receptor is present in caveolae-enriched plasma membranes and binds 1 alpha,25(OH)2-vitamin D3 in vivo and in vitro. *Mol Endocrinol* 2004 November;18(11):2660-71.

123. Clemens TL, Garrett KP, Zhou XY, Pike JW, Haussler MR, Dempster DW. Immunocytochemical localization of the 1,25-dihydroxyvitamin D3 receptor in target cells. *Endocrinology* 1988 April;122(4):1224-30.

124. Kim JY, Son YL, Lee YC. Involvement of SMRT corepressor in transcriptional repression by the vitamin D receptor. *Mol Endocrinol* 2009 February;23(2):251-64.

125. Barsony J, Pike JW, Deluca HF, Marx SJ. Immunocytology with microwave-fixed fibroblasts shows 1 alpha,25-dihydroxyvitamin D3-dependent rapid and estrogen-dependent slow reorganization of vitamin D receptors. *J Cell Biol* 1990 December;111(6 Pt 1):2385-95.

126. Baran DT, Quail JM, Ray R, Leszyk J, Honeyman T. Annexin II is the membrane receptor that mediates the rapid actions of 1alpha,25-dihydroxyvitamin D(3). *J Cell Biochem* 2000 April;78(1):34-46.

127. Khanal RC, Nemere I. The ERp57/GRp58/1,25D3-MARRS receptor: multiple functional roles in diverse cell systems. *Curr Med Chem* 2007;14(10):1087-93.

128. Zanello LP, Norman AW. Rapid modulation of osteoblast ion channel responses by 1alpha,25(OH)2-vitamin D3 requires the presence of a functional vitamin D nuclear receptor. *Proc Natl Acad Sci U S A* 2004 February 10;101(6):1589-94.

129. Zmuda JM, Cauley JA, Ferrell RE. Molecular epidemiology of vitamin D receptor gene variants. *Epidemiol Rev* 2000;22(2):203-17.

130. Valdivielso JM, Fernandez E. Vitamin D receptor polymorphisms and diseases. *Clin Chim Acta* 2006 September;371(1-2):1-12.

131. Bid HK, Konwar R, Aggarwal CG et al. Vitamin D receptor (FokI, BsmI and TaqI) gene polymorphisms and type 2 diabetes mellitus: a North Indian study. *Indian J Med Sci* 2009 May;63(5):187-94.

132. Herdick M, Carlberg C. Agonist-triggered modulation of the activated and silent state of the vitamin D(3) receptor by interaction with co-repressors and co-activators. *J Mol Biol* 2000 December 15;304(5):793-801.

133. Mackey SL, Heymont JL, Kronenberg HM, Demay MB. Vitamin D receptor binding to the negative human parathyroid hormone vitamin D response element does not require the retinoid x receptor. *Mol Endocrinol* 1996 March;10(3):298-305.

134. Chen KS, Deluca HF. Cloning of the human 1 alpha,25-dihydroxyvitamin D-3 24-hydroxylase gene promoter and identification of two vitamin D-responsive elements. *Biochim Biophys Acta* 1995 July 25;1263(1):1-9.

135. Kahlen JP, Carlberg C. Functional characterization of a 1,25-dihydroxyvitamin D3 receptor binding site found in the rat atrial natriuretic factor promoter. *Biochem Biophys Res Commun* 1996 January 26;218(3):882-6.

136. van den Bemd GJ, Jhamai M, Staal A et al. A central dinucleotide within vitamin D response elements modulates DNA binding and transactivation by the vitamin D receptor in cellular response to natural and synthetic ligands. *J Biol Chem* 2002 April 26;277(17):14539-46.

137. Quelo I, Kahlen JP, Rascle A, Jurdic P, Carlberg C. Identification and characterization of a vitamin D3 response element of chicken carbonic anhydrase-II. *DNA Cell Biol* 1994 December;13(12):1181-7.

138. Taketani Y, Miyamoto K, Tanaka K et al. Gene structure and functional analysis of the human Na+/phosphate co-transporter. *Biochem J* 1997 June 15;324 (Pt 3):927-34.

139. Staal A, Van Wijnen AJ, Desai RK et al. Antagonistic effects of transforming growth factor-beta on vitamin D3 enhancement of osteocalcin and osteopontin transcription: reduced interactions of vitamin D receptor/retinoid X receptor complexes with vitamin E response elements. *Endocrinology* 1996 May;137(5):2001-11.

140. Liu M, Lee MH, Cohen M, Bommakanti M, Freedman LP. Transcriptional activation of the Cdk inhibitor p21 by vitamin D3 leads to the induced differentiation of the myelomonocytic cell line U937. *Genes Dev* 1996 January 15;10(2):142-53.

141. Sinkkonen L, Malinen M, Saavalainen K, Vaisanen S, Carlberg C. Regulation of the human cyclin C gene via multiple vitamin D3-responsive regions in its promoter. *Nucleic Acids Res* 2005;33(8):2440-51.

142. Cao X, Ross FP, Zhang L, MacDonald PN, Chappel J, Teitelbaum SL. Cloning of the promoter for the avian integrin beta 3 subunit gene and its regulation by 1,25-dihydroxyvitamin D3. *J Biol Chem* 1993 December 25;268(36):27371-80.

143. Seuter S, Vaisanen S, Radmark O, Carlberg C, Steinhilber D. Functional characterization of vitamin D responding regions in the human 5-Lipoxygenase gene. *Biochim Biophys Acta* 2007 July;1771(7):864-72.

144. Cardus A, Panizo S, Encinas M et al. 1,25-dihydroxyvitamin D3 regulates VEGF production through a vitamin D response element in the VEGF promoter. *Atherosclerosis* 2009 May;204(1):85-9.

145. Dunlop TW, Vaisanen S, Frank C, Molnar F, Sinkkonen L, Carlberg C. The human peroxisome proliferator-activated receptor delta gene is a primary target of 1alpha,25-dihydroxyvitamin D3 and its nuclear receptor. *J Mol Biol* 2005 June 3;349(2):248-60.

146. Peng L, Malloy PJ, Feldman D. Identification of a functional vitamin D response element in the human insulin-like growth factor binding protein-3 promoter. *Mol Endocrinol* 2004 May;18(5):1109-19.

147. Matilainen M, Malinen M, Saavalainen K, Carlberg C. Regulation of multiple insulin-like growth factor binding protein genes by 1alpha,25-dihydroxyvitamin D3. *Nucleic Acids Res* 2005;33(17):5521-32.

148. Wu Y, Craig TA, Lutz WH, Kumar R. Identification of 1 alpha,25-dihydroxyvitamin D3 response elements in the human transforming growth factor beta 2 gene. *Biochemistry* 1999 March 2;38(9):2654-60.

149. Kim MS, Fujiki R, Murayama A et al. 1Alpha,25(OH)2D3-induced transrepression by vitamin D receptor through E-box-type elements in the human parathyroid hormone gene promoter. *Mol Endocrinol* 2007 February;21(2):334-42.

150. Kremer R, Sebag M, Champigny C et al. Identification and characterization of 1,25-dihydroxyvitamin D3-responsive repressor sequences in the rat parathyroid hormone-related peptide gene. *J Biol Chem* 1996 July 5;271(27):16310-6.

151. Alonso M, Segura C, Dieguez C, Perez-Fernandez R. High-affinity binding sites to the vitamin D receptor DNA binding domain in the human growth hormone promoter. *Biochem Biophys Res Commun* 1998 June 29;247(3):882-7.

152. Dong X, Craig T, Xing N et al. Direct transcriptional regulation of RelB by 1alpha,25-dihydroxyvitamin D3 and its analogs: physiologic and therapeutic implications for dendritic cell function. *J Biol Chem* 2003 December 5;278(49):49378-85.

153. Owen TA, Bortell R, Yocum SA et al. Coordinate occupancy of AP-1 sites in the vitamin D-responsive and CCAAT box elements by Fos-Jun in the osteocalcin gene: model for phenotype suppression of transcription. *Proc Natl Acad Sci U S A* 1990 December;87(24):9990-4.

154. Ikeda N, Uemura H, Ishiguro H et al. Combination treatment with 1alpha,25-dihydroxyvitamin D3 and 9-cis-retinoic acid directly inhibits human telomerase reverse transcriptase transcription in prostate cancer cells. *Mol Cancer Ther* 2003 August;2(8):739-46.

155. Gill RK, Christakos S. Identification of sequence elements in mouse calbindin-D28k gene that confer 1,25-dihydroxyvitamin D3- and butyrate-inducible responses. *Proc Natl Acad Sci U S A* 1993 April 1;90(7):2984-8.

156. Toropainen S, Vaisanen S, Heikkinen S, Carlberg C. The down-regulation of the human MYC gene by the nuclear hormone 1alpha,25-dihydroxyvitamin D3 is associated with cycling of corepressors and histone deacetylases. *J Mol Biol* 2010 July 16;400(3):284-94.

157. Xie Z, Bikle DD. Cloning of the human phospholipase C-gamma1 promoter and identification of a DR6-type vitamin D-responsive element. *J Biol Chem* 1997 March 7;272(10):6573-7.

158. Polly P, Carlberg C, Eisman JA, Morrison NA. Identification of a vitamin D3 response element in the fibronectin gene that is bound by a vitamin D3 receptor homodimer. *J Cell Biochem* 1996 March 1;60(3):322-33.

159. Schrader M, Nayeri S, Kahlen JP, Muller KM, Carlberg C. Natural vitamin D3 response elements formed by inverted palindromes: polarity-directed ligand sensitivity of vitamin D3 receptor-retinoid X receptor heterodimer-mediated transactivation. *Mol Cell Biol* 1995 March;15(3):1154-61.

160. Schrader M, Kahlen JP, Carlberg C. Functional characterization of a novel type of 1 alpha,25-dihydroxyvitamin D3 response element identified in the mouse c-fos promoter. *Biochem Biophys Res Commun* 1997 January 23;230(3):646-51.

161. Thompson PD, Jurutka PW, Whitfield GK et al. Liganded VDR induces CYP3A4 in small intestinal and colon cancer cells via DR3 and ER6 vitamin D

responsive elements. *Biochem Biophys Res Commun* 2002 December 20;299(5):730-8.

162. Murayama A, Kim MS, Yanagisawa J, Takeyama K, Kato S. Transrepression by a liganded nuclear receptor via a bHLH activator through co-regulator switching. *EMBO J* 2004 April 7;23(7):1598-608.

163. Yuan W, Pan W, Kong J et al. 1,25-dihydroxyvitamin D3 suppresses renin gene transcription by blocking the activity of the cyclic AMP response element in the renin gene promoter. *J Biol Chem* 2007 October 12;282(41):29821-30.

164. Alroy I, Towers TL, Freedman LP. Transcriptional repression of the interleukin-2 gene by vitamin D3: direct inhibition of NFATp/AP-1 complex formation by a nuclear hormone receptor. *Mol Cell Biol* 1995 October;15(10):5789-99.

165. D'Ambrosio D, Cippitelli M, Cocciolo MG et al. Inhibition of IL-12 production by 1,25-dihydroxyvitamin D3. Involvement of NF-kappaB downregulation in transcriptional repression of the p40 gene. *J Clin Invest* 1998 January 1;101(1):252-62.

166. Towers TL, Freedman LP. Granulocyte-macrophage colony-stimulating factor gene transcription is directly repressed by the vitamin D3 receptor. Implications for allosteric influences on nuclear receptor structure and function by a DNA element. *J Biol Chem* 1998 April 24;273(17):10338-48.

167. Quack M, Carlberg C. Selective recognition of vitamin D receptor conformations mediates promoter selectivity of vitamin D analogs. *Mol Pharmacol* 1999 June;55(6):1077-87.

168. Carlberg C. Current understanding of the function of the nuclear vitamin D receptor in response to its natural and synthetic ligands. *Recent Results Cancer Res* 2003;164:29-42.

169. Jin CH, Pike JW. Human vitamin D receptor-dependent transactivation in Saccharomyces cerevisiae requires retinoid X receptor. *Mol Endocrinol* 1996 February;10(2):196-205.

170. Nolte RT, Wisely GB, Westin S et al. Ligand binding and co-activator assembly of the peroxisome proliferator-activated receptor-gamma. *Nature* 1998 September 10;395(6698):137-43.

171. Nagpal S, Na S, Rathnachalam R. Noncalcemic actions of vitamin D receptor ligands. *Endocr Rev* 2005 August;26(5):662-87.

172. Deeb KK, Trump DL, Johnson CS. Vitamin D signalling pathways in cancer: potential for anticancer therapeutics. *Nat Rev Cancer* 2007 September;7(9):684-700.

173. Urnov FD, Wolffe AP. Chromatin remodeling and transcriptional activation: the cast (in order of appearance). *Oncogene* 2001 May 28;20(24):2991-3006.

174. Nishishita T, Okazaki T, Ishikawa T et al. A negative vitamin D response DNA element in the human parathyroid hormone-related peptide gene binds to vitamin D receptor along with Ku antigen to mediate negative gene regulation by vitamin D. *J Biol Chem* 1998 May 1;273(18):10901-7.

175. Falzon M. DNA sequences in the rat parathyroid hormone-related peptide gene responsible for 1,25-dihydroxyvitamin D3-mediated transcriptional repression. *Mol Endocrinol* 1996 June;10(6):672-81.

176. Simboli-Campbell M, Gagnon A, Franks DJ, Welsh J. 1,25-Dihydroxyvitamin D3 translocates protein kinase C beta to nucleus and enhances plasma membrane association of protein kinase C alpha in renal epithelial cells. *J Biol Chem* 1994 February 4;269(5):3257-64.

177. Hsieh JC, Jurutka PW, Galligan MA et al. Human vitamin D receptor is selectively phosphorylated by protein kinase C on serine 51, a residue crucial to its trans-activation function. *Proc Natl Acad Sci U S A* 1991 October 15;88(20):9315-9.

178. Jurutka PW, Hsieh JC, Haussler MR. Phosphorylation of the human 1,25-dihydroxyvitamin D3 receptor by cAMP-dependent protein kinase, in vitro, and in transfected COS-7 cells. *Biochem Biophys Res Commun* 1993 March 31;191(3):1089-96.

179. Jurutka PW, Hsieh JC, MacDonald PN et al. Phosphorylation of serine 208 in the human vitamin D receptor. The predominant amino acid phosphorylated by casein kinase II, in vitro, and identification as a significant phosphorylation site in intact cells. *J Biol Chem* 1993 March 25;268(9):6791-9.

180. Hsieh JC, Dang HT, Galligan MA et al. Phosphorylation of human vitamin D receptor serine-182 by PKA suppresses 1,25(OH)2D3-dependent transactivation. *Biochem Biophys Res Commun* 2004 November 12;324(2):801-9.

181. Zhai XY, Nielsen R, Birn H et al. Cubilin- and megalin-mediated uptake of albumin in cultured proximal tubule cells of opossum kidney. *Kidney Int* 2000 October;58(4):1523-33.

182. Adams JS, Chen H, Chun RF et al. Novel regulators of vitamin D action and metabolism: Lessons learned at the Los Angeles zoo. *J Cell Biochem* 2003 February 1;88(2):308-14.

183. Wasserman RH. Vitamin D and the dual processes of intestinal calcium absorption. *J Nutr* 2004 November;134(11):3137-9.

184. White C, Gardiner E, Eisman J. Tissue specific and vitamin D responsive gene expression in bone. *Mol Biol Rep* 1998 January;25(1):45-61.

185. Cardus A, Parisi E, Gallego C, Aldea M, Fernandez E, Valdivielso JM. 1,25-Dihydroxyvitamin D3 stimulates vascular smooth muscle cell proliferation through a VEGF-mediated pathway. *Kidney Int* 2006 April;69(8):1377-84.

186. Cardus A, Panizo S, Encinas M et al. 1,25-dihydroxyvitamin D3 regulates VEGF production through a vitamin D response element in the VEGF promoter. *Atherosclerosis* 2009 May;204(1):85-9.

187. Panizo S, Cardus A, Encinas M et al. RANKL Increases Vascular Smooth Muscle Cell Calcification Through a RANK-BMP4-Dependent Pathway. *Circulation Research* 2009 May 8;104(9):1041-8.

188. Li YC, Kong J, Wei M, Chen ZF, Liu SQ, Cao LP. 1,25-Dihydroxyvitamin D(3) is a negative endocrine regulator of the renin-angiotensin system. *J Clin Invest* 2002 July;110(2):229-38.

189. Valdivielso JM, Cannata-Andia J, Coll B, Fernandez E. A new role for vitamin D receptor activation in chronic kidney disease. *Am J Physiol Renal Physiol* 2009 December;297(6):F1502-F1509.

190. Liu M, Iavarone A, Freedman LP. Transcriptional activation of the human p21(WAF1/CIP1) gene by retinoic acid receptor. Correlation with retinoid induction of U937 cell differentiation. *J Biol Chem* 1996 December 6;271(49):31723-8.

191. Kanli A, Savli H. Differential expression of 16 genes coding for cell cycle- and apoptosis-related proteins in vitamin D-induced differentiation of HL-60 cells. *Exp Oncol* 2007 December;29(4):314-6.

192. Penna G, Adorini L. 1 Alpha,25-dihydroxyvitamin D3 inhibits differentiation, maturation, activation, and survival of dendritic cells leading to impaired alloreactive T cell activation. *J Immunol* 2000 March 1;164(5):2405-11.

193. Adorini L, Penna G, Giarratana N et al. Dendritic cells as key targets for immunomodulation by Vitamin D receptor ligands. *J Steroid Biochem Mol Biol* 2004 May;89-90(1-5):437-41.

194. Alvarez JA, Ashraf A. Role of vitamin d in insulin secretion and insulin sensitivity for glucose homeostasis. *Int J Endocrinol* 2010;2010:351385.

195. Hawker NP, Pennypacker SD, Chang SM, Bikle DD. Regulation of human epidermal keratinocyte differentiation by the vitamin D receptor and its coactivators DRIP205, SRC2, and SRC3. *J Invest Dermatol* 2007 April;127(4):874-80.

196. Kim HJ, Abdelkader N, Katz M, McLane JA. 1,25-Dihydroxy-vitamin-D3 enhances antiproliferative effect and transcription of TGF-beta1 on human keratinocytes in culture. *J Cell Physiol* 1992 June;151(3):579-87.

197. Matsumoto K, Hashimoto K, Nishida Y, Hashiro M, Yoshikawa K. Growth-inhibitory effects of 1,25-dihydroxyvitamin D3 on normal human keratinocytes cultured in serum-free medium. *Biochem Biophys Res Commun* 1990 January 30;166(2):916-23.

198. Wiseman H. Vitamin D is a membrane antioxidant. Ability to inhibit iron-dependent lipid peroxidation in liposomes compared to cholesterol, ergosterol and tamoxifen and relevance to anticancer action. *FEBS Lett* 1993 July 12;326(1-3):285-8.

199. Bao BY, Ting HJ, Hsu JW, Lee YF. Protective role of 1 alpha, 25-dihydroxyvitamin D3 against oxidative stress in nonmalignant human prostate epithelial cells. *Int J Cancer* 2008 June 15;122(12):2699-706.

200. Sardar S, Chakraborty A, Chatterjee M. Comparative effectiveness of vitamin D3 and dietary vitamin E on peroxidation of lipids and enzymes of the hepatic antioxidant system in Sprague--Dawley rats. *Int J Vitam Nutr Res* 1996;66(1):39-45.

201. Koren R, Hadari-Naor I, Zuck E, Rotem C, Liberman UA, Ravid A. Vitamin D is a prooxidant in breast cancer cells. *Cancer Res* 2001 February 15;61(4):1439-44.

202. Razzaque MS, Lanske B. Hypervitaminosis D and premature aging: lessons learned from Fgf23 and Klotho mutant mice. *Trends Mol Med* 2006 July;12(7):298-305.

203. Richards JB, Valdes AM, Gardner JP et al. Higher serum vitamin D concentrations are associated with longer leukocyte telomere length in women. *Am J Clin Nutr* 2007 November;86(5):1420-5.

204. Tian J, Liu Y, Williams LA, de ZD. Potential role of active vitamin D in retarding the progression of chronic kidney disease. *Nephrol Dial Transplant* 2007 February;22(2):321-8.

205. Norman AW. The vitamin D Endocrine system: manipulation of structure-function relationships to provide opportunities for development of new cancer chemopreventive and immunosuppressive agents. *J Cell Biochem Suppl* 1995;22:218-25.

206. Noonan W, Koch K, Nakane M et al. Differential effects of vitamin D receptor activators on aortic calcification and pulse wave velocity in uraemic rats. *Nephrol Dial Transplant* 2008 December;23(12):3824-30.

207. Li YC, Qiao G, Uskokovic M, Xiang W, Zheng W, Kong J. Vitamin D: a negative endocrine regulator of the renin-angiotensin system and blood pressure. *J Steroid Biochem Mol Biol* 2004 May;89-90(1-5):387-92.

208. Nonn L, Peng L, Feldman D, Peehl DM. Inhibition of p38 by vitamin D reduces interleukin-6 production in normal prostate cells via mitogen-activated protein kinase phosphatase 5: implications for prostate cancer prevention by vitamin D. *Cancer Res* 2006 April 15;66(8):4516-24.

209. Yoshizawa T, Handa Y, Uematsu Y et al. Mice lacking the vitamin D receptor exhibit impaired bone formation, uterine hypoplasia and growth retardation after weaning. *Nat Genet* 1997 August;16(4):391-6.

210. Li YC, Pirro AE, Amling M et al. Targeted ablation of the vitamin D receptor: an animal model of vitamin D-dependent rickets type II with alopecia. *Proc Natl Acad Sci U S A* 1997 September 2;94(18):9831-5.

211. Erben RG, Soegiarto DW, Weber K et al. Deletion of deoxyribonucleic acid binding domain of the vitamin D receptor abrogates genomic and nongenomic functions of vitamin D. *Mol Endocrinol* 2002 July;16(7):1524-37.

212. Van Cromphaut SJ, Dewerchin M, Hoenderop JG et al. Duodenal calcium absorption in vitamin D receptor-knockout mice: functional and molecular aspects. *Proc Natl Acad Sci U S A* 2001 November 6;98(23):13324-9.

213. Kinuta K, Tanaka H, Moriwake T, Aya K, Kato S, Seino Y. Vitamin D is an important factor in estrogen biosynthesis of both female and male gonads. *Endocrinology* 2000 April;141(4):1317-24.

214. Aihara K, Azuma H, Akaike M et al. Disruption of nuclear vitamin D receptor gene causes enhanced thrombogenicity in mice. *J Biol Chem* 2004 August 20;279(34):35798-802.

215. Asakura H, Aoshima K, Suga Y et al. Beneficial effect of the active form of vitamin D3 against LPS-induced DIC but not against tissue-factor-induced DIC in rat models. *Thromb Haemost* 2001 February;85(2):287-90.

216. Takeyama K, Kitanaka S, Sato T, Kobori M, Yanagisawa J, Kato S. 25-Hydroxyvitamin D3 1alpha-hydroxylase and vitamin D synthesis. *Science* 1997 September 19;277(5333):1827-30.

217. Dardenne O, Prud'homme J, Arabian A, Glorieux FH, St-Arnaud R. Targeted inactivation of the 25-hydroxyvitamin D(3)-1(alpha)-hydroxylase gene (CYP27B1) creates an animal model of pseudovitamin D-deficiency rickets. *Endocrinology* 2001 July;142(7):3135-41.

218. Panda DK, Miao D, Tremblay ML et al. Targeted ablation of the 25-hydroxyvitamin D 1alpha -hydroxylase enzyme: evidence for skeletal, reproductive, and immune dysfunction. *Proc Natl Acad Sci U S A* 2001 June 19;98(13):7498-503.

219. St-Arnaud R, Arabian A, Travers R et al. Deficient mineralization of intramembranous bone in vitamin D-24-hydroxylase-ablated mice is due to elevated 1,25-dihydroxyvitamin D and not to the absence of 24,25-dihydroxyvitamin D. *Endocrinology* 2000 July;141(7):2658-66.

220. Masuda S, Byford V, Arabian A et al. Altered pharmacokinetics of 1alpha,25-dihydroxyvitamin D3 and 25-hydroxyvitamin D3 in the blood and tissues of the 25-hydroxyvitamin D-24-hydroxylase (Cyp24a1) null mouse. *Endocrinology* 2005 February;146(2):825-34.

221. Kallay E, Pietschmann P, Toyokuni S et al. Characterization of a vitamin D receptor knockout mouse as a model of colorectal hyperproliferation and DNA damage. *Carcinogenesis* 2001 September;22(9):1429-35.

222. Pickering JG, Weir L, Rosenfield K, Stetz J, Jekanowski J, Isner JM. Smooth muscle cell outgrowth from human atherosclerotic plaque: implications for the assessment of lesion biology. *J Am Coll Cardiol* 1992 November 15;20(6):1430-9.

223. Gnaiger E. Bioenergetics at low oxygen: dependence of respiration and phosphorylation on oxygen and adenosine diphosphate supply. *Respir Physiol* 2001 November 15;128(3):277-97.

224. Kuznetsov AV, Strobl D, Ruttmann E, Konigsrainer A, Margreiter R, Gnaiger E. Evaluation of mitochondrial respiratory function in small biopsies of liver. *Anal Biochem* 2002 June 15;305(2):186-94.

225. Hutter E, Renner K, Pfister G, Stockl P, Jansen-Durr P, Gnaiger E. Senescence-associated changes in respiration and oxidative phosphorylation in primary human fibroblasts. *Biochem J* 2004 June 15;380(Pt 3):919-28.

226. Renner K, Amberger A, Konwalinka G, Kofler R, Gnaiger E. Changes of mitochondrial respiration, mitochondrial content and cell size after induction of apoptosis in leukemia cells. *Biochim Biophys Acta* 2003 September 23;1642(1-2):115-23.

227. Kim KS, Rosenkrantz MS, Guarente L. Saccharomyces cerevisiae contains two functional citrate synthase genes. *Mol Cell Biol* 1986 June;6(6):1936-42.

228. Lindner V, Fingerle J, Reidy MA. Mouse model of arterial injury. *Circ Res* 1993 November;73(5):792-6.

229. Sullivan TR, Jr., Karas RH, Aronovitz M et al. Estrogen inhibits the response-to-injury in a mouse carotid artery model. *J Clin Invest* 1995 November;96(5):2482-8.

230. Kroemer G, Galluzzi L, Vandenabeele P et al. Classification of cell death: recommendations of the Nomenclature Committee on Cell Death 2009. *Cell Death Differ* 2009 January;16(1):3-11.

231. Owens GK, Geisterfer AA, Yang YW, Komoriya A. Transforming growth factor-beta-induced growth inhibition and cellular hypertrophy in cultured vascular smooth muscle cells. *J Cell Biol* 1988 August;107(2):771-80.

232. Sinuani I, Weissgarten J, Beberashvili I et al. The cyclin kinase inhibitor p57kip2 regulates TGF-beta-induced compensatory tubular hypertrophy: effect of the immunomodulator AS101. *Nephrol Dial Transplant* 2009 August;24(8):2328-38.

233. Eickelberg O, Kohler E, Reichenberger F et al. Extracellular matrix deposition by primary human lung fibroblasts in response to TGF-beta1 and TGF-beta3. *Am J Physiol* 1999 May;276(5 Pt 1):L814-L824.

234. Hautmann MB, Madsen CS, Owens GK. A transforming growth factor beta (TGFbeta) control element drives TGFbeta-induced stimulation of smooth muscle alpha-actin gene expression in concert with two CArG elements. *J Biol Chem* 1997 April 18;272(16):10948-56.

235. Goldsmith AM, Bentley JK, Zhou L et al. Transforming growth factor-beta induces airway smooth muscle hypertrophy. *Am J Respir Cell Mol Biol* 2006 February;34(2):247-54.

236. Owens GK. Differential effects of antihypertensive drug therapy on vascular smooth muscle cell hypertrophy, hyperploidy, and hyperplasia in the spontaneously hypertensive rat. *Circ Res* 1985 April;56(4):525-36.

237. Fukuda N, Satoh C, Hu WY et al. Production of angiotensin II by homogeneous cultures of vascular smooth muscle cells from spontaneously hypertensive rats. *Arterioscler Thromb Vasc Biol* 1999 May;19(5):1210-7.

238. Funakoshi Y, Ichiki T, Ito K, Takeshita A. Induction of interleukin-6 expression by angiotensin II in rat vascular smooth muscle cells. *Hypertension* 1999 July;34(1):118-25.

239. Eickelberg O, Pansky A, Mussmann R et al. Transforming growth factor-beta1 induces interleukin-6 expression via activating protein-1 consisting of JunD homodimers in primary human lung fibroblasts. *J Biol Chem* 1999 April 30;274(18):12933-8.

240. Kolpakov V, Gordon D, Kulik TJ. Nitric oxide-generating compounds inhibit total protein and collagen synthesis in cultured vascular smooth muscle cells. *Circ Res* 1995 February;76(2):305-9.

241. Rockett KA, Brookes R, Udalova I, Vidal V, Hill AV, Kwiatkowski D. 1,25-Dihydroxyvitamin D3 induces nitric oxide synthase and suppresses growth of Mycobacterium tuberculosis in a human macrophage-like cell line. *Infect Immun* 1998 November;66(11):5314-21.

242. Garcion E, Sindji L, Nataf S, Brachet P, Darcy F, Montero-Menei CN. Treatment of experimental autoimmune encephalomyelitis in rat by 1,25-dihydroxyvitamin D3 leads to early effects within the central nervous system. *Acta Neuropathol* 2003 May;105(5):438-48.

243. Cardus A, Panizo S, Parisi E, Fernandez E, Valdivielso JM. Differential effects of vitamin D analogs on vascular calcification. *J Bone Miner Res* 2007 June;22(6):860-6.

244. Dimri GP, Lee X, Basile G et al. A biomarker that identifies senescent human cells in culture and in aging skin in vivo. *Proc Natl Acad Sci U S A* 1995 September 26;92(20):9363-7.

245. Gosselin K, Deruy E, Martien S et al. Senescent keratinocytes die by autophagic programmed cell death. *Am J Pathol* 2009 February;174(2):423-35.

246. Pitkanen S, Merante F, McLeod DR, Applegarth D, Tong T, Robinson BH. Familial cardiomyopathy with cataracts and lactic acidosis: a defect in complex I (NADH-dehydrogenase) of the mitochondria respiratory chain. *Pediatr Res* 1996 March;39(3):513-21.

247. Nagata D, Takeda R, Sata M et al. AMP-activated protein kinase inhibits angiotensin II-stimulated vascular smooth muscle cell proliferation. *Circulation* 2004 July 27;110(4):444-51.

248. Zmijewski JW, Banerjee S, Bae H, Friggeri A, Lazarowski ER, Abraham E. Exposure to hydrogen peroxide induces oxidation and activation of AMP-activated protein kinase. *J Biol Chem* 2010 October 22;285(43):33154-64.

249. Antoniades C, Tousoulis D, Marinou K et al. Asymmetrical dimethylarginine regulates endothelial function in methionine-induced but not in chronic

homocystinemia in humans: effect of oxidative stress and proinflammatory cytokines. *Am J Clin Nutr* 2006 October;84(4):781-8.

250. Ushio-Fukai M, Alexander RW, Akers M, Griendling KK. p38 Mitogen-activated protein kinase is a critical component of the redox-sensitive signaling pathways activated by angiotensin II. Role in vascular smooth muscle cell hypertrophy. *J Biol Chem* 1998 June 12;273(24):15022-9.

251. Tanner FC, Yang ZY, Duckers E, Gordon D, Nabel GJ, Nabel EG. Expression of cyclin-dependent kinase inhibitors in vascular disease. *Circ Res* 1998 February 23;82(3):396-403.

252. Bouillon R, Okamura WH, Norman AW. Structure-function relationships in the vitamin D endocrine system. *Endocr Rev* 1995 April;16(2):200-57.

253. Brouwer DA, van BJ, Ferwerda H et al. Rat adipose tissue rapidly accumulates and slowly releases an orally-administered high vitamin D dose. *Br J Nutr* 1998 June;79(6):527-32.

254. Brown AJ, Dusso A, Slatopolsky E. Vitamin D. *Am J Physiol* 1999 August;277(2 Pt 2):F157-F175.

255. Li YC, Amling M, Pirro AE et al. Normalization of mineral ion homeostasis by dietary means prevents hyperparathyroidism, rickets, and osteomalacia, but not alopecia in vitamin D receptor-ablated mice. *Endocrinology* 1998 October;139(10):4391-6.

256. Kollenkirchen U, Fox J, Walters MR. Normocalcemia without hyperparathyroidism in vitamin D-deficient rats. *J Bone Miner Res* 1991 March;6(3):273-8.

257. Takeda S, Yoshizawa T, Nagai Y et al. Stimulation of osteoclast formation by 1,25-dihydroxyvitamin D requires its binding to vitamin D receptor (VDR) in osteoblastic cells: studies using VDR knockout mice. *Endocrinology* 1999 February;140(2):1005-8.

258. Szeto FL, Sun J, Kong J et al. Involvement of the vitamin D receptor in the regulation of NF-kappaB activity in fibroblasts. *J Steroid Biochem Mol Biol* 2007 March;103(3-5):563-6.

259. Zinser GM, McEleney K, Welsh J. Characterization of mammary tumor cell lines from wild type and vitamin D3 receptor knockout mice. *Mol Cell Endocrinol* 2003 February 28;200(1-2):67-80.

260. Mordan-McCombs S, Valrance M, Zinser G, Tenniswood M, Welsh J. Calcium, vitamin D and the vitamin D receptor: impact on prostate and breast cancer in preclinical models. *Nutr Rev* 2007 August;65(8 Pt 2):S131-S133.

261. Bula CM, Huhtakangas J, Olivera C, Bishop JE, Norman AW, Henry HL. Presence of a truncated form of the vitamin D receptor (VDR) in a strain of VDR-knockout mice. *Endocrinology* 2005 December;146(12):5581-6.

262. Song Y, Kato S, Fleet JC. Vitamin D receptor (VDR) knockout mice reveal VDR-independent regulation of intestinal calcium absorption and ECaC2 and calbindin D9k mRNA. *J Nutr* 2003 February;133(2):374-80.

263. Zierold C, Darwish HM, Deluca HF. Identification of a vitamin D-response element in the rat calcidiol (25-hydroxyvitamin D3) 24-hydroxylase gene. *Proc Natl Acad Sci U S A* 1994 February 1;91(3):900-2.

264. Ellison TI, Eckert RL, MacDonald PN. Evidence for 1,25-dihydroxyvitamin D3-independent transactivation by the vitamin D receptor: uncoupling the receptor and ligand in keratinocytes. *J Biol Chem* 2007 April 13;282(15):10953-62.

265. Bi JX, Shuttleworth J, Al-Rubeai M. Uncoupling of cell growth and proliferation results in enhancement of productivity in p21CIP1-arrested CHO cells. *Biotechnol Bioeng* 2004 March 30;85(7):741-9.

266. Nakano N, Urasawa K, Takagi Y et al. Downregulation of cyclin-dependent kinase inhibitor; p57(kip2), is involved in the cell cycle progression of vascular smooth muscle cells. *Biochem Biophys Res Commun* 2005 December 23;338(3):1661-7.

267. Takahashi K, Nakayama K, Nakayama K. Mice lacking a CDK inhibitor, p57Kip2, exhibit skeletal abnormalities and growth retardation. *J Biochem* 2000 January;127(1):73-83.

268. Liu B, Preisig P. TGF-beta1-mediated hypertrophy involves inhibiting pRB phosphorylation by blocking activation of cyclin E kinase. *Am J Physiol* 1999 August;277(2 Pt 2):F186-F194.

269. Liu B, Preisig PA. Compensatory renal hypertrophy is mediated by a cell cycle-dependent mechanism. *Kidney Int* 2002 November;62(5):1650-8.

270. Owens GK. Influence of blood pressure on development of aortic medial smooth muscle hypertrophy in spontaneously hypertensive rats. *Hypertension* 1987 February;9(2):178-87.

271. Xiang W, Kong J, Chen S et al. Cardiac hypertrophy in vitamin D receptor knockout mice: role of the systemic and cardiac renin-angiotensin systems. *Am J Physiol Endocrinol Metab* 2005 January;288(1):E125-E132.

272. Hannon GJ, Beach D. p15INK4B is a potential effector of TGF-beta-induced cell cycle arrest. *Nature* 1994 September 15;371(6494):257-61.

273. Datto MB, Li Y, Panus JF, Howe DJ, Xiong Y, Wang XF. Transforming growth factor beta induces the cyclin-dependent kinase inhibitor p21 through a p53-independent mechanism. *Proc Natl Acad Sci U S A* 1995 June 6;92(12):5545-9.

274. Cheng T, Shen H, Rodrigues N, Stier S, Scadden DT. Transforming growth factor beta 1 mediates cell-cycle arrest of primitive hematopoietic cells independent of p21(Cip1/Waf1) or p27(Kip1). *Blood* 2001 December 15;98(13):3643-9.

275. Scandura JM, Boccuni P, Massague J, Nimer SD. Transforming growth factor beta-induced cell cycle arrest of human hematopoietic cells requires p57KIP2 up-regulation. *Proc Natl Acad Sci U S A* 2004 October 19;101(42):15231-6.

276. Weber KT, Brilla CG. Pathological hypertrophy and cardiac interstitium. Fibrosis and renin-angiotensin-aldosterone system. *Circulation* 1991 June;83(6):1849-65.

277. Nguyen QT, Colombo F, Rouleau JL, Dupuis J, Calderone A. LU135252, an endothelin(A) receptor antagonist did not prevent pulmonary vascular remodelling or lung fibrosis in a rat model of myocardial infarction. *Br J Pharmacol* 2000 August;130(7):1525-30.

278. Koyama H, Raines EW, Bornfeldt KE, Roberts JM, Ross R. Fibrillar collagen inhibits arterial smooth muscle proliferation through regulation of Cdk2 inhibitors. *Cell* 1996 December 13;87(6):1069-78.

279. Reusch P, Wagdy H, Reusch R, Wilson E, Ives HE. Mechanical strain increases smooth muscle and decreases nonmuscle myosin expression in rat vascular smooth muscle cells. *Circ Res* 1996 November;79(5):1046-53.

280. Wang M, Zhao D, Spinetti G et al. Matrix metalloproteinase 2 activation of transforming growth factor-beta1 (TGF-beta1) and TGF-beta1-type II receptor signaling within the aged arterial wall. *Arterioscler Thromb Vasc Biol* 2006 July;26(7):1503-9.

281. Borland JA, Chester AH, Morrison KA, Yacoub MH. Alternative pathways of angiotensin II production in the human saphenous vein. *Br J Pharmacol* 1998 October;125(3):423-8.

282. Shewale JG, Tang J. Amino acid sequence of porcine spleen cathepsin D. *Proc Natl Acad Sci U S A* 1984 June;81(12):3703-7.

283. Wang F, Duan R, Chirgwin J, Safe SH. Transcriptional activation of cathepsin D gene expression by growth factors. *J Mol Endocrinol* 2000 April;24(2):193-202.

284. Pentz ES, Lopez ML, Cordaillat M, Gomez RA. Identity of the renin cell is mediated by cAMP and chromatin remodeling: an in vitro model for studying cell recruitment and plasticity. *Am J Physiol Heart Circ Physiol* 2008 February;294(2):H699-H707.

285. Chan YC, Leung PS. Involvement of redox-sensitive extracellular-regulated kinases in angiotensin II-induced interleukin-6 expression in pancreatic acinar cells. *J Pharmacol Exp Ther* 2009 May;329(2):450-8.

286. Satou R, Gonzalez-Villalobos RA, Miyata K et al. IL-6 augments angiotensinogen in primary cultured renal proximal tubular cells. *Mol Cell Endocrinol* 2009 November 13;311(1-2):24-31.

287. Libby P. Inflammation in atherosclerosis. *Nature* 2002 December 19;420(6917):868-74.

288. Rikitake Y, Hirata K, Kawashima S, Akita H, Yokoyama M. Inhibitory effect of inducible type nitric oxide synthase on oxidative modification of low density lipoprotein by vascular smooth muscle cells. *Atherosclerosis* 1998 January;136(1):51-7.

289. Narita M. Cellular senescence and chromatin organisation. *Br J Cancer* 2007 March 12;96(5):686-91.

290. Kurz DJ, Decary S, Hong Y, Erusalimsky JD. Senescence-associated (beta)-galactosidase reflects an increase in lysosomal mass during replicative ageing of human endothelial cells. *J Cell Sci* 2000 October;113 (Pt 20):3613-22.

291. Sharpless NE. Ink4a/Arf links senescence and aging. *Exp Gerontol* 2004 November;39(11-12):1751-9.

292. Krishnamurthy J, Torrice C, Ramsey MR et al. Ink4a/Arf expression is a biomarker of aging. *J Clin Invest* 2004 November;114(9):1299-307.

293. Famulski KS, Halloran PF. Molecular events in kidney ageing. *Curr Opin Nephrol Hypertens* 2005 May;14(3):243-8.

294. Martin EA, Robinson PJ, Franklin RA. Oxidative stress regulates the interaction of p16 with Cdk4. *Biochem Biophys Res Commun* 2000 September 7;275(3):764-7.

295. Toussaint O, Medrano EE, von ZT. Cellular and molecular mechanisms of stress-induced premature senescence (SIPS) of human diploid fibroblasts and melanocytes. *Exp Gerontol* 2000 October;35(8):927-45.

296. Chen QM, Bartholomew JC, Campisi J, Acosta M, Reagan JD, Ames BN. Molecular analysis of H2O2-induced senescent-like growth arrest in normal human fibroblasts: p53 and Rb control G1 arrest but not cell replication. *Biochem J* 1998 May 15;332 (Pt 1):43-50.

297. Ross R, Wight TN, Strandness E, Thiele B. Human atherosclerosis. I. Cell constitution and characteristics of advanced lesions of the superficial femoral artery. *Am J Pathol* 1984 January;114(1):79-93.

298. Brandes RP, Fleming I, Busse R. Endothelial aging. *Cardiovasc Res* 2005 May 1;66(2):286-94.

299. Najjar SS, Scuteri A, Lakatta EG. Arterial aging: is it an immutable cardiovascular risk factor? *Hypertension* 2005 September;46(3):454-62.

300. Lock R, Debnath J. Extracellular matrix regulation of autophagy. *Curr Opin Cell Biol* 2008 October;20(5):583-8.

301. Kroemer G, Levine B. Autophagic cell death: the story of a misnomer. *Nat Rev Mol Cell Biol* 2008 December;9(12):1004-10.

302. Motoshima H, Goldstein BJ, Igata M, Araki E. AMPK and cell proliferation--AMPK as a therapeutic target for atherosclerosis and cancer. *J Physiol* 2006 July 1;574(Pt 1):63-71.

303. Zwerschke W, Mazurek S, Stockl P, Hutter E, Eigenbrodt E, Jansen-Durr P. Metabolic analysis of senescent human fibroblasts reveals a role for AMP in cellular senescence. *Biochem J* 2003 December 1;376(Pt 2):403-11.

304. Robinson BH. Human complex I deficiency: clinical spectrum and involvement of oxygen free radicals in the pathogenicity of the defect. *Biochim Biophys Acta* 1998 May 6;1364(2):271-86.

305. Ushio-Fukai M, Zafari AM, Fukui T, Ishizaka N, Griendling KK. p22phox is a critical component of the superoxide-generating NADH/NADPH oxidase system and regulates angiotensin II-induced hypertrophy in vascular smooth muscle cells. *J Biol Chem* 1996 September 20;271(38):23317-21.

306. Herbert KE, Mistry Y, Hastings R, Poolman T, Niklason L, Williams B. Angiotensin II-mediated oxidative DNA damage accelerates cellular senescence in cultured human vascular smooth muscle cells via telomere-dependent and independent pathways. *Circ Res* 2008 February 1;102(2):201-8.

307. Min LJ, Mogi M, Iwanami J et al. Cross-talk between aldosterone and angiotensin II in vascular smooth muscle cell senescence. *Cardiovasc Res* 2007 December 1;76(3):506-16.